

**GAZİANTEP UNIVERSITY GRADUATE
SCHOOL OF NATURAL & APPLIED SCIENCES**

**A NEW APPROACH FOR ELASTOPLASTIC
ANALYSIS OF STRUCTURES:
NEURAL NETWORKS**

**Ph.D THESIS
IN
MECHANICAL ENGINEERING**

**BY
ABDULKADİR ÇEVİK
JUNE 2006**

A New Approach For Elastoplastic Analysis Of Structures:Neural Networks

**PhD Thesis
in
Mechanical Engineering
University of Gaziantep**

**Supervisor:
Assoc. Prof. Dr. İbrahim H. GÜZELBEY**

**by
Abdulkadir ÇEVİK
June 2006**

Approval of the Graduate School of Natural and Applied Sciences

Prof. Dr.Saadettin ÖZYAZICI

Director

I certify that this thesis satisfies all the requirements as a thesis for the degree of Doctor of Philosophy.

Prof. Dr. Melda ÇARPINLIOĞLU

Head of Department

This is to certify that we have read this thesis and that in our opinion it is fully adequate, in scope and quality, as a thesis for the degree of Doctor of Philosophy.

Assoc. Prof. Dr. İbrahim H. GÜZELBEY

Supervisor

Examining Committee Members

- 1..... _____
- 2..... _____
- 3..... _____
- 4..... _____
- 5..... _____

ABSTRACT

A NEW APPROACH FOR ELASTOPLASTIC ANALYSIS OF STRUCTURES: NEURAL NETWORKS

Abdulkadir ÇEVİK

PhD in Mechanical Engineering

Supervisor: Assoc. Prof. Dr. İbrahim H. GÜZELBEY

June 2006, 212 pages

This thesis investigates the applicability of Neural Networks (NN) for elastoplastic analysis of structures by means of a wide range of case studies. All case studies are specific examples of elastoplastic behaviour of structures. Case studies considered in this thesis can be categorized as FEM-based and experimental-based in terms of the origin of training patterns i.e. how they are obtained for the NN modeling. Required training and test data for the FEM-based NN modeling is obtained using ANSYS and from literature. Required training and test data for the experimental-based NN modeling are obtained from literature as a result of a comprehensive literature survey. The experimental based NN modeling consists of several types of materials such as steel, aluminum and composites used in various types of structural members such as beams, columns and plates. Matlab NN Toolbox is used for the NN modeling of case studies. A flexible Matlab program has been developed to select the optimum NN architecture directly. Moreover, the developed program also gives the explicit form of the proposed NN models. The accuracy of the NN results when compared with either FE or experimental results is found to be quite high. In some case studies the NN results are compared with existing design codes and are found to be by far more accurate. As a result of this thesis, it can be concluded that NNs can be effectively used to model elastoplastic behaviour of structures for a wide range of material type and structural members.

Keywords: Neural Networks, Elastoplasticity, Web Crippling, Rotation Capacity, Shear Capacity, Strength Enhancement, Aluminum Alloy Columns, Flexural Buckling, Structures.

ÖZET

YAPILARIN ELASTOPLASTİK ANALİZİ İÇİN YENİ BİR YAKLAŞIM: YAPAY SINIR AĞLARI

Abdulkadir ÇEVİK

Doktora Tezi, Makine Mühendisliği

Tez Yöneticisi: Doç Dr. İbrahim H. GÜZELBEY

Haziran 2006, 212 sayfa

Bu tez Yapay Sinir Ağlarının (YSA) geniş aralıklı örnekler kullanılarak yapıların elastoplastik analizi için kullanılabilirliğini incelemektedir. Bütün örnek çalışmaları, yapıların elastoplastik davranışına ilişkin özgün örneklerdir. Bu tezde verilen örnekler, YSA için eğitim setlerinin elde edilmesine göre Sonlu Elemanlar ya da deneysel tabanlı olmak üzere sınıflandırılabilir. Sonlu Elemanlar tabanlı YSA modellemesi için gereken eğitim ve test setleri, ANSYS kullanılarak ya da literatürden sağlanmıştır. Deneysel tabanlı YSA modellemesi için gereken eğitim ve test setleri ise çok kapsamlı bir literatür taraması sonucu literatürden elde edilmiştir. Deneysel tabanlı YSA modellemesi çelik, alüminyum, kompozit gibi çeşitli malzeme tiplerini ve kiriş, kolon ve plak gibi çeşitli yapı elemanlarını içermektedir. Örnek çalışmaların YSA modellemesi için Matlab NN Toolbox kullanılmıştır. Doğrudan optimum YSA mimarisini seçen esnek bir Matlab programı geliştirilmiştir. Bunun ötesinde geliştirilen program, önerilen YSA modelinin açık formunu da verebilmektedir. YSA sonuçları Sonlu Elemanlar ya da deneysel sonuçları ile karşılaştırılmış ve doğruluğu çok yüksek bulunmuştur. Bazı örnekler için ise YSA sonuçları mevcut tasarım standartları ile de karşılaştırılmış ve onlardan çok daha doğru sonuçlar verdiği görülmüştür. Bu tezin sonucunda YSA larının yapıların elastoplastik analizinde etkili bir şekilde kullanılabileceği görülmüştür.

Anahtar Kelimeler: Yapay Sinir Ağları, Elastoplastisite, Gövde ezilmesi, Dönme kapasitesi, Kesme kapasitesi, Dayanım artışı, Alüminyum alaşımlı kolonlar, Eğilme burkulması, Yapılar.

ACKNOWLEDGEMENTS

I express sincere appreciation to my supervisor Assoc. Prof. Dr. İbrahim H. GÜZELBEY for his guidance and great help and to my family.

TABLE OF CONTENTS	
ABSTRACT	iv
ÖZET	v
ACKNOWLEDGEMENT	vi
LIST OF FIGURES	x
LIST OF TABLES	xiv
LIST OF SYMBOLS	xv
CHAPTER 1 INTRODUCTION	1
1.1 General Introduction	1
1.2 Research Objectives and Tasks	1
1.3 Thesis Layout	3
CHAPTER 2 LITERATURE REVIEW	4
2.1 Engineering Analysis	4
2.2 Neural Networks	7
2.2.1 NNs in structural mechanics	8
2.2.2 NNs in elastoplastic analysis of structures	10
2.2.3. NNs in modeling of material constitutive behaviour	14
2.3. Conclusion	16
CHAPTER 3 THEORY OF PLASTICITY	17
3.1 Introduction	17
3.2 Historical Remarks	19
3.3 Review of Basic Governing Equations of Linear Elasticity	22
3.3.1 Compatibility equations	22
3.3.2 Constitutive equations	23
3.3.3 Equilibrium equations	23
3.4 Plastic Analysis	24
3.4.1 Yielding criteria	24
3.4.1.1 Tresca criterion	25
3.4.1.2 Von Mises criterion	25
3.4.1.3 The Mohr-Coulomb yield criterion	27
3.4.1.4 The Drucker-Prager Criterion	28
3.4.1.5 Hill's Yield Criterion	29
3.4.2 Flow rule	29
3.4.2.1 Associated and non-associated flow rule	29
3.4.3 Hardening rules	31
3.4.3.1 Isotropic hardening	32
3.4.3.2 Kinematic hardening	33
3.4.3.3 Mixed hardening	34
CHAPTER 4 FINITE ELEMENT METHOD	36
4.1 Introduction	36
4.2 Basic review of Finite Element Method	36
4.2.1 Generalised equations of equilibrium	36
4.2.2 Derivation of the B matrix for two-dimensional problems	38
4.2.3 The Finite Element Method and ANSYS	42

CHAPTER 5 NEURAL NETWORKS	46
5.1 Introduction	46
5.2 History of Neural Networks	47
5.3 Elements of Neural Networks	48
5.4 Classification of Neural Networks	51
5.5 Backpropagation Algorithm	54
5.6 Matlab NN Toolbox	56
5.7 Optimal NN Model Selection	57
CHAPTER 6 CASE STUDIES	61
6.1 Introduction	61
6.2 Case Studies	62
6.2.1 The prediction of ultimate strength of metal plates in compression	62
6.2.1.1 Introduction	62
6.2.1.2 Inelastic buckling of plates	63
6.2.1.3 Strength of Metal Plates With Non-Linear Mechanical Properties	64
6.2.1.4 Numerical application	68
6.2.1.5 Results of NN models	68
6.2.1.6 Explicit Formulation of NN Models	70
6.2.1.7 Conclusion	72
6.2.2 Explicit Formulation of Elastoplastic Bending By Neural Networks	73
6.2.2.1 Introduction	73
6.2.2.2 Numerical application	75
6.2.2.3 Explicit formulation of NN models	78
6.2.2.4 Conclusion	83
6.2.3 Prediction of Web Crippling Strength of Cold-Formed Steel Sheetings Using Neural Networks	84
6.2.3.1 Introduction	84
6.2.3.2 Web Crippling of Sheetings	86
6.2.3.3 Current design codes	87
6.2.3.4 Plastic web crippling behaviour of sheetings	88
6.2.3.5 Numerical application	89
6.2.3.6 Closed-Form Solution of Ultimate Concentrated Load (R_u)	97
6.2.3.7 Conclusion	99
6.2.4 Prediction Of Rotation Capacity Of Wide Flange Beams Using Neural Networks	99
6.2.4.1 Introduction	99
6.2.4.2 Rotation Capacity	101
6.2.4.3 Numerical Application	103
6.2.4.4 Closed Form Solution of Available Rotation Capacity	111
6.2.4.5 Conclusion	113
6.2.5 Strength Enhancement of Corner Regions in cold-formed steel	114
6.2.5.1 Introduction	114
6.2.5.2 Strength Enhancement of Corner Regions	115
6.2.5.3 Numerical Application	118
6.2.5.4 Explicit Formulation of NN Models	126
6.2.5.5 Conclusion	130
6.2.6 Flexural Buckling Load Prediction of Aluminium Alloy Columns	130
6.2.6.1 Introduction	130
6.2.6.2 Buckling of Aluminium Alloy Columns	131

6.2.6.3 Numerical Application	134
6.2.6.4 Explicit Formulation of NN Models	136
6.2.6.5 Conclusion	138
6.2.7 Prediction of Buckling Parameters of Hollow Aluminium Columns Using NNs	138
6.2.7.1 Introduction	138
6.2.7.2 Buckling of Axially Compressed Aluminium Extrusions	139
6.2.7.3 Numerical Application	142
6.2.7.5 Conclusion	150
6.2.8 Shear Capacity of RC Beams Without Web Reinforcement	151
6.2.8.1 Introduction	151
6.2.8.2 Shear Strength of RC Beams	151
6.2.8.3 NN Results	154
6.2.8.4 Explicit Formulation of the NN Model	158
6.2.8.5 Conclusion	158
6.2.9 Strength Enhancement for CFRP Confined Concrete Cylinders	159
6.2.9.1 Introduction	159
6.2.9.2 Behavior of FRP Confined Concrete	160
6.2.9.4 Results of NN model	163
6.2.9.5 Explicit Formulation of the NN Model	165
6.2.9.6 Conclusion	167
CHAPTER 7 CONCLUSIONS	168
RECOMMENDATIONS FOR FUTURE WORK	170
APPENDIX	197
VITAE	

LIST OF FIGURES

Fig 5.1 A biological neuron	48
Fig 5.2 Artificial neuron model.....	49
Fig 5.3 Basic elements of an artificial neuron.....	50
Fig 5.4 Threshold activation function	50
Fig 5.5 Piecewise-linear function.....	50
Fig 5.6 Sigmoid (logistic) function	51
Fig 5.8 Schematic presentation of weight correction in BPNN.....	54
Fig 5.9 Backpropagation algorithm	55
Fig 5.10 Optimal NN selection process	59
Fig 5.11 Flowchart of optimal NN selection.....	60
Fig 6.1 Buckling of rectangular plate under uniform compression	68
Fig 6.2 Proposed NN model for the prediction of σ_u	69
Fig 6.3 Performance of NN model for test set	69
Fig 6.5. % Error for test set.....	70
Fig 6.6 % Error for training set.....	70
Fig 6.7 Moment-Curvature relationship.....	74
Fig 6.8. Bilinear strain hardening material model.....	74
Fig 6.9a Optimum NN model for $\sigma_{V_{max}}$	76
Fig 6.9b Optimum NN model for δ_{max}	76
Fig 6.10 Performance of NN model for test set (δ_{max}).....	77
Fig 6.11 Performance of NN model for training set (δ_{max}).....	77
Fig 6.12. % Error for training set (δ_{max}).....	77
Fig 6.13 % Error for test set (δ_{max}).....	77
Fig 6.14 Performance of NN model for test set ($\sigma_{V_{max}}$).....	77
Fig 6.15 Performance of NN model for training set ($\sigma_{V_{max}}$).....	77
Fig 6.16 % Error for training set ($\sigma_{V_{max}}$)	78
Fig 6.17 % Error for test set ($\sigma_{V_{max}}$)	78
Fig 6.18 NN model for maximum plastic Von Mises stress.....	78
Fig 6.19 NN model for maximum plastic deflection	79
Fig 6.20 Web crippling of thin-walled cold-formed steel me.....	85
Fig 6.21 Elastic, elastoplastic and plastic behaviour of a sheet section.....	89
Fig 6.22 Types of failure modes for sheetings.....	89
Fig 6.23 Geometry of cross-section variables.....	90
Fig 6.24 Wing's test set up.....	91
Fig 6.25 Sections for Wing's experiments	91
Fig 6.26 Sections for Wing's experiments II.....	92
Fig 6.27 Optimum NN model	92
Fig 6.28 Prediction of NN and actual values for learning set.....	94
Fig 6.29 Prediction of NN and actual values for testing set.....	94
Fig 6.30 % Error of training set	94
Fig 6.31 % Error of test set	94
Fig 6.32 Actual experimental results/ NN predictions.....	95
Fig 6.33 Trend of r vs. F_y	95
Fig 6.34 Trend of t vs. F_y	95
Fig 6.35 Trend of r vs. L_{sp}	95

Fig 6.36 Trend of b_{tf} vs. F_y	95
Fig 6.37 Trend of b_{tf} vs. r	96
Fig 6.38 Trend of b_{bf} vs. r	96
Fig 6.39 Trend of b_{bf} vs. F_y	96
Fig 6.40 Trend of b_{bf} vs. θ	96
Fig 6.41 Trend of t vs. L_p	96
Fig 6.42 Trend of L_p vs. F_y	96
Fig 6.43 Trend of θ vs. F_y	97
Fig 6.44 Trend of b_w vs. F_y	97
Fig 6.45. General beam behaviour.....	100
Fig 6.46 Definition of rotation capacity.....	102
Fig 6.47 Classical definition for rotation capacity based on normalised moment-rotation relationship.....	103
Fig 6.48a. SB1.....	105
Fig 6.48b SB2.....	105
Fig 6.49 Geometry of cross-section variables.....	106
Fig 6.50 NN model.....	107
Fig 6.51 Optimum NN model.....	108
Fig 6.52 % Error of test set.....	110
Fig 6.53 % Error of training set.....	110
Fig 6.54 Prediction of NN and actual values for testing set.....	110
Fig 6.55 Prediction of NN and actual values for learning set.....	110
Fig 6.57 Overall performance of NN vs. experimental results.....	111
Fig 6.58 Comparison of NN and DUCTROT Results.....	111
Fig 6.59 Proposed NN model for the prediction of $\sigma_{0.2,c}$	119
Fig 6.60 Performance of NN model for test set.....	121
Fig 6.61 Performance of NN model for training set.....	121
Fig 6.62 % Error for test set (NN Model).....	121
Fig 6.63 % Error for training set (NN model).....	121
Fig 6.64 Proposed NN Model for the prediction of $\sigma_{u,c}$	123
Fig 6.65 Performance of NN model for test set.....	125
Fig 6.66 Performance of NN model for training set.....	125
Fig 6.67 % Error for training set.....	126
Fig 6.68 % Error for test set (NN model).....	126
Fig 6.69 Proposed NN model for the prediction of σ_u	135
Fig 6.70 Performance of NN model for test set.....	135
Fig 6.71. Performance of NN model for training set.....	135
Fig 6.72 % Error for test set (NN Model).....	136
Fig 6.73. % Error for training set (NN model).....	136
Fig 6.74 Stress-strain curve of aluminum alloy.....	140
Fig 6.75 Test set-up and cross-section of tested RHS and SHS aluminium columns.....	143
Fig 6.76 Optimum NN model for ultimate buckling resistance (σ_u).....	145
Fig 6.77 % Error for test set.....	145
Fig 6.78 % Error for training set.....	145
Fig 6.79 Performance Of NN model for test set.....	146
Fig 6.80 Performance Of NN model for training set.....	146

Fig 6.81 Optimum NN model for normalized buckling strain ($\frac{\epsilon_{LB}}{\epsilon_0}$).....	146
Fig 6.82 % Error for Test set.....	147
Fig 6.83 % Error for Training set.....	147
Fig 6.84 Performance Of NN model for test set	147
Fig 6.85 Performance of NN model for training set	147
Fig 6.86 Shear Force in RC beam without web reinforcement.....	152
Fig 6.87 Optimum NN model	155
Fig 6.88 % Error of test set for NN model.....	155
Fig 6.89 % Error of train set for NN model	155
Fig 6.90 Performance of test set for NN model	155
Fig 6.91 Performance of train set for NN model	155
Fig 6.92 Overall performance ACI (11.5) code	156
Fig 6.93 Overall performance ACI (11.3) code	156
Fig 6.94 Overall performance EC2 code.....	156
Fig 6.95 Overall performance LRFD code	156
Fig 6.96 Overall Performance of NN model.....	156
Fig 6.97 Distribution of mean of test/predicted for NN model.....	157
Fig 6.98 Distribution of mean of test/predicted for ACI 11.5.....	157
Fig 6.99 Distribution of mean of test/predicted for LRFD	157
Fig 6.100 Distribution of mean of test/predicted for EC2 model	157
Fig 6.101 Distribution of mean of test/predicted for ACI 11.3 model.....	157
Fig 6.102 Typical response of FRP-confined concrete.....	161
Fig 6.103 Proposed NN Model for the prediction of f'_{cc}	164

LIST OF TABLES

Table 5.1. Back propagation training algorithms used in NN training.	58
Table 6.1 Values of (S/\mathcal{X}) for complete set of Finite Element analyses.....	67
Table 6.2 FE results for $(\frac{\sigma_u}{\sigma_{0.2}})$	67
Table 6.3 Statistical parameters of the proposed NN models	69
Table 6.4 Weights between inputs and hidden layer.....	70
Table 6.5 Statistical parameters of the NN used for δ_{\max} and $\sigma_{V \max}$	76
Table 6.6 NN vs ANSYS for test set $(\sigma_{V \max})$	80
Table 6.7 NN vs ANSYS for test set (δ_{\max})	82
Table 6.8 Minimum and maximum values for cross-section variables.	90
Table 6.9 Statistical parameters of optimum NN model.....	92
Table 6.10 NN prediction of R_u and experimental results of test set with geometric and mechanical variables	93
Table 6.11 Experimental database	104
Table 6.12. Minimum and maximum values for cross-section variables.	106
Table 6.13 Statistical parameters of optimum NN model.....	107
Table 6.14 Comparative analysis of NN results with experimental and numerical results	108
Table 6.15 Available test results	116
Table 6.16 Statistical parameters of the proposed NN models	119
Table 6.17 Results of NN models for the prediction of $\sigma_{0.2,c}$	120
Table 6.18 Comparison of the proposed NN models for the Prediction of $\sigma_{0.2,c}$ with previous statistical models	122
Table 6.19 Statistical parameters of the proposed NN models	123
Table 6.20 Results of NN models for the Prediction of $\sigma_{u,c}$	124
Table 6.21 Comparison of the proposed NN models for the prediction of $\sigma_{u,c}$ with previous statistical models	126
Table 6.22 Weight matrix of the first hidden layer of the proposed NN model	128
Table 6.23. Weight matrix of the first hidden layer of the proposed NN model	129
Table 6.24 Material parameters of test specimens	134
Table 6.25 Statistical parameters of the proposed NN model.....	135
Table 6.26 Weight matrix of the first hidden layer of the proposed NN model	137
Table 6.27 Experimental database	144
Table 6.28 Statistical parameters of the proposed NN model.....	146
Table 6.29 Statistical parameters of the proposed NN model.....	147
Table 6.30 Range of variables.....	148
Table 6.31 Current Design Codes	153
Table 6.32 Experimental database and range of variables.....	154
Table 6.33 Statistical parameters of the proposed NN Model	155
Table 6.34. Models for strength enhancement of FRP confined concrete cylinders	162
Table 6.35 Experimental database and ranges of variables	163
Table 6.36 Statistical parameters of the proposed NN model.....	164
Table 6.37. Statistics of performance and accuracy of (f'_{cc}/f'_{co}) of proposed NN model and various models compared to experimental results	165

LIST OF SYMBOLS

\underline{F}	:Force vector
$\underline{\sigma}$:Stress vector
$\underline{\varepsilon}$:Strain vector
$\underline{\varepsilon}_p$:Plastic strain vector
\underline{k}	:Hardening vector
κ	:Hardening parameter
\underline{S}	:Deviatoric stress vector
J_2	:Deviatoric stress
\underline{D}	:Elastic stress strain matrix
$d\lambda$:Proportionality constant
Y	:Yield stress
\underline{B}	:Matrix of derivatives of the nodal shape functions
N_i	:Lagrangian shape function
u, v	:Displacement components
x, y	:Cartesian coordinates
ξ, η	:Natural coordinates
ν	:Poisson's ratio
E	:Young's modulus
E_t	:Tangential modulus
\underline{K}_t	:Tangential stiffness matrix
\underline{K}_σ	:Geometric stiffness matrix
e	: Nondimensional yield stress, ($e = \sigma_{0.2} / E_0$)
E_0	: Initial elastic modulus
n	: Exponent in Ramberg–Osgood expression
α	: Parameter used to define the imperfection parameter (η)
β	: Parameter used to define the imperfection parameter (η)
η	: Imperfection parameter
λ	: Column slenderness, ($\lambda = (\sigma_{0.2} / \sigma_{E_0})^{1/2}$)
λ_0	: Parameter used to define the imperfection parameter (η)
λ_1	: Parameter used to define the imperfection parameter (η)

σ_u : Ultimate stress of single test or mean of several tests conducted at the same length
 σ_{E_0} : Flexural buckling stress based on E_0
 $\sigma_{0.2}$: 0.2% proof (or off-set) stress
 φ : Parameter used to define the nondimensional column strength (χ)
 χ : Nondimensional column design strength
 A_l : Area of the longitudinal reinforcement
 a/d : Shear span to depth ratio
 bw : Web width
 d : Effective depth
 f_c : Concrete compressive strength
 ρ_l : Amount of longitudinal reinforcement
 f'_{co} : Compressive strength of the unconfined concrete cylinder
 f'_{cc} : Compressive strength of the confined concrete cylinder
 p_u : Ultimate confinement pressure
 E_l : Confinement modulus or lateral modulus
 E_f : Modulus of elasticity of the FRP laminate
 nt : Total thickness of FRP layer
 D : Diameter of the concrete cylinder
 L : Length of the concrete cylinder

CHAPTER 1

INTRODUCTION

1.1 General Introduction

The interest in transferring of methods developed in one discipline to the analysis of problems in other disciplines has evidently increased in recent years. This concerns especially the biologically inspired methods of information processing (soft computing techniques). Among those methods Artificial Neural Networks (ANNs) are worth emphasizing. ANNs have been applied to the analysis of a great amount of problems in science and technology (Waszczyszyn and Ziemanski 2001). This concerns also mechanics of structures and materials (Waszczyszyn, 1999, Waszczyszyn, 2000a).

1.2 Research Objectives and Tasks

NNs have been widely used for modeling of material and structure behaviour so far. However up to now no scientific research has been carried out in a general sense to prove the applicability of NNs to model the elastoplastic behavior of structures. This thesis investigates the feasibility of Neural Networks for elastoplastic analysis of structures by means of a wide range of case studies. Case studies considered in this thesis can be categorized under two headings in terms of origin of training patterns i.e. how they are obtained for the NN modeling:

1. FEM based NN Modeling
2. Experimental based NN modeling.

Besides several types of materials and corresponding case studies are modeled and given as follows:

1. Steel Structures:

- Web Crippling
- Rotation Capacity
- Strength Enhancement of Corner Regions in cold-formed steel

2. Aluminum Structures:

- Flexural Buckling Load Prediction of Aluminum Alloy Columns
- Prediction of Buckling Parameters Of Hollow Aluminum Columns

3. Composite Structures

- Shear Capacity Of RC Beams Without Web Reinforcement
- Strength Enhancement For CFRP Confined Concrete Cylinders

A comprehensive literature review has been carried out to determine the types of case studies to be modeled. All the case studies above are particularly preferred as they were related with elastoplastic behaviour.

Matlab NN Toolbox has been used as software due to its flexibility. Thus a new and efficient algorithm has been developed for the selection of optimal NN architecture which has always been a time consuming and cumbersome task in NN studies. NN models are referred as black box models as the neural process can be modeled mathematically in closed-form solution in general. In this thesis however all proposed NN models are presented in explicit form in order to be used for further practical application.

The results of this PhD thesis are very promising: The proposed NN models are by far more accurate compared to current design codes or existing analytical functions related for each case study.

1.3 Thesis Layout

A literature review for NN applications in elastoplastic analysis of structures is summarized in chapter 2.

Fundamental principles of plasticity theory are presented in Chapter 3.

A general background on Finite Element Method with historical remarks is introduced in Chapter 4.

Background information on NNs are given in chapter 5 with a brief historical remark. Basic concepts of NNs are explained (Definition of NNs, Models of a neuron, learning process, backpropagation). Matlab NN Toolbox is shortly reviewed. A Matlab computer program developed for the optimal NN selection process is also explained.

In chapter 6 cases studies of NN applications are presented in details with their results and discussions. Explicit NN formulations of each case study are derived in this chapter.

Final Conclusions are summarized in Chapter 7.

CHAPTER 2

LITERATURE REVIEW

2.1 Engineering Analysis

Engineering analysis is the process of taking given "input" information defining the physical situation at hand and, through an appropriate set of manipulations, converting that input into a different form of information, the "output," which provides the answer to some questions of interest (Gallegher, 1995). The purpose of any engineering analysis is to predict the behavior of an engineering system under specified conditions. In other words: given the input to the system what is the output from the system? The engineering system under analysis could be, for example, a simple elastic beam, a complex nonlinear three-dimensional structure, mechanical equipment or a hydraulic network

Irrespective of what the engineering system (the physical system) is, it *is*, first converted into a mathematical model and the mathematical model is then analyzed to predict its behavior whether the mathematical model is a simple one or a complex one and whether the analysis is a simple hand calculation or an elaborate computerized analysis, results of the analysis will always have a certain amount of uncertainty associated with it. Uncertainties arise because of the approximations and assumptions made in the conversion of the physical system to a mathematical model in the analysis procedure. Traditionally the uncertainty is not quantified but is recognized and accounted for in designs through safety factors (Ayyub, 1997).

The process of mechanical engineering analysis whether using sophisticated computer software or closed-form calculations often involves several fundamental steps, such as properly posing a problem in engineering terms, generating a mechanical idealization, and solving the resulting differential equations. In general, analyzing stress and structural problems often requires posing a problem in

engineering terms developing a mechanical idealization, and solving the differential equations that evolve from the idealization. If the differential equations are simple enough, they can be solved by closed-form methods; for more complicated situations, a numerical solution, perhaps using finite elements, is required (Lepi,1998).

The process of making engineering assumptions to convert a physical problem into mathematical terms is defined as *idealization*. The idealization process renders an equation (or system of equations) that is solved by either closed-form methods or a numerical method, such as the finite element method. To further investigate mechanical idealization, consider six categories of assumptions and simplifications associated with the process of mechanical idealization in solid mechanics problems:

- Linearity
- Boundary condition assumptions
- Stress-strain assumptions
- Geometric simplification
- Material assumptions
- Loading assumptions

Idealization often allows the essence of an intractable problem to be expressed in simplified mathematical form such that analysis can be performed. Without idealization, analyzing many structural problems would be impractical due to difficulties in replicating complex geometry, storing vast amounts of data, and implementing complicated mathematical principles to simulate many subtle responses that would not significantly affect an engineering design decision. Note that idealization is independent of the finite element method, it is used to initiate problems that may be solved by either closed-form methods or numerical means (Lepi,1998).

The ability to properly pose a problem relies upon an understanding of loads, stress metrics, boundary conditions, and material behavior. The problem statement above focuses upon the maximum value of von Mises stress that develops in the structure with the given loading and restraints. It also clearly states the purpose of the

analysis, and the metric that will be used to evaluate the strength of the structure (Lepi, 1998).

The scope of an engineering analysis must often be narrow and well defined in order to be efficient and effective. Using finite element analysis, one cannot typically build a model and then "see what it will tell you." Considerable thought is needed to properly pose an analysis problem, conceive a model that will yield *relevant* results, and use the results to effect an engineering decision (Lepi, 1998).

There exist two major categories of idealizations used in association with the solid mechanics problems, namely, idealizations based upon the presumption of linearity and those that account for non-linear behavior. At the outset, it is important for the analyst to identify which type of idealization is applicable to a particular problem since there are major differences in the way each type is approached (Lepi,1998). This thesis focuses on non-linear behavior or so called elastoplastic behavior of structures. The engineering analysis for this kind of problems is quite complex and time consuming. The advent of computers has shown a significant impact on the way in which engineering analysis is performed introducing two robust techniques:

1. Numerical Techniques,
2. Artificial Intelligence Techniques,

Among numerical techniques, Finite element method has been widely used in the analysis of structures because of the power of the technique and also because of the availability of many commercial finite element programs. Finite element analysis is a numerical analysis of the mathematical models used to represent the behavior of engineering structures. Therefore, mathematical assumptions concerning the representation of the geometry and behavior of the structures have to be made in finite element models. In order to efficiently and accurately perform the finite element analysis of a composite structure, it is necessary to have a qualitative knowledge of the structure behavior and its finite element model (Suong et al, 1998).

The Finite Element Method is an approximate technique. This means that the continuous structure is discretized into a number of continuous elements connected together at a number of nodes. As the number of elements increases, the approximation of the structure becomes more and more accurate approaching the exact solution. The solution obtained from the finite element method therefore is an approximate solution. In general, finite element analysis of structures is performed by following six steps: discretizing the structure, deriving element equations, assembling elements, imposing essential boundary conditions, solving primary unknowns, and calculating secondary quantities (Suong et al, 1998).

On the other hand, Artificial Intelligence (AI) techniques serve as another robust alternative technique for engineering analysis problems. Artificial intelligence emerged as a computer science discipline in the mid 1950s. Since then, it has produced a number of powerful tools, many of which are of practical use in engineering to solve difficult problems normally requiring human intelligence (Pham and Pham, 1999). AI can be defined as the simulation of human intelligence on a machine, so that the machine efficiently identifies and uses the right piece of “Knowledge” at a given step of solving a problem. Thus, AI alternatively may be stated as a subject dealing with computational models that can think and act rationally. The subject of AI spans a wide horizon. It deals with the various kinds of knowledge representation schemes, different techniques of intelligent search, various methods for resolving uncertainty of data and knowledge, different schemes for automated machine learning and many others (Konar,1999).

Some AI tools that are most applicable to engineering problems can be given as knowledge-based systems, fuzzy logic, inductive learning, neural networks and genetic algorithms (Pham and Pham, 1999). Among these tools Neural Networks are worth to emphasize.

2.2 Neural Networks

Over the past few years, interest in artificial neural networks has grown rapidly. Professionals from such diverse fields as engineering, philosophy, physiology, and

psychology recognize the potential offered by this technology and are seeking applications within their disciplines. Recently, the artificial neural network has experienced a surge in popularity and is now one of the most rapidly expanding areas of research across many disciplines. The main reason is in its powerful and adaptive abilities to treat various complex problems. One can be sure that with its further developments, neural networks will strongly impact many conventional disciplines from the standpoint of methodology. In the field of mechanics, the research and application of both neural network and revolutionary computing are especially active and successful. The back propagated multilayered network is one of the main types applied to engineering (Zeng,1998).

2.2.1 NNs in structural mechanics

The application of NNs in structural mechanics has been gaining support in the recent years. The NN models adopted for structural mechanics may have different architectures and may possess different patterns of connectivity. NNs have been used as computational tools in various areas of structural mechanics, amongst them, identification, simulation, assessment, optimization, analysis and design. The range of applications of Backpropagation neural networks in computational structural mechanics may include design, optimization, identification, mesh generation and analysis (Topping and Bahreininejad, 1997). It seems that a paper by Adeli and Yeh (1989) was the first to be published in 1989 in an archival journal. During the last 15 years, ANNs applications in mechanics grew so rapidly that now it would be difficult to point out those problems of mechanics in which ANNs have not been used yet. ANNs have been widely used as an alternative tool for both civil and mechanical engineering disciplines during the last 15 years and have been applied to almost every type of problem in the field of engineering mechanics (Yagawa and Okuda, 1996, Zeng, 1998, Waszczyszyn, 1999, Waszczyszyn, 1998, Waszczyszyn, 1996, Topping and Bahreininejad, 1997).

In the first structural engineering application of neural networks published in an archival journal, Adeli and Yeh (1989) presented a model of machine learning in engineering design based on the concept of self-adjustment of internal control

parameters and perceptron. The problem of structural design was cast in a form to be described by a perceptron without hidden layers (Adeli and Park, 1995)

Vanluchene and Sun (1990) discuss the use of back-propagation learning algorithm in structural engineering. Hung and Adeli (1991) present a two-layer neural network learning model for engineering design by combining the perceptron with a single-layer AND neural net. They reported improvement in the rate of learning compared with the single-layer perceptron learning model. Several other researchers have applied neural networks, mostly back-propagation algorithms, in structural engineering and mechanics and related engineering problems (Hajela and Berke 1991; Ghaboussi et al. 1991; Masri et al. 1993; Kang and Yoon 1994, Adeli and Park, 1995)

An excellent literature review on application of NNs in structural analysis and design can be found in Lu (2000) given as follows:

Due to the high efficient non-linear mapping capacity with incomplete and noisy input, the BPNN is used in areas such as structural analysis and design, material behaviour and damage identification and assessment. In these applications, the training patterns are provided either by finite element analysis or by the test results. On the other hand, the trial and error characteristic of BPNN leads the application to improve the techniques of training neural networks. In the following paragraphs, the application of BPNN is briefly described from these two aspects.

As far as structural analysis and design are concerned, Hajela et al. (1991) used BPNN to represent the force-displacement relationship in static structural analysis. Such models provide computationally efficient capabilities for reanalysis and appear to be well suited for application in numerical optimum design. In the aspect of simulating structural analysis, Lu *et al* (1994) have introduced Kolmogorov's mapping neural network existence theorem into the approximation analysis of a structure. The research results show that three-layer ANNs can be applied to implement exactly the function between the stresses, displacements, and the design

variables of any elastic structure. [3]. Jenkins (1995) considered the application of neural nets to approximate structural analysis and especially to a comparatively simple structure. Chuang et al. (1998) modeled the complicated non-linear relationship between the various input parameters associated with reinforced concrete columns and actual ultimate capacity of the column. Messner (1994) has shown that a neural network may be the best alternative to develop an accurate decision-making system for the preliminary selection of structural systems. Rogers (1994) used a promising technique to simulate a slow, expensive structural analysis with a fast, inexpensive neural network and presented an application of an ANN to the problem of behavior modeling or prediction of behavior instead of a more complicated and time-consuming finite-element-based structural analysis procedure. Yeh (1999) presented a method of optimizing high-performance concrete mix proportioning for a given workability and compressive strength using artificial neural Networks and non-linear programming. Kang and Yoon (1994) described the configuring and training of neural network for truss design application and explored the possible roles for neural network in structural design problems. Mukherjee et al. (1996) mapped the relationship between the slenderness ratio, the modulus of elasticity and the buckling load for columns. As the input is taken directly from the experimental results, factors affecting the buckling load of columns are automatically incorporated in the model to a great extent. Mukherjee and Deshpande (1995) developed a neural network for the initial design of reinforced-concrete rectangular single-span beams. Further, Ghaboussi et al. (1991) modeled the behavior of concrete in the state of plane stress under monotonic biaxial loading and compressive uniaxial cyclic loading. In order to improve the performance of neural networks, Adeli and Hung (1994) developed an adaptive conjugate gradient learning algorithm for training a multilayer feed forward neural network.

2.2.2 NNs in elastoplastic analysis of structures

In recent years, there has been significant improvement in engineering mechanics studies in order to reach high accuracy analysis and reduce computation time. Particularly for nonlinear analysis in engineering mechanics, reducing the computation time of the structural analysis is significantly important. Elasto-plastic

analysis in this field is the basis of many complex mechanical behaviors. Analysis of elastoplastic problems by means of FEM programs is numerically much more laborious than the analysis of elastic problems because of constitutive equations of plasticity. They are not only nonlinear but history dependent and it is difficult to make mathematical manipulations with them, e.g. to invert them. That is why changes of numerical procedures related to plasticity models into neural procedures seem to be very prospective (Mucha and Waszczyszyn, 1994)

Due to the nonlinear relationship between stress and strain in plasticity, many iterations are needed in terms of stress and loading which lead the computing process to become too complicated and the computation time to increase dramatically especially for complex analysis (Sun et al, 2000). In this sense, ANNs are applied as an alternative tool for the simulation of constitutive equations which was originally proposed by Ghaboussi et al (1991). Neural Network-Based Constitutive Modeling has been emphasized well so far in various state of the art reviews (Yagawa and Okuda, 1996, Waszczyszyn, 1998, Kortesios and Panagiotopoulos, 1993, Waszczyszyn, 2000) and PhD thesis (Wu, 1991, Sidarta, 2000, Basheer, 1998)

A constitutive relation stands for a set of curves in stress space, for given set of strains paths. ANN can be trained to reproduce these curves and to interpolate between them (Lefik and Schreffler, 2003). NN constitutive models, unlike commonly-used plasticity models, do not require special integration procedures for implementation in FE analysis. The learning potential of NN material models is realized using an innovative analysis technique known as Autoprogressive Training (Ghaboussi et al, 1998). This technique allows the numerical model, for the first time, to extract the material constitutive relationship from structural systems by using the measurements of loads and displacements. No prior knowledge of the exact variation of stresses and strains within the boundary value problem is required. A NN material model does not use a material stiffness matrix in its formulation. This is considered a basic advantage of this class of models, but represents a potential disadvantage for implementation in implicit FE analysis. On the other hand, Hashash and co-workers (2004) derived a stiffness matrix for NN material models dependent on the current state of the material and the strain increment. In this sense, the NN

material model and proposed stiffness matrix can be adapted in general FE analysis codes using implicit methods such as Newton–Raphson method.

The implementation of neurocomputation in FE programs was first introduced by Mucha and Waszczyszyn (Mucha and Waszczyszyn,1994). In hybrid systems, ANNs are combined with other non-neural tools like FEM where ANN is trained off line and embedded into the FE program. This procedure is called Hybrid NN/FEM approach and has been widely used by Waszczyszyn and coworkers for the analysis of the elastoplastic plane stress problem, elastoplastic bending of beams and plates (Waszczyszyn, and Pabisek,1999a, Waszczyszyn and Pabisek, 2000, Lukaszyk, and Waszczyszyn,1999, Waszczyszyn and Pabisek,1999b, Waszczyszyn et al,1999, Mucha and Waszczyszyn,1997, Waszczyszyn and Ziemianski,2001, Waszczyszyn, 2000, Waszczyszyn,2003, Kaczmarczyk and Waszczyszyn, 2003).

Neural networks can be efficiently applied for massive computing of samples needed in the optimum design or reliability analysis of structures (Hajela and Berke,1991, Papadrakakis et al,1996). In cases when the FE computation of the samples is complex or time consuming, FEM is used for the preparation of neural solvers which could be used instead of the corresponding FE programs. This problem was analyzed in (Kaliszuk Waszczyszyn, 2003), where neural solvers were used for computing trials in the reliability analysis of elastoplastic frames. New possibilities are associated with neural procedures which are trained and tested off line and then they are incorporated in standard FE programs. This approach, related to implementation of FEM/NN hybrid programs, can be more efficient than standard FE programs . This concerns especially the analysis of problems associated with materials of nonlinear characteristics. That is why the author and his associates have been developing the FEM/NN hybrid systems for the analysis of elastoplastic structures since 1996 (Waszczyszyn, 1996). An interesting application of this approach was discussed in (Waszczyszyn and Pabisek, 1998) where a multilayer forward neural network (called also BPNN, i.e. Back-Propagation Neural Network) was used in the simulation of RMA (Return Mapping Algorithm). A corresponding hybrid FEM/BPNN program was efficiently explored there in the analysis of an elastoplastic plane stress problem. An extension of the above approach is related to the formulation of hybrid systems in which FE programs (or their moduli) interact with

neural networks. A good example of such a system is discussed in (Szewczyk and Noor,1996), where a BPNN was used for predicting partial information about the nonlinear response of FE systems. Another approach was proposed in papers by P.D. Panagiotopoulos and his associates (Kortesis and Panagiotopoulos, 1993 Theocaris and Panagiotopoulos,1993) for the analysis of elastic deformable bodies with unilateral constraints. The main idea of Panagiotopoulos' approach lies in using the FE matrices for calibration of a HTNN (Hopfield-Tank Neural Network) and then interacting of HTNN with a FE program. This approach was generalized in (Pabisek and Waszczyszyn,2001)for the analysis of an elastoplastic plane stress problem with a contact frictionless boundary zone. An efficient application of neurocomputing and FEM was explored for structural updating. An FE program is used for computing patterns with structural imperfections which correspond to the predicted characteristics of the tested material models (laboratory models or full scale real structures). A BPNN is used for inverse analysis and after training the network is applied for calibrating the imperfection parameters in FE models exploring corresponding measurements on the material model (Ziemianski,1999, Waszczyszyn,2003)

From FEM point of view, the analysis of constitutive equations is relatively time-consuming and complicated as it requires the computation of the actual stress vector and consistent stiffness matrix at each Gauss point of plane finite elements which is performed by return mapping algorithm (RMA). In this sense, the NN is trained for the simulation of a generalized RMA (Return Mapping Algorithm) and used for elastoplastic plane problems. On the other hand, Waszczyszyn and co-workers also applied hybrid NN/FDM (Finite difference Method) techniques for the elastoplastic bending analysis of beams where the trained NNs were used in FDM equations (Lukaszyk and Waszczyszyn 1999, Waszczyszyn et al 1999, Waszczyszyn 2000b).

In all studies above related with elastoplastic analysis of structures, NNs are used as so called black box tools. This is often criticized as being their major disadvantage as no understanding of the underlying relationship between inputs and outputs can be gained and no explicit relationship between inputs and outputs can be obtained. Furthermore, NNs are not capable of explaining in an understandable form the process through which a given decision was made.

2.2.3. NNs in modeling of material constitutive behaviour

Another important application of NNs is in the field of material modeling of constitutive behavior. In these studies, a conceptually different approach based on artificial neural networks is used for modeling the mechanical behavior of materials. An important advantage of the NN material model is that it can easily be implemented in the finite element (FE) analysis similar to any other mathematical constitutive model and used in the analysis of any type of boundary value problem. As an integrated part of a structural analysis procedure, material modeling becomes increasingly important as the need increases to investigate complex structural behavior with the availability of sophisticated computational method and powerful computational hardware. A material model, conventionally described as a mathematical model that represents the constitutive law of the material behavior, is becoming complicated as it is required to represent complex material behavior (Sidarta, 2000). An excellent Literature review can be found in (Sidarta, 2000, Basheer, 1998)

Research concerning the application of NN to problems in computational mechanics, in particular the constitutive modeling of the material behavior, started in the early 1990's by Ghaboussi and his co-workers (Ghaboussi et al. 1990, 1991; Wu 1991). Since then research in this field has expanded (Penumadu et al. 1994; Ellis et al. 1995; Penumadu and Chameau 1997; Zhu et al. 1998). The NN material modeling approach offers a fundamentally different approach to modeling the constitutive behavior of materials. The NN material model is developed through learning from examples, which are obtained from experimental test data. During the learning process (training), the NN adapts to the new environment and self-organizes to eventually learn the underlying constitutive material behavior present in the material data. The discovered knowledge is stored in NN connection weights. An advantage of using the NN material modeling approach is the NN model's flexibility to adapt to new environments, which allows the NN model to be further trained to learn new information or behavior previously unexplained by the model when new experimental results are available. The development of NN material models, which is very attractive for modeling complex material behavior, has a

fundamentally different approach. First, the representation of the material behavior has to be determined. In the finite element (FE) analysis, a strain-controlled material model, which relates the states of strains in the input level to the states of stresses as the output of the model with possible inclusion of any other important parameters in the input vector, is of interest. A comprehensive set of states of strains and stresses has to be provided for the training, since the development of a NN material model is through learning from examples and in turn the quality of the trained NN model is greatly dependent upon the quality of the examples (Sidarta, 2000).

Ghaboussi et al. (1991) used standard backpropagation with automatic node generation for network structure optimization. The stress-strain data of uniform plain concrete specimens were digitized in stress-controlled mode and represented in one-point scheme in which the future stress-strain state was expressed as function of the immediately preceding state. The input layer of the constitutive network contained states of stress and strain in the two principal directions, and the corresponding required stress increments in both directions. The output layer contained the corresponding two incremental strains. The predictions of the monotonic model was relatively good; however, there is no indication whether the predicted stress-strain curves were simulated by generating strain increments or by using experimental strain increments. In the second investigation Ghaboussi et al. (1991) used one experimental stress-strain curve representing behavior of plain concrete in uniaxial cyclic loading. In order to model the hysteresis, the experimental data were digitized (coded) into three-point scheme of representation. The input layer contained three successive states of stress and strain and the single stress increment, while the output layer included the next (i.e. fourth) state of strain represented by the incremental strain. The results of the three training/testing episodes indicated that the larger the number of cycles used in training, the better the prediction of subsequent cycles. Overall, the degree of accuracy was much lower than that found in monotonic loading model (Basheer,1998).

2.3. Conclusion

As a results of the comprehensive literature survey, the following outcomes are obtained:

Although NNs are widely applied in structural engineering applications, the specific field of NN application for elastoplastic analysis of structures needs further contributions. Applications of NNs in this field are scarce. Moreover, there is no study covering all aspects of NN applications of elastoplastic analysis of structures for different material types based on real experimental results. Thus this thesis aims to present a comprehensive study in this specific area.

Studies performed in analysis of structures by NNs are in general material specific i.e. a single material type is investigated. There is no study covering behaviour of various material types at the same time. Thus there is no comparative study of NNs for different material types.

NNs are treated as black box in structural analysis problems. There is no study that presents the proposed NN model in explicit form for practical use.

One of the major tasks in NN studies is obviously the determination of the optimum NN architecture which is based on trial and error processes. This is the most difficult and time consuming part of the study. However, there is no well established study in the fields of structural analysis by NNs covering the automatic selection of the optimum NN architecture. This will save much more time and simplify NN applications to a great extent.

CHAPTER 3

THEORY OF PLASTICITY

3.1 Introduction

Theory of plasticity is the name given to the mathematical study of stress and strain in plastically deformed solids, especially metals. This follows the well-established precedent set by the 'theory of elasticity', which deals with methods of calculating stress and strain in elastically deformed solids, and not, as a literal interpretation suggests, with the physical explanation of elasticity (Hill, 1998).

Both the theory of elasticity and the theory of plasticity are phenomenological in nature. They are the formalization of experimental observations of the macroscopic behavior of a deformable solid and do not inquire deeply into the physical and chemical basis of this behavior (Chen and Han, 1988).

A complete account of the theory and application of plasticity must deal with two equally important aspects: (1) the general technique used in the development of stress-strain relationships for elastic-plastic materials with work hardening as well as strain softening; and (2) the general numerical solution procedure for solving an elastic-plastic structural problem under the action of loads or displacements, each of which varies in a specified manner (Chen and Han, 1988).

The first task of plasticity theory is to set up relationships between stress and strain under a complex stress state that can describe adequately the observed plastic deformation. This is a difficult task. However, deformational rules for metals that, in general, agree well with experimental evidence have been firmly established and successfully used in engineering applications. Moreover, in recent years, plasticity theories have also been extended and applied to study the deformational behavior of

geological materials, such as rocks, soils, and concretes. The extension of plasticity theory to non-metallic materials is probably the most active research subject in the field of mechanics of materials at present, and various material models have been developed (Chen and Han, 1988).

The second task of the theory is to develop numerical techniques for implementing these stress-strain relationships in the analysis of structures. Because of the nonlinear nature of the plastic deformation rules, solutions of the basic equations of solid mechanics inevitably present considerable difficulties. However, in recent years, the rapid development of high-speed computers and modern techniques of finite-element analysis has provided engineers with a powerful tool for the solution of virtually any nonlinear structural problem. It has also provoked newer developments and wider applications of the classical plasticity theory. Research activities in this field have increased tremendously during the last decade and it is obvious that it will continue to do so in the future (Chen and Han, 1988).

Any material body deforms when it is subjected to external forces. The deformation is called elastic if it is reversible; that is, if the deformation vanishes instantaneously as soon as forces are removed. A reversible but time-dependent deformation is known as viscoelastic; in this case, the deformation increases with time after application of load, and it decreases slowly after the load is removed. The deformation is called plastic, if it is irreversible or permanent. A brittle material such as glass, concrete, or rock under low hydrostatic pressure can only have elastic deformation before it fails under ultimate load. On the other hand, metals and rocks under high confining pressure can undergo substantial plastic deformation before failure and therefore are known as ductile materials (Akhtar and Sujian, 1995).

The theory of plasticity deals with the stress-strain and load-deflection relationships for a plastically deforming ductile material or structure. The establishment of these relationships should follow two steps: (1) the experimental observation and (2) the mathematical representation. The stress states that are normally achieved in any experiment are simple and uniform, but the ultimate goal of any plasticity theory is a general mathematical formulation that can predict the plastic

deformation of materials under complex loading and boundary condition (Akhtar and Sujian, 1995).

The theories of plasticity can be established into two categories: One group is known as mathematical theories of plasticity, and the other is physical theories of plasticity. Mathematical theories are formulated to represent the experimental observations as general mathematical formulations. This group of theories does not require a deep knowledge of the physics of plastic deformation and is based on hypotheses and assumptions from experimental results. Therefore the mathematical theories are phenomenological in nature and are referred to as phenomenological *theories*. The physical theories, on the other hand, attempt to quantify plastic deformation at the microscopic level and explain why and how the plastic deformation occurs, the movements of atoms and the deformation of the crystal; and grains are important considerations. The responses of metals, viewed as aggregates of single crystals or polycrystals, to applied loads are derived from those of their building blocks, namely single crystals and single-crystal grains (Akhtar and Sujian, 1995).

3.2 Historical Remarks

It is generally regarded that the origin of plasticity, as a branch of mechanics of continua, dates back to a series of papers from 1864 to 1872 by Tresca on the extrusion of metals, in which he proposed the first yield condition, which states that a metal yields plastically when the maximum shear stress attains a critical value. The actual formulation of the theory was done in 1870 by St. Venant, who introduced the basic constitutive relations for what today we would call rigid, perfectly plastic materials in plane stress. The salient feature of this formulation was the suggestion of a flow rule stating that the principal axes of the strain increment (or strain rate) coincide with the principal axes of stress. It remained for Levy later in 1870 to obtain the general equations in three dimensions. A generalization similar to the results of Levy was arrived at independently by von Mises in a landmark paper in 1913, accompanied by his well-known, pressure-insensitive yield criterion (y_2 -theory, or octahedral shear stress yield condition) (Chen and Han, 1988).

In 1871, Levy, adopting Saint Venant's conception of an ideal plastic material, proposed three dimensional relations between stress and rate of plastic strain. There seems to have been no further significant advance until the close of the century when Guest investigated the yielding of hollow tubes under combined axial tension and internal pressure, and obtained results broadly in agreement with the maximum shear-stress criterion. During the next decade, many similar experiments were performed, mainly in England with slightly differing conclusions. Various yield criteria were suggested, but for many metals, as later and more accurate work was to show, the most satisfactory was that advanced by von Mises (1913) on the basis of purely mathematical considerations; it was interpreted by Hencky some years afterwards as implying that yielding occurred when the elastic shear-strain energy reached a critical value. Von Mises also independently proposed equations similar to Levy's (Hill, 1998).

In 1924, Prandtl extended the St. Venant-Levy-von Mises equations for the plane continuum problem to include the elastic component of strain, and Reuss in 1930 carried out their extension to three dimensions. In 1928 von Mises generalized his previous work for a rigid, perfectly plastic solid to include a general yield function and discussed the relation between the direction of plastic strain rate (increment) and the regular or smooth yield surface, thus introducing formally the concept of using the yield function as a plastic potential in the incremental stress-strain relations of flow theory. As is well known now, the von Mises yield function may be regarded as a plastic potential for the St. Venant-Levy-von Mises-Prandtl-Reuss stress-strain relations. The appropriate flow rule associated with the Tresca yield condition, which contains singular regimes (i.e., corners or discontinuities derivatives with respect to stress), was discussed by Reuss in 1932 and 1933 (Chen and Han, 1988).

Since greater emphasis was placed on problems involving flow or perfect plasticity in the years before 1940, the development of incremental constitutive relationships for hardening materials proceeded more slowly. For example, in 1928, Prandtl attempted to formulate general relations for hardening behavior, and Melan, in 1938, generalized the foregoing concepts of perfect plasticity and gave incremental relations for hardening solids with smooth (regular) yield surface. Also, uniqueness theorems for elastic-plastic incremental problems were discussed by Melan in 1938

for both perfectly plastic and hardening materials based on some limiting assumptions. The nearly twenty years after 1940 saw the most intensive period of development of basic concepts and fundamental ingredients in what is now referred to as the classical theory of metal plasticity. Independently of the work of Melan in 1938, Prager, in a significant paper published in 1949, arrived at a general framework (similar to that discussed by Melan in 1938) for the plastic constitutive relations for hardening materials with smooth (regular) yield surfaces. The yield function (also termed the loading function) and the loading-unloading conditions were precisely formulated. Such conditions as the continuity condition (near neutral loading), the consistency condition (for loading from plastic states), the uniqueness condition, and the condition of irreversibility of plastic deformation were formulated and discussed. Also, the interrelationship between the convexity of the (smooth) yield surface, the normality to the yield surface, and the uniqueness of the associated boundary-value problem was clearly recognized. In 1958, Prager further extended this general framework to include thermal effects (nonisothermal plastic deformation), by allowing the yield surface to change its shape with temperature. (Chen and Han , 1988).

A very significant concept of work hardening, termed the material stability postulate, was proposed by Drucker in 1951 and amplified in his further papers. With this concept, the plastic stress-strain relations together with many related fundamental aspects of the subject may be treated in a unified manner. We may note here that Drucker in 1959 also extended his postulate to include time-dependent phenomena such as creep and linear viscoelasticity. Based on this postulate, uniqueness of solution for perfectly plastic and work-hardening solids has been proved, and various variational theorems have been formulated (Chen and Han ,1988).

3.3 Review of Basic Governing Equations of Linear Elasticity

3.3.1 Compatibility equations

Using Cauchy's strain for small strain problems, the strain tensor is expressed in terms of displacement components as follows:

$$\varepsilon_{ij} = \frac{1}{2} \left(\frac{\partial u_i}{\partial x_j} + \frac{\partial u_j}{\partial x_i} \right) \quad (3.1)$$

Alternatively it can be expressed in a matrix form for three dimensional analyses as follows:

$$\underline{\varepsilon}_{ij} = \begin{bmatrix} \varepsilon_x & \varepsilon_{xy} & \varepsilon_{xz} \\ \varepsilon_{yx} & \varepsilon_y & \varepsilon_{yz} \\ \varepsilon_{zx} & \varepsilon_{zy} & \varepsilon_z \end{bmatrix} \quad (3.2)$$

Because of the symmetry of the strain matrix, it can be represented in terms of the engineering strains as the strain vector which is:

$$\underline{\varepsilon} = \{ \varepsilon_x \ \varepsilon_y \ \varepsilon_z \ \gamma_{xy} \ \gamma_{yz} \ \gamma_{zx} \} \quad (3.3)$$

where

$$\gamma_{xy} = 2\varepsilon_{xy} \quad \gamma_{yz} = 2\varepsilon_{yz} \quad \gamma_{zx} = 2\varepsilon_{zx}$$

since Equation (3.1) represents 6 strain components, defined in terms of 3 displacement components, differential operations can be used to eliminate displacement components, and the resulting equations, known as the compatibility equations, can be expressed as follows:

$$\frac{\partial^2 \varepsilon_{ii}}{\partial x_j^2} + \frac{\partial^2 \varepsilon_{jj}}{\partial x_i^2} = 2 \frac{\partial^2 \varepsilon_{ij}}{\partial x_i \partial x_j} \quad (3.4)$$

and

$$\frac{\partial^2 \varepsilon_{ii}}{\partial x_j \partial x_k} = \frac{\partial}{\partial x_i} \left(\frac{\partial \varepsilon_{ij}}{\partial x_k} - \frac{\partial \varepsilon_{jk}}{\partial x_i} + \frac{\partial \varepsilon_{ki}}{\partial x_j} \right) \quad (3.5)$$

3.3.2 Constitutive equations

Linear elastic behavior of homogeneous and isotropic materials can be defined in terms of material properties such as Young's Modulus (E) and Poisson's ratio (ν), and Shear Modulus (G) by means of the generalized Hooke's law expressed as follows:

$$\begin{aligned}\varepsilon_x &= \frac{1}{E}[\sigma_x - \nu(\sigma_y + \sigma_z)], \quad \gamma_{xy} = \frac{1}{G}\tau_{xy} \\ \varepsilon_y &= \frac{1}{E}[\sigma_y - \nu(\sigma_z + \sigma_x)], \quad \gamma_{yz} = \frac{1}{G}\tau_{yz} \\ \varepsilon_z &= \frac{1}{E}[\sigma_z - \nu(\sigma_x + \sigma_y)], \quad \gamma_{zx} = \frac{1}{G}\tau_{zx}\end{aligned}\quad (3.6)$$

Equation (3.6) can be represented in the following matrix form:

$$\underline{\varepsilon} = \underline{C} \underline{\sigma} \quad (3.7)$$

which can be inverted as follows:

$$\underline{\sigma} = \underline{D} \underline{\varepsilon} \quad (3.8)$$

where

$$\underline{D} = \underline{C}^{-1}$$

The stress components can be written in a matrix form as follows:

$$\begin{bmatrix} \tau_{ij} \end{bmatrix} = \begin{bmatrix} \sigma_x & \tau_{xy} & \tau_{xz} \\ \tau_{yx} & \sigma_y & \tau_{yz} \\ \tau_{zx} & \tau_{zx} & \sigma_z \end{bmatrix} \quad (3.9)$$

$$\underline{\sigma} = \{ \sigma_x \quad \sigma_y \quad \sigma_z \quad \tau_{xy} \quad \tau_{yz} \quad \tau_{zx} \} \quad (3.10)$$

3.3.3 Equilibrium equations

The requirements of equilibrium in a body should satisfy two conditions, the moment and force (including surface traction) equilibrium conditions. If the stress tensor is symmetric, it will satisfy moment equilibrium, i.e.

$$\tau_{ij} = \tau_{ji} \quad (3.11)$$

and from force equilibrium it can be shown that

$$\sum_i \frac{\partial \tau_{ji}}{\partial x_i} + X_j = 0, \quad j = 1, 2, 3 \quad (3.12)$$

where X_j represents the components of body force.

3.4 Plastic Analysis

Computational plasticity requires to describe the plastic strain and stress increments. This can be preceded by means of the following conditions in the associated plasticity; the instantaneous yield surface must be convex, the plastic strain increment vector must be on the outward normal to the instantaneous yield surface and the rate of change of plastic strain must be a linear function of the rate of change of the stress (Guzelbey, 1992). These conditions can be satisfied under the assumption of the elasto-plastic behavior of a given material under multiaxial stresses obtained in terms of its uniaxial behavior. Due to the classical theory of plasticity, elasto-plastic equations are derived based upon the yield criteria, flow rules and hardening rules (Erklig, 2003).

3.4.1 Yielding criteria

The term yield refers to the onset of inelastic behavior. There have been many different yield criteria suggested by different researchers and engineers. Coulomb set down the first useful yield criterion in 1773. It forms one of the cornerstones of our understanding of the way soils behave. On the other hand, the yield criteria suggested for ductile metals is a bit simpler than geomaterials, and many of the basic ideas can be developed in a simpler context (David, 2002)

A yield criterion is a necessary condition to know whether a material is in elastic region or not. A yield criterion can be visualized as a mathematical function and can be defined by the yield surfaces. Yield surface is generally expressed as follows:

$$F(\underline{\sigma}, \underline{k}) = 0 \quad (3.13)$$

where \underline{k} is the hardening vector, which is generally a function of the plastic strain ε_p and a scalar hardening parameter κ , i.e.

$$F(\underline{\sigma}, \underline{\varepsilon}_p, \kappa) = 0 \quad (3.14)$$

There are several yield criteria in the literature, the most popular ones for metals and alloys can be summarized as follows:

3.4.1.1 Tresca criterion

The first yield criterion for metals was suggested by the French engineer H. Tresca in 1864. His experiments suggested that plastic behavior would commence when the maximum shear stress reached a critical value which is the maximum shear stress in uniaxial loading (David, 2002). Tresca's criterion takes the maximum shear stress as the decisive factor for yielding. If the principal stresses are in the following order (Guzelbey, 1992):

$$\sigma_1 \geq \sigma_2 \geq \sigma_3 \quad (3.15)$$

then Tresca's yielding condition is given by:

$$|\sigma_1 - \sigma_3| = Y \quad (3.16)$$

i.e. Tresca's equivalent stress can be defined as follows

$$\bar{\sigma}^T = |\sigma_1 - \sigma_3| \quad (3.17)$$

and yield surface equation can therefore be expressed as

$$F = \bar{\sigma}^T - Y = 0 \quad (3.18)$$

where Y is the yield stress.

3.4.1.2 Von Mises criterion

The second yield criterion of general interest for metals was suggested by R. von Mises in 1913. He suggested that yield will occur when the value of the deviatoric stress reaches a critical value (David, 2002)

This criterion suggests that a component under multiaxial stress state will yield when its distortion energy reaches the value of the distortion energy of uniaxial tension at yield (Guzelbey, 1992).

Distortion energy for multiaxial-stress is

$$\bar{U}_s = \frac{1}{2} \underline{S}^t \underline{\varepsilon} \equiv \frac{J_2}{G} \quad (3.19)$$

Where \underline{S} is the deviatoric stress vector and J_2 is the deviatoric stress invariant.

Uniaxial distortion energy at yield is expressed as follows:

$$U = \frac{1}{6G} Y^2 \quad (3.20)$$

From the equality of distortion energies, it can be deduced that the condition for yield is

$$Y = \sqrt{3J_2} \quad (3.21)$$

This leads to the definition of the following Von Mises equivalent stress

$$\bar{\sigma} = \sqrt{3J_2} \quad (3.22)$$

which can be expressed explicitly in terms of stress components as follows:

$$\bar{\sigma} = \frac{1}{\sqrt{2}} \left[(\sigma_x - \sigma_y)^2 + (\sigma_y - \sigma_z)^2 + (\sigma_z - \sigma_x)^2 + 6(\tau_{xy}^2 + \tau_{yz}^2 + \tau_{zx}^2) \right]^{\frac{1}{2}} \quad (3.23)$$

Hence, the corresponding Von Mises yield surface can be defined in terms of the following equation:

$$F = \bar{\sigma} - Y = 0 \quad (3.24)$$

An alternative explanation for Mises' criterion was supplied by the German engineer H. Hencky in 1924. When a ductile metal yields on a microscopic level, displacements occurring between the atoms that make up the crystal lattice are observed. These are called dislocations. A dislocation can move through the lattice, displacing one atom after another producing a small, irrecoverable deformation. Very large numbers of dislocations may occur as the applied stress reaches the yield

criterion, and they will be manifest on a macroscopic level as a plastic deformation. This is not exactly the situation one envisions in a soil as it approaches failure, but some similarities may exist. On a macroscopic level both a ductile metal and a soft clay may appear to flow when the stresses become severe. Both metals and soils often exhibit localisation of deformation within relatively narrow regions or bands when failure is imminent. Workers in geotechnical engineering have often attempted to adapt aspects of metal plasticity theories for use in soil mechanics. The reverse, however, is also true since the very first practical yield criterion was derived specifically for soil. It was the work of the great French engineer Charles Augustus Coulomb (David,2002).

3.4.1.3 The Mohr-Coulomb yield criterion

Coulomb wrote his first scientific paper in 1773. In it he considered a number of problems involving the strength of building materials prevalent in his day, namely wood, stone, masonry and soil. His interest in soil stemmed from the design of retaining walls. As a military engineer he had been involved in the construction of several large earth-retaining structures. He began by observing that all the materials derived strength from two sources: cohesion and friction. His observations of real soils suggested that failure will usually be associated with a surface of rupture within the soil mass. (David,2002) Coulomb's equation relates the normal and shear stresses on a failure plane (Gao and Davies, 2002):

$$\tau = C - \sigma_n \tan \phi \quad (3.25)$$

where τ is the shear stress, σ_n is the normal stress, C is the cohesion, and ϕ is the angle of internal friction. Both C and ϕ are experimentally determined material constants. This criterion may be written for $\sigma_1 \geq \sigma_2 \geq \sigma_3$ as

$$\frac{\sigma_1 - \sigma_3}{2} = c \cos \phi - \frac{\sigma_1 + \sigma_3}{2} \sin \phi \quad (3.26)$$

For frictionless materials ($\phi = 0$), the Mohr-Coulomb criterion reduces to the Tresca criterion.

3.4.1.4 The Drucker-Prager Criterion

This yield criteria was proposed in 1952 by two of the most prominent researchers from the field of both metal and soil plasticity: D. C. Drucker and W. Prager. They suggested that the von Mises yield criterion could be modified easily by introducing a dependence on the mean stress. In order to represent the experimental data located between the Tresca and Mises yield surfaces. Drucker proposed the following criterion (Banabic et al,2000):

$$J_2'^3 - C_D J_3'^2 = F \quad (4.88)$$

where J_2' and J_3' are the second and third invariants of the stress tensor, respectively, and C_D is a constant. Eq. 4.25 may be generalized in the form

$$J_2'^{3p} - C_D J_3'^{2p} = F \quad (4.89)$$

p being an integer. Under plane-stress conditions ($\sigma_3 = 0$), the Drucker yield criterion becomes:

$$\frac{\sigma_1}{\sigma_u} = \left[\frac{\left(\frac{1}{3}\right)^{3p} - C_D \left(\frac{2}{27}\right)^{2p}}{\{(1 - \alpha + \alpha^2)/3\}^{3p} - C_D \{(2 - \alpha)(1 - 2\alpha)(1 + \alpha)/27\}^{2p}} \right]^{1/6} \quad (3.26)$$

where σ_u is the uniaxial yield stress and $\alpha = \sigma_2 / \sigma_1$

Eq. 3.26 is reduced to the Von Mises yield criterion when p tends to infinity. Due to the restrictions related to positive definiteness and convexity, there are some limitations for the value of C_D . In order to have a positive definite form, it is necessary that

$$C_D \leq \left[\frac{27(1 - \alpha + \alpha^2)^3}{\{(2 - \alpha)(1 - 2\alpha)(1 + \alpha)\}^2} \right]^p \quad (\text{Banabic et al,2000}) \quad (3.28)$$

3.4.1.5 Hill's Yield Criterion

In 1948 Hill proposed an anisotropic yield criterion as a generalization of the Von-Mises criterion. The material is supposed to have an anisotropy with three orthogonal symmetry planes. The yield criterion is expressed by a quadratic function of the following type:

$$2f(\sigma_{ij}) = F(\sigma_y - \sigma_z)^2 + G(\sigma_z - \sigma_x)^2 + H(\sigma_x - \sigma_y)^2 + 2L\tau_{yz}^2 + 2M\tau_{zx}^2 + 2N\tau_{xy}^2 = 1$$

Here f is the yield function; F , G , H , L , M and N are constants specific to the anisotropy state of the material, and x , y , z are the principal anisotropic axes.

When describing the anisotropy of metals, the Hill 1948 yield criterion has the advantage that its basic assumptions are easy to understand. This explains its wide use in practice (Banabic et al,2000).

3.4.2 Flow rule

Von Mises suggested that the plastic strain increment is related to the yield surface. This relationship is written by Zienkiewicz (1971) as follows:

$$d\underline{\varepsilon}_p = d\lambda \frac{\partial F}{\partial \underline{\sigma}} = d\lambda \underline{a} \quad (3.29)$$

where $d\lambda$ is a proportionality constant, F is the yield surface function and

$$\underline{a} = \frac{\partial F}{\partial \underline{\sigma}} = \left(\frac{\partial F}{\partial \sigma_x} \quad \frac{\partial F}{\partial \sigma_y} \quad \dots \quad \frac{\partial F}{\partial \tau_{zx}} \right) \quad (3.30)$$

3.4.2.1 Associated and non-associated flow rule

The classical theory of plasticity was originally developed based on the observed mechanical behavior of metals. Therefore, the fundamental plasticity principles or rules,

such as normality, consistency, and stability, describe the behavior of metals successfully. However, the behavior of concrete or soil is considerably different from that of metals, rendering some of the fundamental rules of the classical theory inappropriate for describing its mechanical behavior (Lade, 1988, Iswandi, 1994)

One of the distinguishing characteristics of metals is that their yielding behavior is insensitive to the applied hydrostatic pressure. This implies that yielding or plastic flow in the material is controlled solely by the deviatoric component of the stress state. As a result, the plastic volumetric change in the material can be assumed negligible during the occurrence of plastic flow (it is only the deviatoric components of the strain that contribute to the plastic flow). This yielding behavior of metals can be well described by either the von Mises or the Tresca yield criteria combined with an associated flow (or normality) rule (Chen and Han, 1988, Iswandi, 1994).

On the other hand, the yielding behaviour of concrete (and in general, that of frictional materials) is profoundly influenced by the presence of hydrostatic pressure (Chen, 1988; Desai and Siriwardane, 1984). The strength of these materials is known to be generated from the friction and cohesion between their material constituents. It is well established that the strength of frictional mechanisms is sensitive to the presence of normal (or confining) stresses. Hence, for frictional materials, the higher the applied normal compressive stresses (or confining stresses), the higher the resulting strength; however, it is also known that the rate of strength increase due to confinement decreases with increasing normal stresses (Iswandi, 1994, Chen, 1988).

Another distinguishing characteristic of concrete and other frictional materials is that they exhibit volume and, therefore, density change when they are subjected to compressive or shear loading (Lade, 1988). When concrete is subjected to this type of loading, it initially undergoes volume contraction. However, just prior to failure, concrete invariably exhibits a volume increase (or dilatancy), caused by the propagation of microcracks in the material microstructure. Therefore, in order to get realistic results for stresses and deformations in concrete, the expansive behaviour of this material under mechanical loads ought to be considered in the nonlinear analysis of concrete structures, particularly for structures subjected to triaxial states of stress. As has been mentioned earlier, the classical theory of plasticity combining an

associated flow rule can facilitate inclusion of this dilatancy behaviour in the constitutive description of the material. However, reported experimental and analytical results have shown that the use of associated flow rules results in an unrealistically high estimate for the plastic volumetric expansion of concrete test specimens (Iswandi, 1994, Hu and Schnobrich, 1989).

For some plane-stress problems, such as in modelling concrete beams, accurate representation of the dilatancy may not be necessary because in this problem, dilatancy of the material during loading can be released through the nearby free boundaries or surfaces of the beams without generating any internal stresses (Vermeer and de Borst, 1984). Therefore, in such cases, out-of-plane expansion will have no significant effect on strength. On the other hand, for kinematically restrained problems (such as plane-strain problems, and confined columns) or other three-dimensional problems, such as floating vessels, offshore platforms etc., inaccurate representation of dilatancy behaviour in the analysis may result in incorrect estimation of the strength and deformability of the material, especially in the case of pressure sensitive materials like concrete (Iswandi,1994). Thus, to characterize the dilatancy behavior of concrete in a reliable way, it is necessary to use a non-associated flow rule, which assumes that the plastic strain increment vector is not normal to the yield surface. Such a rule is adopted in this study; note that application of a non-associative rule requires defining a function that relates the plastic strain increment in the material with the associated stress increment. As has been mentioned in the previous section, this function is referred to as "*plastic potential*". Because the amount of plastic dilatancy in the material is controlled through this function, selection of an appropriate plastic potential for the material being considered is a very important step towards the successful development of a constitutive model using plasticity theory (Iswandi,1994).

3.4.3 Hardening rules

A hardening rule is usually employed so as to define the instantaneous yield surface during plastic deformation. In this work, the yield surfaces can be formulated as follows:

3.4.3.1 Isotropic hardening

This rule states that the instantaneous yield surface will deform uniformly during plastic deformation. In this case, the yield surface can be formulated as follows (Guzelbey, 1992):

$$F(\underline{\sigma}, Y(k)) = 0 \quad (3.31)$$

where k is a function of the plastic strain history. If the history of the process is taken into account throughout the effective plastic strain, ε_p , then this type of hardening is called as strain hardening. If the hardening parameter depends on the total plastic work, this is known as work hardening. Throughout this work, work hardening will be used in the analysis in which case k may be defined as the amount of plastic work done during plastic deformation as follows (Guzelbey, 1992):

$$dk = dW_p = \underline{\sigma}' d\underline{\varepsilon}_p \quad (3.32)$$

In the case of simple tension test, the work hardening may be found by

$$dk = dW_p = Y d\overline{\varepsilon}_p \quad (3.33)$$

These two equations are accepted as equivalent to each other, i.e.

$$dk = Y d\overline{\varepsilon}_p = d\underline{\varepsilon}_p' \underline{\sigma} = d\lambda \underline{\sigma}' \underline{\sigma} \quad (3.34)$$

From yield surface function, applying the Euler's theorem (Nayak and Zienkiewicz, 1972) and using Equation (3.40), the hardening and flow parameters are defined as follows:

$$dk = -Y \frac{\partial F}{\partial Y} d\lambda \quad (3.35)$$

and

$$d\lambda = -\frac{d\overline{\varepsilon}_p}{\left(\frac{\partial F}{\partial Y}\right)} \quad (3.36)$$

Although the yield surface is given by Equation (3.37), the physical problems force us to use the following explicit form as a special case of the implicit form:

$$F(\underline{\sigma}, Y) = f(\underline{\sigma}) - Y = 0 \quad (3.37)$$

Applying Euler's theorem to Equation (3.43) the following form is obtained:

$$\left(\frac{\partial F}{\partial \underline{\sigma}}\right)' \underline{\sigma} - Y = 0 \quad (3.38)$$

so

$$d\kappa = f(\underline{\sigma})d\lambda \quad (3.39)$$

and

$$d\lambda = d\overline{\varepsilon}_p \quad (3.40)$$

The parameter A can be represented in the following form for isotropic hardening:

$$A = \left(\frac{\partial F}{\partial Y} \right)^2 H' \quad (3.41)$$

where

$$H' = \frac{dY}{d\varepsilon_p}$$

For the yield surface defined by means of Equation (3.43), the parameter A is given by:

$$A = H' \quad (3.42)$$

The parameter H' can be defined in terms of the tangential modulus as follows:

$$H' = \frac{d\sigma}{d\varepsilon_p} = \frac{E_t}{1 - \frac{E_t}{E}} \quad (3.43)$$

where

$$E_t = \frac{d\sigma}{d\varepsilon} \quad (3.44)$$

3.4.3.2 Kinematic hardening

The Bauschinger effect can be represented by the kinematic hardening model and for this case, it is assumed that the yield surface translates in the stress space as a rigid body (Guzelbey, 1992).

The yield surface for kinematic hardening is expressed as follows:

$$F(\underline{\sigma} - \underline{\alpha}, Y_0) = 0 \quad (3.45)$$

where $\underline{\alpha}$ is a shift vector for the translation of the initial yield surface and

Y_0 is the initial yield stress.

The shift vector increment is given by Prager (1955) as follows:

$$d\underline{\alpha} = C d\varepsilon_p \quad (3.46)$$

The Ziegler's modification (Zeigler, 1959) of the Prager hardening rule has been given as follows:

$$d\underline{\alpha} = d\mu(\underline{\sigma} - \underline{\alpha}) \quad (3.47)$$

where C is a parameter which characterises the hardening behaviour of material.

Parameters $d\lambda$, A , $d\mu$ and C can be defined as follows for kinematic hardening:

$$d\lambda = \frac{1}{C} \frac{\underline{a}^t d\underline{\sigma}}{\underline{a}^t \underline{a}} \quad (3.48)$$

$$A = C \underline{a}^t \underline{a} \quad (3.49)$$

$$d\mu = \frac{C \underline{a}^t d\underline{\epsilon}_p}{Y_0} \quad (3.50)$$

For a uniaxial case it can be proven that:

$$C = \frac{2}{3} H' \quad (3.51)$$

3.4.3.3 Mixed hardening

Allen (1980) gives a combination of isotropic and kinematic work hardening rules, which has been used by Guzelbey (1992) as mixed hardening for the correctness of isotropic hardening with kinematic hardening to predict the Bauschinger effect during cyclic loadings (Erklig,2003).

Mixed hardening model simulates the yield surface's deformation (isotropic hardening) and translation (kinematic hardening) in space, and the yield surface equation is given by:

$$F(\underline{\sigma} - \underline{\alpha}, Y_r) = 0 \quad (3.52)$$

where $\underline{\alpha}$ is the translation of the centre of the yield surface.

$\underline{\sigma} - \underline{\alpha} = \underline{\sigma}_r$ is the reduced stress vector which is measured from the centre of the translated yield surface. Y_r is the current reduced yield stress in simple tension.

The plastic strain increment is expressed as follows:

$$d\underline{\epsilon}_p = d\underline{\epsilon}_p^{(i)} + d\underline{\epsilon}_p^{(k)} \quad (3.53)$$

where the superscripts show the isotropic and kinematic models contribution, and

$$d\underline{\epsilon}_p^{(i)} = M d\underline{\epsilon}_p \quad (3.54)$$

$$d\underline{\varepsilon}_p^{(k)} = (1-M)d\underline{\varepsilon}_p \quad (3.55)$$

where M is a material parameter in the range $-1 \leq M \leq 1$ which defines the share of isotropic hardening in the total amount of hardening. The yield surface for mixed hardening can be written in following form (Guzelbey, 1992):

$$F = F(\underline{\sigma} - \underline{\alpha}, (\underline{\varepsilon})_p^{(k)}, Y_r) \quad (3.56)$$

and the hardening parameters are given by:

$$d\lambda = \frac{d\underline{\varepsilon}_p^{-(i)}}{M \left(\frac{\partial F}{\partial Y_r} \right)} \quad (3.57)$$

$$A = (1-M)C \underline{a}^t \underline{a} + M \left(\frac{\partial F}{\partial Y_r} \right)^2 \frac{dY_r}{d\underline{\varepsilon}_p^{-(i)}} \quad (3.58)$$

where

$$\frac{dY_r}{d\underline{\varepsilon}_p^{-(i)}} = H'(\underline{\sigma}, \underline{\varepsilon})$$

For the special case of a material with an idealised stress-strain diagram,

$$C = \frac{2}{3} \frac{dY_r}{d\underline{\varepsilon}_p^{-(i)}} = \frac{2}{3} H' \quad (3.59)$$

and $d\mu$ of Ziegler's model is

$$d\mu = \frac{C(1-M)\underline{a}^t d\underline{\varepsilon}_p}{-Y_r \frac{\partial F}{\partial Y_r}} \quad (3.60)$$

CHAPTER 4

FINITE ELEMENT METHOD

4.1 Introduction

Numerical methods are extremely powerful tools for engineering analysis. With the advent of computers, there has been a tremendous explosion in the development and use of numerical methods. Of these, the finite element method and its variants are the most commonly used methods in the analysis of practical engineering problems. The finite element method is based on the idea that every system is physically composed of different parts and hence its solution may be represented in parts. In addition, the solution over each part is represented as a linear combination of undetermined parameters and known functions of position and possibly time. The parts can differ from each other in shape, material properties, and physical behavior. Even when the system is of one geometric shape and made of one material, it is simpler to represent its solution in a piecewise manner (Reddy, 2004).

4.2 Basic review of Finite Element Method

4.2.1 Generalised equations of equilibrium

Consider an engineering structure in equilibrium under an initial mechanical loading. A virtual displacement is applied and according to the principle of virtual work:

$$d\chi = dU - dW = 0 \quad (4.1)$$

where $d\chi$, dU and dW represent the variations of total potential energy, strain energy and work done by external force, due to the applied virtual displacement.

An equivalent nodal force vector \underline{F} may be defined such that:

$$dW = d\underline{\delta}^t \underline{F} \quad (4.2)$$

where $d\underline{\delta}$ represents the variation of the nodal displacement vector, and the variation of strain energy can be expressed as follows:

$$dU = \iiint_{\Omega} d\underline{\varepsilon}^t \underline{\sigma} \, dx dy dz \quad (4.3)$$

where Ω represents the domain of the component

Displacement components can be interpolated over each finite element, and it is possible to derive a matrix \underline{B} such that:

$$d\underline{\varepsilon} = \underline{B} d\underline{\delta} \quad (4.4)$$

over every finite element.

If the domain Ω is discretised into n finite elements, then Equation (4.3) may be rewritten, using Equation (4.4), as follows:

$$dU = d\underline{\delta}^t \left[\sum_{e=1}^n \iiint_{\Omega_e} \underline{B}^t \underline{\sigma} \, dx \, dy \, dz \right] \quad (4.5)$$

Substituting from Equation (4.2) and (4.5) into (4.1), it can be shown that:

$$d\chi = d\underline{\delta}^t \left[\sum_{e=1}^n \iiint_{\Omega_e} \underline{B}^t \underline{\sigma} \, dx \, dy \, dz - \underline{F} \right] = 0 \quad (4.6)$$

Since Equation (4.6) is valid for any arbitrary virtual displacement, it can be deduced that:

$$\sum_{e=1}^n \iiint_{\Omega_e} \underline{B}^t \underline{\sigma} \, dx \, dy \, dz - \underline{F} = 0 \quad (4.7)$$

which represents the generalised equation of equilibrium.

4.2.2 Derivation of the \underline{B} matrix for two-dimensional problems

It should be noted in advance that the following derivation of the \underline{B} matrix is valid both for elastic and plastic cases. From the definition of Green's strain tensor given in Chapter 3, the engineering strain components for two-dimensional problems may be expressed in terms of the following vectors:

$$\underline{\varepsilon} = \underline{\varepsilon}_S + \underline{\varepsilon}_L \quad (4.8)$$

where

$$\underline{\varepsilon} = \{ \varepsilon_x \quad \varepsilon_y \quad \gamma_{xy} \}$$

and $\underline{\varepsilon}_S$ represents, of course, the Cauchy's or small strain vector and $\underline{\varepsilon}_L$ represents the complementary or higher order terms in Green's strain components.

$$\underline{\varepsilon}_S = \begin{bmatrix} \frac{\partial u}{\partial x} \\ \frac{\partial v}{\partial y} \\ \frac{\partial u}{\partial y} + \frac{\partial v}{\partial x} \end{bmatrix} \quad (4.9)$$

$$\underline{\varepsilon}_L = \frac{1}{2} \begin{bmatrix} \left(\frac{\partial u}{\partial x} \right)^2 + \left(\frac{\partial v}{\partial x} \right)^2 \\ \left(\frac{\partial v}{\partial y} \right)^2 + \left(\frac{\partial u}{\partial y} \right)^2 \\ 2 \left(\frac{\partial u}{\partial x} \frac{\partial u}{\partial y} + \frac{\partial v}{\partial x} \frac{\partial v}{\partial y} \right) \end{bmatrix} \quad (4.10)$$

The variation of the above vectors can be expressed in terms of displacement components (u, v) and their variations as follows.

$$d\underline{\varepsilon}_S = \begin{bmatrix} \frac{\partial du}{\partial x} \\ \frac{\partial dv}{\partial y} \\ \frac{\partial du}{\partial y} + \frac{\partial dv}{\partial x} \end{bmatrix} \quad (4.11)$$

and

$$d\underline{\varepsilon}_L = \begin{bmatrix} \left(\frac{\partial u}{\partial x}\right)\left(\frac{\partial du}{\partial x}\right) + \left(\frac{\partial v}{\partial x}\right)\left(\frac{\partial dv}{\partial x}\right) \\ \left(\frac{\partial u}{\partial y}\right)\left(\frac{\partial du}{\partial y}\right) + \left(\frac{\partial v}{\partial y}\right)\left(\frac{\partial dv}{\partial y}\right) \\ \left(\frac{\partial u}{\partial x}\right)\left(\frac{\partial du}{\partial y}\right) + \left(\frac{\partial u}{\partial y}\right)\left(\frac{\partial du}{\partial x}\right) + \left(\frac{\partial v}{\partial x}\right)\left(\frac{\partial dv}{\partial y}\right) + \left(\frac{\partial v}{\partial y}\right)\left(\frac{\partial dv}{\partial x}\right) \end{bmatrix} \quad (4.12)$$

Defining a slope vector $\underline{\theta}$ such that:

$$\underline{\theta} = \left\{ \begin{matrix} \frac{\partial u}{\partial x} & \frac{\partial v}{\partial x} & \frac{\partial u}{\partial y} & \frac{\partial v}{\partial y} \end{matrix} \right\} \quad (4.13)$$

then Equation (4.12) may be rewritten as follows:

$$d\underline{\varepsilon}_L = \underline{A}d\underline{\theta} \equiv d\underline{A} \underline{\theta} \quad (4.14)$$

where

$$\underline{A} = \begin{bmatrix} \frac{\partial u}{\partial x} & \frac{\partial v}{\partial x} & 0 & 0 \\ 0 & 0 & \frac{\partial u}{\partial y} & \frac{\partial v}{\partial y} \\ \frac{\partial u}{\partial y} & \frac{\partial v}{\partial y} & \frac{\partial u}{\partial x} & \frac{\partial v}{\partial x} \end{bmatrix} \quad (4.15)$$

Notice that the \underline{A} matrix can be expressed in terms of $\underline{\theta}$ components as follows:

$$\underline{A} = \begin{bmatrix} \theta_1 & \theta_2 & 0 & 0 \\ 0 & 0 & \theta_3 & \theta_4 \\ \theta_3 & \theta_4 & \theta_1 & \theta_2 \end{bmatrix} \quad (4.16)$$

Writing displacement components at any point inside an element in terms of nodal values and shape functions, i.e.

$$\begin{aligned} u(x, y) &= \sum_i u_i N_i(\xi, \eta) \\ v(x, y) &= \sum_i v_i N_i(\xi, \eta) \end{aligned} \quad (4.17)$$

where N_i represents Lagrangian shape functions in terms of intrinsic coordinates ξ, η , then it can be proved that:

$$d\underline{\varepsilon}_S = \underline{B}_S d\underline{\delta} \quad (4.18)$$

$$d\underline{\theta} = \underline{G} d\underline{\delta} \quad (4.19)$$

$$d\underline{\varepsilon}_L = \underline{A} \underline{G} d\underline{\delta} = \underline{B}_L d\underline{\delta} \quad (4.20)$$

where

$$\underline{B}_S = \begin{bmatrix} \dots & \frac{\partial N_i}{\partial x} & 0 & \dots \\ \dots & 0 & \frac{\partial N_i}{\partial y} & \dots \\ \dots & \frac{\partial N_i}{\partial y} & \frac{\partial N_i}{\partial x} & \dots \end{bmatrix} \quad (4.21)$$

and

$$\underline{G} = \begin{bmatrix} \dots & \frac{\partial N_i}{\partial x} & 0 & \dots \\ \dots & 0 & \frac{\partial N_i}{\partial x} & \dots \\ \dots & \frac{\partial N_i}{\partial y} & 0 & \dots \\ \dots & 0 & \frac{\partial N_i}{\partial y} & \dots \end{bmatrix} \quad (4.22)$$

$$\underline{B}_L = \underline{A} \underline{G} \quad (4.23)$$

Hence, it can be deduced from equations (4.4), (4.8), (4.18) and (4.20) that:

$$\underline{B} = \underline{B}_S + \underline{B}_L \quad (4.24)$$

Notice also that, the variation of the \underline{B} matrix due to a virtual displacement is:

$$d\underline{B} = d\underline{B}_L \quad (4.25)$$

and the total strain vector is:

$$\underline{\varepsilon} = \int_0^{\underline{\delta}} (\underline{B}_S + \underline{B}_L) d\underline{\delta} = \left(\underline{B}_S + \frac{1}{2} \underline{B}_L \right) \underline{\delta} \quad (4.26)$$

Generally speaking, Equation (4.7) represents a non-linear system of equations. If an approximate solution is found, in terms of $\underline{\delta}$, $\underline{\sigma}$, \underline{B} , then:

$$\underline{R} = \underline{F} - \sum_e \iiint_{\Omega_e} \underline{B}^t \underline{\sigma} \, dx dy dz \quad (4.27)$$

represents the residual force vector from such an approximation. If the exact solution is represented by

$$\underline{\sigma}_{ex} = \underline{\sigma} + \Delta \underline{\sigma} \quad (4.28)$$

$$\underline{B}_{ex} = \underline{B} + \Delta \underline{B} \quad (4.29)$$

then from Eq. (4.7):

$$\sum_e \iiint_{\Omega_e} (\underline{B} + \Delta \underline{B})^t (\underline{\sigma} + \Delta \underline{\sigma}) \, dx dy dz - \underline{F} = \underline{0}$$

i.e. by neglecting $\Delta \underline{B}^t \Delta \underline{\sigma}$ term:

$$\sum_e \left[\iiint_{\Omega_e} \underline{B}^t \Delta \underline{\sigma} \, dx dy dz + \iiint_{\Omega_e} \Delta \underline{B}^t \underline{\sigma} \, dx dy dz \right] \approx \underline{R} \quad (4.30)$$

The value of $\Delta \underline{\sigma}$ may be approximated as follows:

$$\Delta \underline{\sigma} = \underline{D}_t \Delta \underline{\varepsilon} = \underline{D}_t \underline{B} \Delta \underline{\delta} \quad (4.31)$$

where \underline{D}_t may represent a tangential stress-strain matrix, and $\underline{D}_t = \underline{D}_{ep}$ for elasto-plastic analysis.

The term $\Delta \underline{B}^t \Delta \underline{\sigma}$ may be simplified as follows:

$$\Delta \underline{B}^t \underline{\sigma} = \Delta \underline{B}_L^t \underline{\sigma} = \underline{G}^t \Delta \underline{A} \underline{\sigma}$$

i.e.

$$\Delta \underline{B}^t \underline{\sigma} = \underline{G}^t \underline{S} \underline{G} \Delta \underline{\delta} \quad (4.32)$$

where

$$\underline{S} = \begin{bmatrix} \sigma_x & 0 & \tau_{xy} & 0 \\ 0 & \sigma_x & 0 & \tau_{xy} \\ \tau_{xy} & 0 & \sigma_y & 0 \\ 0 & \tau_{xy} & 0 & \sigma_y \end{bmatrix} \quad (4.33)$$

Using Equations (4.31) and (4.32), then Equation (4.30) may be rewritten in the following matrix form:

$$(\underline{K}_t + \underline{K}_\sigma)\Delta\underline{\delta}=\underline{R} \quad (4.34)$$

where

$$\underline{K}_t = \sum_e \iiint_{\Omega_e} \underline{B}^t \underline{D} \underline{B} dx dy dz \quad (4.35)$$

$$\underline{K}_\sigma = \sum_e \iiint_{\Omega_e} \underline{G}^t \underline{S} \underline{G} dx dy dz \quad (4.36)$$

Equation (4.34) represents the linearised finite element equations of equilibrium, and an iterative algorithm is required in order to obtain an accurate solution.

4.3 The Finite Element Method and ANSYS

In recent years, the use of finite element analysis as a design tool has grown rapidly. Easy-to-use comprehensive packages such as ANSYS have become a common tool in the hands of design engineers. ANSYS is a comprehensive general-purpose finite element computer program which is released in 1971. ANSYS has been a leading FEA program for well over 20 years being capable of performing static, dynamic, heat transfer, fluid flow, and electromagnetism analyses. Today, one will find ANSYS in use in many engineering fields, including aerospace, automotive, electronics, and nuclear. In order to use ANSYS or any other FEA computer program intelligently, the user should first fully understand the underlying basic concepts and limitations of the finite element method. There are various sources of error that can contribute to incorrect results which include the following (Moaveni, 2003):

- Wrong input data, such as physical properties and dimensions
- Selecting inappropriate types of elements
- Poor element shape and size after meshing
- Applying wrong boundary conditions and loads

A typical analysis in ANSYS involves three distinct steps (Moaveni, 2003):

1. *Preprocessing*: Using the PREP7 processor, you provide data such as the geometry, materials, and element type to the program.
2. *Solution*: Using the Solution processor, you define the type of analysis, set boundary conditions, apply loads, and initiate finite element solutions.
3. *Postprocessing*: Using POST1 (for static or steady state problems) or POST26. A general organization of ANSYS is presented in Fig 4.1

The simplest way to communicate with ANSYS is by using the ANSYS menu system, called the Graphical User Interface (GUI). The GUI provides an interface between you and the ANSYS program. The program is internally driven by ANSYS commands. However, by using the GUI, you can perform an analysis with little or no knowledge of ANSYS commands. This process works because each GUI function ultimately produces one or more ANSYS commands that are automatically executed by the program (Moaveni, 2003).

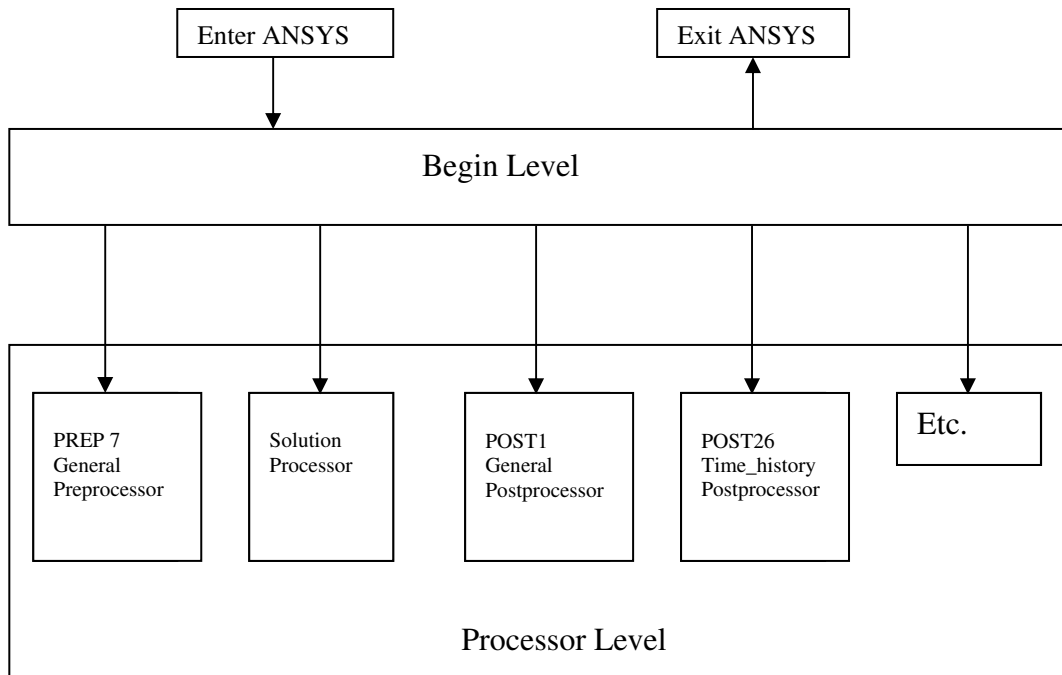


Fig 4.1 General Organization of ANSYS (Moaveni, 2003)

There are three processors that are used most frequently: (1) the *preprocessor* (PREP7), (2) the *processor* (SOLUTION), and (3) the general *postprocessor* (POST1). The preprocessor (PREP7) contains the commands needed to build a model (Moaveni, 2003);

- Define element types and options
- Define element real constants
- Define material properties
- Create model geometry
- Define meshing controls
- Mesh the object created.

ANSYS provides more than one hundred various elements to be used to analyze different problems. Selecting the correct element type is a very important part of the analysis process. A good understanding of finite element theory will benefit you the most in this respect, helping you choose the correct element for your analysis. In ANSYS, each element type is identified by a *category name* followed by a *number*. For example, two-dimensional solid elements have the category name PLANE. Furthermore, PLANE42 is a four-node quadrilateral element used to model structural solid problems. The element is defined by four nodes having two degrees of freedom at each node, translation in the x and y directions (Moaveni, 2003).

The solution *processor* (SOLUTION) has the commands that allow the user to apply boundary conditions and loads. For example, for structural problems, you can define displacement boundary conditions and forces, or for heat transfer problems, you can define boundary temperatures or convective surfaces. Once all the information is made available to the solution processor (SOLUTION), it solves for the nodal solutions. The general *postprocessor* (POST1) contains the commands that allow you to list and display results of an analysis (Moaveni, 2003):

- Read results data from results file
- Read element results data

- Plot results
- List results

There are other processors that allow you to perform additional tasks. For example, the *time-history postprocessor* (POST26) contains the commands that allow the user to review results over time in a transient analysis at a certain point in the model. The *design optimization processor* (OPT) allows the user to perform a design optimization analysis (Moaveni, 2003).

CHAPTER 5

NEURAL NETWORKS

5.1 Introduction

Artificial Intelligence (AI) comprises methods, tools, and systems for solving problems that normally require the intelligence of humans. The term *intelligence* is always defined as the ability to learn effectively, to react adaptively, to make proper decisions, to communicate in language or images in a sophisticated way, and to understand. The main objectives of AI are to develop methods and systems for solving problems, usually solved by the intellectual activity of humans, for example, image recognition, language and speech processing, planning, and prediction, thus enhancing computer information systems; and to develop models which simulate living organisms and the human brain in particular, thus improving our understanding of how the human brain works (Kasabov, 1996).

The main AI directions of development are to develop methods and systems for solving AI problems without following the way humans do so, but providing similar results, for example, expert systems; and to develop methods and systems for solving AI problems by modeling the human way of thinking or the way the brain works physically, for example, artificial neural networks (Kasabov, 1996).

Artificial Neural Networks (ANN) can be defined as computer models that mimic the biological nervous system in general. There are many definitions of NNs in literature which can be summarized as follows:

A Neural Network is a ‘machine’ that is designed to model the way in which the brain performs a particular task or function of interest, the network is usually

implemented using electronic components or simulated in software on a digital computer (Hecht-Nielsen,1990).

Haykin (1994) defines a neural network as a massively parallel distributed processor that has a natural propensity for storing experiential knowledge and making it available for use. It resembles the brain in two respects:

- Knowledge is acquired by the network through a learning process.
- Interneuron connection strengths known as synaptic weights are used to store the knowledge.

On the other hand according to Nigrin (1993); a neural network is a circuit composed of a very large number of simple processing elements that are neural based. Each element operates only on local information. Furthermore each element operates asynchronously; thus there is no overall system clock.

Another widely accepted definition of NNs is given by Zurada (1992) as follows: Artificial neural systems, or neural networks, are physical cellular systems which can acquire, store, and utilize experiential knowledge.

5.2 History of Neural Networks

The first step toward artificial neural networks came in 1943 when Warren McCulloch, a neurophysiologist, and a young mathematician, Walter Pitts, wrote a paper on how neurons might work. They modeled a simple neural network with electrical circuits. In 1949, Donald Hebb proposed 'Hebb rule' which states that nets can learn from their experience in a training environment. 'Hebb rule' has always played a striking role in the field of ANN studies (Hebb, 1949). Throughout 1950s scientists implemented models called perceptrons based on the work of McCulloch and Pitts. In 1957, Rosenblatt invented the *Perceptron* which has been a milestone in ANN studies. Widrow and Hoff developed the models called ADALINE and MADALINE in 1959 which was the first neural network to be applied to a real world problem. In 1968, Marvin Minsky published some intrinsic limitations of neural Networks which slowed down the implementations of ANN drastically (Minsky, 1969). The studies in the field ANN almost stopped for more than a decade until

Hopfield invented The Hopfield network in 1982 whose dynamics were guaranteed to converge. After this novel invention, ANN studies have raised again. Backpropagation was invented in 1986 by Rumelhart, Hinton and Williams which opened a new era in ANN applications (Rumelhart,1986).

5.3 Elements of Neural Networks

The basic element of a neural network is the artificial neuron as shown in Figure 3 which is actually the mathematical models of biological neuron model shown in Figure 5.1. A biological neuron is made up of four main parts: dendrites, synapses, axon and the cell body. The dendrites receive signals from other neurons. The axon of a single neuron serves to form synaptic connections with other neurons. The cell body of a neuron sums the incoming signals from dendrites. If input signals are sufficient to stimulate the neuron to its threshold level, the neuron sends an impulse to its axon. On the other hand, if the inputs do not reach the required level, no impulse will occur. The analogy between a biological neuron model and an artificial neuron model is shown in Figure 5.1 and Figure 5.2.

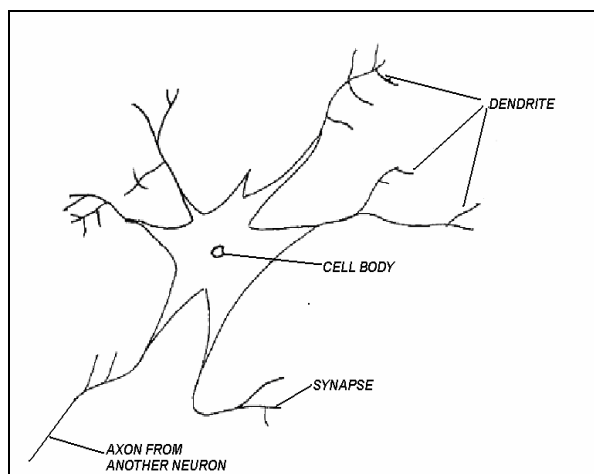


Fig 5.1 A biological neuron. (Wasserman, 1989)

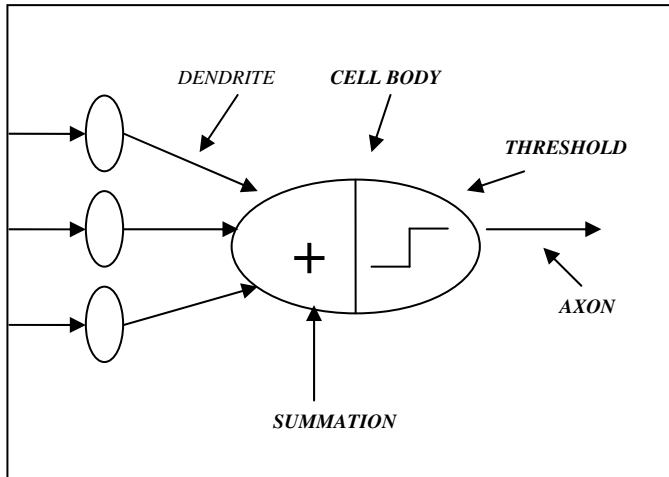


Fig 5.2 Artificial neuron model

The artificial neuron consists of three main components namely as weights, bias, and an activation function (Fig 5.3). Each neuron receives inputs x_1, x_2, \dots, x_n , attached with a weight w_i which shows the connection strength for that input for each connection. Each input is then multiplied by the corresponding weight of the neuron connection. A bias b_i can be defined as a type of connection weight with a constant nonzero value added to the summation of inputs (Fig 5.3) and corresponding weights u , given in Equation (5.1) .

$$u_i = \sum_{j=1}^H w_{ij} x_j + b_i \quad (5.1)$$

The summation u_i is transformed using a scalar-to-scalar function called an "activation or transfer function", $F(u_i)$ yielding a value called the unit's "activation", given in Equation 5.2.

$$Y_i = f(u_i) \quad (5.2)$$

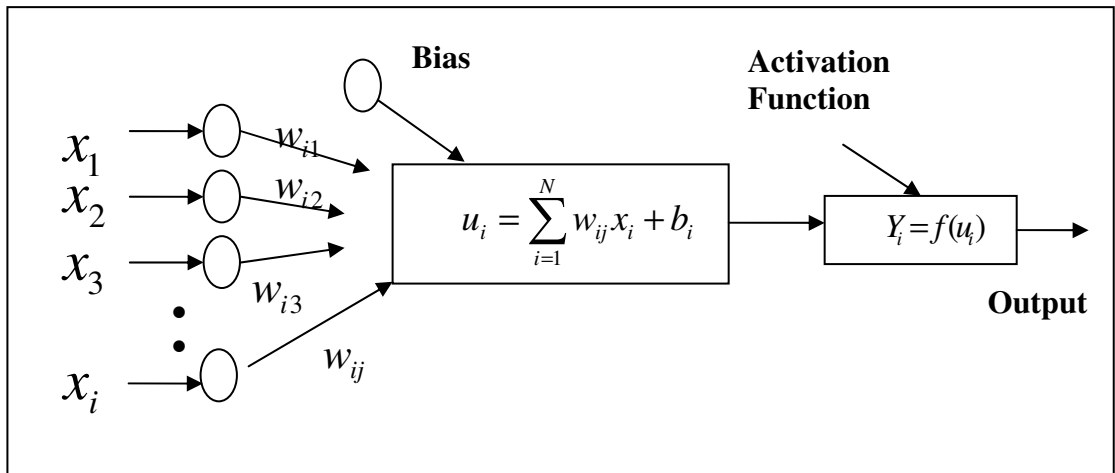


Fig 5.3 Basic elements of an artificial neuron .

Activation functions serve to introduce nonlinearity into neural networks which makes NNs so powerful. The activation function is also referred to as a squashing function. There are a number of different types of activation function and some common examples are provided below:

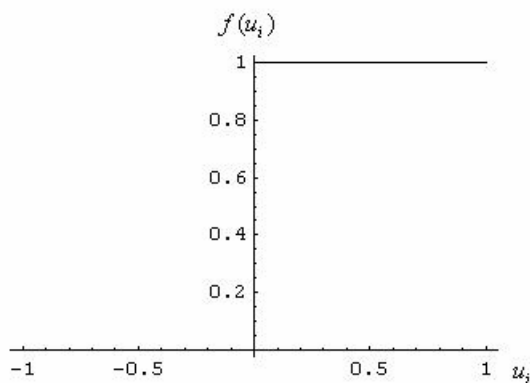


Fig 5.4: Threshold activation function.

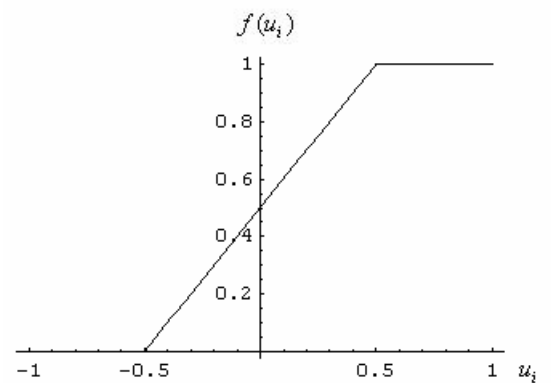


Fig 5.5: Piecewise-linear function

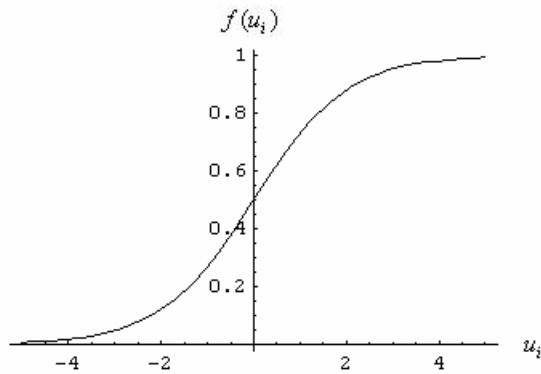


Fig 5.6: Sigmoid (logistic) function.

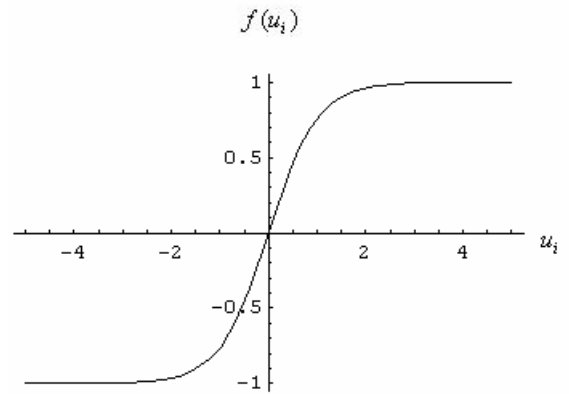


Fig 5.7: Hyperbolic tangent function.

5.4 Classification of Neural Networks

Neural Network models can be classified in a number of ways. Using the network architecture as basis, there are three major types of neural networks:

- *Recurrent networks* - the units are usually laid out in a two-dimensional array and are regularly connected. Typically, each unit sends its output to every other unit of the network and receives input from these same units. Recurrent networks are also called *feedback networks*. Such networks are "clamped" to some initial configuration by setting the activation values of each of the units. The network then goes through a stabilization process where the network units change their activation values and slowly evolve and converge toward a final configuration of "low energy". The final configuration of the network after stabilization constitutes the output or response of the network. This is the architecture of the Hopfield Model (www.comp.nus.edu.sg)
- *Feed forward networks* – these networks distinguish between three types of units: input units, hidden units, and output units. The activity of this type of network propagates forward from one layer to the next, starting from the input layer up to the output layer. Sometimes called multilayered networks, feed forward networks are very popular because this is the inherent architecture of the Backpropagation Model.

- *Competitive networks*– these networks are characterized by lateral inhibitory connections between units within a layer such that the competition process between units causes the initially most active unit to be the only unit to remain active, while all the other units in the cluster will slowly be deactivated. This is referred to as a "winner-takes-all" mechanism. Self-Organizing Maps, Adaptive Resonance Theory, and Rumelhart & Zipser's Competitive Learning Model are the best examples for these types of networks (www.comp.nus.edu.sg).

The network architecture can be further subdivided into whether the network structure is fixed or not. There are two broad categories:

- *Static architecture* – most of the seminal work on neural networks were based on static network structures, whose interconnectivity patterns are fixed *a priori*, although the connection weights themselves are still subject to training. Perceptrons, multi-layered perceptrons, self-organizing maps, and Hopfield networks all have static architecture.
- *Dynamic architecture* – some neural networks do not constrain the network to a fixed structure but instead allow nodes and connections to be added and removed as needed during the learning process as adaptivity. Some examples are Grossberg's Adaptive Resonance Theory and Fritzke's "Neural Gas". Some adding-pruning approaches to Multi-Layered Perceptron networks have also been widely studied.

Yet another basis for classifying neural network models is according to the mode of learning adapted. In this case, there are two major categories (www.comp.nus.edu.sg):

- *Supervised learning* – these are generally the learn-by-example methods where user-supplied information are provided with each training pattern. These guide the neural network in adjusting its parameters. The perceptrons and backpropagation networks are classic examples of supervised learning models.

- *Unsupervised learning* – some neural network models do not need category information to accompany each training pattern, although such information would still be required in the interpretation and labeling of the resultant networks. Classical examples of these are Kohonen’s self-organizing maps and Grossberg’s Adaptive Resonance Theory.

It also makes sense to classify neural network models on the basis of their over-all task:

- *Pattern association* – the neural network serves as an associative memory by retrieving an associated output pattern given some input pattern. The association can be *auto-associative* or *hetero-associative*, depending on whether or not the input and output patterns belong to the same set of patterns.
- *Classification* – the network seeks to divide the set of training patterns into a pre-specified number of categories. Binary-valued output values are generally used for classification, although continuous-valued outputs (coupled with a labeling procedure) can do classification just as well.
- *Function approximation* – the network is supposed to compute some mathematical function. The network's output represents the approximated value of the function given the input pattern as parameters. In certain areas, *regression* may be the more natural term.

There are other bases for classifying neural network models, but these are less fundamental than those mentioned earlier. Some of these include the type of input patterns that can be admitted (binary, discrete valued, real values), or the type of output values that are produced (www.comp.nus.edu.sg).

5.5 Backpropagation Algorithm

Back propagation algorithm is one of the most widely used supervised training methods for training multilayer neural networks due to its simplicity and applicability. It is based on the generalized delta rule and was popularized by Rumelhart and coworkers (1986). As it is a supervised learning algorithm, there is a pair of inputs and corresponding output. The algorithm is simply based on a weight correction procedure shown schematically in Fig. 5.8. It consists of two passes: a forward pass and a backward pass. In the forward pass, first, the weights of the network are randomly initialized and an output set is obtained for a given input set where weights are kept as fixed. The error between the output of the network and the target value is propagated backward during the backward pass and used to update the weights of the previous layers as shown in Fig 5.9 (Zupan,1993).

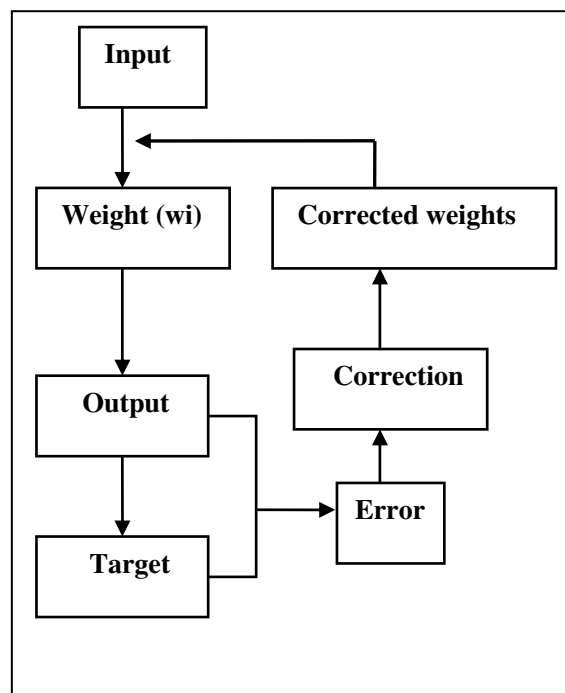


Fig 5.8 Schematic presentation of weight correction in BPNN

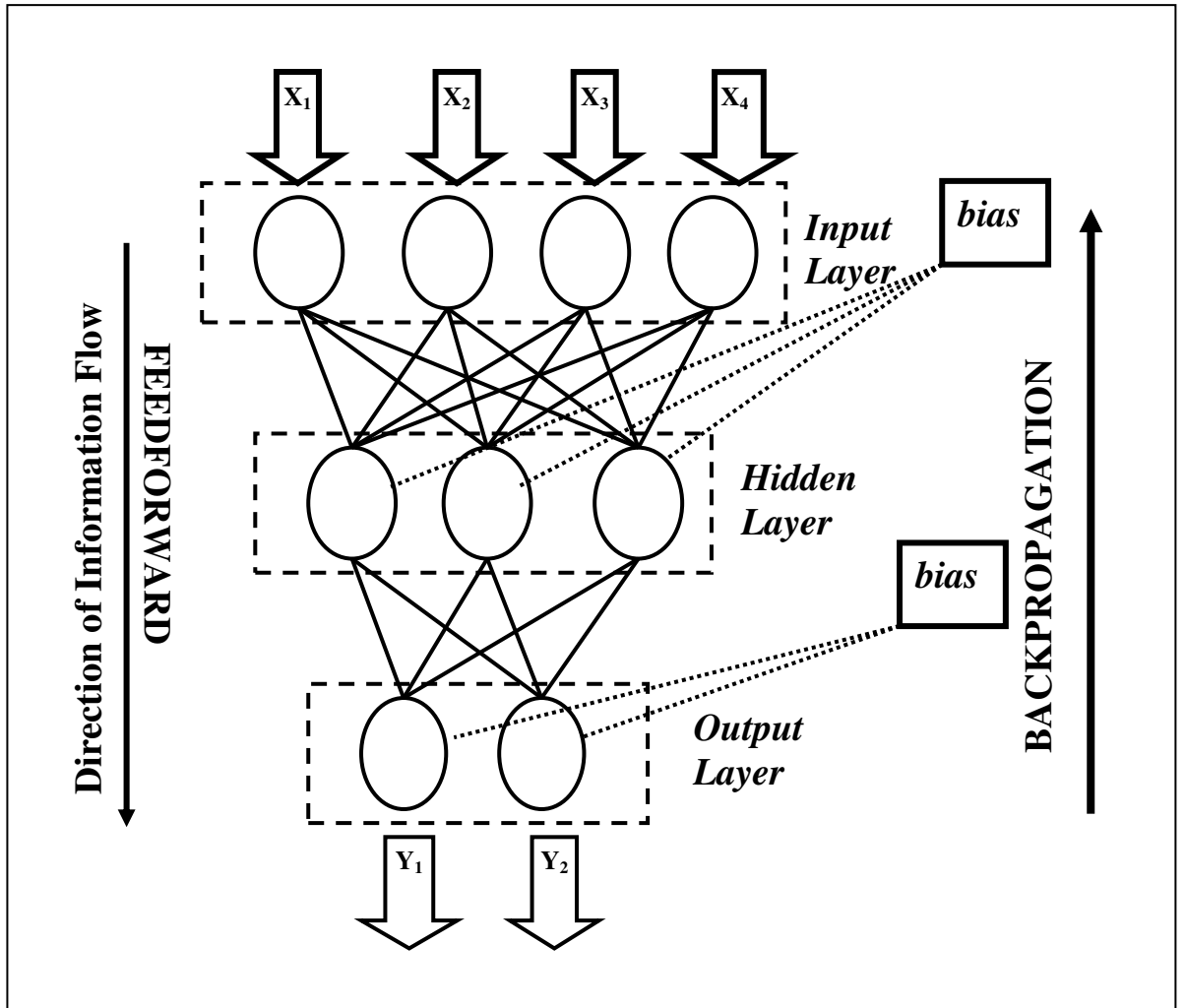


Fig 5.9 Backpropagation algorithm

The main goal of BPNN is mapping of input, i.e. vector x into output, i.e. vector y :

This can be written in short:

$$X_i \xrightarrow{BPNN} Y_i \quad (5.3)$$

For the output layer the error δ_j^{last} can be given as the difference between the target

value Y_i and the network output out_j^{last} :

$$\delta_j^{last} = (Y_i - out_j^{last}) out_j^{last} (1 - out_j^{last}) \quad (5.4)$$

The weight correction is given as

$$\Delta w_{ji}^l = w_{ji}^{l(new)} - w_{ji}^{l(old)} \quad (5.5)$$

Combining Equations 5.4 and 5.5 the weight correction in a hidden layer can be generalized as follows:

$$\Delta w_{ji}^l = \eta \left(\sum_{k=1}^r \delta_k^{l+1} w_{kj}^{l+1} \right) out_j^l (1 - out_j^l) out_i^{l-1} + \mu \Delta w_{ji}^{l(previous)} \quad (5.6)$$

where η is the learning rate and μ is the momentum constant .

Equation 5.5 can be also be expressed in condensed form as:

$$\Delta w_{ji}^l = \eta \delta_j^l out_i^{l-1} + \mu \Delta w_{ji}^{l(previous)} \quad (5.7)$$

5.6 Matlab NN Toolbox

In this thesis, Matlab NN toolbox is used for NN modeling. Matlab NN toolbox is preferred due to its flexibility. As a result, an optimal NN selection algorithm program has been developed which is almost impossible for other NN software available in market.

The toolbox consists of a set of functions and structures that handle neural networks, so the user does not need to write code for all activation functions, training algorithms. The toolbox is based on the network object. This object contains information about everything that concern the neural network, e.g. the number and structure of its layers, the connectivity between the layers, etc. Matlab provides high-level network creation functions, like `newlin` (create a linear layer), `newp` (create a perceptron) or `newff` (create a feed-forward backpropagation network) to allow an easy construction (www.igi.tugraz.at).

A graphical user interface has been added to the toolbox. This interface allows you to:

- Create networks
- Enter data into the GUI
- Initialize, train, and simulate networks
- Export the training results from the GUI to the command line workspace
- Import data from the command line workspace to the GUI (www.igi.tugraz.at)

The User can handle almost all main parameters related with NN model and obtain them very easily. Architecture parameters and the subobject structures given by the Toolbox are as follows:

inputs: {1x1 cell} of inputs
layers: {1x1 cell} of layers
outputs: {1x1 cell} containing 1 output
targets: {1x1 cell} containing 1 target
biases: {1x1 cell} containing 1 bias
inputWeights: {1x1 cell} containing 1 input weight
layerWeights: {1x1 cell} containing no layer weights

In this thesis, by the aid of these NN parameters, closed form solutions of the proposed NN models are also derived and presented. This will open the black box as NNs are often referred to as. The analytical form of the NN models will enable them to be used for further practical applications.

5.7 Optimal NN Model Selection

The performance of a NN model mainly depends on the network architecture and parameter settings. One of the most difficult tasks in NN studies is to find this optimal Network architecture which is based on determination of numbers of optimal layers and neurons in the hidden layers by trial and error approach. The assignment of initial weights and other related parameters may also influence the performance of the NN in a great extent. However there is no well defined rule or procedure to have optimal network architecture and parameter settings where trial and error method still remains valid. This process is very time consuming.

Various Backpropagation Training Algorithms are used in this thesis given in Table 5.1. Matlab NN toolbox randomly assigns the initial weights for each run each time which considerably changes the performance of the trained NN even all parameters and NN architecture are kept constant. This leads to extra difficulties in the selection of optimal Network architecture and parameter settings. To overcome this difficulty, a program has been developed in Matlab which handles the trial and error process automatically. The program tries various number of layers and neurons in the hidden layers both for first and second hidden layers for a constant epoch for several times and selects the best NN architecture with the minimum MAPE (Mean Absolute %

Error) or RMSE (Root Mean Squared Error) of the testing set, as the training of the testing set is more critical. For instance, NN architecture with 1 hidden layer with 7 nodes is tested 10 times and the best NN is stored where in the second cycle the number of hidden nodes is increased up to 8 and the process is repeated. The best NN for cycle 8 is compared with cycle 7 and the best one is stored as best NN. This process is repeated N times where N denotes the number of hidden nodes for the first hidden layer. This whole process is repeated for changing number of nodes in the second hidden layer. Moreover, this selection process is performed for different back propagation training algorithms such as trainlm, trainscg and trainbfg given in Table 5.1. The program begins with simplest NN architecture i.e. NN with 1 hidden node for the first and second hidden layers and ends up with optimal NN architecture as shown in Figure 5.10. The flowchart of the whole process is shown in Figure 5.11.

Table 5.1. Back propagation training algorithms used in NN training.

MATLAB Function name	Algorithm
trainbfg	BFGS quasi-Newton back propagation
traincgf	Fletcher-Powell conjugate gradient back propagation
traincgp	Polak-Ribiere conjugate gradient back propagation
traingd	Gradient descent back propagation
traingda	Gradient descent with adaptive lr back propagation
traingdx	Gradient descent w/momentum & adaptive linear back propagation
trainlm	Levenberg-Marquardt back propagation
trainoss	One step secant back propagation
trainrp	Resilient back propagation (Rprop)
trainscg	Scaled conjugate gradient back propagation

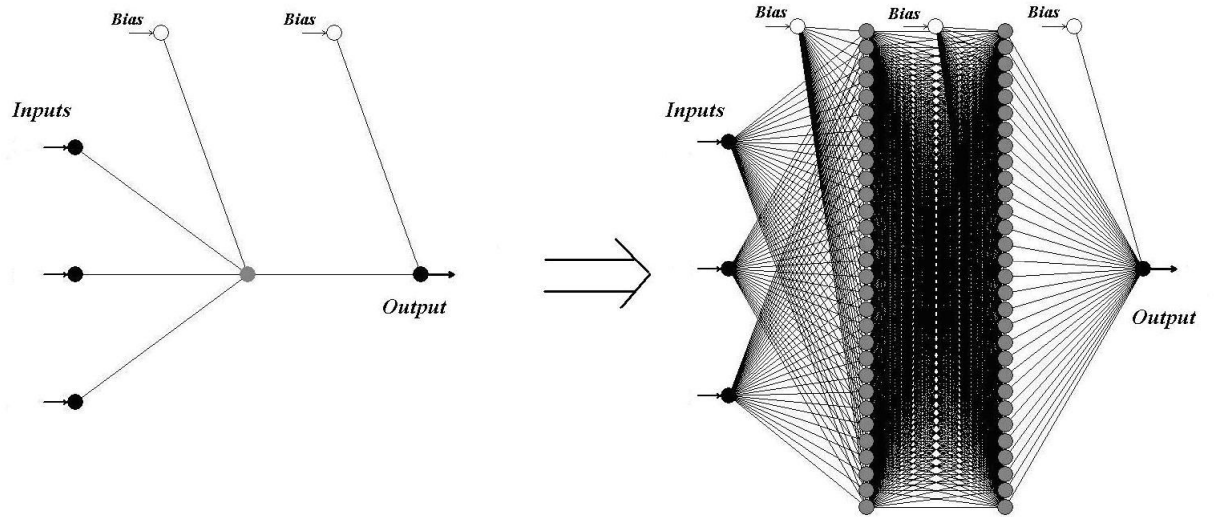


Fig 5.10 Optimal NN selection process

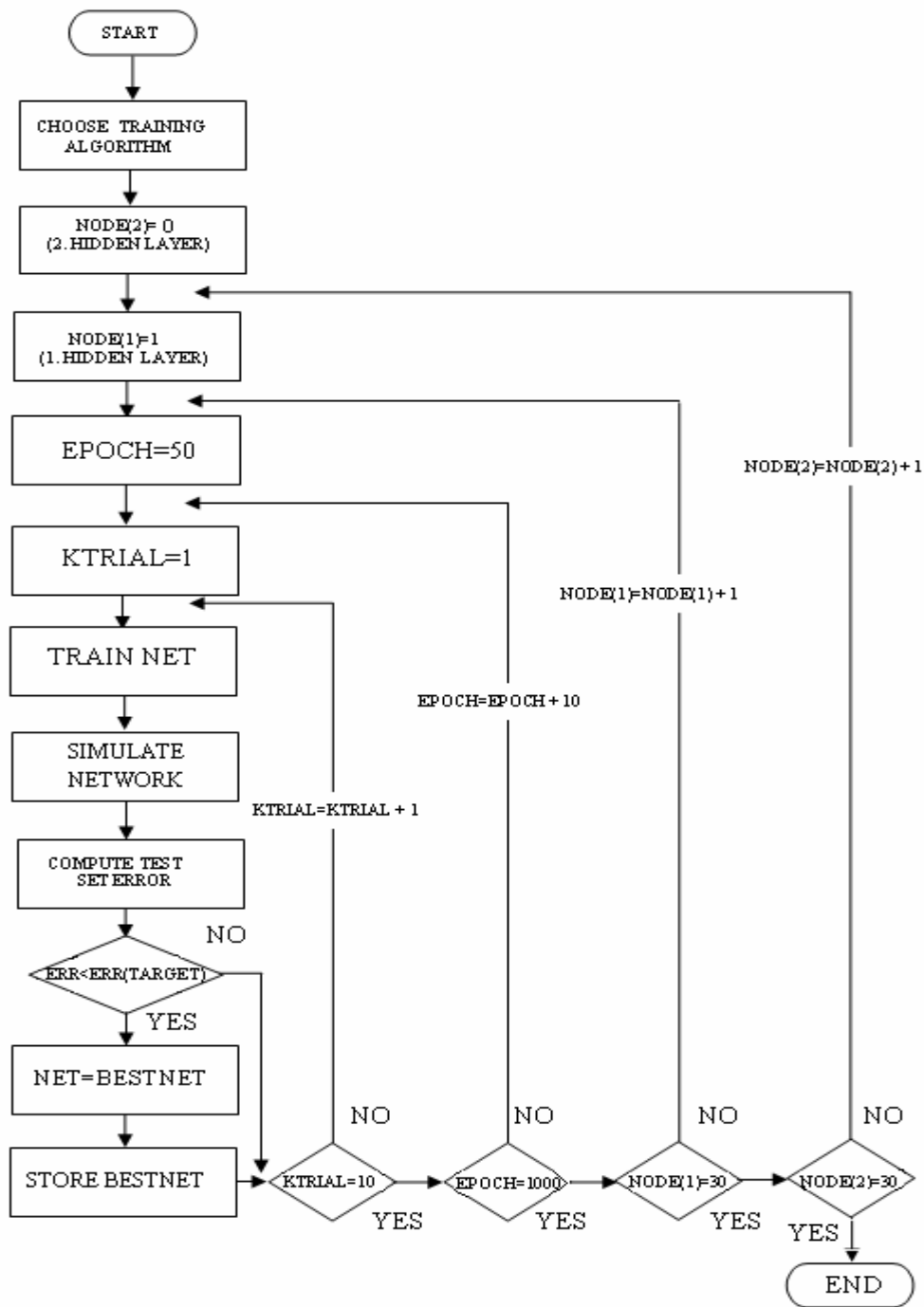


Fig 5.11 Flowchart of optimal NN selection

CHAPTER 6

CASE STUDIES

6.1 Introduction

In this chapter, the feasibility of NNs to be used for elastoplastic analysis of structures is investigated by means of a number of case studies. These case studies can be categorized under 2 headings with respect to the databases used for the NN training.

a) FEM based NN Training

b) Experimental based NN Training

The experimental based case studies consist of different material types given as follows: Steel, aluminum, concrete and composite materials. Case studies can be categorized as follows:

a) FEM based NN Training

- The Prediction Of Ultimate Strength Of Metal Plates In Compression
- Explicit Formulation of Elastoplastic Bending By Neural Networks

b) Experimental based NN Training

Steel Structures:

- Prediction Of Web Crippling Strength Of Cold-Formed Steel Sheetings Using Neural Networks
- Prediction Of Rotation Capacity Of Wide Flange Beams Using Neural Networks

- Strength Enhancement of Corner Regions in cold-formed steel

Aluminum Structures:

- Flexural Buckling Load Prediction of Aluminium Alloy Columns
- Prediction of Buckling Parameters Of Hollow Aluminium Columns

Composite Structures

- Shear Capacity Of RC Beams Without Web Reinforcement
- Strength Enhancement For CFRP Confined Concrete Cylinders

6.2 Case Studies

6.2.1 The prediction of ultimate strength of metal plates in compression

6.2.1.1 Introduction

This case study presents two plate strength formulations applicable to metals with nonlinear stress strain curves, such as aluminium and stainless steel alloys obtained by Neural Networks (NN). The proposed NN models are based on well-defined FE results available in literature. The proposed formulations enable to determine the buckling strength of rectangular plates in terms of Ramberg-Osgood parameters. The strength curves obtained by the proposed NN formulations show perfect agreement with FE results. The formulations are later compared with related codes and results are found to be quite satisfactory.

Although studies on buckling of columns go back to the end of 19th century, viable theoretical solutions for plastic buckling of plates have been proposed throughout late 1930s and 1940s. (Singer, 2004). The theory of plastic buckling of columns is well developed however, several aspects in the theory of plastic buckling of plates

are still controversial. Determination of plastic buckling load of a plate is significantly more difficult than its elastic counterpart as the stress-strain relationship beyond the proportional limit is more complex. In the case of plastic buckling of columns, the stresses are uniaxial whereas in the case of plates the stresses are two or three dimensional which brings extra difficulties in the proper representation of the stress-strain relationship. Thus numerical methods are strongly recommended for stability analysis of plates in plastic region (Szilard, 2004). This study offers an alternative novel approach for the formulation of plate strength using NNs. NNs are used for closed-form solution of plate strength applicable to metals with nonlinear stress strain curves, such as aluminium and stainless steel alloys. The formulation is based on well-established FE results from literature. The formulation is proposed in terms of Ramberg-Osgood parameters. Results of the Soft computing formulations agree well with FE results. The proposed NN model is seen to be more accurate than the related codes.

6.2.1.2 Inelastic buckling of plates

The phenomenon of buckling can be categorized (by plasticity) into three classes, namely elastic buckling, elastic-plastic buckling and plastic buckling where the last two are called inelastic buckling. Elastic-plastic buckling occurs after a local region inside the plate deforms plastically. Plastic buckling refers to buckling that occurs in the regime of gross yielding, i.e., after the plate has yielded over large areas (Paik and Thayamballi, 2003).

Plastic buckling analysis of plates may be based on three classes namely incremental (flow) theory of plasticity, deformation theory and slip theory. The successes of these methods are still controversial. For example, the deformation theory gives a better prediction of critical buckling loads for long, simply-supported plates; the incremental theory gives better results for cylinders under compression and torsion. On the other hand, hybrid methods are also available based on both the deformation theory and the incremental theory (Wang and Reddy, 2004).

6.2.1.3 Strength of Metal Plates With Non-Linear Mechanical Properties

Metals with non-linear mechanical properties, such as stainless steel, aluminium or brass do not have a yield plateau as do ordinary hot-rolled carbon structural steels, which for compression design purposes can be modeled as elastic-perfectly-plastic. However, the mechanical response of many modern cold-formed structural shapes of carbon steel, including tubulars, is becoming increasingly nonlinear because of residual stresses introduced during cold-forming. The strength of the component plates of such sections can also be determined using the strength curve formulation developed by Bezkorovainy et al. (Bezkorovainy,2002).

In the absence of a yield plateau, it is common practice to define an equivalent yield stress for nonlinear metals. This is usually chosen as the 0.2% proof stress, defined as the stress with a *plastic* strain of 0.2%. It is also common practice to represent the stress-strain curve by a Ramberg-Osgood curve (Ramberg and Osgood 1943), which is defined in terms of the initial elastic modulus (E_0), a proof stress, and a parameter n that defines the sharpness of the knee of the stress-strain curve. If the proof stress is chosen as the 0.2% proof stress ($\sigma_{0.2}$), the Ramberg-Osgood function takes the form (Bezkorovainy et al, 2003)

$$\varepsilon = \frac{\sigma}{E_0} + 0.002 \left(\frac{\sigma}{\sigma_{0.2}} \right)^n \quad (6.1)$$

The proportionality stress for such metals is defined as the 0.01% proof stress ($\sigma_{0.01}$). Thus the parameter n can be defined as:

$$n = \frac{\ln(20)}{\ln(\sigma_{0.2} / \sigma_{0.01})} \quad (6.2)$$

Thus it is possible to define the strength of a plate which depends on the stress-strain curve in terms of the Ramberg-Osgood parameters (E_0 , n , $\sigma_{0.2}$) as the stress-strain curve can be defined in terms of the Ramberg-Osgood parameters. Based on this approach, Rasmussen and Rondall (1997a) developed equations for the strength of metal columns, which was later modified design curves for stainless steel (Rasmussen and Rondal, 1997b) and aluminum columns (Rasmussen and Rondal,2000).

The study of Bezkorovainy et al (2003) is based on a similar study of Rasmussen and Rondall (1997a) for uniformly compressed metal plates simply supported along four edges. Bezkorovainy et al (2002) have first performed FE analysis to obtain strength curves for large number Ramberg-Osgood parameters. The FE model produced agreement with tests on stainless steel plates to within a few percent. The FE model can therefore be expected to be accurate. The width of the plate was 100 mm in all analyses, while the thickness was varied to produce a set of predetermined plate slenderness values,

$$\lambda = \sqrt{\frac{\sigma_{0.2}}{\sigma_{cr}}} \quad (6.3)$$

Where σ_{cr} = elastic critical stress

$$\sigma_{cr} = \frac{4\pi^2 E_0 \tau}{12(1-\nu^2)} \left(\frac{t}{b}\right)^2 \quad (6.4)$$

Strength curves were determined for all (n,e) -permutations of the n - and e -values given in Table 6.1 where e is defined as:

$$e = \frac{\sigma_{0.2}}{E_0} \quad (6.5)$$

For each (n,e) -combination, the plate strength was determined for the slenderness values, $\lambda = 0.5, 0.75, 1, 1.25, 1.5, 2, 2.5, 3$ given in Table 6.1.

The plate strength (s) is given as the average ultimate stress (σ_u) nondimensionalised with respect to the 0.2% proof stress ($\sigma_{0.2}$), where the ultimate stress is the maximum load obtained in the FE analysis divided by the cross-sectional area. S is expressed as:

$$S = \sigma_u / \sigma_{0.2} \quad (6.6)$$

Having obtained plate strength curves for a wide range of n - and e -values, Bezkorovainy et al (2002) derived analytical approximations to these curves i.e., a nondimensional plate strength (χ) by adopting a generalized Winter-curve given in the following form:

$$\chi = (\alpha/\lambda) - (\beta/\lambda^2) \quad (6.7)$$

Where λ is the plate slenderness and α and β are calculated functions of the Ramberg-Osgood parameters derived by Bezkorovainy et al (2002) given as follows:

$$\alpha = \begin{cases} 0.92 + 0.07 \tanh\left(\frac{n-3}{2.1}\right) - (0.026 \exp[-0.55(n-3)] + 0.019)(6 - 2000e) & 3 \leq n \leq 10 \quad (6.8) \\ \alpha_{10} + (1 - \alpha_{10}) \frac{n-10}{90} & 10 < n \leq 100 \quad (6.9) \end{cases}$$

$$\beta = \begin{cases} 0.18 + 0.045 \tanh\left(\frac{n-3}{2.5}\right) - (0.01 \exp[-1.6(n-3)] + 0.005)(6 - 2000e) & 3 \leq n \leq 10 \quad (6.10) \\ \beta_{10} + (0.22 - \beta_{10}) \frac{n-10}{90} & 10 \leq n \leq 100 \quad (6.11) \end{cases}$$

Table 6.1 Values of (S/λ) for complete set of Finite Element analyses.

λ	e=0.001				e=0.0015				e=0.002				e=0.0025				e=0.003			
	n=3	n=5	n=10	n=100	n=3	n=5	n=10	n=100	n=3	n=5	n=10	n=100	n=3	n=5	n=10	n=100	n=3	n=5	n=10	n=100
0.5	0.97	1.01	0.98	0.98	1.00	1.04	1.00	0.99	0.99	1.01	1.02	0.99	0.98	0.99	1.02	1.00	0.95	0.97	1.02	1.01
0.75	0.98	0.97	0.98	1.00	1.04	1.01	1.00	1.00	1.05	1.01	1.00	1.01	1.04	1.00	1.00	1.01	1.03	1.00	1.00	1.02
1	0.94	0.93	0.99	1.04	1.00	0.95	0.99	1.04	1.00	0.96	0.99	1.03	1.00	0.96	0.99	1.04	0.98	0.96	0.98	1.04
1.25	0.96	0.909	0.98	1.00	1.00	0.95	0.97	0.99	1.01	0.95	0.96	1.00	0.98	0.95	0.96	1.01	0.98	0.95	0.95	1.01
1.5	0.98	0.913	0.97	0.99	1.02	0.95	0.97	0.99	1.02	0.96	0.97	0.99	1.01	0.97	0.97	0.99	0.98	0.95	0.96	1.01
2	1.03	0.94	1.00	1.01	1.06	0.99	1.01	1.01	1.06	1.00	1.01	1.00	1.05	0.99	1.00	1.03	1.02	0.99	1.00	1.04
2.5	1.07	0.97	1.02	1.02	1.12	1.04	1.02	1.03	1.09	1.03	1.03	1.06	1.13	1.06	1.04	1.03	1.09	1.05	1.03	1.06
3	1.08	1.01	1.06	1.06	1.13	1.04	1.06	1.06	1.07	1.03	1.05	1.00	1.09	1.04	1.03	1.08	1.06	1.02	1.04	1.06

Table 6.2 FE results for $(\frac{\sigma_u}{\sigma_{0.2}})$

λ	e=0.001				e=0.0015				e=0.002				e=0.0025				e=0.003			
	n=3	n=5	n=10	n=100	n=3	n=5	n=10	n=100	n=3	n=5	n=10	n=100	n=3	n=5	n=10	n=100	n=3	n=5	n=10	n=100
0.500	0.970	1.118	1.083	0.976	0.971	1.110	1.082	0.967	0.934	1.041	1.081	0.950	0.899	0.986	1.060	0.942	0.848	0.935	1.039	0.935
0.750	1.267	1.237	1.214	1.174	1.289	1.245	1.213	1.151	1.250	1.204	1.188	1.140	1.191	1.155	1.164	1.118	1.136	1.120	1.141	1.108
1.000	1.516	1.417	1.451	1.471	1.539	1.400	1.421	1.442	1.471	1.370	1.392	1.400	1.409	1.328	1.364	1.386	1.324	1.288	1.324	1.359
1.250	1.863	1.629	1.683	1.672	1.846	1.648	1.631	1.621	1.778	1.596	1.581	1.605	1.649	1.548	1.549	1.589	1.579	1.502	1.503	1.559
1.500	2.227	1.890	1.918	1.916	2.201	1.903	1.878	1.877	2.096	1.863	1.839	1.839	1.980	1.826	1.802	1.803	1.838	1.736	1.749	1.804
2.000	3.029	2.478	2.510	2.496	2.955	2.526	2.482	2.445	2.808	2.473	2.431	2.372	2.650	2.375	2.358	2.394	2.458	2.306	2.312	2.371
2.500	3.866	3.112	3.111	3.073	3.830	3.231	3.045	3.039	3.539	3.101	3.012	3.064	3.492	3.097	2.980	2.918	3.213	2.979	2.893	2.945
3.000	4.629	3.821	3.808	3.771	4.581	3.810	3.728	3.692	4.115	3.658	3.617	3.413	3.988	3.584	3.477	3.612	3.698	3.414	3.441	3.476

6.2.1.4 Numerical application

The main focus of this study is to obtain closed-form solutions of plate strength given schematically in Fig. 6.1 by means of NNs. Data needed for the training process is obtained from Bezkorovainy et al (2002) who have performed a wide range of FE analysis on plate strength in terms of e , n , and λ and have compared these FE results with the results of analytical equation they have derived given in Equations 6.8-6.11. They have presented the (S / χ) values in table 6.1. Thus to obtain the FE results, Equations 6.8-6.11 have been used to find the nondimensional χ values and in return the FE results have been obtained from Table 6.1. This study is based on the soft computing modeling of these FE results given in Table 6.2. Among the FE results, a number of cases have been randomly selected as test and training sets.

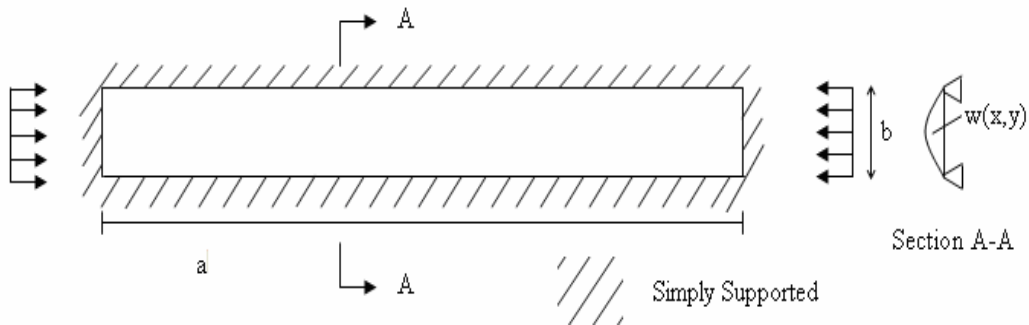


Fig 6.1 Buckling of rectangular plate under uniform compression (traction)
(Bezkorovainy,2003)

6.2.1.5 Results of NN models

The optimal NN architecture in this part was found to be 5-3-1 NN architecture with logistic sigmoid transfer function (logsig). The training algorithm was quasi-Newton back propagation (BFGS). The optimum NN model is given in Figure 6.2. Statistical parameters of learning and training sets of NN model are presented in Table 5.3. The % errors and Prediction of NN and actual values of learning and testing sets and their corresponding correlation are given in Figures 6.3-6.6. The overall comparison of the

proposed NN model results with FE results and results obtained from Equations 6.8-6.11 is given in Table A.1. The overall accuracy and correlation of NN models are quite satisfactory compared to FE results.

Table 6.3 Statistical parameters of the proposed NN models

	MSE	RMSE	SSE	MAPE (%)
NN Train Set	0.0015	0.039	0.224	1.65
NN Test Set	0.0116	0.108	0.163	3.22

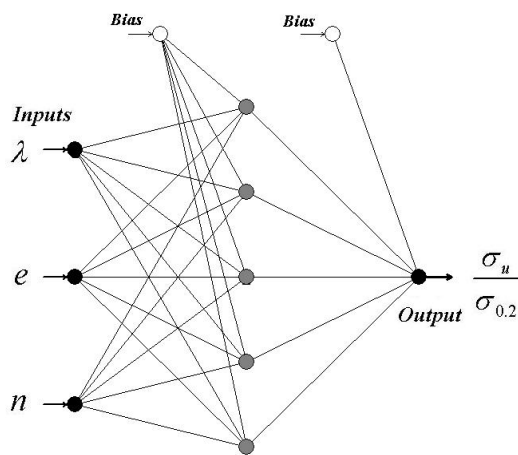


Fig 6.2 Proposed NN model for the prediction of σ_u

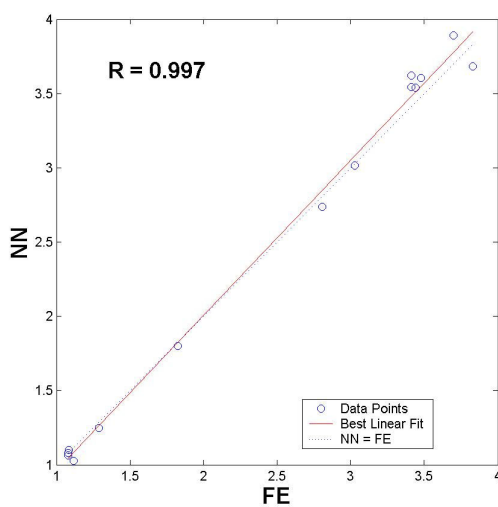


Fig 6.3 Performance of NN model for test set

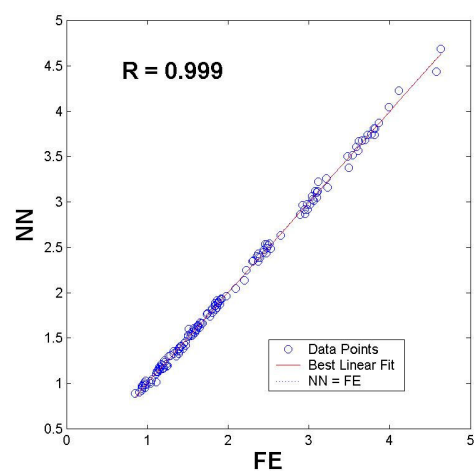


Fig 6.4 Performance of NN model for training set

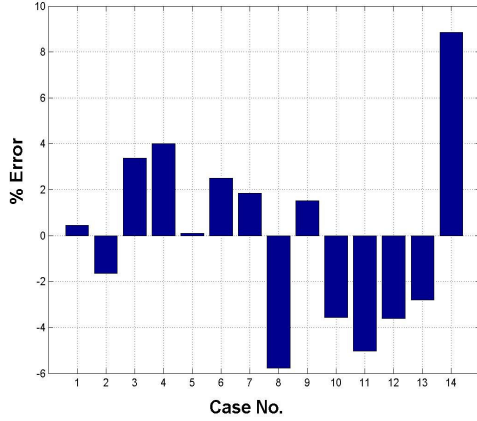


Fig 6.5. % Error for test set

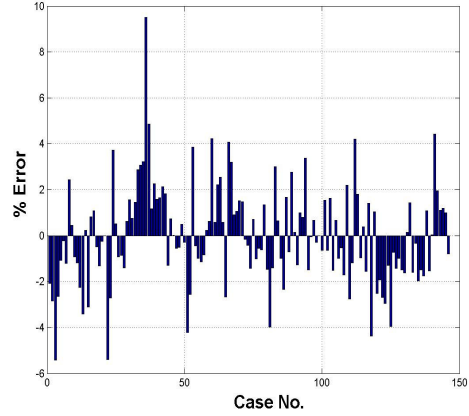


Fig 6.6 % Error for training set

6.2.1.6 Explicit Formulation of NN Models

The explicit formulation for the proposed NN model is obtained by using the well trained NN parameters which are biases, and weights for the input and hidden layer and the normalization factors both for inputs and output proposed NN model. Related weights in the derivations of NN based formulations are given in Tables 6.4. Each input is multiplied by a connection weight. Thus the main focus is to obtain the explicit formulation as follows:

$$\frac{\sigma_u}{\sigma_{0.2}} = f(\lambda, e, n) \quad (6.12)$$

Revisiting Eqn 5.1
$$u_i = \sum_{j=1}^H w_{ij} x_j + b_i$$

Where each input is multiplied by its corresponding weight and its bias is added. w_{ij} is the weight matrix of the first hidden layer in Table 6.4.

Table 6.4 Weights between inputs and hidden layer

Weights	Number of hidden layer neurons (<i>i</i>)				
	1	2	3	4	5
$w1i$	1.3448	-1.3696	-2.2788	2.6218	-0.5745
$w2i$	-2.9353	-3.2153	-6.0831	-6.4065	7.6174
$w3i$	6.2338	-5.5639	1.4444	1.8013	4.4988

and X_j is the corresponding parameter vector given as

$\mathbf{X} = [\lambda, e, n]$ where

b_i is the bias matrix to the first hidden layer given as

$$\mathbf{b} = [221.3 \quad -4.37 \quad -5.42 \quad -2.82 \quad -2.85]$$

The summation u_i is transformed using a scalar-to-scalar function called an "activation or transfer function", $F(u_i)$ yielding a value called the unit's "activation".

$$Y_i = f(u_i)$$

Following the steps above leads to:

$$u_1 = (-222.8 * \lambda) + (-18.6 * e) + (-306.3 * n) + 221.3$$

$$u_2 = (-1.73 * \lambda) + (1.38 * e) + (332.1 * n) - 4.37$$

$$u_3 = (-1.8 * \lambda) + (0.19 * e) + (0.08 * n) - 5.42$$

$$u_4 = (-6.44 * \lambda) + (-0.56 * e) + (-73.8 * n) - 2.82$$

$$u_5 = (-4.74 * \lambda) + (0.20 * e) + (-0.55 * n) - 2.85$$

The activation function used in this study is logistic transfer function (logsig)

$$f(u_i) = \left(\frac{1}{1 + e^{-u_i}} \right) \text{ performed for each hidden node in the first hidden layer}$$

Thus the output is

$$O = 1 / (1 + \exp - (\sum (w2_i * f(u_i)) + b2))$$

Where $w2_i$ is the weight vector to the output layer given as

$$w2_i = [0.028 \quad -13.37 \quad -16.92 \quad -34.49 \quad -0.33]$$

and $b2$ is the bias added which is

$$b2 = 30.7$$

It should be noted that the inputs entering the network have been normalized before the training as

$$\lambda^* = \lambda / 3 \quad e^* = e / 0.003 \quad n^* = n / 100$$

These steps given so far may seem to be too complex particularly for those who do not have a neural network background. The same steps can be given in a simpler form as follows:

$$\frac{\sigma_u}{\sigma_{0.2}} = f(\lambda, e, n)$$

$$\frac{\sigma_u}{\sigma_{0.2}} = 5 * \left(\frac{1}{1 + e^{-W}} \right)$$

Where W=

$$(0.028) * \left(\frac{1}{1 + e^{-U1}} \right) + (-13.37) * \left(\frac{1}{1 + e^{-U2}} \right) + (-19.92) * \left(\frac{1}{1 + e^{-U3}} \right) + (-34.49) * \left(\frac{1}{1 + e^{-U4}} \right) + (-0.33) * \left(\frac{1}{1 + e^{-U5}} \right) + 30.7$$

$$U1 = (-74.25 * \lambda) + (-621.4 * e) + (-3.063 * n) + 221.3$$

$$U2 = (-0.576 * \lambda) + (45.9 * e) + (3.32 * n) - 4.37$$

$$U3 = (-0.6 * \lambda) + (6.37 * e) + (0.0008 * n) - 5.42$$

$$U4 = (-2.148 * \lambda) + (-18.6 * e) + (-0.738 * n) - 2.82$$

$$U5 = (-1.58 * \lambda) + (6.74 * e) + (-0.0055 * n) - 2.85$$

It should be noted that the proposed explicit formulation of the NN models presented above are valid only for the ranges of training set.

6.2.1.7 Conclusion

This case study presents an alternative NN based approach for the prediction of nondimensional ultimate strength of metal plates in compression with non-linear mechanical properties. The proposed NN model is based on well-defined FE results of nondimensional ultimate strength of metal plates in compression with non-linear mechanical properties from literature. The ultimate plate strength is obtained in terms of λ , e , n being plate slenderness ratio, $\frac{\sigma_{0.2}}{E_0}$ and Ramberg Osgood parameter.

The closed-form solutions are also presented for the NN models. The results of the

proposed NN model are quite satisfactory compared to FE results. A very high accuracy and a perfect correlation which are better than existing analytical formulations has been obtained for the NN model since a new optimum NN selection algorithm has been used for the selection of optimum NN architecture. This study presents the robustness NNs for the explicit formulation and analysis of various engineering problems where it is difficult to obtain an analytic expression from experimental and numerical results.

6.2.2 Explicit Formulation of Elastoplastic Bending By Neural Networks

6.2.2.1 Introduction

In this study, an application of Neural Networks on nonlinear mechanics problems is presented by the neurocomputation of the elastoplastic analysis of a cantilever beam based on Back Propagation Artificial Neural Networks (BPNN). BPNN is proposed as a tool for analysis and formulation of the elastoplastic behaviour of the cantilever beam in the plastic range. The training patterns for BPNNs are prepared by ANSYS. All necessary processes for neural networks are conducted using MATLAB tools. Explicit formulations for maximum plastic deflection and maximum plastic normal stresses are obtained by using the parameters of the trained NNs. It is shown that there is a good agreement with the neurocomputed results, explicit formulation and those of theoretical analyzed solution of the elastoplastic problem. Parametric case studies are performed to show the generalization capability of the trained NNs. Thus, this study aims to open the Neural Networks' Black box and to present a pioneering work in this field.

The maximum plastic deflection and normal stress for a uniformly loaded cantilever beam are formulated explicitly by utilizing trained NN parameters.

Assuming $\delta s \approx \rho \delta \theta$ and $\rho = ds/d\theta$ given in Fig 6.7

The 'curvature' of the beam, κ , is given as:

$$\kappa = \frac{1}{\rho} = \frac{d\theta}{ds} \quad (6.13)$$

where

$$K = \begin{cases} M/EI & \text{(elastic range)} \\ f(M) & \text{(elastoplastic) range} \end{cases} \quad (6.14)$$

$$K = \begin{cases} M/EI & \text{(elastic range)} \\ f(M) & \text{(elastoplastic) range} \end{cases} \quad (6.15)$$

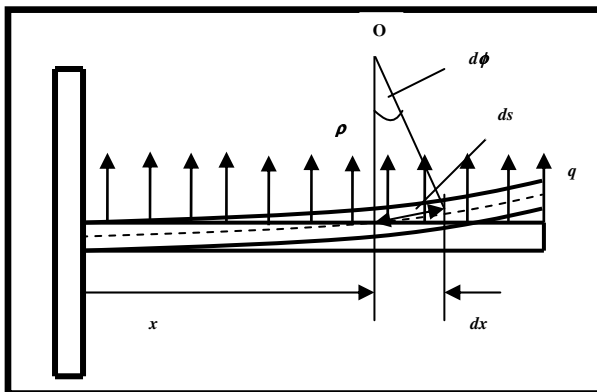


Fig 6.7 Moment-Curvature relationship

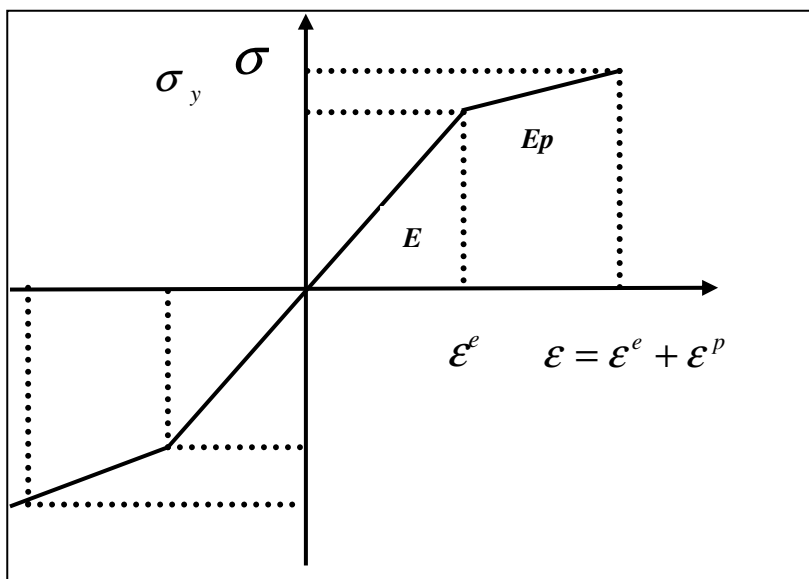


Fig 6.8. Bilinear strain hardening material model

6.2.2.2 Numerical application

The training patterns for NNs have been obtained by ANSYS. The cantilever beam cross section is rectangular with unit thickness and it is uniformly distributed loaded (Fig 6.7). A Bilinear strain hardening material model (Fig 6.8) with a strain hardening parameter $\chi = E_p/E = 0.1$ is chosen where, E_p , E being the plastic tangential modulus and the elasticity modulus respectively. The maximum plastic deflection δ_{\max} and maximum plastic Von Mises stresses $\sigma_{V\max}$ are obtained. The variables taken are $E \in [210\text{GPa}, 30\text{GPa}]$, $\sigma_y \in [350\text{MPa}, 50\text{MPa}]$ and the plastic load ratio $L_r \in [1, 10]$ being a dimensionless parameter. To generalize the training case, $L_r = q/q_y$ is taken where q and q_y being the uniformly distributed load applied and uniformly distributed yield load to reach yield stress respectively. The calculations are done for the case where $L/H=10$.

Afterwards, a simple relationship between different L/H ratios for the maximum plastic deflection and maximum plastic normal stress are derived which enabled the explicit formulation to be generalized for all cases i.e. for various L/H values. A wide range of variables are chosen to represent a general model for NN with a data set of 348 training patterns and 65 testing patterns. All necessary neural procedures are performed by MATLAB NN Toolbox. The optimal network architectures for both cases are given in Figures 6.9a and 6.9b with hyperbolic sigmoidal transfer function and the learning algorithm used is Levenberg–Marquardt (LM) learning algorithms for both cases. The training test set errors for maximum plastic deflection and maximum plastic Von Mises stress are given in figures 6.10-6.17 for both cases. As seen, the errors are quite satisfactory for each case for test set and training sets. Results of the network training show a perfect match between target output and the NN output. Other statistical parameters are presented in Table 6.5.

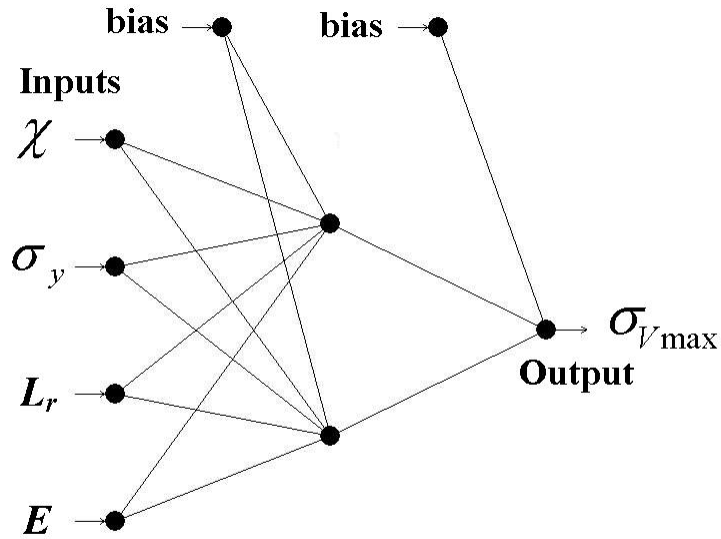


Fig 6.9a Optimum NN model for $\sigma_{V\max}$

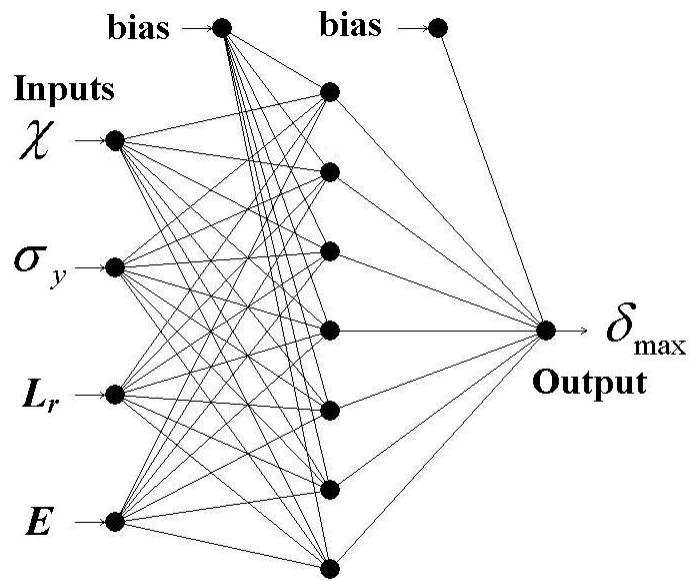


Fig 6.9b Optimum NN model for δ_{\max}

Table 6.5 Statistical parameters of the NN used for δ_{\max} and $\sigma_{V\max}$

	MSE	RMSE	SSE	MAPE (%)
NN Train Set (δ_{\max})	7.82E-06	0.002797	0.002652	5.929
NN Test Set (δ_{\max})	5.32E-05	0.007293	0.003404	6.860
NN Train Set ($\sigma_{V\max}$)	56.734	7.5322	19573	1.295
NN Test Set ($\sigma_{V\max}$)	272.42	16.505	17707	4.451

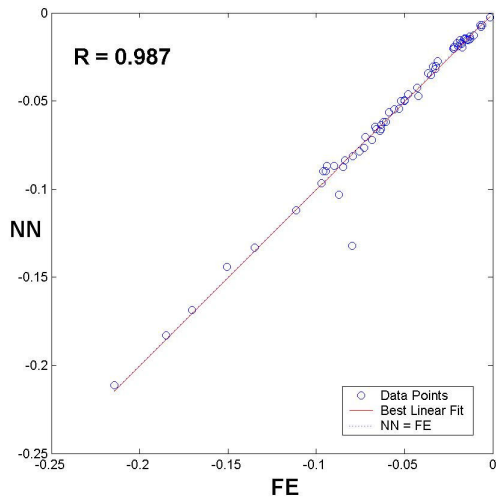


Fig 6.10 Performance of NN model for test set (δ_{\max})

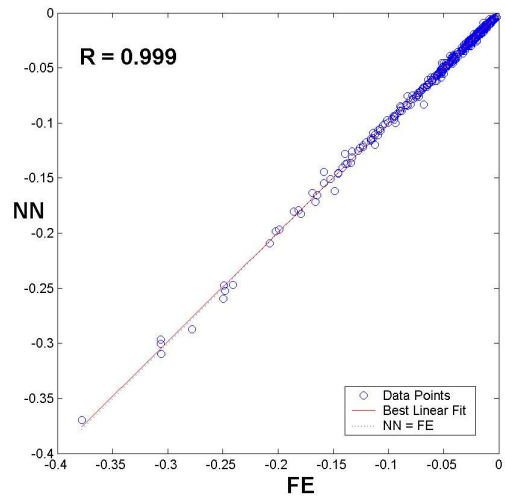


Fig 6.11 Performance of NN model for training set (δ_{\max})

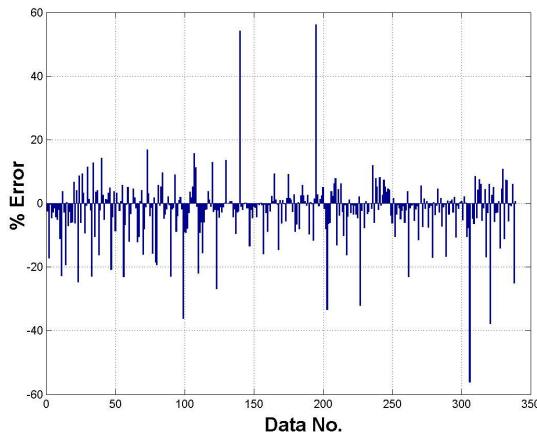


Fig 6.12. % Error for training set (δ_{\max})

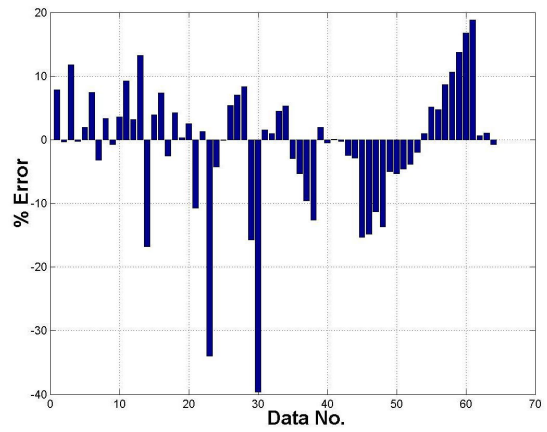


Fig 6.13 % Error for test set (δ_{\max})

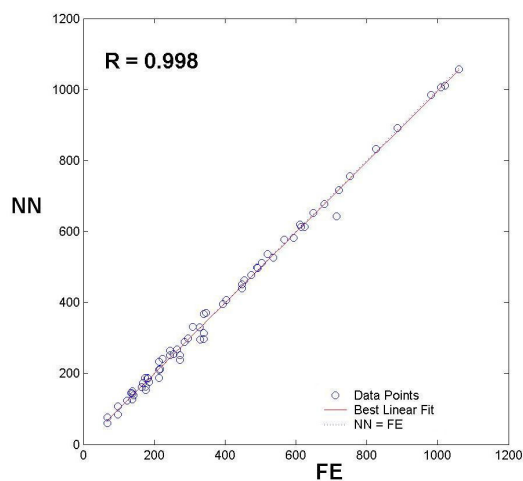


Fig 6.14 Performance of NN model for test set ($\sigma_{V\max}$)

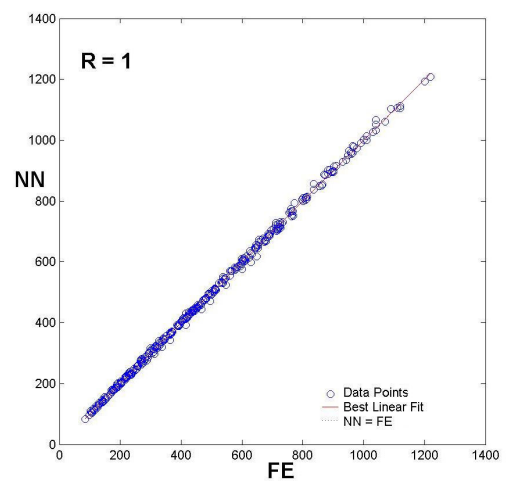


Fig 6.15 Performance of NN model for training set ($\sigma_{V\max}$)

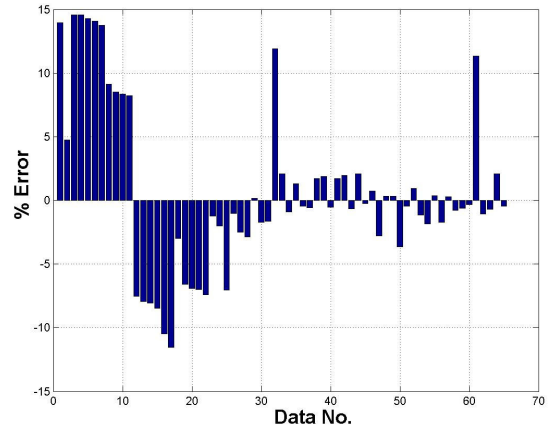
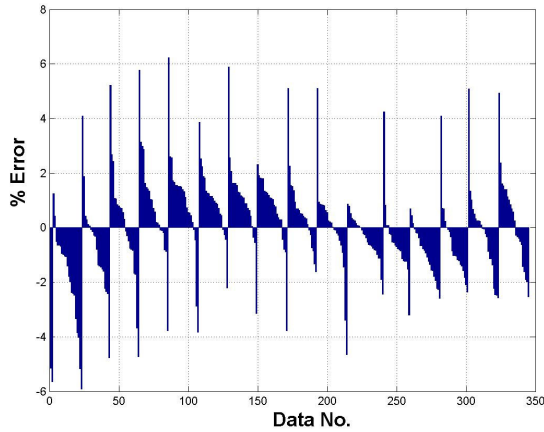


Fig 6.16 % Error for training set (σ_{Vmax}) Fig 6.17 % Error for test set (σ_{Vmax})

6.2.2.3 Explicit formulation of NN models

The trained NN in this case, does not serve as a black box subroutine of a computer program for the calculation of a step like hybrid ANN/FE applications anymore. It is itself an independent program to compute maximum plastic deflection and maximum plastic normal stress for a given set of E, σ_y, L_r and L/H values as shown in Figures 6.18-6.19.

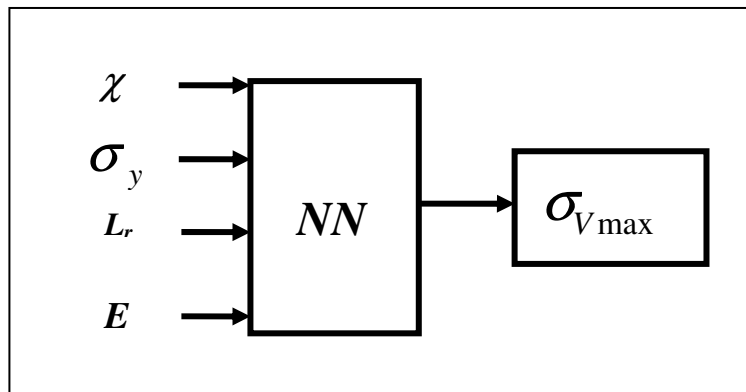


Fig 6.18 NN model for maximum plastic Von Mises stress

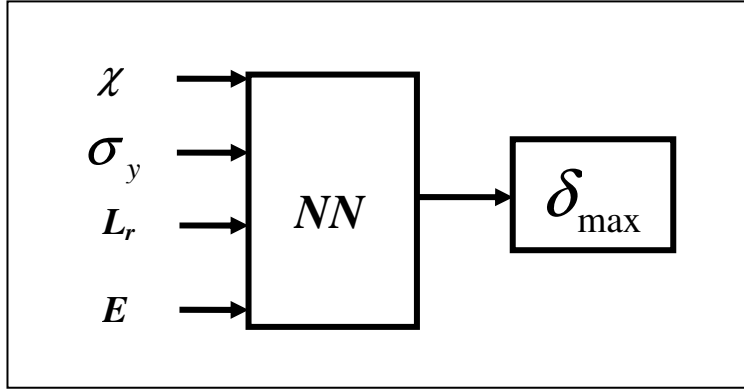


Fig 6.19 NN model for maximum plastic deflection

Furthermore, it is actually an explicit formulation that computes directly maximum plastic deflection, δ_{\max} and maximum plastic Von Mises stress $\sigma_{V\max}$ given as

$$\delta_{\max} = f(\chi, \sigma_y, E, L_r)$$

$$\sigma_{V\max} = f(\chi, \sigma_y, E, L_r)$$

The explicit formulation of maximum plastic Von Mises stress $\sigma_{V\max}$ obtained by the same way following the same steps in the previous case study and using the weights of the corresponding trained NN. The same steps can be given in a simpler form as follows:

$$\sigma_{V\max} = 1500 * \left(\frac{2}{1 + e^{-2W}} - 1 \right)$$

$$\text{Where } W = (-3.3) * \left(\frac{2}{1 + e^{-2U_1}} - 1 \right) + (2.6) * \left(\frac{2}{1 + e^{-2U_2}} - 1 \right) - 0.713$$

$$U_1 = (0.27 * \chi) + (-0.0006 * \sigma_y) + (0.00002 * E) + (0.26 * L_r) - 1.76$$

$$U_2 = (0.31 * \chi) + (0.00045 * \sigma_y) + (-0.00001 * E) + (0.28 * L_r) - 1.7$$

Following the same steps can be for δ_{\max} given as follows leads to:

$$\delta_{\max} = \left(\frac{2}{1 + e^{-2W}} - 1 \right)$$

$$\text{Where } W = (-2.4) * \left(\frac{2}{1 + e^{-2U_1}} - 1 \right) + (-2.99) * \left(\frac{2}{1 + e^{-2U_2}} - 1 \right) + (6.73) * \left(\frac{2}{1 + e^{-2U_3}} - 1 \right) +$$

$$(0.35)*\left(\frac{2}{1+e^{-2U_4}}-1\right) + (3.0)*\left(\frac{2}{1+e^{-2U_5}}-1\right) + (-0.065)*\left(\frac{2}{1+e^{-2U_6}}-1\right) + (4.5)*\left(\frac{2}{1+e^{-2U_7}}-1\right) - 4.35$$

$$U1= (0.86 * \chi) + (0.002 * \sigma_y) + (-0.014 * E) + (0.26* L_r) - 2.31$$

$$U2= (81.36* \chi) + (-0.066* \sigma_y) + (-0.047 * E) + (-5.35* L_r) + 37.3$$

$$U3= (5.3 * \chi) + (-0.002 * \sigma_y) + (0.007 * E) + (-0.2* L_r) + 2.17$$

$$U4= (-0.99* \chi) + (-0.003* \sigma_y) + (-0.005 * E) + (0.33* L_r) - 1.51$$

$$U5= (79 * \chi) + (-0.06 * \sigma_y) + (-0.05 * E) + (-5.2* L_r) + 36.25$$

$$U6= (-1.2* \chi) + (0.002* \sigma_y) + (-0.004 * E) + (0.41* L_r) - 1.03$$

$$U7= (-4.2* \chi) + (0.002 * \sigma_y) + (-0.007 * E) + (0.033* L_r) - 1.67$$

The NN results for the test sets for both cases are given in Tables 6.6 and 6.7 respectively.

Table 6.6 NN vs ANSYS for test set ($\sigma_{V_{max}}$)

χ	σ_y (MPa)	E(GPa)	L_r	NN (MPa)	ANSYS (MPa)
0.1	70	210	0.87	59.06	67.30
0.35	180	90	0.87	176.64	185.00
0.1	180	210	0.87	153.62	176.00
0.1	350	150	0.87	296.81	340.00
0.1	280	210	0.87	238.01	272.00
0.1	220	130	0.87	187.59	214.00
0.1	100	130	0.87	84.92	96.60
0.2	140	190	0.87	126.45	138.00
0.2	350	130	0.87	313.28	340.00
0.2	180	110	0.87	162.41	176.00
0.2	280	190	0.87	251.33	272.00
0.5	350	170	0.87	367.73	340.00
0.5	250	70	0.87	265.09	244.00
0.5	140	70	0.87	150.13	138.00
0.5	220	150	0.87	233.82	214.00
0.5	100	150	0.87	107.92	96.60
0.5	70	190	0.87	76.07	67.30
0.35	140	70	1.37	172.15	167.00
0.5	280	130	1.37	371.40	347.00
0.5	140	210	1.37	188.04	175.00
0.5	250	210	1.37	332.20	309.00
0.5	180	130	1.37	240.79	223.00

Table 6.6 Cont'd

0.2	220	70	1.53	268.29	265.00
0.35	140	210	1.53	185.69	182.00
0.5	100	190	1.53	145.22	135.00
0.2	220	210	1.70	289.00	286.00
0.35	100	190	1.70	142.54	139.00
0.5	350	110	1.70	535.35	520.00
0.2	180	190	1.87	254.62	255.00
0.5	280	70	1.87	463.02	455.00
0.5	310	90	1.87	511.27	503.00
0.1	220	210	1.87	294.86	330.00
0.2	140	170	2.03	212.55	217.00
0.5	280	210	2.03	496.43	492.00
0.2	100	150	2.20	161.89	164.00
0.35	70	170	2.20	123.54	123.00
0.5	250	190	2.20	476.64	474.00
0.2	250	90	2.37	439.52	447.00
0.2	350	150	2.37	612.50	624.00
0.5	220	170	2.37	450.43	448.00
0.2	280	110	2.53	526.97	536.00
0.2	310	130	2.53	582.53	594.00
0.5	180	150	2.53	395.62	393.00
0.2	70	130	2.70	138.09	141.00
0.5	140	130	2.70	329.80	329.00
0.1	350	110	2.87	715.83	721.00
0.5	100	110	2.87	252.01	245.00
0.1	280	70	3.03	612.91	615.00
0.1	310	90	3.03	677.68	680.00
0.5	70	90	3.03	187.87	181.00
0.1	280	210	3.20	652.02	649.00
0.5	350	70	3.37	1010.50	1020.00
0.1	250	190	3.37	619.14	612.00
0.1	220	170	3.53	577.55	567.00
0.35	350	70	3.53	1006.20	1010.00
0.1	180	150	3.70	498.66	490.00
0.35	350	210	3.70	1056.80	1060.00
0.1	140	130	3.87	406.12	403.00
0.35	280	170	3.87	891.41	886.00
0.35	310	190	3.87	984.35	981.00
0.1	220	210	3.87	642.20	715.00
0.1	100	110	4.03	299.23	296.00
0.35	250	150	4.03	831.95	826.00
0.1	70	90	4.17	209.62	214.00
0.35	220	130	4.17	755.49	752.00

Table 6.7 NN vs ANSYS for test set (δ_{\max})

χ	σ_y (MPa)	E(GPa)	L_r	NN (m)	ANSYS (m)
0.5	310	210	2.700	-0.026	-0.030
0.5	310	190	1.533	-0.015	-0.016
0.5	310	190	3.700	-0.050	-0.050
0.5	310	170	2.533	-0.030	-0.034
0.5	310	150	1.367	-0.017	-0.017
0.5	310	150	3.367	-0.055	-0.056
0.5	310	130	2.200	-0.034	-0.037
0.5	310	130	4.167	-0.087	-0.085
0.5	310	110	3.033	-0.064	-0.067
0.5	310	90	3.867	-0.112	-0.111
0.5	310	70	2.700	-0.087	-0.090
0.5	350	210	1.533	-0.015	-0.016
0.5	350	210	3.533	-0.046	-0.048
0.5	350	190	2.367	-0.028	-0.031
0.5	350	170	0.867	-0.013	-0.011
0.5	350	170	3.200	-0.050	-0.052
0.5	350	150	2.033	-0.030	-0.032
0.5	350	150	4.033	-0.081	-0.079
0.5	350	130	2.867	-0.057	-0.059
0.5	350	110	3.700	-0.097	-0.097
0.5	350	90	2.533	-0.071	-0.072
0.5	350	70	1.367	-0.047	-0.042
0.5	350	70	3.367	-0.133	-0.135
0.1	70	210	0.867	-0.003	-0.002
0.1	70	90	4.167	-0.079	-0.075
0.1	100	110	4.033	-0.084	-0.084
0.1	140	130	3.867	-0.090	-0.095
0.1	180	150	3.700	-0.090	-0.096
0.1	220	170	3.533	-0.087	-0.094
0.1	250	190	3.367	-0.103	-0.087
0.1	280	210	3.200	-0.132	-0.080
0.1	280	70	3.033	-0.211	-0.214
0.1	310	90	3.033	-0.183	-0.185
0.1	350	110	2.867	-0.144	-0.151
0.2	70	130	2.700	-0.015	-0.015
0.2	100	150	2.200	-0.013	-0.013
0.2	140	170	2.033	-0.015	-0.014
0.2	180	190	1.867	-0.015	-0.014
0.2	220	210	1.700	-0.015	-0.013
0.2	220	70	1.533	-0.032	-0.033
0.2	250	90	2.367	-0.064	-0.063
0.2	280	110	2.533	-0.066	-0.066
0.2	310	130	2.533	-0.062	-0.062
0.2	350	150	2.367	-0.054	-0.053
0.35	70	170	2.200	-0.007	-0.007
0.35	100	190	1.700	-0.007	-0.006
0.35	140	210	1.533	-0.008	-0.007
0.35	140	70	1.367	-0.020	-0.017

Table 6.6 Cont'd

0.35	180	90	0.867	-0.013	-0.011
0.35	220	130	4.167	-0.077	-0.073
0.35	250	150	4.033	-0.072	-0.068
0.35	280	170	3.867	-0.067	-0.064
0.35	310	190	3.867	-0.066	-0.063
0.35	350	210	3.700	-0.062	-0.061
0.35	350	70	3.533	-0.169	-0.170
0.5	70	90	3.033	-0.017	-0.018
0.5	100	110	2.867	-0.019	-0.020
0.5	140	130	2.700	-0.020	-0.022
0.5	180	150	2.533	-0.020	-0.022
0.5	220	170	2.367	-0.019	-0.022
0.5	250	190	2.200	-0.017	-0.020
0.5	280	210	2.033	-0.016	-0.019
0.5	280	70	1.867	-0.049	-0.050
0.5	310	90	1.867	-0.042	-0.043
0.5	350	110	1.700	-0.035	-0.035

6.2.2.4 Conclusion

This case study proposes a novel approach of explicit formulation for elastoplastic analysis of structures by NNs. However, Neural Networks are often treated as "black box" modeling tools; they can be explicitly formulated as carried out in this study. A simple uniformly loaded cantilever beam problem is chosen as a case study with bilinear isotropic hardening. The aim is to find the explicit formulation of maximum von Mises stress and maximum plastic deflection by NNs. Results of the network training show that there is a perfect match between target output and the NN output both for maximum von Mises stress and maximum plastic deflection. Thus, novel explicit formulations of the problem are derived for the maximum normal stress and maximum plastic deflection by using the weights of the trained NNs.

6.2.3 Prediction of Web Crippling Strength of Cold-Formed Steel Sheetings Using Neural Networks

6.2.3.1 Introduction

This section considers the use of neural networks to predict the web crippling strength of cold-formed steel decks. Web crippling is critical for slender webs as in the case of trapezoidal sheetings which are widely used in roofing applications. The elasto-plastic behaviour of web crippling is quite complex and difficult to handle. There is no well established analytical solution due to complex plastic behaviour. This leads to significant errors in various design codes. The objective of this study is to provide a fast and accurate method of predicting the web crippling strength of cold-formed steel sheetings and to introduce this in a closed-form solution which has not been obtained so far. The training and testing patterns of the proposed NN are based on well established experimental results from literature. The trained NN results are compared with the experimental results and current design codes (NAS 2001) and found to be considerably more accurate. Moreover, a trained neural network gives the results significantly more quickly than the design codes and FE models. The web crippling strength is also introduced in closed-form solution based on the parameters of the trained NN. Extensive parametric studies are also performed and presented graphically to examine the effect of geometric and mechanical properties on web crippling strength.

Structural steel is mainly used in two forms as hot-rolled and cold-formed. Hot-rolled members are more widely used than cold-formed steel members but cold-formed steel members have various advantages such as: high strength/weight ratio, ease of transportation and construction, mass production, and faster installation. Thus the use of cold-formed steel members may enable a more economic design than hot-rolled steel structural members.

In spite of the fact that use of cold-formed steel members go back to 1850s, it has not found an extensive application until 1940s. The flexibility in usage, size and shape of cold-formed steel members enabled them to be effectively and increasingly used in

almost every structural application throughout 1980s and 1990s. This extensive and increasing use necessitates comprehensive research in this field. Detailed information can be found in Yu (2000) and Hancock (2001).

Web crippling is a significant failure type for cold-formed steel members which is a form of localized buckling that occurs at points of transverse concentrated loading and supports. In general cold-formed steel members are unstiffened against transverse loading which leads to web crippling or so called web crushing as in the case of sheetings shown in Fig 1. Cold formed members are more susceptible to web crippling than hot-rolled sections as their depth-to-thickness ratios of the webs are higher and the webs are inclined rather than vertical. Moreover the load acting eccentric to the web causes initial bending in the web even before crippling takes place (Fig. 6.20).

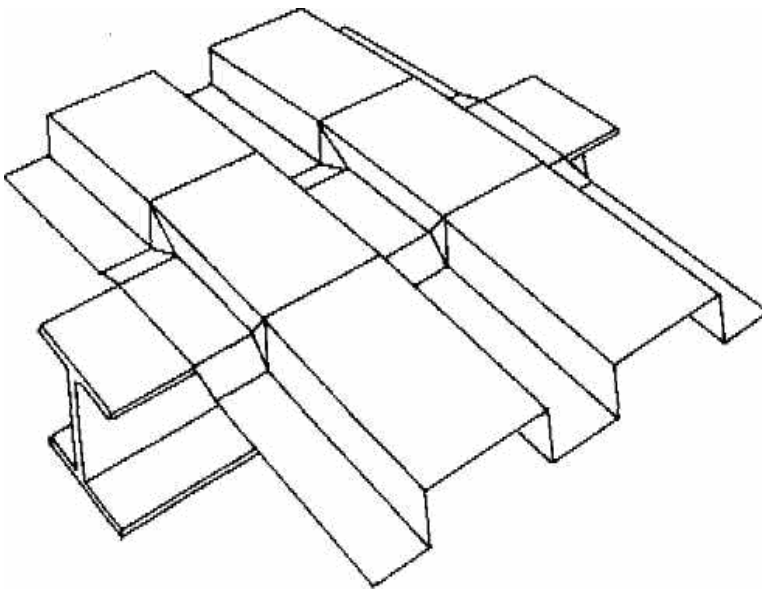


Fig 6.20 Web crippling of thin-walled cold-formed steel members (Reinsch, 1983)

The theoretical analysis of web crippling of sheetings is cumbersome due to various factors such as initial imperfection of web element which affects web buckling, local yielding in the region of load application, instability of the web element which leads to a complex elastoplastic behaviour of the member. This difficulty in theoretical based analysis leads research in this field to be experimentally based and thus the design codes to be empirical being valid for the range of variables tested (Young and Hancock, 2001).

Finite element modeling has been used to model web crippling behaviour as well. On the other hand some authors have also proposed so-called mechanical models for web crippling strength predictions. The main focus of this study is to propose an alternative novel approach in this field using NNs. The prediction and the closed form solution of ultimate concentrated load for trapezoidal sheetings are presented by means of NNs followed by extensive parametric studies for the first time in literature.

6.2.3.2 Web Crippling of Sheetings

Web crippling studies of Cold-Formed Steel Decks can be categorized under 3 groups: Experimental studies, FE modeling and Mechanical Models.

a) Experimental studies

In USA Winter and Pian (1946) conducted the first research on web crippling. Their studies were developed by Hetrakul and Yu (1978) and Yu (1981) at Missouri-Rolla which was used in specifications in USA. The experimental studies (Zetlin and Winter, 1952, Andersson and Bergfors, 1973, Keulers, 1981, Wing, 1981, Santaputra, 1986, Tsai and Crisinel, 1996, Studnicka, 1990, Tomà and Stark, 1973, Tomà and Stark, 1974, Wu et al, 1998, Bakker, 1992, Hofmeyer, 2000) on sheetings, sheet sections, and hat sections can be divided into three groups:

1. Members loaded by a pure concentrated load and a negligible small bending moment.
2. Members loaded by pure bending moment.
3. Members loaded by combined concentrated load and bending moment.

b) FE modeling

FE models have also been widely used for the modeling of sheetings and offer many advantages compared to experimental work as they are inexpensive, flexible and can simulate impractical experimental situations (Santaputra, 1986, Sharp, 1991,

Talja,1992, Landolfo and Mazzolani,1995, Vaessen,1995, Schafer and Peköz,1997, Davies and Jiang,1997, Landolfo and Mazzolani,1994) although FEA is time consuming approach. On the other hand how realistic FEA results are compared to experimental values can be scope of another study.

c) Mechanical Models

Some researchers have also proposed so-called mechanical models as an alternative method for the modeling of sheetings. (Reinsch,1983, Tsai and Crisinel,1996,Bakker,1992,Vaessen,1995,RSD,1974, Park and Lee,1996,Lindner et al,1996, Schafer and Peköz, 1998,Davies et al,1999, Rhodes and Nash,1999). These mechanical models are based on mechanics rather than curve fitting of experimental results and describe the behaviour of sheetings

6.2.3.3 Current design codes

Current design codes for sheeting are based on the prediction of the concentrated load and bending moment separately and the maximal allowable interaction of load and moment. The case study in this section deal with the prediction of ultimate concentrated load acting on the sheeting. The prediction of the ultimate concentrated load (web crippling strength) of sheetings in current design codes is based on experiments results. The sheet sections are subjected to a concentrated load with a small bending moment which does not have a significant effect on the value of concentrated load. The ultimate load is recorded finally. Four loading conditions are introduced in The United States and Canadian code namely as : Exterior Two Flange (ETF), Exterior One Flange (EOF), Interior Two Flange (ITF), and Interior One Flange (IOF) loading. On the other hand Eurocode introduces one category for ETF, EOF, and ITF loading and one category (category 2) for IOF loading (Hofmeyer et al, 2001).

Current design rules for sheeting are not precise. As various codes are compared, (the code used in the United States of America (AISI,1996), the code used in Europe (ENV,1993), and the code used in Canada (CSA,1995) the ultimate concentrated load prediction R_u , can differ between +18 and -58 % which indicates that design

codes do not give realistic results for prediction of web crippling strength of sheetings (Hofmeyer,2000)

6.2.3.4 Plastic web crippling behaviour of sheetings

The web crippling behaviour of sheetings is quite complex due to its complicated plastic behaviour. Hofmeyer (2000) has performed three point bending tests on sheetings where he defined the elastic, elastoplastic and plastic behaviour of sheetings in detail shown in Fig. 6.21. If a sheet section is loaded in a three point bending test, the entire sheet section will first behave elastically. If the sheet section is deformed further, a local part of the sheet section will behave plastically which means that if the section is unloaded, this local part will remain deformed. The behaviour from the start of loading until first local plastic behaviour is defined as elastic behaviour. During further increase of deformation, increasingly local parts will become plastic until no other parts will become plastic. The behaviour from first local plastic behaviour until no other parts will become plastic is defined as elasto-plastic behaviour. Further increase of the deformation leads to more plastic deformation in all local plastic parts. However, no new local plastic parts will occur. At that moment, further sheet section behaviour is defined as plastic behaviour. For elasto-plastic and plastic behaviour, elastic deformations still can increase in elastic areas of the section. For plastic behaviour however, these elastic deformations are negligible compared to plastic deformations. The ultimate concentrated load can be obtained as the maximum load on the curve. However the prediction of the plastic behaviour of sheet section becomes a cumbersome task. Various methods have been proposed to overcome this difficulty such as ultimate load simplifications for the description of elastic and plastic curves (Hofmeyer, 2000). Hofmeyer (2000) has observed three different yield line patterns after ultimate load during his experiments on web crippling behaviour of sheetings. Before ultimate load, no yield lines were visible. These yield line patterns all have their own specific load versus web crippling deformation curve which are used to define post-failure modes. Three post-failure modes are defined as rolling post-failure mode, yield arc post-failure mode and yield eye post-failure mode shown in Fig 6.22.

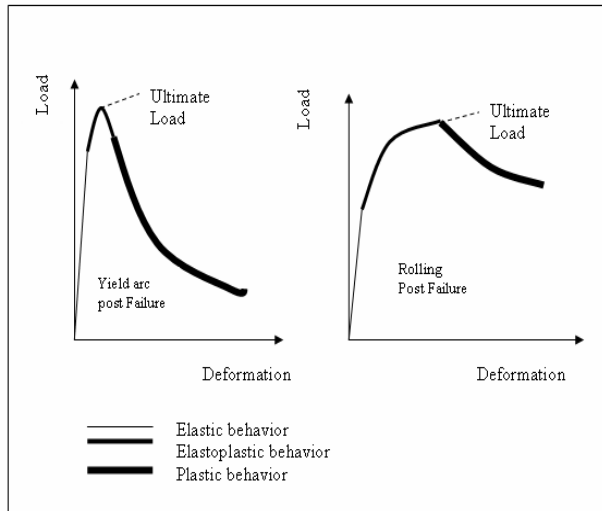


Fig 6.21 Elastic, elastoplastic and plastic behaviour of a sheet section (Hofmeyer,2000)

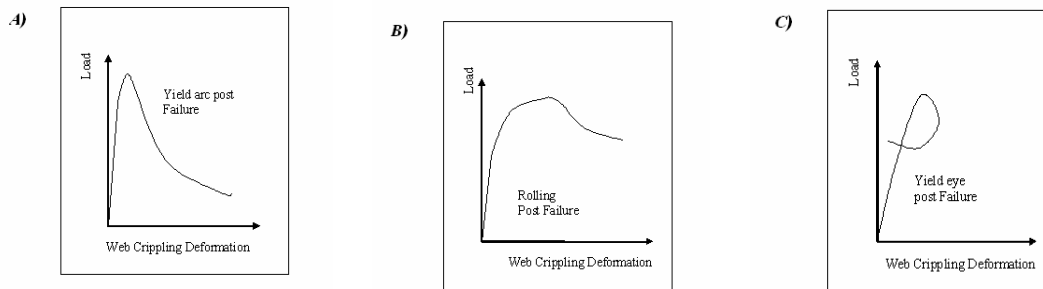


Fig 6.22 Types of failure modes for sheetings (Hofmeyer, 2000)

6.2.3.5 Numerical application

The main focus of this section is to predict the web crippling strength of cold-formed steel decks and its closed-form solution by means of NNs based on experimental results from literature. Therefore an extensive literature survey has been performed for experimental results on sheeting, sheet sections, and hat sections (Zetlin and Winter,1952, Andersson and Bergfors,1973, Keulers,1981, Wing,1981, Santaputra,1986, Tsai and Crisinel,1996, Studnicka,1990, Tomà and Stark,1973, Tomà and Stark,1974, Wu et al ,1998, Bakker,1992, Hofmeyer,2000).

Among these experimental studies on members loaded by pure concentrated load or a pure concentrated load and a negligible small bending moment were examined and

Wing's (1981), Tsai and Crisinel (1996) and Toma and Stark's (1973) experimental results were selected and used as training and test sets for NN training. The variables in these test set up were practical variables whereas there were impractical variables in the remaining test set ups. The sheet section variables used in these experimental studies is given in Fig 6.23 and the ranges of variables are presented in Table 6.8. The most comprehensive one of these studies is found to be Wing's (1981) study conducted by 241 experiments for varying section variables. Wing's test set up and profiles used in his study are given in Figs 6.24-6.26. Tsai and Crisinel (1996) and Toma and Stark's (1973) each performed 12 experiments. Among these 265 tests 37 test were used as test set and the remaining as training set for NN training.

Table 6.8 Minimum and maximum values for cross-section variables.

Variable	Minimum value	Maximum value
Angle (θ)	45 deg.	90 deg.
Steel plate thickness (t)	0.6 mm	1.57 mm
Web height (b_w)	24.1 mm	197 mm
Bottom flange width (b_{bf})	38.9 mm	134.9 mm
Span length (L_{sp})	318 mm	3556 mm
Top flange width (b_{tf})	21.8 mm	119 mm
Load-bearing plate width (L_p)	25.4 mm	160 mm
Corner radius (r)	1.92 mm	11.9 mm
Yield stress (F_y)	231 MPa	372 MPa

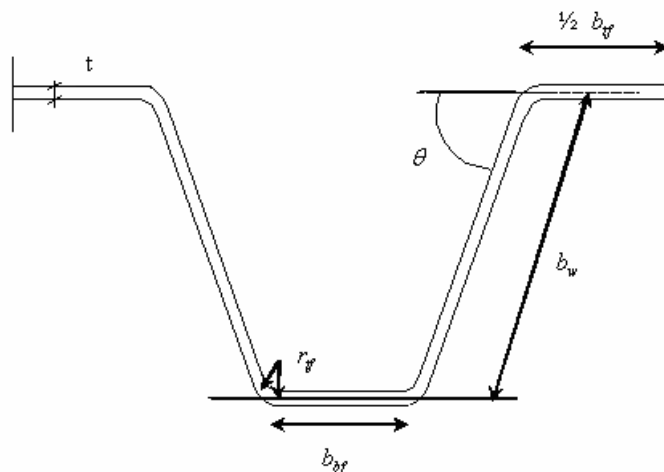


Fig 6.23 Cross-sectional paramaters

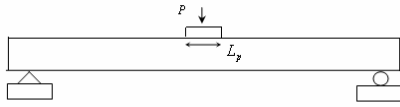


Fig 6.24 Wing's test set up.

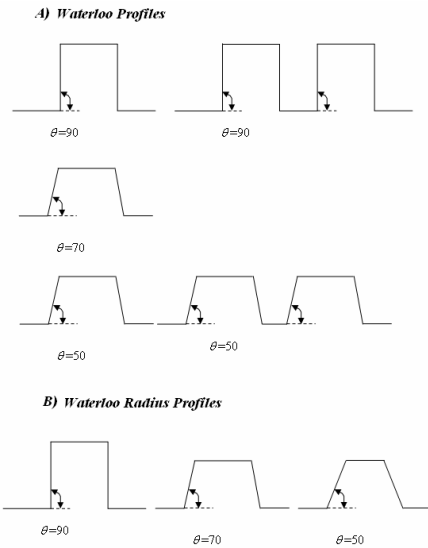


Fig 6.25 Sections for Wing's experiments I (Wing,1981). (a) Waterloo profiles; (b) Waterloo radius profiles

The patterns used in test set are randomly selected among the experimental database. Among these 265 tests 37 tests were used as test set and the remaining as training set for NN training. The optimal NN architecture in this study was found to be 9-5-1 NN architecture with hyperbolic tangent sigmoid transfer function (tansig). The training algorithm was quasi-Newton backpropagation (BFGS). The optimum NN model is given in Fig 6.27. Statistical parameters of normalized values of learning and training sets are presented in Table 6.9. The % errors and Prediction of NN and actual values of learning and testing sets are given in Figs 6.28-6.31. The prediction of the proposed NN model vs. actual experimental values and a comparison with calculated values according to NAS 2001 (North American Specification for the Design of Cold-Formed Steel Structural Members) are given in Table 6.10. The performance of the proposed NN model vs. experimental result is shown in Fig 6.32.

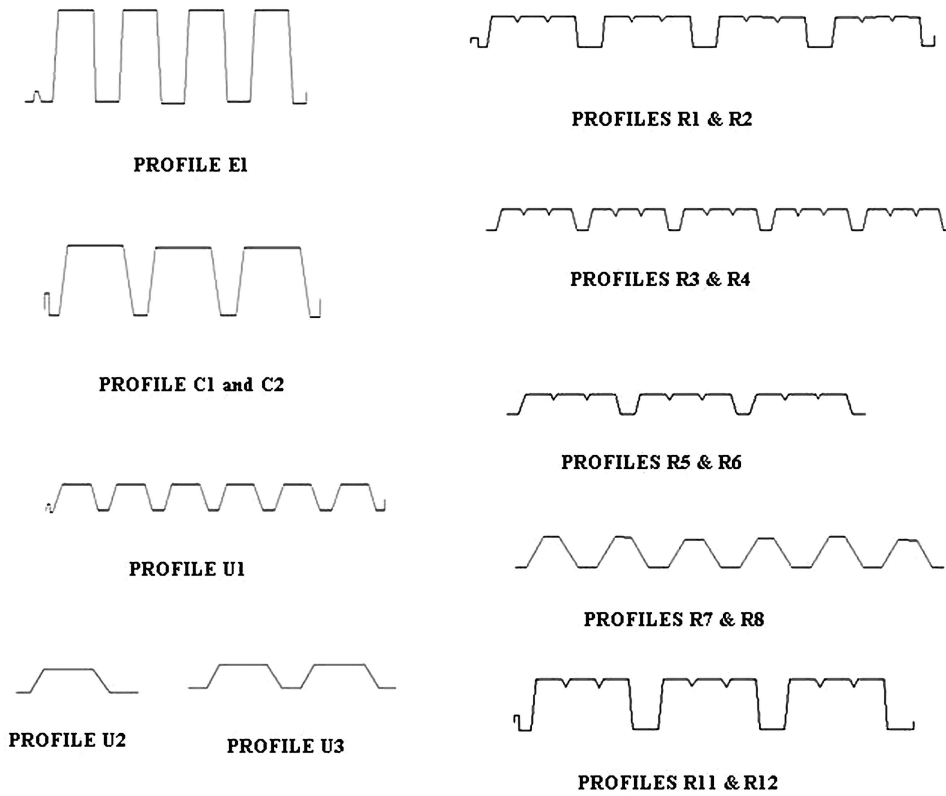


Fig 6.26 Sections for Wing's experiments II (Wing, 1981)

Table 6.9 Statistical parameters of optimum NN model

	MSE	RMSE	SSE	MAPE(%)	Correlation Coefficient (R)
Test Set	0.00054959	0.023443	0.020335	7.0011	0.995
Training set	0.00034346	0.018533	0.099947	6.946	0.996

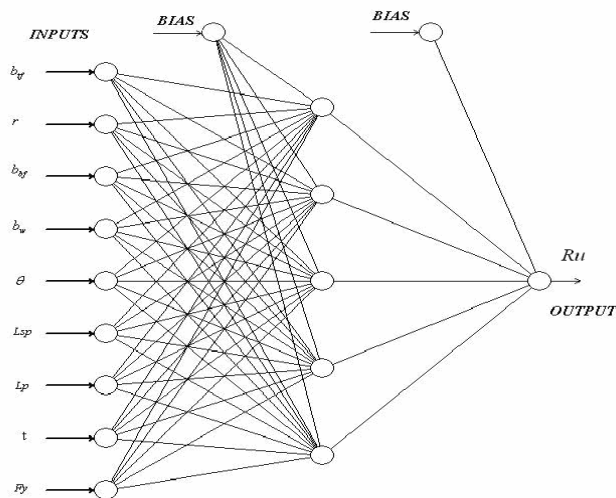


Fig 6.27 Optimum NN model

Table 6.10 NN prediction of R_u and experimental results of test set with geometric and mechanical variables

Exp.	btf (mm)	r (mm)	bbf (mm)	bw (mm)	θ (°)	Lsp (mm)	Lp (mm)	t (mm)	F_y (MPa)	Rtest (N)	RNN (N)	Rtest/RNN	NAS 2001	RNN/NAS 2001
Tsai	35.2	6.4	56.4	100.6	78.7	560	100	0.83	294	4363	4871.7	0.9	3555	1.37
Tsai	62.5	8.4	55.4	61.6	75.4	1200	100	0.85	306	2690	2733.9	0.98	3807	0.72
Toma	119	4.6	42.1	40	72	1080	55	0.72	317	1688	1725.7	0.98	2722	0.63
Toma	77	6.6	70.9	70	81	1080	100	0.71	333	2830	2846.4	0.99	3084	0.92
Wing	95.5	2.69	100.4	95.8	90	940	50.8	0.61	265.4	2447	2347.7	1.04	1660	1.41
Wing	96.5	2.87	63.8	98.6	50	508	25.4	0.97	274.4	3229	3959.1	0.82	2656	1.49
Wing	94.5	3.15	99.4	97	90	775	25.4	1.52	231	9902	10572	0.94	7014	1.51
Wing	95	3.15	106.5	98.8	70	1003	25.4	1.52	231	9012	9110.5	0.99	6580	1.38
Wing	94.5	3.15	54.3	98.8	70	516	25.4	1.52	231	8790	9883.4	0.89	6580	1.50
Wing	95	3.15	66.6	100.3	50	521	25.4	1.52	231	8452	9463.5	0.89	5356	1.77
Wing	97	2.69	50.6	97	90	1727	25.4	0.61	265.4	890	881.25	1.01	1337	0.66
Wing	97.5	3.15	100.3	97.8	90	318	127	1.52	231	23753	22411	1.06	11010	2.04
Wing	95	2.69	100.3	95.5	90	2337	76.2	0.62	269.6	1388	1477	0.94	1999	0.74
Wing	94.5	2.69	101.5	96	90	1016	50.8	0.62	269.6	2242	2337	0.96	1741	1.34
Wing	95.5	2.69	74.7	96.3	90	1016	50.8	0.61	269.6	2019	1924.9	1.05	1684	1.14
Wing	95.5	2.68	75	96.3	90	711	76.2	0.61	269.6	2402	2601.7	0.92	1934	1.35
Wing	96	2.68	74.4	196.6	90	584	152.4	0.6	337.8	3825	4707.6	0.81	2588	1.82
Wing	96	2.71	74.9	197.1	90	432	76.2	0.66	317.8	4048	3788.5	1.07	2292	1.65
Wing	88.4	6.33	83.7	89.4	90	1321	50.8	1.54	302	8229	8578	0.96	10406	0.82
Wing	98.6	5.09	104.9	94.7	70	2946	50.8	0.63	317.8	1219	1279.2	0.95	1774	0.72
Wing	94.5	7.13	105.4	91.4	70	1321	50.8	1.54	302	9795	9486.1	1.03	9587	0.99
Wing	97.5	7.92	125.2	98	50	1321	50.8	1.55	288.2	10987	10056	1.09	7381	1.36
Wing	96.5	10.3	130.2	91.9	50	1321	50.8	1.54	302	9724	10283	0.95	7323	1.40
Wing	93	5.28	82.4	91.9	90	1321	101.6	1	299.2	4777	4484.9	1.07	5632	0.80
Wing	92.5	11.9	103.3	87.9	70	1321	101.6	1.54	302	10871	10642	1.02	10732	0.99
Wing	93	6.78	84.2	87.1	90	508	101.6	0.85	284.1	5560	5420.4	1.03	3719	1.46
Wing	43.7	4.76	75.9	76.5	85	1334	76.2	1.57	293	8505	8451.6	1.01	12326	0.69
Wing	35.1	3.56	77.6	128.5	81.5	3556	50.8	0.76	282	1139	968.63	1.18	2468	0.39
Wing	35.1	3.56	77.6	128.5	81.5	1588	101.6	0.76	282	2616	2496.3	1.05	3113	0.80
Wing	32	4.35	38.9	75.4	70	1702	38.1	0.79	291.6	1032	1072.3	0.96	2510	0.43
Wing	32	4.35	38.9	75.4	70	1651	38.1	0.79	291.6	1165	1103.9	1.06	2510	0.44
Wing	32	4.35	38.9	75.4	70	368	38.1	0.79	291.6	3318	3088.1	1.07	2510	1.23
Wing	21.8	1.92	61	24.1	45	1626	38.1	0.65	336.5	916	1122.9	0.82	1867	0.6
Wing	95	2.71	100	96	70	508	25.4	0.64	265.4	2847	2867.8	0.99	1386	2.07
Wing	95	2.69	100.6	95.8	90	1016	76.2	0.61	269.6	2642	2534.6	1.04	1935	1.31
Wing	101.1	6.85	126	99.1	50	1321	50.8	1	299.2	4653	4637.2	1	3264	1.42
Wing	32	4.35	38.9	75.4	70	699	50.8	0.79	291.6	1886	2150.5	0.88	2740	0.78

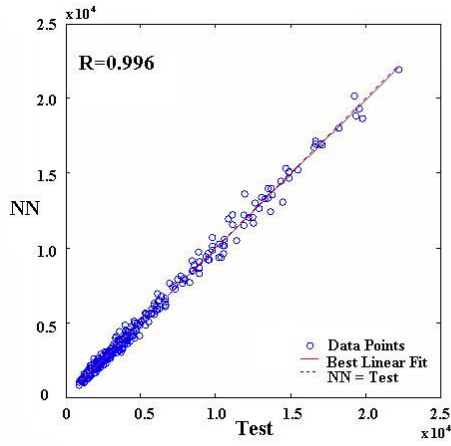


Fig 6.28 Prediction of NN and actual values for learning set

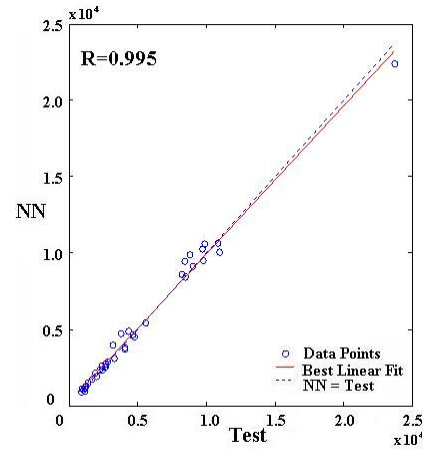


Fig 6.29 Prediction of NN and actual values for testing set

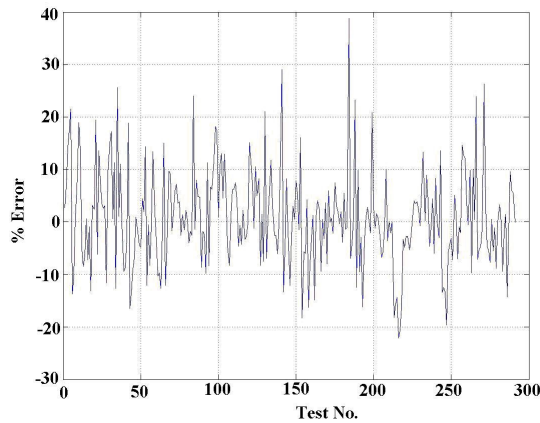


Fig 6.30 % Error of training set

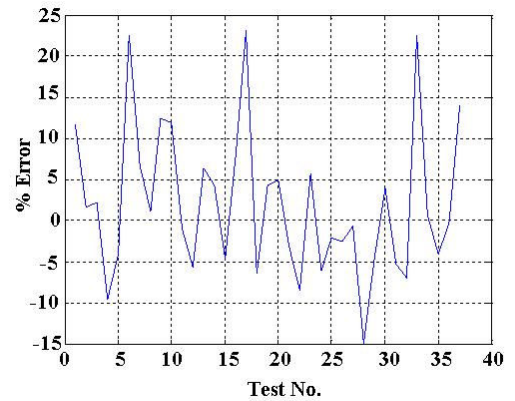


Fig 6.31 % Error of test set

It is obvious from statistical results ($R=0.995$) above that the proposed ANN model accurately learned to map the relationship between the ultimate concentrated load R_u and its geometric and mechanical properties. Thus the trained ANN proposed in this study was used to conduct an extensive parametric study to investigate the effect of changing geometric parameters and yield strength on the ultimate concentrated load of sheetings. The trend of R_u for various parameters is shown in Figs 6.33-6.44. Interesting outcomes are observed on the graphs of trends. The relationship of geometric parameters with yield strength (F_y) is found to be directly proportional and linearly dependent which was as expected. The trend of geometric parameters with each other shows a parabolic relationship in general. One of the most striking result is that top flange width (b_{tf}) does not have a significant effect on ultimate concentrated load and can be neglected which is also indicated in Eurocode

(ENV,1993). A detailed parametric study should perhaps be the scope of another article.

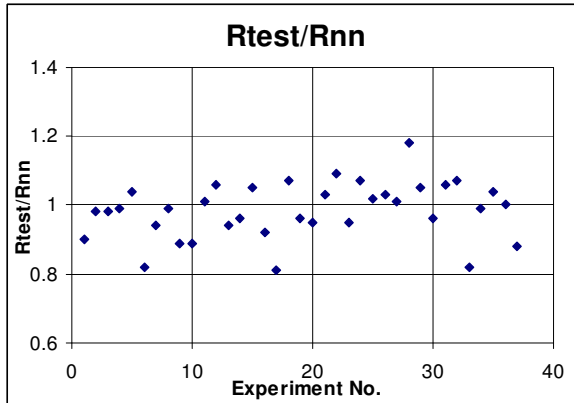


Fig 6.32 Actual experimental results/ NN predictions

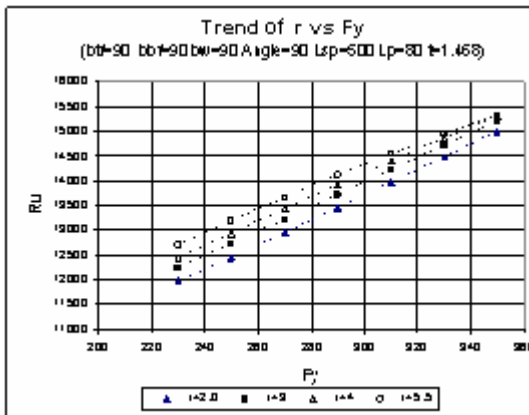


Fig 6.33 Trend of r vs. F_y

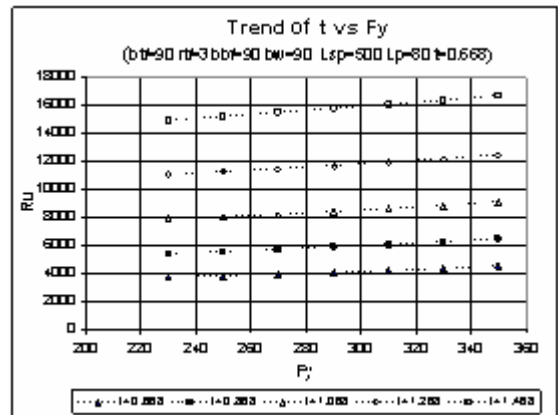


Fig 6.34 Trend of t vs. F_y

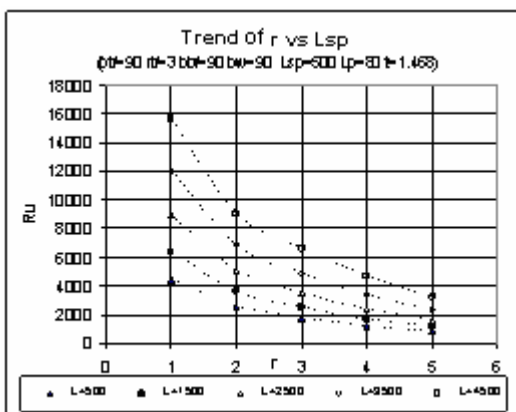


Fig 6.35 Trend of r vs. L_{sp}

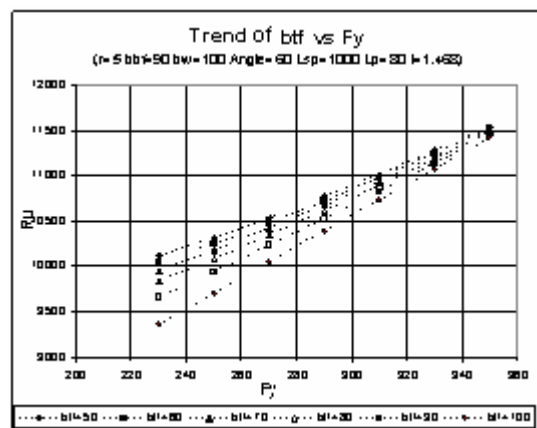


Fig 6.36 Trend of b_{tf} vs. F_y

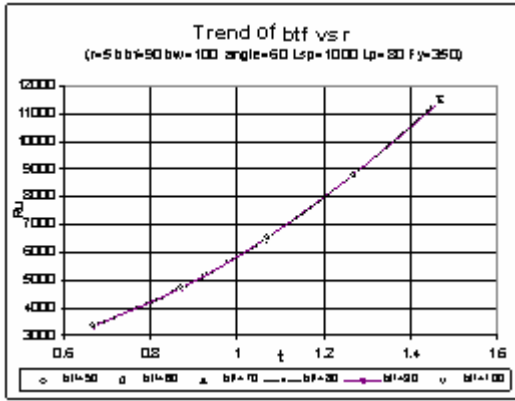


Fig 6.37 Trend of b_{tf} vs. r

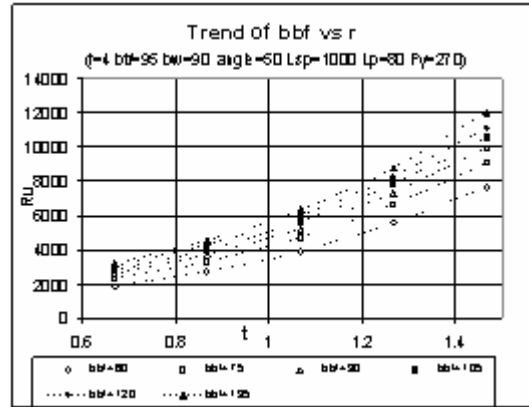


Fig 6.38 Trend of b_{bf} vs. r

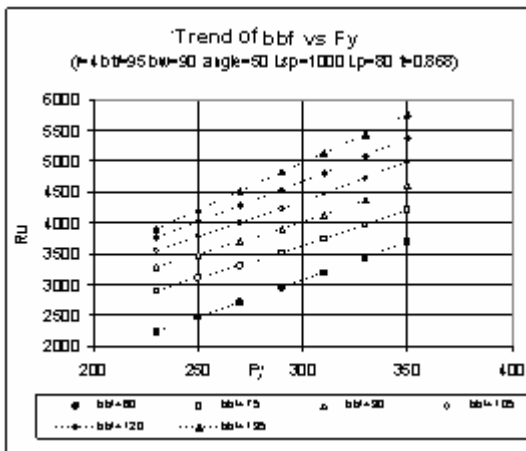


Fig 6.39 Trend of b_{bf} vs. F_y

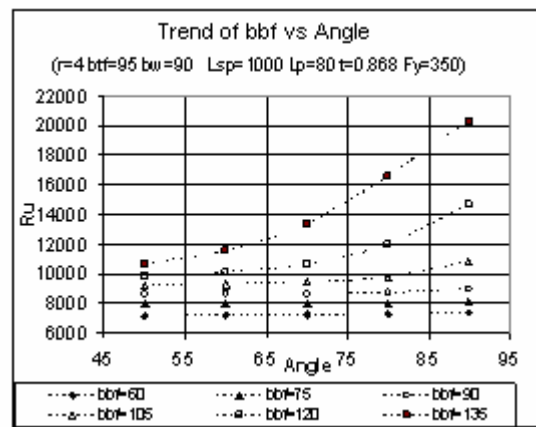


Fig 6.40 Trend of θ vs. bbf

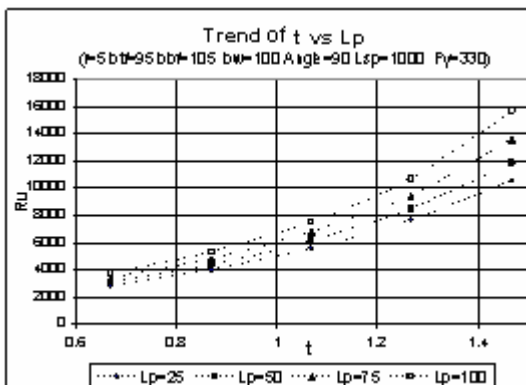


Fig 6.41 Trend of t vs. L_p

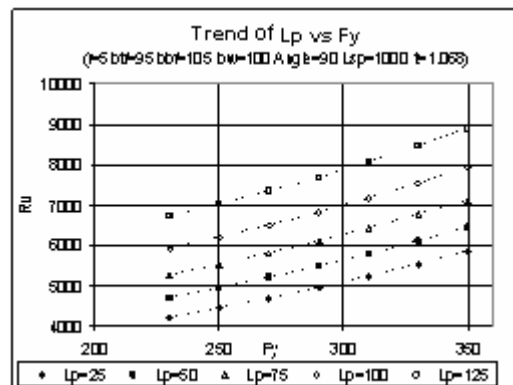


Fig 6.42 Trend of L_p vs. F_y

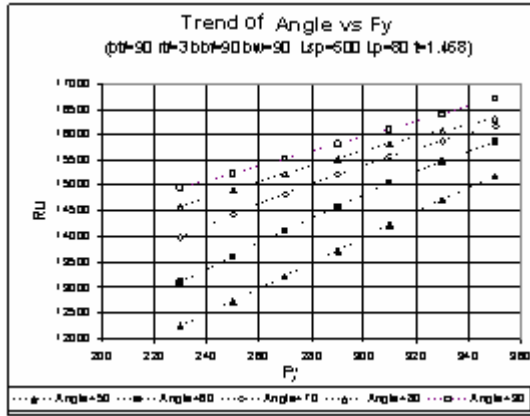


Fig 6.43 Trend of θ vs. F_y

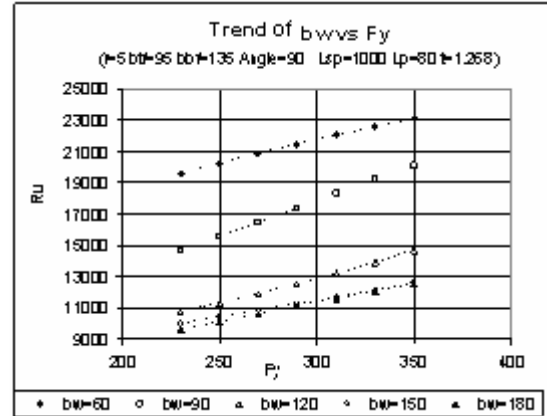


Fig 6.44 Trend of b_w vs. F_y

6.2.3.6 Closed-Form Solution of Ultimate Concentrated Load (R_u)

The aim of this study is to obtain the concentrated Load R_u in explicit form as

$$R_u = f(b_{ff}, r, b_{bf}, b_w, \theta, L_{sp}, L_p, t, F_y)$$

Using trained NN parameters. Following the same procedure given in previous case studies one can get

$$u_1 = (-6.3992 * b_{ff}) + (0.064638 * r) + (-7.004 * b_{bf}) + (5.9736 * b_w) + (-4.6755 * \theta) \\ + (1.291 * L_{sp}) + (-2.0631 * L_p) + (-6.2691 * t) + (-1.9978 * F_y) + 19.91$$

$$u_2 = 31305 * b_{ff} + (0.60695 * r) + (-0.60872 * b_{bf}) + (-1.6494 * b_w) + (0.7681 * \theta) + \\ (9.7193 * L_{sp}) + (-1.4085 * L_p) + (-2.7943 * t) + (1.1545 * F_y) + 1.05$$

$$u_3 = (-0.10556 * b_{ff}) + (2.9594 * r) + (5.4054 * b_{bf}) + (-0.87409 * b_w) + (0.96795 * \theta) + \\ (-0.32996 * L_{sp}) + (-1.6918 * L_p) + (-.5065 * t) + (1.7634 * F_y) - 0.26$$

$$u_4 = (-0.07071 * b_{ff}) + (0.0559 * r) + (-0.50931 * b_{bf}) + (-0.3624 * b_w) + \\ (-0.03758 * \theta) + (1.2201 * L_{sp}) + (-0.47406 * L_p) + (-2.2025 * t) + (-.0226 * F_y) + 2.82$$

$$u_5 = (-4.0521 * b_{ff}) + (1.6647 * r) + (-2.3898 * b_{bf}) + (-4.9121 * b_w) + (3.6499 * \theta) +$$

$$(15.952 * L_{sp}) + (-1.8613 * L_p) + (-2.3345 * t + 2.7774 * F_y) + 3.91$$

Where the activation function is hyperbolic tangent sigmoid transfer function (tansig)

$$f(u_i) = \left(\frac{2}{1 + e^{-2(u_i)}} - 1 \right)$$

Hence the output

$$O = \sum (w_{2_i} * f(u_i)) + b_2$$

$$\begin{aligned} &= \left(\frac{2}{1 + e^{-2u_1}} - 1 \right) * w_{2_1} + \left(\frac{2}{1 + e^{-2u_2}} - 1 \right) * w_{2_2} + \left(\frac{2}{1 + e^{-2u_3}} - 1 \right) * \\ &w_{2_3} + \left(\frac{2}{1 + e^{-2u_4}} - 1 \right) * w_{2_4} + \left(\frac{2}{1 + e^{-2u_5}} - 1 \right) * w_{2_5} + b_2 \\ &= \left(\frac{2}{1 + e^{-2u_1}} - 1 \right) * (-0.371) + \left(\frac{2}{1 + e^{-2u_2}} - 1 \right) * (-0.331) + \left(\frac{2}{1 + e^{-2u_3}} - 1 \right) * (2.821) + \\ &\left(\frac{2}{1 + e^{-2u_4}} - 1 \right) * (-0.492) + \left(\frac{2}{1 + e^{-2u_5}} - 1 \right) * (0.167) + (-1.779) \end{aligned}$$

It should be noted that the inputs entering the network have been normalized before the training as

$$b_{tf} = b_{tf}^* / 100 \quad ; \quad r = r^* / 10; \quad b_{bf} = b_{bf}^* / 150; \quad b_w = b_w^* / 200; \quad \theta = \theta^* / 90;$$

$$L_{sp} = L_{sp}^* / 5000; \quad L_p = L_p^* / 200; \quad t = t^* / 2; \quad F_y = F_y^* / 500$$

And the output before the training has been normalized by 20000 thus the final output should be

$$R_u = O * 20000$$

6.2.3.7 Conclusion

This case study reports findings of a novel NN application to model web crippling strength of trapezoidal sheetings as a function of various influencing parameters. There is no well established mathematical formulation of web crippling strength as the plastic behaviour is too complicated leading 3 different types of failure modes. There have been attempts to model this complex web crippling behaviour of sheeting either by FE modeling or so called mechanical models but current design codes in this field remain still inaccurate. This study not only proposes a new NN approach for the prediction of web crippling strength of sheetings but also presents a closed form solution of web crippling strength of sheetings with a very high correlation ($R=0.995$) with experimental results from literature. It opens the so called black box which NNs are often indicated as. The proposed NN approach is quite fast compared to FE modeling and mechanical models and very practical for use. The results of the proposed NN are compared with NAS (2001) and are found to be quite more accurate. Another advantage of the proposed ANN model is its wide range of the input parameters which enables the NN model to be used in practical applications. The well trained NN model is also used to conduct parametric studies. The effect of geometric and mechanical parameters on web crippling strength of sheetings is graphically presented in details. It is found that top flange width does not have a significant effect on web crippling strength consistent with various design codes. The results of this study are very promising.

6.2.4 Prediction Of Rotation Capacity Of Wide Flange Beams Using Neural Networks

6.2.4.1 Introduction

This study proposes Neural Networks (NN) as a new approach for the estimation and explicit formulation of available rotation capacity of wide flange beams. Rotation capacity is an important phenomena which determines the plastic behaviour

of steel structures. Thus the database for the NN training is directly based on extensive experimental results from literature. The results of the NN approach are compared with numerical results obtained by a specialized computer. Available rotation capacity is also introduced in a closed form solution based on the proposed NN model. The proposed NN method is seen to be more accurate than numerical results, practical and fast compared to FE models.

The behavior of a wide flange beam can be generalized into; Elastic, Inelastic and Plastic categories as shown in Figure 6.45. In any case the failure of beam will be due to one of the following: local plate buckling of the compression flange, local plate buckling of the web in flexural compression, or lateral-torsional buckling. The plastic behaviour category is of special concern in this study as it permits moment redistribution in indeterminate structures (Yura et al, 1978).

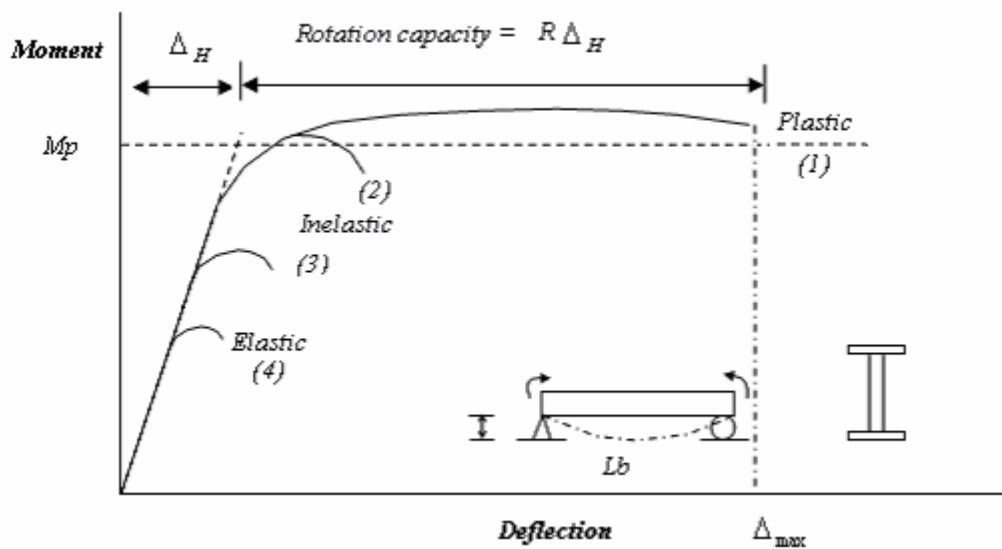


Fig 6.45. General beam behaviour (Yura et al, 1978).

Plastic analysis and design enables the full cross sectional capacity of a beam to be used by notionally allowing a *plastic hinge* to form. This hinging occurs when the plastic moment strength, M_p , is reached at a discrete point along the beam (i.e. the entire cross section has yielded). At such a location, the cross section can no longer resist increasing moment and hence large rotations occur, with constant resistance, M_p , being maintained. In the case of an indeterminate structure, such a scenario allows for moment re-distribution to occur. However, it is critical that in addition to the cross section reaching its plastic moment capacity, the beam must also be ductile

enough to maintain M_p while continuing to deform (rotate) through a sufficient angle so that moment redistribution can take place. A common structural ductility or deformation capacity measure is termed plastic rotation capacity (Steven, 2000).

The estimation of plastic rotation capacity is of significant importance for plastic and seismic analysis and design of steel structures. Similarly the moment redistribution in a steel structure also depends on the rotation capacity of the section. Thus the determination of rotation capacity of steel structures becomes an important task.

This case study focuses on the prediction of available rotation capacity of wide flange steel beams. Theoretical, empirical and approximate methods have been proposed for the determination of available rotation capacity of wide flange steel beams in literature which have been reported by Gioncu and Petcu (1997a, 1997b). In order to find how realistic results are, these studies should be compared with experimental tests. Thus an alternative approach for the prediction of rotation capacity of wide flange steel beams using NNs is presented for the first time in literature. Backpropagation NNs are used for the training of the NN model. The results of the proposed NN model based on experimental studies are compared with numerical results and are seen to be very accurate. Moreover an explicit solution of rotation capacity for wide flange beams in terms of geometric and mechanical parameters will be introduced by using the well trained NN parameters. The proposed NN approach is quite accurate, fast and practical compared to FE approach.

6.2.4.2 Rotation Capacity

There are various definitions of Rotation Capacity in literature as a non-dimensional parameter. Salmon and Johnson defined rotation capacity as a method of quantifying deformation capacity within a cross-section prior to instability eroding the cross-sectional capacity (Salmon and Johnson, 1996). According to Lay and Galambos (1965) rotation capacity is, $R = \theta_h / \theta_p$, in which θ_p is the elastic rotation at the initial attainment of the plastic moment M_p and θ_h is the plastic rotation at the point when moment drops below M_p .

A widely used definition for rotation capacity is proposed by ASCE (1971) (Fig 6.46):

$R = \theta_2 / \theta_1$ where θ_1 refers to the theoretical rotation at which the full plastic capacity is achieved and θ_2 is the rotation when the moment capacity drops below M_p on the unloading portion Kemp (1985) defined rotation capacity as $R = \theta_{hm} / \theta_p$ in which θ_{hm} is the plastic rotation up to the maximum moment on the moment rotation curve.

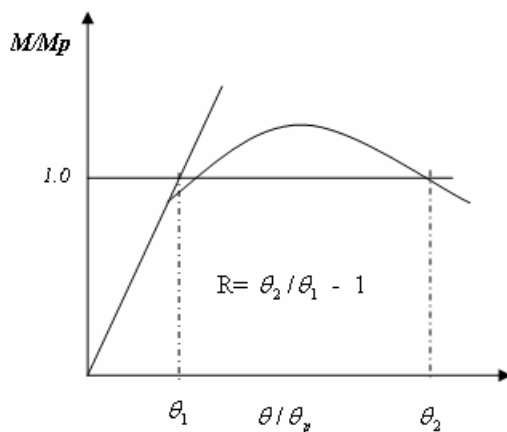


Fig 6.46 Definition of rotation capacity (ASCE, 1971)

The behaviour of laterally restrained beams is commonly divided into three or four classes of behaviour as illustrated in Fig 6.47. The Australian Standard AS 4100 (1998) and AISC (1997) have three classes (compact, non-compact, and slender). A compact or Class 1 section is suitable for plastic design, and can sustain the plastic moment (M_p) for a sufficiently large rotation capacity (R) to allow for moment redistribution in a statically indeterminate system (Wilkinson and Hancock, 2002)

On the other hand Eurocode 3 (2003) defines 4 classes of cross-sections to identify the extent to which the resistance and rotation capacity of cross sections is limited by its local buckling resistance as follows:

- Class 1 cross-sections are those which can form a plastic hinge with the rotation capacity required from plastic analysis without reduction of the resistance.
- Class 2 cross-sections are those which can develop their plastic moment resistance, but have limited rotation capacity because of local buckling.
- Class 3 cross-sections are those in which the stress in the extreme compression fibre of the steel member assuming an elastic distribution of stresses

can reach the yield strength, but local buckling is liable to prevent development of the plastic moment resistance.

– Class 4 cross-sections are those in which local buckling will occur before the attainment of yield stress in one or more parts of the cross-section.

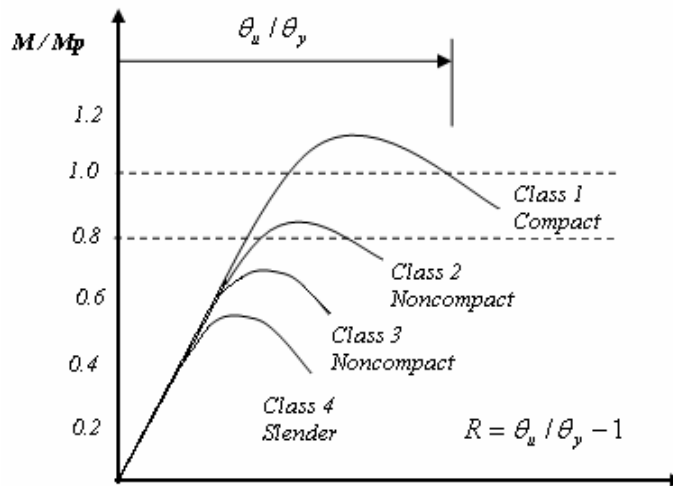


Fig 6.47. Classical definition for rotation capacity based on normalised moment-rotation relationship.

6.2.4.3 Numerical Application

The main focus of this study is the prediction of rotation capacity of wide flange steel beams using NNs and its closed –form solution by means of NNs based on experimental results from literature. Therefore an extensive literature survey has been performed for experimental results shown in Table 1. The experimental results in this field are dispersed. Standard beams are used in experimental studies (SB1, SB2) shown in Fig 6.48a-6.48b. SB1 is used in the experimental studies given in Table 6.11. The geometry of cross-section variables of tested beams is shown in Fig. 6.49. The ranges of variables i.e. the maximum and minimum values of cross-section variables where the proposed NN model will be valid are given in Table 6.12.

Table 6.11 Experimental database

Ref.	Exp No	b (mm)	d(mm)	t _f (mm)	t _w (mm)	L (mm)	F _{yi} (MPa)	F _w (MPa)
Lukey and Adams (1969) ⁽ⁱ⁾	1	36.95	191.3	5.28	4.45	1036	371	395
	2	43.05	191.3	5.28	4.45	1254	371	395
	3	47	191.3	5.28	4.45	1396	371	395
	4	48.4	191.3	5.26	4.45	1448	371	395
	5	50.95	241.2	5.26	4.6	1372	371	350
	6	36.85	241.2	5.26	4.6	960	371	350
	7	42.95	241.2	5.26	4.6	1168	371	350
	8	44.45	241.2	5.26	4.6	1280	371	350
	9	46.75	241.2	5.26	4.6	1296	371	350
	10	51.3	191.3	5.28	4.45	1554	371	395
	11	88	235.1	10.8	7.65	2946	283	308
	12	101.75	235.1	10.8	7.65	3480	283	308
Kuhlman (1986,1989) ⁽ⁱⁱ⁾	13	70.5	278	8	5	3404	236	217
	14	75	278	8	5	3704	236	217
	15	80	277	8.5	5.5	4000	449	217
	16	80	261	8	6	2540	287	260
	17	80	258	8	5	2636	287	252
	18	80	259	8	4	2716	287	252
	19	80	280	8	5	1796	287	252
	20	80	280	8	5	2196	287	252
	21	80	275	8	5	2598	287	252
	22	80	237.2	10.4	5.5	3508	333	709
	23	80	148.6	10.2	5.5	2304	333	709
	24	80	200	10	5.5	2204	333	709
	25	80	278	10	6	2000	333	341
	26	80	279	10	6	2804	333	349
	27	80	279	10	6	2402	333	349
	28	85	279	8	5	2802	236	217
	29	85	279	10	6	2406	333	349
	30	91	278	8	5.5	3002	236	217
	31	91.5	278.4	10.3	6	2500	333	349
	32	95	278	8	5.5	3400	236	217
33	95	278.6	10.2	6	2700	333	349	
34	70.5	239.6	10.2	5.5	3000	333	709	
35	75	239	10	5.5	3200	333	709	
36	80.5	269	10	5.5	2100	333	709	
Spangemacher (1991) ⁽ⁱⁱⁱ⁾	37	109.2	185.2	16.1	9.4	3500	278	286
	38	109.3	186.5	16.3	9.8	3500	486	532
	39	109.3	184.9	16.2	9.4	3500	486	532
	40	109.5	186.1	16.3	9.6	3500	278	286
	41	110	188	10.5	7.5	3000	282	308
	42	110.5	189	11	7.4	4000	282	308
	43	111	192.6	10.7	7.5	4000	420	437
	44	117.8	185.4	10.3	7.25	4000	275	302
	45	117.8	186.1	11.1	7.65	4000	430	448
	46	139.5	246.6	17.7	10.8	4000	248	252
	47	139.7	241.2	17.8	10.9	3000	248	252
	48	140	243.4	12.8	7.5	4000	276	311

Table 6.11 cont'd

	49	140	240.8	12.6	8	3000	276	311
	50	140.5	250.4	12.6	9	3000	504	535
	51	140.5	249.6	12.7	9.3	4000	504	535
	52	141.5	246.9	17.3	11.35	3000	489	535
	53 ^a	141.6	249.9	17.4	11.5	3000	489	535
	54 ^a	141.7	246.4	17.3	11.3	3000	489	535
	55 ^a	112.8	188.3	11	7.5	3000	420	437
	56	150.3	320	15	10	3000	817	813
	57	150.3	320	15	10	3000	486	990
	58	150.3	320	15	10	3000	248	323
	59	142	249.7	17.4	11.5	4000	489	539
	60	141.7	246.4	17.4	11.4	3000	489	539
Boreave et al. (1993) ^(iv)	61	100	159.5	14.9	9.4	3000	409	426
	62	100.1	153.9	14.7	9.5	3000	375	421
	63	100.2	156.6	14.6	9.6	3000	261	291
	64	100.3	155.1	14.1	8.8	3000	303	342
	65	100.7	154.4	15.1	9.5	3000	445	462
Kemp (1985,1991) ^(v)	66	75	217.8	8.09	6.65	3660	340	358
	67	72.5	217.4	10.57	6.82	3660	285	329
	68	74.5	217.9	8.56	6.78	1830	340	353
	69	74.5	217.1	1.44	6.78	1830	294	300
	70	77	120.3	9.83	7.44	3660	313	300
	71 ^a	53	273.9	7.05	5.85	3660	332	388
	72 ^a	70	209.5	10.77	6.76	1830	288	329
Suzuki et al (1994) ^(vi)	73	75	132	9	6	1200	291	340
	74	75	132	9	6	1200	527	340
	75	75	132	9	6	1200	291	509
	76	75	132	9	6	1200	526	509
	77	75	132	9	6	1800	291	340
	78	75	132	9	6	1800	291	509
	79	75	132	9	6	1800	291	686
	80	75	132	9	6	1800	526	509
	81 ^a	75	132	9	6	1200	291	340

^a Eliminated experiments from statistical analysis due experimental deficiencies

(i) Tested on 12 specimens (rolled wide-flange beams

(ii) 24 specimens (built-up welded wide-flange sections) are tested

(iii) Tested 34 rolled wide flange beams, where 24 of these are used as the remaining 10 specimens were not used on which shear failure is observed.

(iv) Five hot rolled section were tested.

(v) 12 built-up welded I-beams was tested, but only 7 beams due to missing data

(vi) 9 built-up welded hybrid beams are tested.

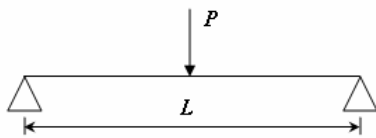


Fig 6.48a. SB1

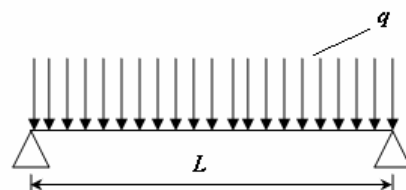


Fig 6.48b. SB2

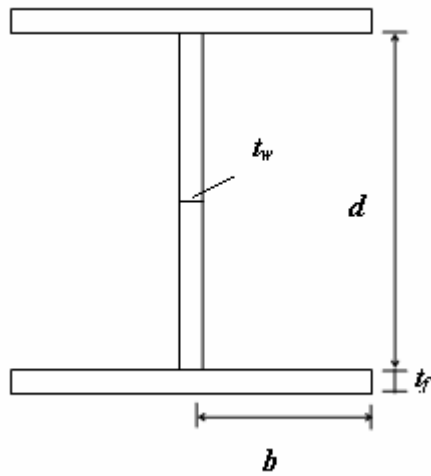


Fig 6.49 Cross-sectional parameters

Table 6.12. Minimum and maximum values for cross-section variables.

Variable	Minimum value	Maximum value
Half length of flange b (mm)	36.95	150.4
Height of web d (mm)	120.3	320
Thickness of flange t_f (mm)	1.44	17.3
Thickness of web t_w (mm)	4	11.5
Length of beam L (mm)	960	4000
Yield strength of flange F_{yf} (MPa)	236	817
Yield strength of web F_{yw} (MPa)	217	990

The NN model of this study is shown in Fig 6.50. The optimal NN architecture was found to be 7-17-1 NN architecture with hyperbolic tangent sigmoid transfer function (tansig). Back-propagation Neural networks are adopted in this work, as they have a high capability of data mapping. The training algorithm was quasi-Newton backpropagation (BFGS). The optimum NN model is given in Figure 6.51. Statistical parameters of learning and training sets for normalized outputs are presented in Table 6.13. The % errors and Prediction of NN and actual values of learning and testing sets are given in Figures 6.52-6.55. The performances of NN model and DUCTROT in overall are given in Figures 6.56 and 6.57. The prediction of the proposed NN model, actual experimental values and numerical results are given in

Table 6.14. The numerical results are obtained by a specialized computer program (DUCTROT) developed by Petcu and Gioncu (2003) which is based on local plastic mechanism. The main factors influencing the rotation capacity are included in program: section type, material properties, member dimensions, moment variation, buckling type, influence of strain rate, influence of cyclic loading, etc. The validation of computer program is performed by Petcu and Gioncu comparing the obtained values with experimental and numerical results. The result accuracy is confirmed by this comparison. The performance of NN model and numerical results are presented in Fig 6.58. The results indicate that the proposed NN model performs quite well compared to numerical results.

Table 6.13 Statistical parameters of optimum NN model

	MSE()	RMSE	SSE	MAPE(%)	Correlation Coefficient (R)
Test Set	0.0005	0.0233	0.0054	6.959	0.990
Training set	0.0003	0.0171	0.019	5.293	0.997

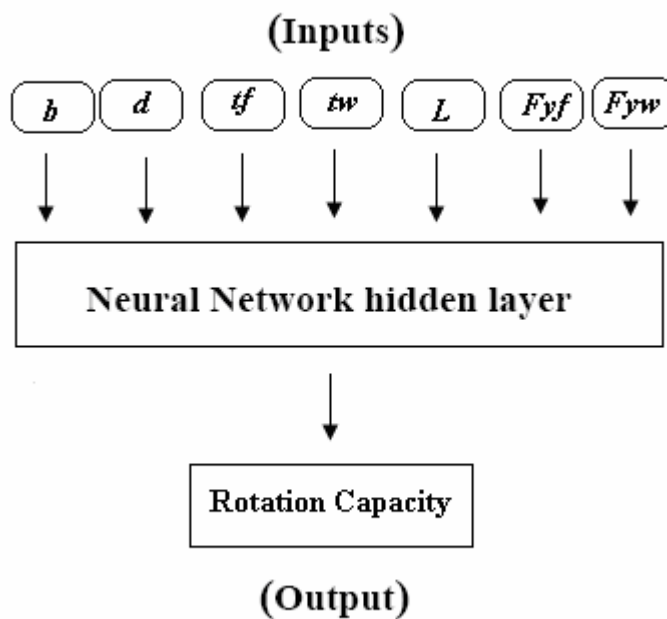


Fig 6.50 NN model

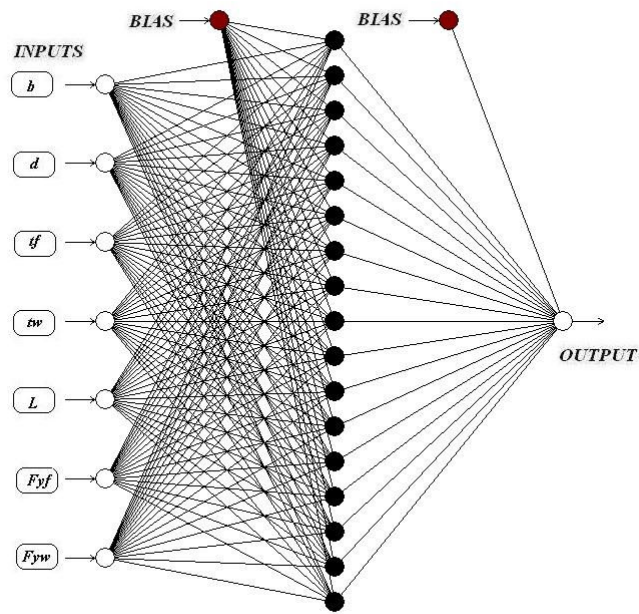


Fig 6.51 Optimum NN model

Table 6.14 Comparative analysis of NN results with experimental and numerical results

* Bold Sets are test sets

Ref.	Exp No	R_E	R_{NN}	$R_{DUCTROT}$	$R_{DUCTROT}/R_E$	R_{NN}/R_E
Lukey and Adams (1969)	1	10.4	10.501	8	0.77	1.01
	2	6.7	5.8913	7.6	1.13	0.879
	3	3.4	3.8415	7.4	2.17	1.13
	4	3.2	3.2257	7	2.19	1.008
	5	4.2	3.8324	6.8	1.62	0.912
	6	13.7	13.556	7.9	0.58	0.989
	7	8	7.8534	7.3	0.91	0.982
	8	6.5	5.9556	6.9	1.06	0.916
	9	4.2	5.2793	7.1	1.68	1.257
	10	2.9	2.3847	7.2	2.48	0.822
	11	13.6	13.256	10.7	0.79	0.975
	12	11.8	11.666	7.9	0.67	0.989
Kuhlman (1986,1989)	13	8	8.1781	7.9	0.99	1.022
	14	7	6.8058	11.9	1.7	0.972
	15	1	1.0461	3.3	3.3	1.046
	16	12.7	11.978	12.3	0.97	0.943
	17	8.6	7.8664	16.5	1.92	0.915
	18	4.6	4.2461	5.2	1.13	0.923
	19	13.5	13.623	13.2	0.98	1.009

Table 6.14 cont'd

	20	11.5	10.801	10.1	0.88	0.939
	21	7.8	7.9685	8.3	1.07	1.022
	22	3.6	3.8928	3.8	1.05	1.081
	23	10.5	10.549	13.3	1.27	1.005
	24	9.5	9.1749	7.8	0.82	0.966
	25	12	12.336	11.2	0.93	1.028
	26	7.2	7.7291	4.1	0.57	1.073
	27	8.7	9.9222	9	1.03	1.14
	28	5.5	7.4625	8.2	1.49	1.357
	29	10	8.7757	9.7	0.97	0.878
	30	8.9	7.828	6.8	0.76	0.88
	31	6.7	6.9439	10.2	1.52	1.036
	32	7.6	7.2833	13.5	1.78	0.958
	33	5.2	5.4081	4	0.76	1.04
	34	5.1	5.15	4.69	0.92	1.01
	35	3.8	3.44	3.8	1	0.91
	36	6.6	6.66	5.21	0.79	1.01
Spangemacher (1991)	37	19.8	19.103	15.4	0.78	0.965
	38	6.4	7.3038	9.1	1.42	1.141
	39	7.8	6.9657	9.3	1.19	0.893
	40	18.9	19.385	11.5	0.61	1.026
	41	12	11.851	7.7	0.64	0.988
	42	9.3	9.641	6.2	0.67	1.037
	43	1.5	1.456	3.9	2.6	0.971
	44	10.3	10.326	19.6	1.9	1.003
	45	2.6	2.1458	3.7	1.44	0.825
	46	20.5	20.506	14.1	0.69	1
	47	34.1	34.022	19.8	0.58	0.998
	48	6.4	6.4972	7.6	1.18	1.015
	49	19	19.145	9.3	0.49	1.008
	50	6.4	6.1561	5.8	0.9	0.962
	51	4.1	4.328	3.1	0.76	1.056
	52	10.4	9.9356	9.4	0.9	0.955
	56	0.9	0.89634	4.3	4.78	0.996
	57	2.7	2.8713	5.1	1.88	1.063
	58	16.9	16.966	14.9	0.88	1.004
	59	8.3	8.19	7.06	0.85	0.99
	60	9.5	9.9	9.41	0.99	1.04
Boreave et al. (1993)	61	9.2	10.663	10.8	1.17	1.159
	62	12.1	12.549	11.7	0.97	1.037
	63	24.3	24.436	16.5	0.68	1.006
	64	16.8	16.645	13.6	0.81	0.991
	65	10	9.2012	9.9	0.99	0.92
Kemp (1985,1991)	66	2.7	3.1854	2.7	0.99	1.18
	67	6.6	6.5085	9.5	1.44	0.986

Table 6.14 cont'd

	68	15.2	15.976	12.2	0.8	1.051
	69	14.8	14.755	10.4	0.7	0.997
	70	8.4	8.261	6.2	0.74	0.983
Suzuki et al (1994)	73	33.4	33.75	30.06	0.9	1.01
	74	19.2	19.09	26.88	1.4	0.99
	75	22.3	21.67	13.6	0.61	0.97
	76	9.4	9.47	11.75	1.25	1.01
	77	27.2	27.13	25.3	0.93	1
	78	18.5	19.04	19.61	1.06	1.03
	79	15.7	15.87	17.43	1.11	1.01
	80	7.7	6.99	3.85	0.5	0.91

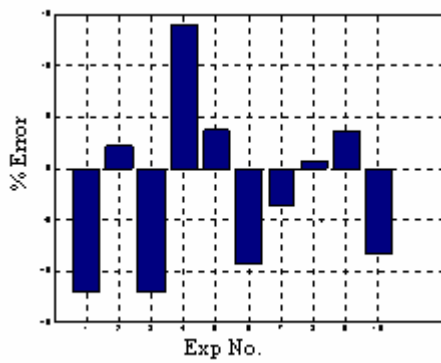


Fig 6.52 % Error of test set

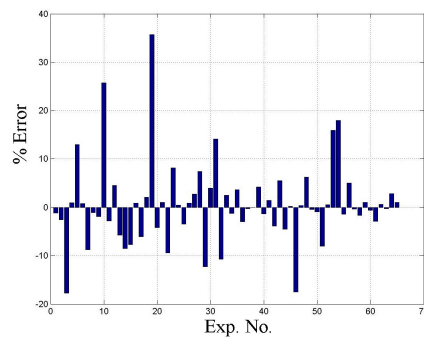


Fig 6.53 % Error of training set

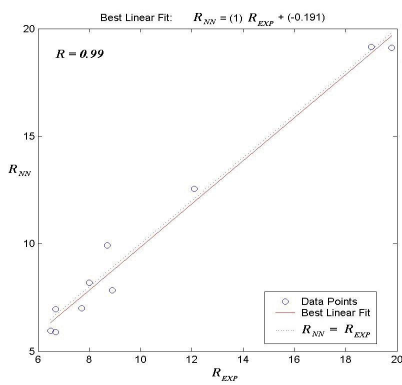


Fig 6.54 Prediction of NN and actual values for testing set

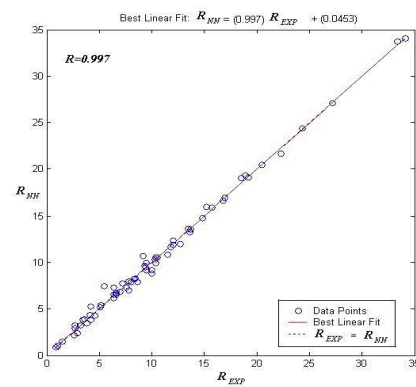


Fig 6.55 Prediction of NN and actual values for learning set

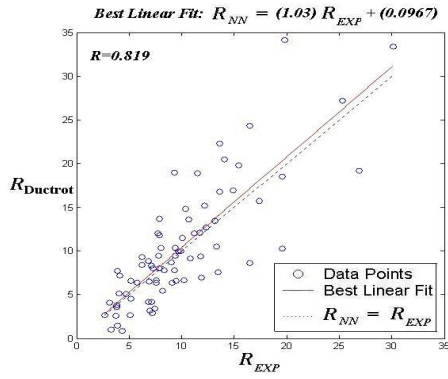


Fig 6.56 Overall performance of DUCTROT vs. experimental results

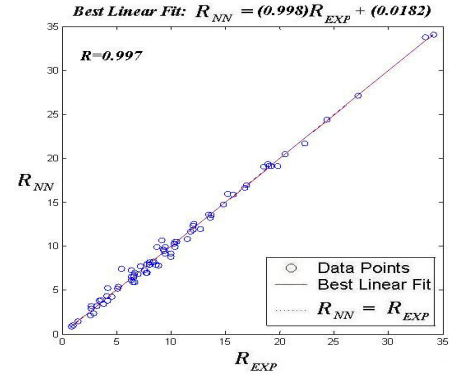


Fig 6.57 Overall performance of NN vs. experimental results

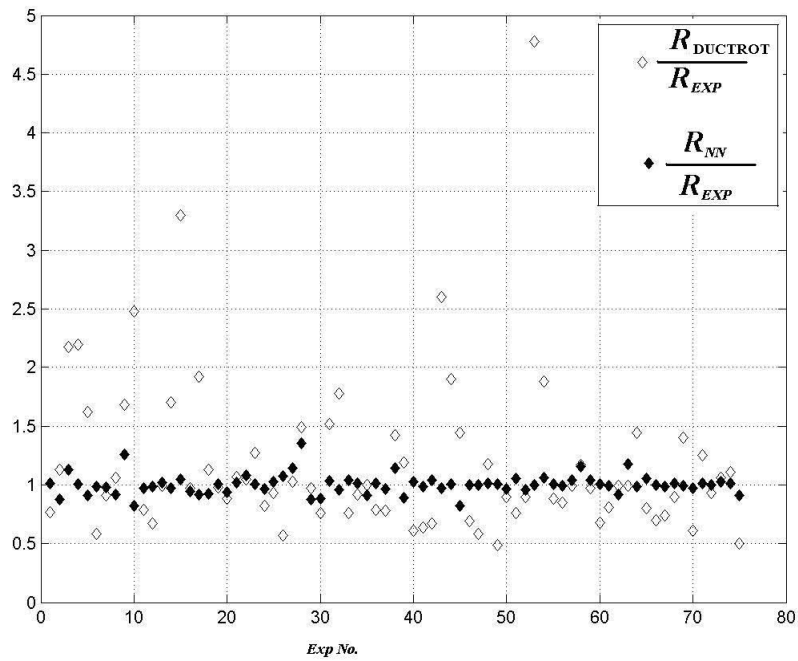


Fig 6.58 Comparison of NN and DUCTROT Results (NN Results/Experimental Results) vs. (DUCTROT results/experimental results)

6.2.4.4 Closed Form Solution of Available Rotation Capacity

The main focus is to obtain the explicit formulation of available rotation as a function of geometric and mechanical properties of a steel beam as follows:

$$R = f(b, d, t_f, t_w, L, F_{yf}, F_{yw})$$

$$R = 30 * \left(\frac{2}{1 + e^{-2W}} - 1 \right)$$

Where

W=

$$\begin{aligned} & (-0.49) * \left(\frac{2}{1 + e^{-2U_1}} - 1 \right) + (-1.23) * \left(\frac{2}{1 + e^{-2U_2}} - 1 \right) + (0.76) * \left(\frac{2}{1 + e^{-2U_3}} - 1 \right) + (- \\ & 0.21) * \left(\frac{2}{1 + e^{-2U_4}} - 1 \right) + (-0.54) * \left(\frac{2}{1 + e^{-2U_5}} - 1 \right) + (0.46) * \left(\frac{2}{1 + e^{-2U_6}} - 1 \right) + \\ & (0.26) * \left(\frac{2}{1 + e^{-2U_7}} - 1 \right) + (0.43) * \left(\frac{2}{1 + e^{-2U_8}} - 1 \right) + (0.18) * \left(\frac{2}{1 + e^{-2U_9}} - 1 \right) + \\ & (-1.1) * \left(\frac{2}{1 + e^{-2U_{10}}} - 1 \right) + (0.34) * \left(\frac{2}{1 + e^{-2U_{11}}} - 1 \right) + (-0.72) * \left(\frac{2}{1 + e^{-2U_{12}}} - 1 \right) + \\ & (0.94) * \left(\frac{2}{1 + e^{-2U_{13}}} - 1 \right) + (-0.32) * \left(\frac{2}{1 + e^{-2U_{14}}} - 1 \right) + (-0.28) * \left(\frac{2}{1 + e^{-2U_{15}}} - 1 \right) + \\ & (-0.44) * \left(\frac{2}{1 + e^{-2U_{16}}} - 1 \right) + (-0.42) * \left(\frac{2}{1 + e^{-2U_{17}}} - 1 \right) + 1.2761 \end{aligned}$$

And the values for U_i are given as

$$U_1 = (-0.0030*b) + (-0.0069*d) + (-0.0446*t_f) + (-0.1268*t_w) + (-0.0064*L) + (-0.0057*F_{yf}) + (0.0216*F_{yw}) + (7.7055)$$

$$U_2 = (0.0118*b) + (-0.0087*d) + (-0.1200*t_f) + (0.2558*t_w) + (0.0042*L) + (0.0020*F_{yf}) + (-0.0182*F_{yw}) + (-4.0409)$$

$$U_3 = (0.0164*b) + (-0.0079*d) + (0.0216*t_f) + (0.1022*t_w) + (-0.0049*L) + (-0.0009*F_{yf}) + (-0.0350*F_{yw}) + (1.0284)$$

$$U_4 = (-0.0068*b) + (0.0111*d) + (-0.0763*t_f) + (0.2126*t_w) + (-0.0026*L) + (-0.0018*F_{yf}) + (-0.0391*F_{yw}) + (1.4254)$$

$$U_5 = (0.0197*b) + (-0.0007*d) + (0.1097*t_f) + (-0.0679*t_w) + (0.0077*L) + (-0.0009*F_{yf}) + (0.0058*F_{yw}) + (-4.3808)$$

$$U_6 = (0.0215*b) + (0.0088*d) + (0.1084*t_f) + (0.1463*t_w) + (0.0101*L) + (-0.0008*F_{yf}) + (0.0038*F_{yw}) + (-9.5772)$$

$$U_7 = (-0.0198*b) + (-0.0032*d) + (0.0735*t_f) + (-0.1733*t_w) + (-0.0055*L) + (-0.0039*F_{yf}) + (0.0148*F_{yw}) + (6.3085)$$

$$U_8 = (0.0159*b) + (0.0002*d) + (0.1253*t_f) + (0.0094*t_w) + (0.0052*L) + (-0.0048*F_{yf}) + (-0.0317*F_{yw}) + (0.32208)$$

$$U_9 = (-0.0137*b) + (0.0009*d) + (0.1260*t_f) + (0.2475*t_w) + (0.0054*L) + (-0.0005*F_{yf}) + (0.0183*F_{yw}) + (-3.6989)$$

$$U_{10} = (0.0134*b) + (-0.0058*d) + (0.1183*t_f) + (-0.2687*t_w) + (0.0063*L) + (-0.0025*F_{yf}) + (-0.0136*F_{yw}) + (2.9629)$$

$$U_{11} = (-0.0214*b) + (0.00001*d) + (-0.0104*t_f) + (-0.2379*t_w) + (-0.0034*L) + (-0.0025*F_{yf}) + (0.0329*F_{yw}) + (1.5795)$$

$$U_{12} = (-0.0149*b) + (0.0066*d) + (-0.1811*t_f) + (0.0459*t_w) + (0.0050*L) + (0.0030*F_{yf}) + (0.0046*F_{yw}) + (-3.0545)$$

$$U_{13} = (-0.0059*b) + (0.0020*d) + (-0.1195*t_f) + (0.2602*t_w) + (0.0047*L) + (0.0006*F_{yf}) + (-0.0310*F_{yw}) + (-2.4884)$$

$$U_{14} = (0.0166*b) + (0.0118*d) + (0.0131*t_f) + (-0.2199*t_w) + (-0.0024*L) + (-0.0038*F_{yf}) + (-0.0087*F_{yw}) + (2.6819)$$

$$U_{15} = (0.0270*b) + (-0.0004*d) + (-0.1223*t_f) + (0.1090*t_w) + (0.0034*L) + (0.0010*F_{yf}) + (0.0177*F_{yw}) + (-2.087)$$

$$U_{16} = (-0.0011*b) + (0.0041*d) + (0.1165*t_f) + (0.1084*t_w) + (0.0092*L) + (0.0041*F_{yf}) + (-0.0070*F_{yw}) + (-7.7875)$$

$$U_{17} = (-0.0149*b) + (-0.0144*d) + (0.1253*t_f) + (0.1583*t_w) + (0.0019*L) + (-0.0005*F_{yf}) + (-0.0144*F_{yw}) + (-0.53283)$$

It should be noted that the proposed explicit formulation of the NN model presented above is valid for the ranges of training set given in Table 6.12.

6.2.4.5 Conclusion

This case study presents a new and efficient approach for the prediction of available rotation capacity of wide flange beams using NNs. The database used for NN training is based on experimental results from literature. Backpropagation NNs are used for training process. The proposed NN model shows perfect agreement with experimental results ($R = 0.997$) where its accuracy is also quite high (MAPE=%5.1). Numerical results of the same database are obtained by a specialized computer program (DUCTROT) and are used for comparative analysis. The correlation and accuracy of numerical results with experimental results is found to be quite poor ($R = 0.0819$ and MAPE= % 35). Thus NN results are seen to be by far

more accurate compared to numerical results. The proposed NN model is valid for the ranges of the training set. The explicit formulation of available rotation capacity based on proposed NN model is also obtained and presented. As a result the proposed NN model and formulation of the available rotation capacity of wide flange beams is quite accurate, fast and practical for use compared to FE models.

6.2.5 Strength Enhancement of Corner Regions in cold-formed steel

6.2.5.1 Introduction

This case study presents an alternative NN approach for predicting the enhanced strength of the corner regions of cold-formed stainless steel sections. Strength enhancement of the corner regions is primarily due to plastic strains that occur during cold-forming process of stainless steel. Neural networks are proposed as a soft computing technique for the prediction of strength enhancement. Training and test sets for the NN models are collected from test results available in literature. The results of the NN models are compared with previous experimental and statistical studies from literature and found to be quite satisfactory. The explicit formulations of the proposed NN models are also presented.

The use of stainless steel tubular sections in structural applications is increasing day by day. There are various codes concerning the design of cold-formed stainless steel sections (ASCE, 1991, AUST/NZS, 2001, EUROCEODE 3, 1996)

The plastic behaviour of stainless steel is quite complicated to be modeled. Several models exist for the modeling of plastic behaviors of steel which are valid for simple load cases in general. However for more complicated loading cases simple models can not depict the plastic behaviour of stainless steels as in the case of cold-working process (Gozzi, 2003). Cold-working process of the virgin material causes significant enhancement of mechanical behaviour of stainless steel. Stainless steel shows significant strain hardening which leads to strength enhancement in the corner regions of cold-formed sections having 0.2% proof strengths much higher than that

of the flat material. In spite of the fact that utilization of strength enhancement in corner regions may lead to an economic design in stainless steel structural applications, it is not allowed to use it without testing, if material is welded after cold working (EUROCEODE 3, 1996). Therefore the load carrying capacity is in general underestimated. In these situations the load carrying capacity should be modified by a correction factor considering the effect of strength enhancement in corner regions. For instance strength enhancement in corner regions may have significant effect on load carrying capacity as in the case of stocky sections since they have larger proportion of corner area.

Various statistical models have been proposed in literature (Van der Berg and Van der Merwe, 1992, Ashraf et al., 2005) for the prediction of 0.2% proof strength and ultimate strength of corner regions.

This case study proposes an alternative method for the strength enhancement in corner regions based Neural Networks. In cases where a structural problem is too difficult to be modeled mathematically, NNs may serve as a robust alternative for the solution of such problems.

6.2.5.2 Strength Enhancement of Corner Regions

Karren (1967) has performed the first study on strength enhancement of Carbon steel. Karen performed a series of tests and observed 2 important parameters effecting the strength enhancement at corners: r_i/t and σ_u/σ_y of the virgin material where r_i , t , σ_u and σ_y are radius, thickness, corresponding strength values. The first study on strength enhancement of stainless steel sections has been performed by Coetzee et al. (1990). They studied the corner effect on lipped channel section formed by press barking.

As a result of an extensive study Van den Berg and Van der Merwe (1992) proposed the following equations for the prediction of corner 0.2% proof strength as follows:

$$\sigma_{0.2,c} = \frac{B_c \sigma_{0.2,v}}{\left(\frac{r_i}{t}\right)^m} \quad (6.16)$$

Where

$$B_c = 3.289 \left(\frac{\sigma_{u,v}}{\sigma_{0.2,v}} \right) - \left(\frac{\sigma_{u,v}}{\sigma_{0.2,v}} \right)^2 - 1.34 \quad (6.17)$$

$$m = 0.06 \left(\frac{\sigma_{u,v}}{\sigma_{0.2,v}} \right) + 0.031 \quad (6.18)$$

where

$\sigma_{0.2,v}$ = 0.2% proof strength of virgin material

$\sigma_{u,v}$ = ultimate strength of virgin material

$$\sigma_{0.2,c} = \frac{1.881\sigma_{0.2,v}}{\left(\frac{r_i}{t} \right)^{0.194}} \quad (6.19)$$

Experimental studies on strength enhancement at corners of stainless steel hollow sections have been performed by Gardner (2002), Rasmussen and Hancock (1993). Tests on cold-worked austenitic (Grade 1.4318) stainless steel RHS have been continued by Gardner and Talja (2003). All available test results are given in Table 6.15. The soft computing models in this study are based on these experimental results given in Table 6.15.

Table 6.15 Available test results

*Bold values are test sets

Reference	Virgin Material		r_i / t	Corner Material	
	$\sigma_{0.2,v}$ (MPa)	$\sigma_{u,v}$ (MPa)		$\sigma_{0.2,c}$ (MPa)	$\sigma_{u,c}$ (MPa)
	224	395	1.8	370	431
	224	395	1.87	374	431
	224	395	3	365	424
	224	395	3.26	353	418
	224	395	4.2	350	420
	224	395	4.31	334	412
	224	395	5.36	328	409
	224	395	5.97	317	403
	224	395	6.24	322	405
	224	395	7.09	305	399
	277	435	1.61	423	508

Table 6.15 cont'd

	277	435	2.25	450	518
	277	435	3.08	437	506
	277	435	3.16	420	497
	277	435	4.09	409	496
	277	435	4.33	392	493
	277	435	5.1	371	482
	277	435	5.64	379	484
	277	435	6.25	396	486
	277	435	6.7	371	487
	295	671	1.99	452	775
	295	671	2.22	425	762
	295	671	3.4	407	759
	295	671	3.43	397	744
	295	671	4.43	398	753
	295	671	4.47	374	–
	295	671	5.75	362	730
	295	671	5.85	358	725
	295	671	6.63	366	732
	295	671	7.03	–	–
	304	518	1.94	471	574
	304	518	2.39	488	583
	304	518	3.12	458	564
	304	518	3.53	–	–
	304	518	4.32	451	560
	304	518	4.61	442	553
	304	518	5.3	435	551
	304	518	6.09	415	547
	304	518	6.54	418	548
(Van der Berg and Ven der Merwe,1992)	304	518	7.27	407	548
	277	621	1.37	487	710
	277	621	1.42	486	700
	277	621	2.05	445	676
	277	621	2.13	444	685
	296	685	1.15	552	836
	296	685	1.28	520	811
	296	685	2.23	471	795
	296	685	2.24	464	793
	299	462	1.35	519	532
	299	462	1.38	528	541
	299	462	2.2	486	525
Coetzee et al. (1990).	299	462	2.25	482	523
	291	628	1.2	594	820
	275	6230	0.68	587	820
	304	613	1.6	563	844
	318	612	0.92	631	802
Gardner (2002)	289	600	1.46	572	809
Rasmussen and Hancock (1993)	297	614	0.83	580	805
	361	755	2.09	614	941
Gardner and Talja (2003).	548	986	1.8	807	1162

In a recent study Ashraf et al. (2005) compared available test results with predictions of Van den Berg and Van der Merwe's model and proposed alternative power models based on test results given in Table 6.15. He proposed a general expression for the relationship given as:

$$\frac{\sigma_{0.2,c}}{\sigma_{u,v}} = \frac{C_1}{\left(\frac{r_i}{t}\right)^{C_2}} \quad (6.20)$$

Where

$$C_1 = -0.382 \left(\frac{\sigma_{u,v}}{\sigma_{0.2,v}} \right) + 1.711$$

$$C_2 = 0.176 \left(\frac{\sigma_{u,v}}{\sigma_{0.02,v}} \right) - 0.1496$$

Ashraf also proposed a relationship for the prediction of $\sigma_{u,c}$ given as follows:

$$\sigma_{u,c} = 0.75 \sigma_{0.2,c} \left(\frac{\sigma_{u,v}}{\sigma_{0.2,v}} \right) \quad (6.21)$$

6.2.5.3 Numerical Application

The main focus of this study is to predict the enhanced strength of the corner regions of cold-formed stainless steel sections and its closed-form solution by means of NNs based on experimental results from literature. Therefore an extensive literature survey has been performed for available experimental results. Experimental results in Table 6.15 were and used as training and test sets for NN training.

6.2.5.3 a) Results of NN and Models for the Prediction of $\sigma_{0.2,c}$

The optimal NN architecture in this part was found to be 3-5-1 NN architecture with hyperbolic tangent sigmoid transfer function (tansig). The training algorithm was quasi-Newton back propagation (BFGS). The optimum NN model is given in Fig 6.59. Statistical parameters of learning and training sets of NN model are presented in Table 6.16. The prediction of the proposed NN model vs. actual experimental

values is given in Table 6.17. The % errors and Prediction of NN and actual values of learning and testing sets and their corresponding correlation are given in Figs 6.60-6.63. The % errors and. The overall comparison of the proposed NN model results with various statistical models is given in table 6.18.

Table 6.16 Statistical parameters of the proposed NN models

	MSE	RMSE	SSE	MAPE (%)
NN Train Set	144.66	12.027	7232.8	2.1014
NN Test Set	207.49	14.404	1659.9	2.4525

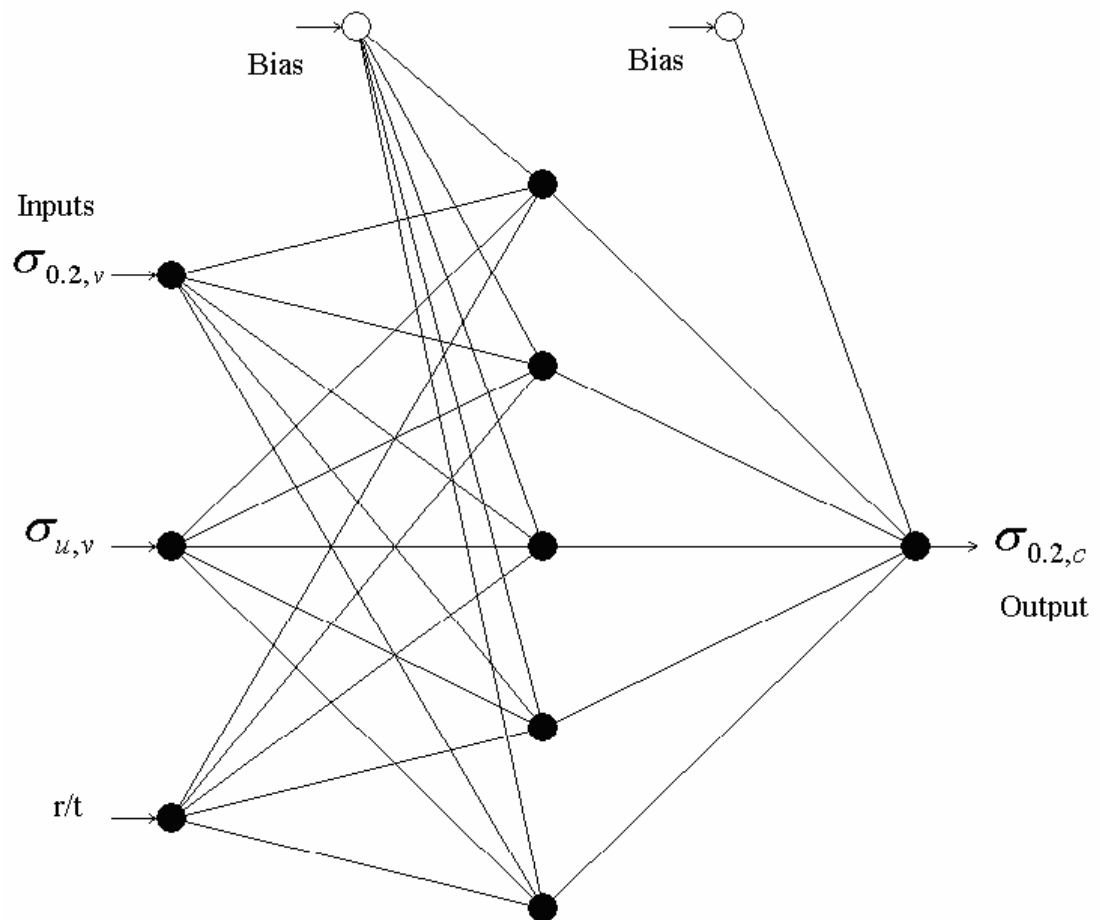


Fig 6.59 Proposed NN model for the prediction of $\sigma_{0.2,c}$

Table 6.17 Results of NN models for the prediction of $\sigma_{0.2,c}$

*Bold values are test set

Reference	$\sigma_{0.2,v}$ (MPa)	$\sigma_{u,v}$ (MPa)	r/t	$\sigma_{0.2,c}$ (Exp.)	$\sigma_{0.2,c}$ (NN)	NN/Exp.
	224	395	1.8	370	369.46	1.00
	224	395	1.87	374	369.03	0.99
	224	395	3	365	359.82	0.99
	224	395	3.26	353	357.11	1.01
	224	395	4.2	350	345.99	0.99
	224	395	4.31	334	344.62	1.03
	224	395	5.36	328	332.18	1.01
	224	395	5.97	317	325.43	1.03
	224	395	6.24	322	321.85	1.00
	224	395	7.09	305	298.56	0.98
	277	435	1.61	423	437.57	1.03
	277	435	2.25	450	427.96	0.95
	277	435	3.08	437	415.78	0.95
	277	435	3.16	420	414.61	1.05
	277	435	4.09	409	401.27	0.98
	277	435	4.33	392	397.98	1.02
	277	435	5.1	371	388.53	1.05
	277	435	5.64	379	383.75	1.01
	277	435	6.25	396	381.3	0.96
	277	435	6.7	371	381.75	1.03
	295	671	1.99	452	464.86	0.99
	295	671	2.22	425	449.65	1.03
	295	671	3.4	407	406.11	1.06
	295	671	3.43	397	405.45	1.00
	295	671	4.43	398	384.69	1.00
	295	671	4.47	374	383.84	1.02
	295	671	5.75	362	361.28	1.03
	295	671	5.85	358	360.57	1.00
	295	671	6.63	366	366.67	1.01
	304	518	1.94	471	490.78	1.03
	304	518	2.39	488	481.62	1.04
	304	518	3.12	458	465.42	0.99
	304	518	4.32	451	437.52	1.00
	304	518	4.61	442	431.51	1.02
	304	518	5.3	435	420.6	0.98
	304	518	6.09	415	416.03	0.97
	304	518	6.54	418	416.17	1.00
(Van der Berg and Ven der Merwe,1992)	304	518	7.27	407	411.7	1.00
	277	621	1.37	487	512.2	1.05
	277	621	1.42	486	506.7	1.04
	277	621	2.05	445	441.14	0.99
	277	621	2.13	444	433.54	0.98
	296	685	1.15	552	533.22	0.97

Table 6.17 cont'd

Coetzee et al. (1990).	296	685	1.28	520	520.53	1.00
	296	685	2.23	471	460.47	0.98
	296	685	2.24	464	460.12	0.99
	299	462	1.35	519	517.44	1.00
	299	462	1.38	528	516.65	0.98
	299	462	2.2	486	495.77	1.02
	299	462	2.25	482	494.54	1.03
Gardner (2002)	291	628	1.2	594	568.91	0.96
	275	623	0.68	587	581.79	0.99
	304	613	1.6	563	563.71	1.00
	318	612	0.92	631	616.03	0.98
	289	600	1.46	572	545.44	0.95
Rasmussen and Hancock (1993)	297	614	0.83	580	609.05	1.05
Gardner and Talja (2003).	361	755	2.09	614	616.56	1.00
	548	986	1.8	807	808.85	1.00

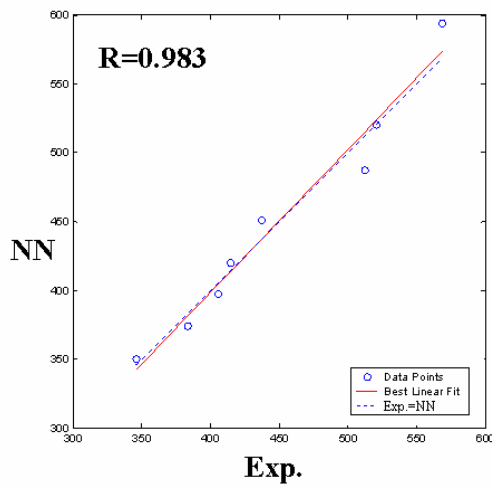


Fig 6.60 Performance of NN model for test set

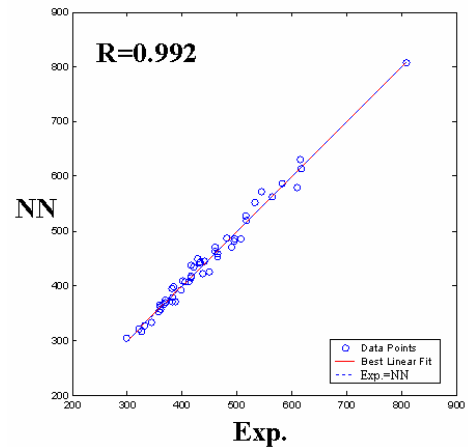


Fig 6.61 Performance of NN model for training set

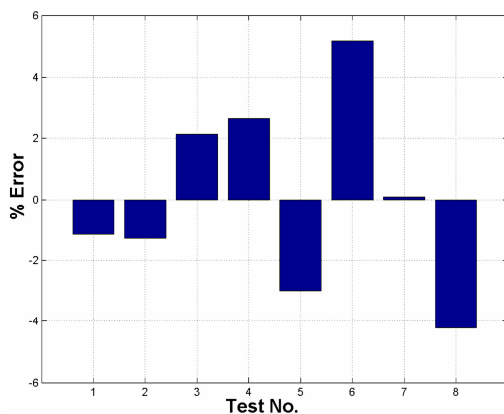


Fig 6.62 % Error for test set (NN Model)

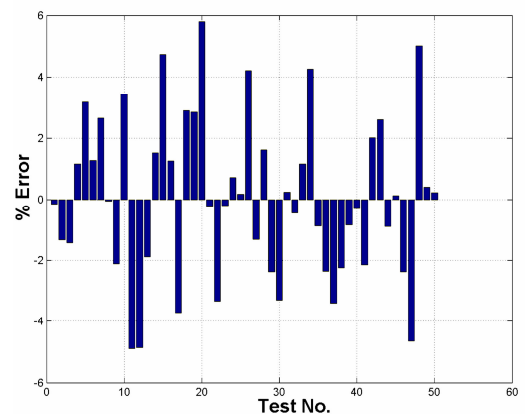


Fig 6.63 % Error for training set (NN model)

Table 6.18 Comparison of the proposed NN models for the Prediction of $\sigma_{0.2,c}$ with previous statistical models

Reference	No. Of Exp	Model Van der berg Eqn 1-3	Std dev Pred./Test Model Van der berg Eqn 1-3	Simple Power Model Eqn. 4	Std dev Pred./Test Model Eqn. 4	Power Model Eqns 5-7 using σ_u	Std dev Pred./Test Model Eqns 5-7 using σ_u	Avg of Pred./Test NN Model	Std dev Pred./Test NN Model
Coetzee et al. (1990)	12	0.92	0.02	1.01	0.01	0.99	0.02	1.00	0.03
Van der Berg and Van der Merwe, (1992)	40	1.00	0.03	1.01	0.06	1.00	0.04	1.01	0.03
Rasmussen and Hancock (1993)	1	0.94	-	1.00	-	1.01	-	1.00	-
Gardner (2002)	5	0.87	0.04	0.92	0.04	0.93	0.04	0.98	0.02
Gardner and Talja (2003)	2	1.00	-	1.05	-	1.06	-	1.03	-
All test results	60	0.97	0.05	1.00	0.06	1.00	0.04	1.00	0.03

6.2.5.3 b) Results of NN models for the prediction of $\sigma_{u,c}$

The optimal NN architecture in this part was found to be 3-7-1 NN architecture with hyperbolic tangent sigmoid transfer function (tansig). The training algorithm was quasi-Newton back propagation (BFGS). The optimum NN model is given in Fig

6.64. Statistical parameters of learning and training sets of NN training are presented in Table 6.19. The prediction of the proposed NN model vs. actual experimental values is given in Table 6.20. The % errors and Prediction of NN model and actual values of learning and testing sets and their corresponding correlation are given in Figs 6.65-6.68. The overall comparison of the proposed NN model results with various statistical models is given in Table 6.21.

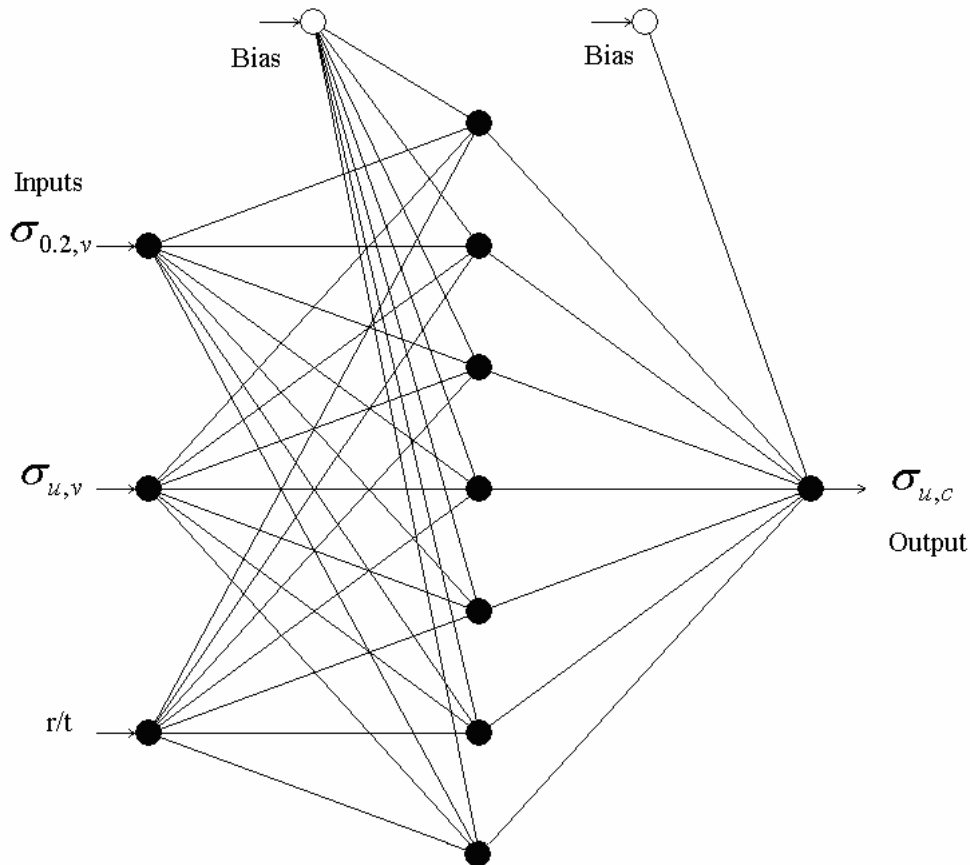


Fig 6.64 Proposed NN Model for the prediction of $\sigma_{u,c}$

Table 6.19 Statistical parameters of the proposed NN models

	MSE	RMSE	SSE	MAPE (%)
NN Train Set	83.527	9.1393	4176.3	0.96626
NN Test Set	329.89	18.163	2309.3	2.4476

Table 6.20 Results of NN models for the Prediction of $\sigma_{u,c}$

*Bold values are test set

Reference	$\sigma_{0.2,v}$ (MPa)	$\sigma_{u,v}$ (MPa)	r/t	$\sigma_{0.2,c}$ (Exp)	$\sigma_{0.2,c}$ (NN)	NN/Exp.
	224	395	1.80	431.00	445.56	1.03
	224	395	1.87	431.00	445.14	1.03
	224	395	3	424	421.48	0.99
	224	395	3.26	418	419.81	1.00
	224	395	4.20	420	413.59	0.98
	224	395	4.31	412	412.84	1.00
	224	395	5.36	409	405.49	0.99
	224	395	5.97	403	401.03	1.00
	224	395	6.24	405	399.01	0.99
	224	395	7.09	399	392.47	0.98
	277	435	1.61	508	514.65	1.01
	277	435	2.25	518	513.06	0.99
	277	435	3.08	506	505.96	1.00
	277	435	3.16	497	494.78	1.00
	277	435	4.09	496	491.52	0.99
	277	435	4.33	493	490.85	1.00
	277	435	5.10	482	488.64	1.01
	277	435	5.64	484	487.04	1.01
	277	435	6.25	486	485.18	1.00
	277	435	6.70	487	483.77	0.99
	295	671	1.99	775	775.75	1.00
	295	671	2.22	762	774.59	1.02
	295	671	3.40	759	768.42	1.01
	295	671	3.43	744	768.26	1.03
	295	671	4.43	753	753.03	1.00
	295	671	5.75	730	738.32	1.01
	295	671	5.85	725	737.71	1.02
	295	671	6.63	732	732.86	1.00
	304	518	1.94	574	575.99	1.00
	304	518	2.39	583	574.91	0.99
	304	518	3.12	564	573.11	1.02
	304	518	4.32	560	553.36	0.99
	304	518	4.61	553	552.59	1.00
	304	518	5.30	551	550.71	1.00
	304	518	6.09	547	548.48	1.00
	304	518	6.54	548	547.18	1.00

Table 6.20 cont'd

Van der Berg and Ven der Merwe (1992)	304	518	7.27	548	545.01	0.99
	277	621	1.37	710	690.11	0.97
	277	621	1.42	700	689.76	0.99
	277	621	2.05	676	685.87	1.01
	277	621	2.13	685	685.38	1.00
	296	685	1.15	836	836	1.00
	296	685	1.28	811	790.71	0.97
	296	685	2.23	795	770.23	0.97
	296	685	2.24	793	770.18	0.97
	299	462	1.35	532	528.18	0.99
	299	462	1.38	541	528.13	0.98
	299	462	2.20	525	526.66	1.00
Coetzee et al. (1990)	299	462	2.25	523	526.57	1.01
	304	613	1.60	820	811.75	0.99
	318	612	0.92	844	829.16	0.98
	289	600	1.46	802	795.32	0.99
	291	628	1.20	820	790.17	0.96
Gardner (2002)	275	623	0.68	820	819.98	1.00
Rasmussen and Hancock (1993)	297	614	0.83	809	811.33	1.00
	361	755	2.09	805	835.34	1.04
Gardner and Talja (2003)	548	986	1.80	941	941	1.00

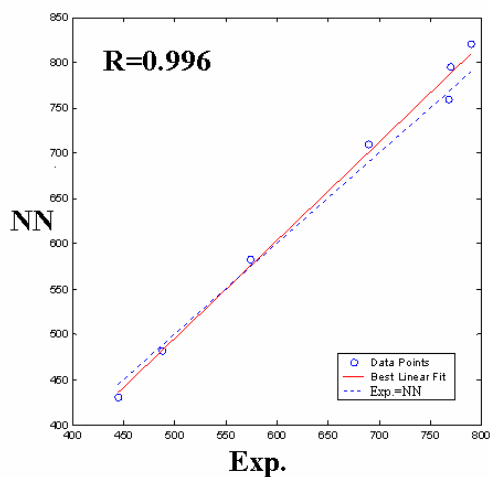


Fig 6.65 Performance of NN model for test set

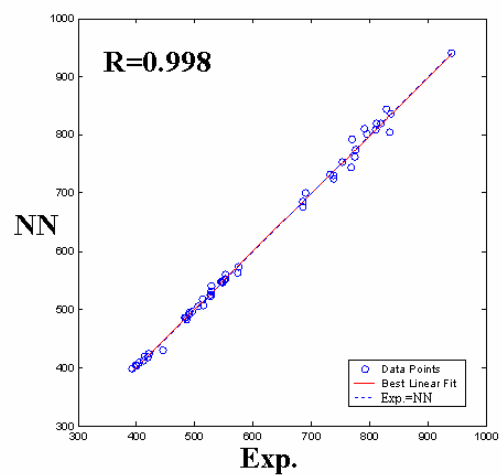


Fig 6.66 Performance of NN model for training set

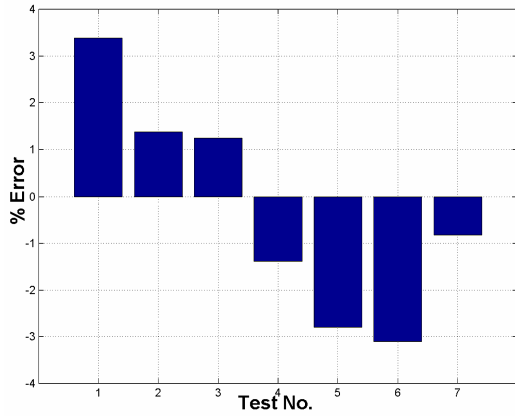


Fig 6.67 % Error for training set (NN model)

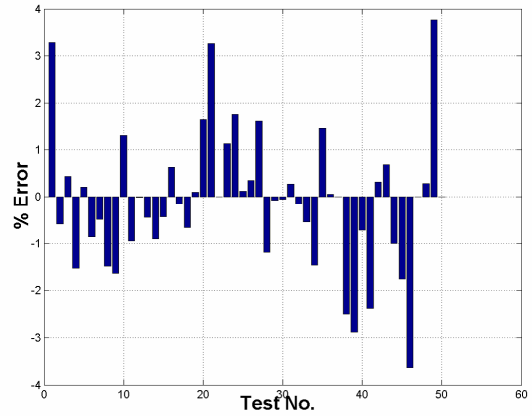


Fig 6.68 % Error for test set (NN model)

Table 6.21 Comparison of the proposed NN models for the prediction of $\sigma_{u,c}$ with previous statistical models

Reference	No. Of Exp	Pred./Test Model based on Eqn 4	Std dev Pred./Test Model Based on Eqn 4	Pred./Test Model based on Eqn 5	Std dev Pred./Test Model Based on Eqn 5	Avg of Pred./Test NN Model	Std dev Pred./Test NN Model
Coetzee et al. (1990)	12	1.11	0.05	1.09	0.06	1.00	0.03
Van der Berg and Ven der Merwe (1992)	40	0.98	0.07	0.98	0.08	1.00	0.03
Rasmussen and Hancock (1993)	1	1.11	–	1.13	–	1.05	–
Gardner (2002)	5	1.04	0.09	1.05	0.10	0.98	0.02
Gardner and Talja (2003)	2	1.14	0.09	1.13	0.07	1.00	0.003
All test results	60	1.02	0.09	1.02	0.09	1.00	0.03

6.2.5.4 Explicit Formulation of NN Models

The main focus is to obtain the explicit formulation of strength enhancement of 0.2% proof and ultimate strength of virgin material due to cold-working as follows:

$$\sigma_{0.2,c} = f(\sigma_{0.2,v}, \sigma_{u,v}, r_i/t)$$

$$\sigma_{u,c} = f(\sigma_{0.2,v}, \sigma_{u,v}, r_i/t)$$

6.2.5.4 a) Explicit Formulation of Enhanced 0.2% Proof Strength

w_{ij} is the weight matrix of the first hidden layer given in table 7 and X_j is the corresponding parameter vector given as

$\mathbf{X} = [(\sigma_{0.2,v}, \sigma_{u,v}, r_i/t)]$ where

b_i is the bias matrix to the first hidden layer given as

$$\mathbf{b} = [4.4358 \ -11.743 \ 4.1495 \ 3.9927 \ 2.8927 \ -1.7135 \ -6.8101 \]$$

The summation u_i is transformed using a scalar-to-scalar function called an "activation or transfer function", $F(u_i)$ yielding a value called the unit's "activation".

Following the steps above leads to:

$$u_1 = (-10.443 * \sigma_{0.2,v}) + (7.2253 * \sigma_{u,v}) + (1.046 * r_i/t)$$

$$u_2 = (3.8411 * \sigma_{0.2,v}) + (4.2688 * \sigma_{u,v}) + (1.8934 * r_i/t)$$

$$u_3 = (6.0138 * \sigma_{0.2,v}) + (-9.1724 * \sigma_{u,v}) + (-3.5332 * r_i/t)$$

$$u_4 = (5.9001 * \sigma_{0.2,v}) + (-9.1399 * \sigma_{u,v}) + (-3.0234 * r_i/t)$$

$$u_5 = (2.6697 * \sigma_{0.2,v}) + (-5.5196 * \sigma_{u,v}) + (-0.39746 * r_i/t)$$

$$u_6 = (-2.1414 * \sigma_{0.2,v}) + (-3.8593 * \sigma_{u,v}) + (5.1458 * r_i/t)$$

$$u_7 = (-3.0475 * \sigma_{0.2,v}) + (3.4746 * \sigma_{u,v}) + (5.0314 * r_i/t)$$

The activation function used in this study is hyperbolic tangent sigmoid transfer function (tansig)

$$f(u_i) = \left(\frac{2}{1 + e^{-2(u_i)}} - 1 \right) \text{ performed for each hidden node in the first hidden layer}$$

Thus the output is

$$O = \Sigma (w2_i * f(u_i)) + b2$$

where $w2_i$ is the weight vector to the output layer given as

$$w2_i = [-0.83853 \ -5.8502 \ -2.9442 \ 3.9058 \ -1.7232 \ -0.80867 \ 7.8143]$$

and $b2$ is the bias added which is

$$b2 = 3.1659$$

It should be noted that the inputs entering the network have been normalized before the training as

$$\sigma_{0.2,v} = \sigma_{0.2,v}^* / 400 \quad \sigma_{u,v} = \sigma_{u,v}^* / 800 \quad r_i / t = (r_i / t)^* / 10$$

And the output before the training has been normalized by 700 thus the final output is

$$R = \left(\frac{2}{1 + e^{-2o}} - 1 \right) * 700$$

The proposed NN models are valid for the range of variables given in table 6.15

Table 6.22 Weight matrix of the first hidden layer of the proposed NN model

[i,j]	1	2	3
1	-10.443	7.2253	1.046
2	3.8411	4.2688	1.8934
3	6.0138	-9.1724	-3.5332
4	5.9001	-9.1399	-3.0234
5	2.6697	-5.5196	-0.39746
6	-2.1414	-3.8593	5.1458
7	-3.0475	3.4746	5.0314

6.2.5.4 b) Explicit Formulation of Enhanced Ultimate Strength

w_{ij} is the weight matrix of the first hidden layer given in table 7 and X_j is the corresponding parameter vector given as

$$\mathbf{X} = [(\sigma_{0.2,v}, \sigma_{u,v}, r_i / t)]$$

b_i is the bias matrix to the first hidden layer given as

$$\mathbf{b} = [-33.35 \ 14.505 \ 275.47 \ 13.019 \ 1.4697]$$

Following the steps above leads to:

$$u_1 = (-26.323 * \sigma_{0.2,v}) + (-25.018 * \sigma_{u,v}) + (-2.4366 * r_i / t)$$

$$u_2 = (13.022 * \sigma_{0.2,v}) + (-312 * \sigma_{u,v}) + (52.037 * r_i / t)$$

$$u_3 = (-243.69 * \sigma_{0.2,v}) + (-138.21 * \sigma_{u,v}) + (0.031021 * r_i / t)$$

$$u_4 = (-47.705 * \sigma_{0.2,v}) + (-103.11 * \sigma_{u,v}) + (245.64 * r_i / t)$$

$$u_5 = (4.0463 * \sigma_{0.2,v}) + (-1.8046 * \sigma_{u,v}) + (-0.25829 * r_i / t)$$

The activation function used in this study is hyperbolic tangent sigmoid transfer function (tansig)

$$f(u_i) = \left(\frac{2}{1 + e^{-2(u_i)}} - 1 \right)$$
 performed for each hidden node in the first hidden layer

Thus the output is

$$O = \sum (w2_i * f(u_i)) + b2$$

where $w2_i$ is the weight vector to the output layer given as

$$w2_i = [-35.279 \quad -38.721 \quad -0.15546 \quad -0.8331 \quad 15.748]$$

and $b2$ is the bias added which is

$$b2 = -11.596$$

It should be noted that the inputs entering the network have been normalized before the training as

$$\sigma_{0.2,v} = \sigma_{0.2,v}^* / 400 \qquad \sigma_{u,v} = \sigma_{u,v}^* / 800 \qquad r_i/t = (r_i/t)^* / 10$$

And the output before the training has been normalized by 1000 thus the final output is

$$R = \left(\frac{2}{1 + e^{-2O}} - 1 \right) * 1000$$

It should be noted that the proposed NN formulations are valid for the range of variables given in the experimental database in Table 6.15.

Table 6.23. Weight matrix of the first hidden layer of the proposed NN model

[i,j]	1	2	3
1	-26.323	-25.018	-2.4366
2	13.022	-312	52.037
3	-243.69	-138.21	0.031021
4	-47.705	-103.11	245.64
5	4.0463	-1.8046	-0.25829

6.2.5.5 Conclusion

This case study proposes NN approach for strength enhancement at corner regions of stainless steel structures. Experimental data used for the training of soft computing models are obtained from literature. The proposed NN models are later compared with previous statistical models. NN results are found to be more accurate than statistical models. Proposed NN models are based on experimental training data from literature where they are further verified by test data from literature that they have not been trained before. This is significantly important as the use of training and test set is an important indicator of the reliability and generalization capabilities of the proposed soft computing models. The reliability of such models actually depends on the presence of test sets. Furthermore the NN models are presented in explicit formulation which enables them to be used fast and practically. The results of this study are very promising and show that the impact of NN techniques will be felt increasingly in the field of plastic behaviour and modeling of structures in coming years.

6.2.6 Flexural Buckling Load Prediction of Aluminium Alloy Columns

6.2.6.1 Introduction

This study presents the application of NNs for strength prediction of heat-treated extruded aluminium alloy columns failing by flexural buckling. The training and test sets for soft computing models are obtained from experimental results available in literature. The proposed NN model is presented in explicit form to be used in practical applications. The accuracy of the proposed NN model is compared with existing codes and is found to be more accurate.

The structural applications of aluminium members have experienced a fast growth in the last few years, mostly because these members exhibit several distinct advantages, namely high strength/weight ratios, corrosion resistance, pleasing appearance, ease

of maintenance, fabrication versatility and, last but not least, increasingly competitive prices (Galambos,1998, Mazzolani,2002, Goncalves and Camotim,2004).

These advantages enable aluminium columns to be widely used in structural applications. The buckling phenomenon for aluminium columns is a complex task which involves various failure types and leads to difficulties in the prediction of critical buckling load. Particularly for cases where plastic buckling is observed the process becomes too complicated. As in the case of flexural buckling of aluminium alloy columns, the behaviour of the aluminium section is determined by the stress-strain curves of the material. The stress–strain curves of aluminium alloys are nonlinear which can be modeled closely using the Ramberg-Osgood expression. Apart from the material nonlinearity, the production process also strongly affects the flexural buckling of aluminium alloy columns i.e. heat-treated aluminium alloys have significantly higher proof stresses yield strength than non-heat-treated aluminium alloys (Rasmussen and Rondal,2000).

This case study aims to present an alternative approach for flexural buckling load prediction of heat treated aluminium alloy columns by using NNs which has not been evaluated yet in this field so far. The accuracy of the proposed soft computing models are compared with available analytic expressions and related codes and are presented as explicit formulations.

6.2.6.2 Buckling of Aluminium Alloy Columns

There has been significant experimental research on aluminium column testing in literature. A review of these studies can be found in Chou and Rhodes (1997) and Singer et al. (2002) .The flexural strength of aluminium alloy columns has been the scope of extensive experimental and numerical research conducted during the 1960s and 1970s at the European Convention for Constructional Steelwork (ECCS). As a result of these tests, reference column curves were proposed referred to as the ECCS a-, b- and c-curves for aluminium alloys where a- and b-curves were adopted by the

(ECCS, 1978) , applying to heat-treated and non-heat-treated alloys respectively. The reason why different curves were adopted for heat-treated and non-heat-treated alloys respectively is the greater softening of non-heat-treated alloys compared to heat-treated alloys. Since the ECCS column curves were not suitable for design as they were in tabular form, An analytic expression was presented by Frey and Rondal (1978) and Rondal and Maquoi (1979) and adopted by ECCS. Rondal (1980) expressed another simple expression based on a Perry-type column curve using an imperfection parameter given as:

$$\eta = \alpha(\beta - \lambda)(\lambda^2 - \lambda_0^2)^{1/2} \quad (6.22)$$

For columns failing by flexural buckling, the pre-standard Eurocode9 (1998) uses the same Perry-type curve as that specified in Eurocode3 (1992) and the same linear form of the imperfection parameter given as

$$\eta = \alpha(\lambda - \lambda_0) \quad (6.23)$$

Eqn. 6.23 has also been adopted in the ISO (1992) Recommendations. Moreover Rasmussen and Rondal (1996) described a general design procedure applicable to metals and presented an appropriate form for round-house type materials given as:

$$\eta = \alpha(\lambda - \lambda_0)^\beta - \lambda_0 \quad (6.24)$$

This design procedure is subsequently applied to aluminium alloy columns by Rasmussen and Rondal (2000). The mechanical properties are firstly assumed in terms of the Ramberg–Osgood parameters, involving the initial Young’s modulus (E_0), the 0.2% proof stress ($\sigma_{0.2}$) and the parameter (n) which controls the sharpness of the knee of the stress–strain curve. The Ramberg–Osgood parameters are assumed to have been obtained from curve fits of measured stress–strain curves obtained from stub column tests of the finished product. Secondly, a Perry curve is adopted as strength curve by modifying the imperfection parameter to be expressed by Eqn 6.24 where the constants α, β, λ_0 and λ_1 can be expressed in terms of Ramberg–Osgood parameters ($E_0, \sigma_{0.2}, n$) (Rasmussen and Rondal ,2000). Thus, the non-dimensional column strength is calculated using

$$X = \frac{1}{\varphi + \sqrt{\varphi^2 - \lambda^2}} \quad (6.25)$$

$$\varphi = \frac{1}{2}(1 + \eta + \lambda^2) \quad (6.26)$$

Where the constants α, β, λ_0 and λ_1 can be expressed in terms of material parameters i.e. in terms of $e, \sigma_{0.2}/E_0$ and n as follows:

$$\alpha(n, e) = \frac{1.5}{(e^{0.6} + 0.03)(n(\frac{0.0048}{e^{0.55}})^{1.4} + 1.3)} + \frac{0.002}{e^{0.6}} \quad (6.27)$$

$$\beta(n, e) = \frac{0.36 \exp(-n)}{e^{0.45} + 0.007} + \tanh\left(\frac{n}{180} + \frac{6 \times 10^{-6}}{e^{1.4}} + 0.04\right) \quad (6.28)$$

$$\lambda_0(n, e) = 0.82 \left(\frac{e}{e + 0.0004} - 0.01n \right) \geq 0.2 \quad (2.29)$$

$$\lambda_1(n, e) = 0.8 \frac{e}{e + 0.0018} \left(1 - \left[\left(\frac{n - 55}{n + \frac{6e - 0.0054}{e + 0.0015}} \right)^2 \right]^{0.6} \right) \quad (6.30)$$

In Eqns (6.26) and (6.27) χ and λ are defined as:

$$\chi = \frac{\sigma_u}{\sigma_{0.2}} \quad (6.31)$$

$$\lambda = \sqrt{\frac{\sigma_u}{\sigma_{E_0}}} \quad (6.32)$$

$$\sigma_{E_0} = \frac{\pi^2 E_0}{(L/r)^2} \quad (6.33)$$

Where $\sigma_{0.2}$, L and r are the ultimate stress, effective length and radius of gyration respectively (Rasmussen and Rondal, 2000). The accuracy of the procedure applied to aluminium alloys is demonstrated by comparisons with established numerical solutions. This study presents a significant contribution in this field by using soft computing techniques for the flexural buckling load prediction of aluminium alloy columns.

6.2.6.3 Numerical Application

The main focus of this study is strength prediction of heat-treated extruded aluminium alloy columns failing by flexural buckling and its closed –form solution by means of NNs based on experimental results from literature. Therefore an extensive literature survey has been performed for available experimental results on flexural buckling load of heat-treated aluminium columns. Experimental results (104 tests) in Table 6.24 given with related material parameters were used as training and test sets for NN training. The datasets for test and training are randomly selected among experimental results.

Table 6.24 Material parameters of test specimens

Reference	Ref. no.	Type (axis)	Production	Alloy	E_0 (MPa)	$\sigma_{0.2}$ (MPa)	n
Djalaly and Sfintesco [25]	1	I (minor)	France	2017	72 600	310	7.15
	2	I (minor)	France	7020	70 630	320	18.12
	3	I (minor)	France	6081	68 670	288	16.16
Bernard et al. [26]	4	I (minor)	Switzerland	7020	75 880	335	24.15
	5	I (minor)	Switzerland	7020	78 264	325	26.56
	6	CHS	Belgium	7020	72 170	340	35.78
	7	CHS	Switzerland	6082	67 300	299	29.45
	8	CHS	Norway	6082	74 650	245	19.94
Kloppel and Barsch [27]	9	I (major)	Germany	7020	72 100	330	33.6
	10	I (major)	Germany	6082	72 100	293	29.9
	11	CHS	Germany	7020	72 100	330	33.6
	12	CHS	Germany	6082	72 100	293	29.9
Arnault [28]	13	I (minor)	France	2017	73 575	312	11.9
	14	I (minor)	France	6081	68 670	288	66.3
	15	I (minor)	France	6082	68 670	315	22.5
	16	I (minor)	France	7020	71 120	322	37.3

The optimal NN architecture in this part was found to be 5-13-1 NN architecture with hyperbolic tangent sigmoid transfer function (tansig). The training algorithm was quasi-Newton back propagation (BFGS). The optimum NN model is given in Fig 6.69. Statistical parameters of learning and training sets of NN model are presented in Table 6.25. The prediction of the proposed NN model vs. actual experimental values and their comparison with previously proposed formulation by Rasmussen and Rondal (2000) for $\alpha=0.3$ & $\alpha=0.4$ and EC9 and ISO is given in Table A.2. The % errors and Prediction of NN and actual values of learning and testing sets and their corresponding correlation are given in Figs 6.70-6.73. The

results of proposed NN model are more accurate compared to existing models proposed by Rasmussen and Rondal (2000) and related codes (Eurocode9 (1998) and ISO (1992)).

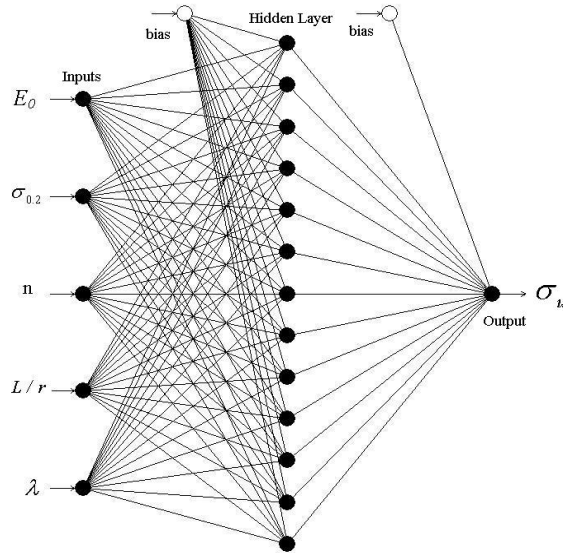


Fig 6.69 Proposed NN model for the prediction of σ_u

Table 6.25 Statistical parameters of the proposed NN model

	MSE	RMSE	SSE	MAPE (%)
NN Train Set	105.24	10.26	3578	3.79
NN Test Set	210.5	14.51	9050	6.84

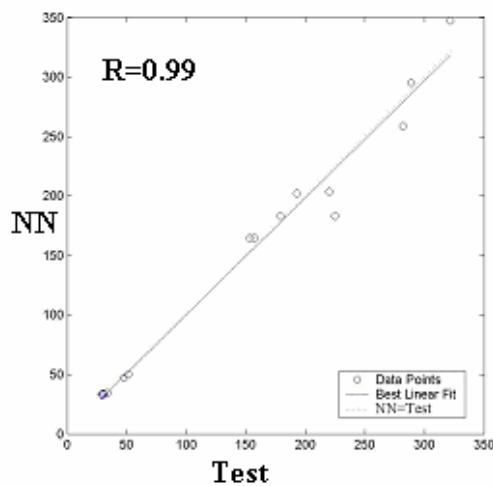


Fig 6.70 Performance of NN model for test set

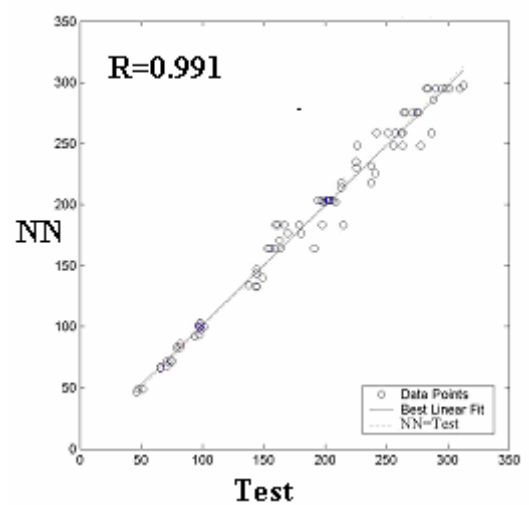


Fig 6.71. Performance of NN model for training set

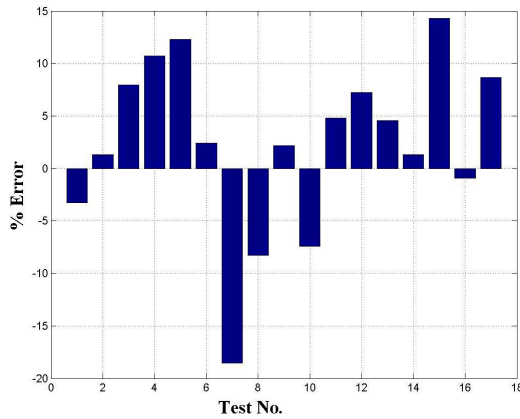


Fig 6.72 % Error for test set (NN Model)

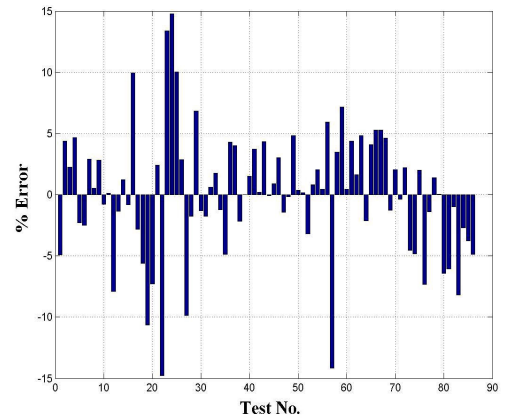


Fig 6.73. % Error for training set (NN model)

6.2.6.4 Explicit Formulation of NN Models

The main focus is to obtain the explicit formulation as follows:

$$\sigma_u = f(E_0, \sigma_{0.2}, n, L/r, \lambda)$$

w_{ij} is the weight matrix of the first hidden layer given in table 6 and X_j is the corresponding parameter vector given as

$$\mathbf{X} = [E_0, \sigma_{0.2}, n, L/r, \lambda]$$

where

b_i is the bias matrix to the first hidden layer given as

$$\mathbf{b} = [-24.08 \ -5.217 \ -18.96 \ 15.814 \ -6.951 \ -22.23 \ 0.823 \ -21.384 \ 3.941 \ -5.958 \ 28.886 \ -16.49 \ 10.17]$$

The summation u_i is transformed using a scalar-to-scalar function called an "activation or transfer function", $F(u_i)$ yielding a value called the unit's "activation".

$$Y_i = f(u_i)$$

Following the steps above leads to:

$$u_1 = (16.78 * E_0) + (7.60 * \sigma_{0.2}) + (19.13 * n) + (9.56 * (L/r)) + (24.04 * \lambda)$$

$$u_2 = (16.00 * E_0) + (-1.83 * \sigma_{0.2}) + (6.16 * n) + (-20.92 * (L/r)) + (-89.58 * \lambda)$$

$$u_3 = (19.88 * E_0) + (-7.80 * \sigma_{0.2}) + (19.33 * n) + (11.05 * (L/r)) + (-86.48 * \lambda)$$

.....

.....

$$u_{13} = (0.5 * E_0) + (3.47 * \sigma_{0.2}) + (2.42 * n) + (-4.08 * (L/r)) + (-165.25 * \lambda)$$

The activation function used in this study is hyperbolic tangent sigmoid transfer function (tansig)

$$f(u_i) = \left(\frac{2}{1 + e^{-2(u_i)}} - 1 \right) \text{ performed for each hidden node in the first hidden layer}$$

Thus the output is

$$O = \sum (w_{2_i} * f(u_i)) + b_2$$

Where w_{2_i} is the weight vector to the output layer given as

$$w_{2_i} = [-1.762 \quad -0.0646 \quad -3.697 \quad -3.0086 \quad 5.65 \quad 1.062 \quad 0.1079 \quad -0.522 \quad -1.1177 \quad 3.74 \quad 6.066 \quad 7.195 \quad 7.203]$$

and b_2 is the bias added which is

$$b_2 = 3.86$$

It should be noted that the inputs entering the network have been normalized before the training as

$$E_0^* = E_0 / 100000 \quad \sigma_{0.2}^* = \sigma_{0.2} / 100 \quad n^* = n / 500 \quad (L/r)^* = (L/r) / 500$$

$$\lambda^* = \lambda / 100$$

And the output before the training has been normalized by 3000 thus the final output

$$R = \left(\frac{2}{1 + e^{-2O}} - 1 \right) * 3000$$

It should be noted that the NN formulation above is valid for the range of variables given in Table 6.26.

Table 6.26 Weight matrix of the first hidden layer of the proposed NN model

[i,j]	1	2	3	4	5
1	16.78	7.60	19.13	9.56	24.04
2	16.00	-1.83	6.16	-20.92	-89.58
3	19.88	-7.80	19.33	11.05	-86.48
4	-23.77	13.90	13.39	9.67	-52.45
5	9.15	-0.82	7.31	-16.98	91.21
6	27.60	-6.24	20.51	4.99	72.65
7	-2.06	0.37	-3.73	-8.86	-0.67
8	16.27	-10.41	-3.80	15.13	99.69
9	-15.91	0.35	-7.25	-11.32	-86.20
10	8.64	-7.36	-19.16	5.14	-157.93
11	20.83	11.34	-17.09	-4.23	-165.58
12	18.27	-13.79	26.13	-10.45	32.91
13	0.50	3.47	2.42	-4.08	-165.25

6.2.6.5 Conclusion

This case study presents NNs for strength prediction of extruded aluminium alloy columns failing by flexural buckling. Experimental data used for the training of soft computing models are obtained from literature. The proposed NN model is later compared with existing models proposed by Rasmussen and Rondal (2000) and related codes (EC9 and ISO). NN results are found to be more accurate than previous analytic expression and codes. Furthermore the NN models are presented in explicit formulation which enables them to be used fast and practically. The results of this study are very promising.

6.2.7 Prediction of Buckling Parameters of Hollow Aluminium Columns using NNs

6.2.7.1 Introduction

In this case study NNs are proposed as an alternative tool for the prediction of buckling parameters of Hollow Aluminium Columns, namely as ultimate buckling load and normalized buckling strain being valid both for elastic and plastic ranges. The NN models for both parameters are based on experimental results from literature. The closed form solutions of the buckling parameters are also derived based on the well trained NN parameters. The prediction of normalized of NN model is compared with existing formulation and is found to be by far more accurate. The prediction accuracy of the proposed NN models are both satisfactory.

Applications of aluminum can be divided as structural and nonstructural. Structural applications are those for which the size of the part is driven primarily by the load which it must support; Nonstructural applications are the rest where half the transportation and building and construction of aluminum applications are structural. The forms of aluminum used in structural components include extrusions, flat-rolled products, castings and forgings where the most widely used forms are extrusions and the flat-rolled products (Kissel and Ferry, 2002).

Aluminium extrusions used in structural applications are in general thin-walled with complex cross-sectional shapes which may lead to several types of instability including overall and cross-sectional instability modes as well as mode interactions. Thus the prediction of buckling behaviour of these complex cross-sections is complicated where the case of buckling in plastic range adds extra difficulties. Current design rules do not provide an accurate description of the actual buckling behaviour of arbitrary cross-sections in plastic range (Mennink, 2002). This study aims to obtain a unified explicit formulation of 2 main buckling parameters namely as ultimate buckling load and normalized buckling strain of RHS and SHS aluminium columns being valid for elastic and plastic ranges at the same time using NNs. NN applications are treated as black-box applications. However this study opens this black box and introduces the NN application in a closed form solution. The prediction of ultimate buckling load and normalized buckling is of significance importance for hollow section aluminum columns as it will provide an accurate description of the actual buckling behaviour.

6.2.7.2 Buckling of Axially Compressed Aluminium Extrusions

With only a third of the weight and a self-protecting surface, the material has clear advantages over steel but it also behaves very differently with a high buckling tendency, no yield plateau and complex strain-hardening characteristics (Mazzolani, 2001). The ultimate load and deformation capacity of an extruded aluminium column is often determined by instability a (buckling) phenomenon which is in general observed as local and distortional buckling. Existing design rules for instability are limited with respect to cross-sectional instability; only a very limited range of cross-sections is covered and only with a limited accuracy. The contrast with the complexity of cross-sections used in practice is manifest. Without validated and conservative design rules, daily practice might lead to disturbingly inaccurate and even unsafe results. The actual cross-sectional instability behaviour (local and distortional buckling) of aluminium extrusions with arbitrary cross-sectional shapes is unknown (Mennink, 2002).

On the other hand the material characteristic also plays a significant role on the buckling behaviour aluminum alloy columns. The stress-strain curve of aluminum alloys is non-linear or so-called horse type which can be modeled by a bi- or tri-linear curve. This approach has been allowed in different codes, for example the Eurocode 9 (CEN, 1999). It is usually convenient to identify three separate regions, see Figure 6.74: (1) Elastic behaviour, (2) Inelastic behaviour, and (3) Strain-hardening behaviour (Faella et al., 2000, Mazzolani, 1995, Dwight, 1999).

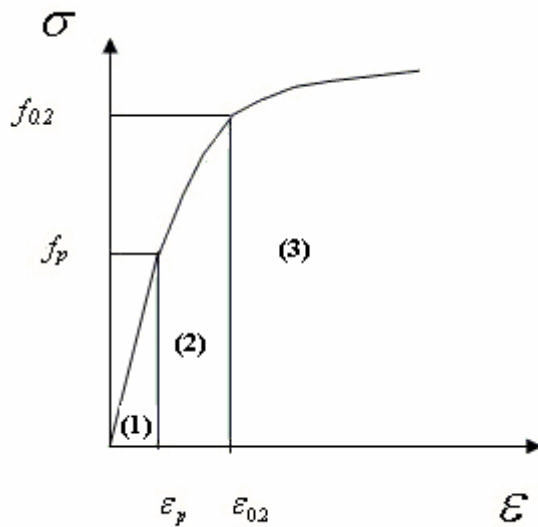


Fig 6.74 Stress-strain curve of aluminum alloy

The Ramberg-Osgood law is the most widely used model that represents stress-strain relationship of aluminum alloys in the following form:

$$\varepsilon = \frac{\sigma}{E} + 0.002 \left(\frac{\sigma}{f_{0.2}} \right)^n \quad (6.34)$$

Where n refers to the strain hardening rate and $f_{0.2}$ is the 0.2% proof strength of the material characteristic, E is the elasticity modulus and f_p is the *proportional* limit of the material characteristic. In the case of buckling in the elastic-plastic range, the critical stress can be computed by properly modifying the Eulerian value through a factor h depending on the stress-strain relationship of the material; i.e., in the case of plastic local buckling, the critical stress can be computed as

$$\sigma_{cr,p} = \eta \sigma_{cr,e} \quad (6.35)$$

where the nondimensional factor η is dependent on the stress-strain curve of the material. On the basis of a review of all formulations for the factor proposed in the technical literature by different researchers the following relationship has been considered (Faella et al., 2000):

$$\eta = \frac{E_s}{E} \left[0.50 + 0.50 \sqrt{0.25 + 0.75 \frac{E_t}{E_s}} \right] \quad (6.36)$$

Which is based on the study of Li and Reid (1992)

where E_t = tangent modulus; and E_s = secant modulus. In spite of the fact that Eqn 6.36 gives satisfactory results when applied for predicting the ultimate loadbearing capacity of aluminum alloy SHS (Langseth and Hopperstad, 1995, Mazzolani et al., 1996a) members subjected to local buckling, it should be noted that to computation of the η factor given by Eqn 6.36 requires the stress-strain curve of the material that is which is obviously a difficult task .

Effective width method is also used effectively for the ultimate load capacity of SHS (Langseth and Hopperstad, 1995, Mazzolani et al., 1996a) and RHS (Mazzolani et al., 1996b) aluminum alloy columns subjected to local buckling under uniform compression..

Faella et al (2000) have presented a practical formulation for normalized buckling strain of aluminum SHS and RHS columns based on normalized elastic buckling strain of plates. The normalized elastic buckling strain of a plate with a geometry of b and t being plate width and thickness, respectively; and λ_p = plate slenderness ratio, $\nu = 0.3$ and the case which edges are simply supported is given as:

$$\frac{\varepsilon_{cr}}{\varepsilon_0} = \frac{\pi^2}{\lambda_p^2 \varepsilon_0} = \frac{\pi^2}{\left(1.652 \frac{b}{t}\right)^2 \varepsilon_0} = \frac{3.62}{\beta^2} \quad (6.37)$$

Where

$$\beta = (b/t)\sqrt{\varepsilon_0} \quad (6.38)$$

and

$$\varepsilon_0 = f_{0.2} / E \quad (6.39)$$

Based on experimental results on SHS the empirical relationship for evaluating the normalized buckling strain has been formulated as:

$$\frac{\varepsilon_{LB}}{\varepsilon_0} = \frac{C_1}{\beta_a^{C_2+C_3\beta_a}} \quad (6.40)$$

where $\beta_a = (a - t_b)\sqrt{\varepsilon_0/t_a}$ is the plate slenderness parameter of the elements constituting the member section. The coefficients C_1 , C_2 , and C_3 have been derived directly from the experimental data by using a regression analysis carried out by means of the least squares method. Finally with reference to all profiles (i.e., including RHS members), the relationship for evaluating the normalized buckling strain has been derived according to the following mathematical structure (Faella et al., 2000):

$$\frac{\varepsilon_{LB}}{\varepsilon_0} = \frac{3.62}{\beta_a^{2.28+0.16\beta_a}} \chi^{-0.45} \quad (6.41)$$

$$\text{Where } \chi = \frac{\beta_b}{\beta_a} \quad (6.42)$$

and

$$\beta_b = (b - t_a)\sqrt{\varepsilon_0/t_b} \quad (6.43)$$

6.2.7.3 Numerical Application

The main focus of this study is the prediction of buckling parameters of RHS and SHS Aluminium Columns, namely as ultimate buckling load and normalized buckling strain and their closed-form solution by means of NNs based on experimental results. The experimental database used for the NN training is obtained from Faella et al. (2000) which presents, an extensive experimental program devoted

to the evaluation of the ultimate resistance of aluminum alloy hollow members subjected to local buckling under uniform compression within the activities of CEN-TC250/SC9, the technical committee charged with the preparation of Eurocode 9 on Aluminum Structures. The experimental database consists of both rectangular hollow sections and square hollow sections made of 6000-series alloys and produced by the major European aluminum industries. A total of 80 tests have been carried out: 24 tests regarding 12 different SHS profiles and 56 tests concerning 27 different RHS profiles. The tests have been performed at the Material and Structure Laboratory of the Department of Civil Engineering of Salerno University (Faella et al., 2000). A simple sketch of the test set up is given in Fig 6.75. With reference to the profiles used for specimen preparation, the material characteristics and geometry of tests specimens are given in Table 6.27. The test and training set are selected randomly from the experimental database. As usual, the exponent n has been calibrated according to the values of $f_{0.1}$ and $f_{0.2}$. Ultimate Strength, f_t is used in the model instead of $f_{0.2}$ as n already reflects the effect of $f_{0.2}$.

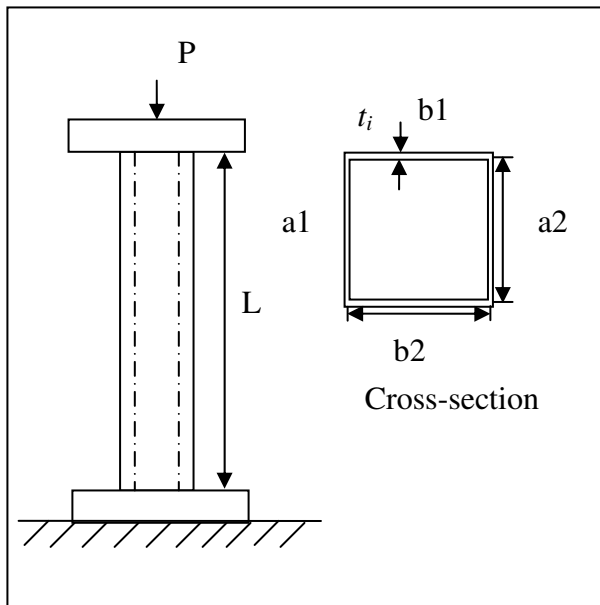


Fig 6.75 Test set-up and cross-section of tested RHS and SHS aluminium columns

Table 6.27 Experimental database

Specimen	Alloy	Country	E	F_0	$f_{0.1}$	n	f_t	anom	b(nom)	Ta	Tb	A_{nom}	A	B	Ta'	Ta''	Tb'	Tb''	A
SHS1	6060 T6	D	67.52	214.4	207.8	22.4	241.3	15	15	2	2	104	15	15	1.9	1.9	1.9	1.9	100
SHS2	6060 T6	D	72.27	223.6	215.6	19.1	244.3	40	40	4	4	576	40.1	40.05	4.05	4.15	4.1	4.05	588
SHS3	6060 T6	D	64.86	222.5	217.2	28.9	244.8	50	50	3	3	564	51.15	50	3.1	3.1	3.05	3.15	582
SHS4	6060 T6	D	64.09	202.6	198.1	30.6	225.2	50	50	4	4	736	50.4	50.35	4.45	4.1	4.2	4.3	786
SHS5	6060 T6	D	70.21	175.7	169.9	20.6	202.9	70	70	4	4	1,056	70.15	70.1	4.1	4.2	4.2	4	1,089
SHS6	6060 T6	D	71.73	194.2	189.2	26.8	220.3	80	80	4	4	1,216	79.9	79.85	4.3	4.2	4.35	4.2	1,289
SHS7	6060 T6	D	70.76	209.8	204.8	28.4	228.3	100	100	4	4	1,536	100	99.8	3.9	4	3.95	3.85	1,507
SHS8	6060 T6	I	71.96	158.2	149.3	12	186.6	60	60	2	2	464	60.4	60.35	2.3	2.25	2.25	2.25	526
SHS9	6060 T6	I	65.13	186.7	182.1	27.5	203.9	80	80	2	2	624	80.4	80.2	2.1	2.1	2.1	2	649
SHS10	6060 T6	D	65.32	293.5	286	26.9	323.7	100	100	6	6	2,256	100.3	99.9	6	5.95	6	6.1	2,263
SHS11	6060 T6	D	75.25	208.9	186.5	11.3	252.1	150	150	5	5	2,900	150.2	150.1	5.2	4.75	5	4.7	2,854
SHS12	6082 T6	N	68.37	258.4	245.5	13.4	300.1	150	150	5	5	2,900	149.9	149.9	5.2	5	5	5.25	2,961
RHS1	6060 T6	D	62.81	218.7	212.4	23.6	250.9	34	20	3	3	288	34	20	3	3	3	3	288
RHS2	6060 T6	D	69.75	202	197.5	31.1	214.3	40	30	4	4	496	39.9	29.9	4.1	3.9	4	4	494
RHS3	6060 T6	D	68.44	210.7	205.3	26.5	233.3	50	20	4	4	496	50.1	20	3.9	4.2	4.4	3.9	505
RHS4	6060 T6	D	70.87	217.4	209.8	19.5	242.5	50	30	3	3	444	50	30.25	3	3.05	3.25	2.9	451
RHS5	6060 T6	D	69.7	221.6	218.4	48.4	244.5	50	40	3	3	425	50.25	40.3	2.8	2.6	2.6	2.8	460
RHS6	6060 T6	D	77.76	212.5	204.8	18.6	235	60	34	3	3	528	60.2	34.1	3	3	3	3	530
RHS7	6060 T6	D	62.76	234.6	229.4	31.3	258.9	60	40	3	3	564	60.2	40.1	2.6	2.5	2.6	2.5	486
RHS8	6060 T6	D	63.51	222	216.3	26.6	258.6	80	40	4	4	896	80.25	40.1	4	4	3.9	3.9	892
RHS9	6060 T6	D	70.2	216.6	213.3	45.2	242.2	100	40	4	4	1,056	99.8	40.1	4	4	4	3.9	1,052
RHS10	6060 T6	D	68.95	215.8	209.8	24.7	227.3	120	50	4	4	1,296	120.3	50.6	4.15	4.15	4.3	4.25	1,360
RHS11	6060 T6	D	68.8	224.6	213.4	13.5	255.5	150	40	4	4	1,456	150.5	40.8	4.1	4.1	4	4.1	1,498
RHS12	6060 T6	D	74.54	212.3	204.6	18.7	246.8	180	40	4	4	1,696	181.2	40.8	4.2	4.2	3.9	4.3	1,787
RHS13	6060 T6	D	68.5	216	211.5	33.3	236.6	100	50	4	4	1,136	100.1	50.25	4	3.9	3.9	4	1,125
RHS14	6060	F	62.45	219.6	215.2	34.7	242.8	60	40	2	2	384	60.1	40.1	2	2.3	2	2.1	405
RHS15	6060	F	69.33	188.9	184	26.8	212.4	80	40	4	4	896	79.9	40	4	3.9	3.9	3.9	882
RHS16	6060	F	60	225.4	222.4	53	260.5	80	40	2	2	464	80.2	40.25	2.3	1.85	2.15	2	483
RHS17	6060 T6	I	69.26	234.3	230	37.5	253.3	60	40	2	2	384	59.9	40	2	1.9	2	2	378
RHS18	6082	N	68.04	264.8	258.3	27.8	285	100	25	2	2	484	100.3	25.7	2.3	2.3	2.3	2.3	558
RHS19	6060	N	69.32	209.7	205.5	33.7	229.4	120	60	2.5	2.5	875	119.9	61	2.7	2.7	2.6	2.6	937
RHS20	6060	N	65.23	235.2	224.2	14.6	282.8	200	100	5	5	2,900	200	99.9	5	4.7	4.8	5	2,824
RHS21	6082	N	67.49	251.3	246	32.9	276.9	47	40	2.5	2.5	410	47	40	2.8	2.95	2.95	2.8	467
RHS22	6082 T6	N	72.04	320	317.3	83.7	353.4	180	70	4.5	4.5	2,169	179.5	70	4.5	4.65	4.65	4.65	2,208
RHS23	6082 TF	GB	71.85	309.2	306.7	90.7	329.9	153	70	4.5	6.5	2,147	153	71.6	4.35	5.35	6.85	6.85	2,309
RHS24	6082 T6	GB	71.36	340	336.9	77.4	362.1	200	180	15.1	9	8,519	200.5	179.2	15.3	15.3	9.15	9.3	8,660
RHS25	6082 TF	GB	68.84	323	315.7	30.3	342.8	120	100	4.5	6.5	2,156	120.5	100.35	4.6	4.9	6.7	6.85	2,268
RHS26	6082	GB	71.6	132.7	131.6	84.4	184.8	200	180	6	6	4,272	201	181.5	6	6.2	6.5	5.7	4,373
RHS27	6061 T6	GB	69.05	297.9	294.1	53.2	325	219	68	4.5	6	2,941	219.8	68	4.4	5	6	6	3,070

6.2.7.3 a) Results of NN Model for Ultimate resistance

The optimal NN architecture in this part was found to be 4-17-1 NN architecture with hyperbolic tangent sigmoid transfer function (tansig). The training algorithm was quasi-Newton back propagation (BFGS). The optimum NN model is given in Fig. 6.76. Statistical parameters of learning and training sets of NN model are presented in Table 6.27. The % errors and Prediction of NN and actual values of learning and testing sets and their corresponding correlation are given in Figs 6.77-6.80. Statistical parameters of the proposed NN model are presented in Table 6.28. Results of NN model is presented in Table A.3.

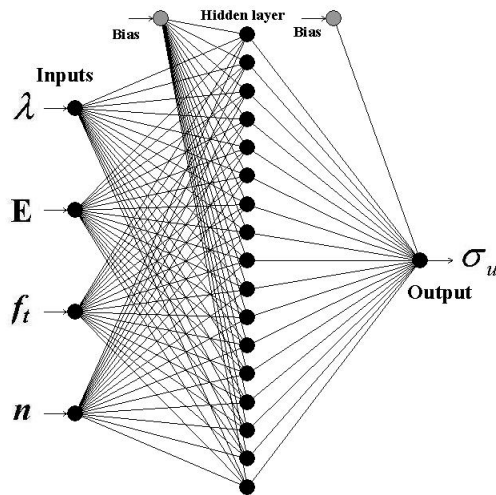


Fig 6.76 Optimum NN model for ultimate buckling resistance (σ_u)

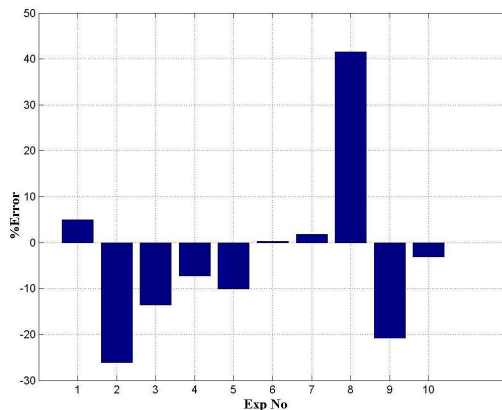


Fig 6.77 % Error for test set

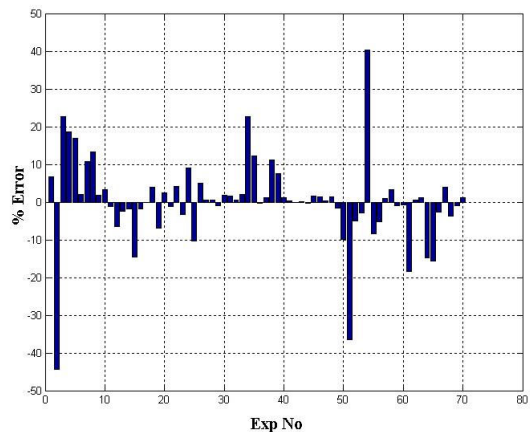


Fig 6.78 % Error for training set

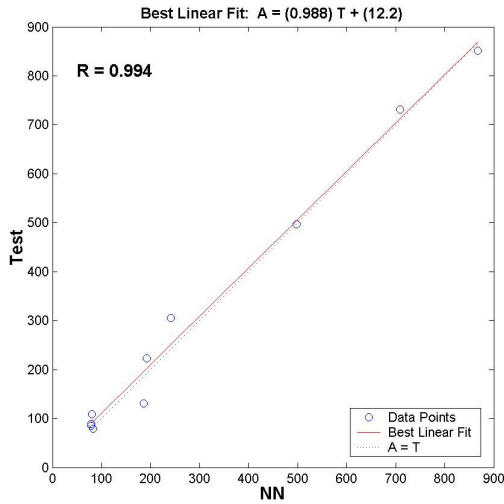


Fig 6.79 Performance Of NN model for test set

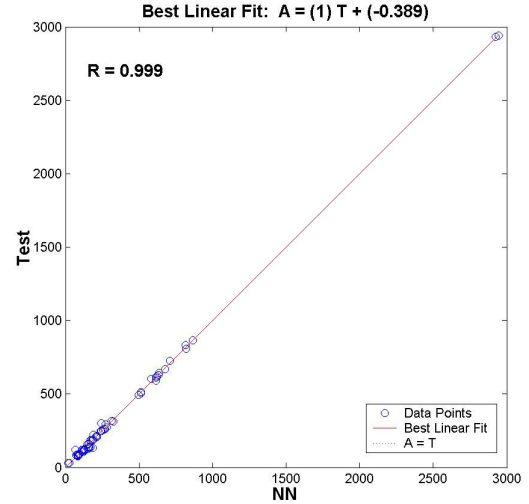


Fig 6.80 Performance Of NN model for training set

Table 6.28 Statistical parameters of the proposed NN model

	MSE	RMSE	SSE	MAPE (%)
NN Train Set	257.07	16.034	17995	6.6151
NN Test Set	958.11	30.953	9581.1	12.948

6.2.7.3 b) Results of NN Model for Normalized Buckling strain

The optimal NN architecture in this part was found to be 4-10-1 NN architecture with hyperbolic tangent sigmoid transfer function (tansig). The training algorithm was quasi-Newton back propagation (LM). The optimum NN model is given in Fig. 6.81. Statistical parameters of learning and training sets of NN model are presented in Table 6.29. The % errors and Prediction of NN and actual values of learning and testing sets and their corresponding correlation are given in Figs 6.82-6.85. Results of NN model is presented in Table A.3.

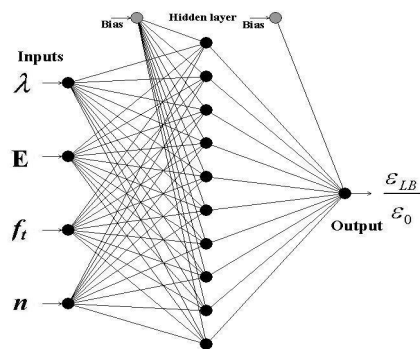


Fig 6.81 Optimum NN model for normalized buckling strain ($\frac{\epsilon_{LB}}{\epsilon_0}$)

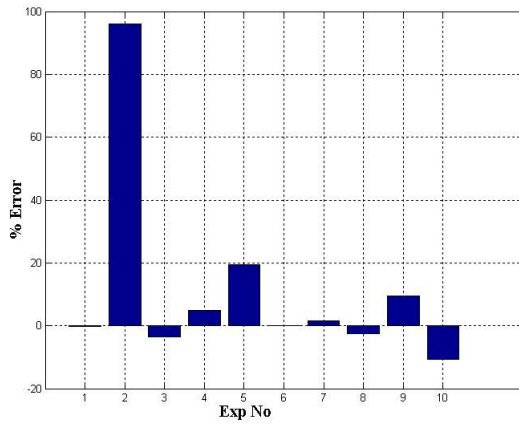


Fig 6.82 % Error for Test set

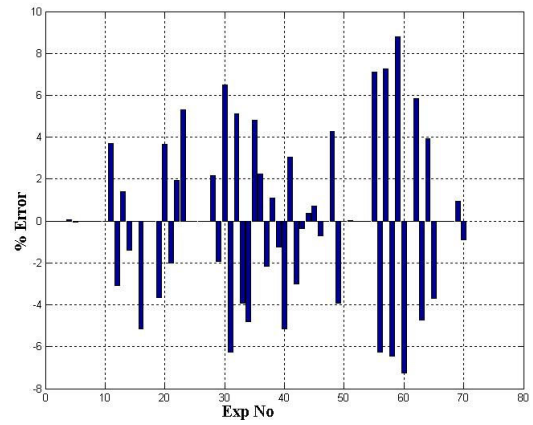


Fig 6.83 % Error for Training set

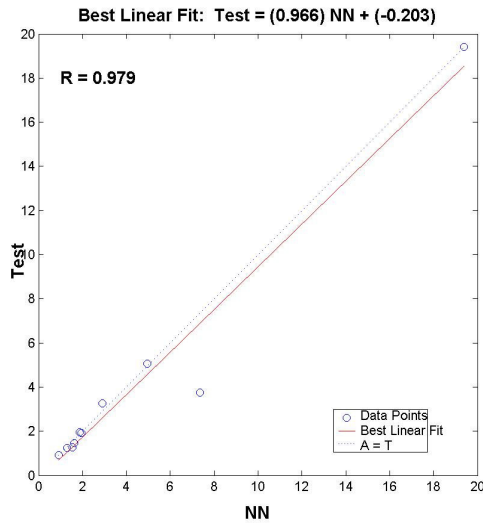


Fig 6.84 Performance Of NN model for test set

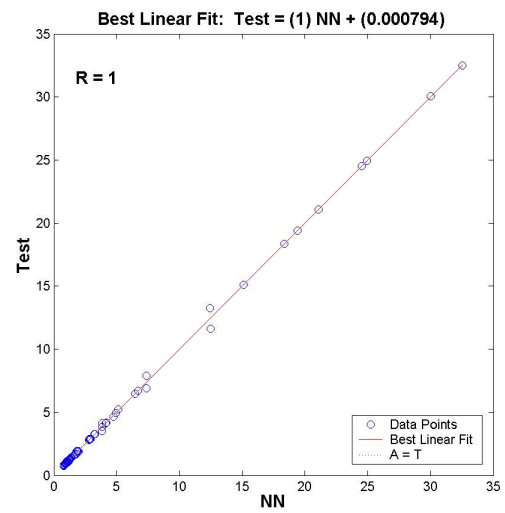


Fig 6.85 Performance of NN model for training set

Table 6.29 Statistical parameters of the proposed NN model

	MSE	RMSE	SSE	MAPE (%)
NN Train Set	0.031129	0.17643	2.179	2.263
NN Test Set	1.3191	1.1485	13.191	14.845

It should be noted that the Proposed NN models are valid within the ranges of the training set as given in table 6.30

Table 6.30 Range of variables

	λ	E	Ft	n
Max Value	57.73	77.8	362.1	91
Min Value	19.86	60	184.8	11

6.2.7.4 a) Closed Form Solution Of Ultimate Buckling resistance (σ_u)

The main aim of this part of the case study is to obtain the closed form solution of Ultimate Buckling resistance (σ_u) based on the trained NN parameters as a function slenderness ratio, Elasticity Modulus, Yield stress and Ramberg-Osgood parameters that reflects the sharpness of stress-strain diagram given as follows:

$$\sigma_u = f(\lambda, E, f_b, n)$$

$$\sigma_u = 3000 * \left(\frac{2}{1 + e^{-2W}} - 1 \right)$$

Where W=

$$\begin{aligned} & (0.132) * \left(\frac{2}{1 + e^{-2U_1}} - 1 \right) + (-0.145) * \left(\frac{2}{1 + e^{-2U_2}} - 1 \right) + (1.857) * \left(\frac{2}{1 + e^{-2U_3}} - 1 \right) + \\ & (1.304) * \left(\frac{2}{1 + e^{-2U_4}} - 1 \right) + (-0.065) * \left(\frac{2}{1 + e^{-2U_5}} - 1 \right) + (-1.081) * \left(\frac{2}{1 + e^{-2U_6}} - 1 \right) + \\ & (0.034) * \left(\frac{2}{1 + e^{-2U_7}} - 1 \right) + (1.694) * \left(\frac{2}{1 + e^{-2U_8}} - 1 \right) + (0.334) * \left(\frac{2}{1 + e^{-2U_9}} - 1 \right) + (- \\ & 0.76) * \left(\frac{2}{1 + e^{-2U_{10}}} - 1 \right) + (-0.153) * \left(\frac{2}{1 + e^{-2U_{11}}} - 1 \right) + (-0.253) * \left(\frac{2}{1 + e^{-2U_{12}}} - 1 \right) + \\ & (-0.245) * \left(\frac{2}{1 + e^{-2U_{13}}} - 1 \right) + (-1.588) * \left(\frac{2}{1 + e^{-2U_{14}}} - 1 \right) + (-0.314) * \left(\frac{2}{1 + e^{-2U_{15}}} - 1 \right) + (- \\ & 1.654) * \left(\frac{2}{1 + e^{-2U_{16}}} - 1 \right) + (1.612) * \left(\frac{2}{1 + e^{-2U_{17}}} - 1 \right) + 0.547 \end{aligned}$$

And the values for U_i are given as

$$U_1 = (-0.030 * \lambda) + (-0.236 * E) + (0.001 * Ft) + (-0.035 * n) + 20.953$$

$$U_2 = (0.053 * \lambda) + (-0.037 * E) + (0.030 * Ft) + (0.098 * n) + -6.526$$

$$U_3 = (0.023 * \lambda) + (0.087 * E) + (0.027 * Ft) + (-0.200 * n) - 13.108$$

$$U_4 = (0.011 * \lambda) + (0.181 * E) + (-0.012 * Ft) + (0.060 * n) - 2.930$$

$$\begin{aligned}
U_5 &= (-0.170 * \lambda) + (0.160 * E) + (-0.003 * F_t) + (0.017 * n) - 3.160 \\
U_6 &= (-0.016 * \lambda) + (-0.284 * E) + (-0.004 * F_t) + (-0.005 * n) + 17.809 \\
U_7 &= (-0.061 * \lambda) + (0.072 * E) + (-0.004 * F_t) + (0.102 * n) - 4.184 \\
U_8 &= (-0.086 * \lambda) + (-0.018 * E) + (0.016 * F_t) + (-0.008 * n) - 12.770 \\
U_9 &= (-0.108 * \lambda) + (0.297 * E) + (0.015 * F_t) + (-0.133 * n) - 18.143 \\
U_{10} &= (-0.072 * \lambda) + (0.040 * E) + (-0.024 * F_t) + (0.018 * n) + 9.373 \\
U_{11} &= (0.085 * \lambda) + (-0.191 * E) + (0.013 * F_t) + (-0.096 * n) 15.781 \\
U_{12} &= (0.075 * \lambda) + (0.319 * E) + (-0.005 * F_t) + (0.008 * n) - 20.803 \\
U_{13} &= (-0.071 * \lambda) + (-0.189 * E) + (-0.006 * F_t) + (-0.161 * n) 18.455 \\
U_{14} &= (-0.056 * \lambda) + (0.015 * E) + (0.021 * F_t) + (-0.026 * n) - 15.517 \\
U_{15} &= (-0.105 * \lambda) + (0.265 * E) + (0.010 * F_t) + (-0.134 * n) - 14.906 \\
U_{16} &= (-0.062 * \lambda) + (0.204 * E) + (0.014 * F_t) + (0.021 * n) - 20.346 \\
U_{17} &= (-0.083 * \lambda) + (0.063 * E) + (0.015 * F_t) + (0.071 * n) - 13.171
\end{aligned}$$

6.2.7.4 b) Closed Form Solution Of Normalized Buckling Strain $\left(\frac{\varepsilon_{LB}}{\varepsilon_0}\right)$

The main aim of this part of the study is to obtain the closed form solution of Normalized Buckling Strain $\left(\frac{\varepsilon_{LB}}{\varepsilon_0}\right)$ based on the trained NN parameters as a function slenderness ratio, Elasticity Modulus, Yield stress and Ramberg-Osgood parameters that reflects the sharpness of stress-strain diagram given as follows:

$$\frac{\varepsilon_{LB}}{\varepsilon_0} = f(\lambda, E, f_b, n)$$

$$\frac{\varepsilon_{LB}}{\varepsilon_0} = 40 * \left(\frac{2}{1 + e^{-2W}} - 1 \right)$$

Where W=

$$\begin{aligned}
&(-0.397) * \left(\frac{2}{1 + e^{-2U_1}} - 1 \right) + (-4.771) * \left(\frac{2}{1 + e^{-2U_2}} - 1 \right) + (1.01) * \left(\frac{2}{1 + e^{-2U_3}} - 1 \right) + \\
&(-0.535) * \left(\frac{2}{1 + e^{-2U_4}} - 1 \right) + (-2.192) * \left(\frac{2}{1 + e^{-2U_5}} - 1 \right) + (5.65) * \left(\frac{2}{1 + e^{-2U_6}} - 1 \right) + \\
&(-5) * \left(\frac{2}{1 + e^{-2U_7}} - 1 \right) + (0.445) * \left(\frac{2}{1 + e^{-2U_8}} - 1 \right) + (2.35) * \left(\frac{2}{1 + e^{-2U_9}} - 1 \right) +
\end{aligned}$$

$$(-5.686 * \left(\frac{2}{1 + e^{-2U_{10}}} - 1 \right) + 6.25$$

$$U_1 = (0.075 * \lambda) + (-0.26 * E) + (0.076 * F_t) + (-0.224 * n) + 6.872$$

$$U_2 = (0.011 * \lambda) + (-0.097 * E) + (-0.019 * F_t) + (0.002 * n) + 9.147$$

$$U_3 = (0.062 * \lambda) + (-0.21 * E) + (0.048 * F_t) + (-0.062 * n) - 3.478$$

$$U_4 = (0.232 * \lambda) + (-0.095 * E) + (0.122 * F_t) + (-0.052 * n) - 28.243$$

$$U_5 = (0.05 * \lambda) + (0.147 * E) + (-0.224 * F_t) + (0.034 * n) - 7.53$$

$$U_6 = (0.019 * \lambda) + (0.12 * E) + (-0.023 * F_t) + (0.015 * n) - 4.019$$

$$U_7 = (-0.019 * \lambda) + (0.023 * E) + (-0.002 * F_t) + (-0.017 * n) + 2.037$$

$$U_8 = (0.42 * \lambda) + (0.072 * E) + (0.04 * F_t) + (-0.115 * n) - 22.9$$

$$U_9 = (-0.021 * \lambda) + (-0.207 * E) + (0.019 * F_t) + (-0.01 * n) + 10.8$$

$$U_{10} = (0.114 * \lambda) + (0.356 * E) + (-0.008 * F_t) + (0.114 * n) - 24.11$$

6.2.7.5 Conclusion

This case study presents a novel approach for the prediction of buckling parameters of RHS and SHS aluminum columns based on NNs. The NN approach in the prediction of ultimate load capacity and normalized buckling strain of RHS and SHS aluminum columns is quite new which has not been proposed in literature so far. The NN models are based on well established experimental data from literature. The closed form solutions for ultimate load capacity and normalized buckling strain based on the well trained NNs are also presented. The results of the NN model for the prediction of normalized buckling strain is also compared with results obtained from existing formulation proposed in literature and are found to be by far more accurate. The results of the NN model for the prediction of ultimate load capacity are quite satisfactory as well.

6.2.8 Shear Capacity of RC Beams Without Web Reinforcement

6.2.8.1 Introduction

This case study addresses the availability NNs for the prediction of shear capacity of RC beams without web reinforcement. The proposed NN model is based on a wide range of experimental data gathered from literature. The accuracy of the proposed NN model is compared with current design codes (ACI-318, EC2, LRFD) and found to be by far more accurate. Moreover the proposed NN model is also given in explicit form for practical use.

The shear strength of RC beams without web reinforcement has been an important phenomena in structural engineering and tremendous amount of research has been performed throughout the 20th century. Thus the knowledge of shear behavior and its failure mechanism has improved significantly. However the subject still needs further study due to the complexity of the shear transfer mechanism and affecting parameters. For reinforced concrete beams without shear reinforcement, the provisions for shear design in current codes are based on empirical equations, due to the complex mechanism of shear transfer, various failure types and interdependent internal forces in beams. The use of these empirical equations to predict the shear strength is not satisfactory. Thus several models based on rational approach are proposed (Peng, 1999).

6.2.8.2 Shear Strength of RC Beams

The purpose of web reinforcement in RC beams (Fig 6.86) is to ensure that shear failure does not occur and that the full flexural capacity can be used. Prior to inclined cracking, the strain in the stirrups is equal to the corresponding strain in the concrete and, therefore, the stress in the stirrups prior to inclined cracking will be relatively small. Stirrups do not prevent inclined cracks from forming as they come into play only after cracks have formed (Cladera, 2003).

Numerous approaches have been proposed in literature to model the shear behavior of RC beams. Among these, the plastic theory is effectively used. The application of

plastic theory to shear in reinforced concrete has now been studied for more than 30 years (Nielsen and Braestrup, 1975, Ashour and Morley, 1994, Miller, 1976, Ibell, 1998). The theory of plasticity offers useful tools for establishing the carrying capacity of structural members. Application of the theory of plasticity to structural engineering is based on the following two theorems:

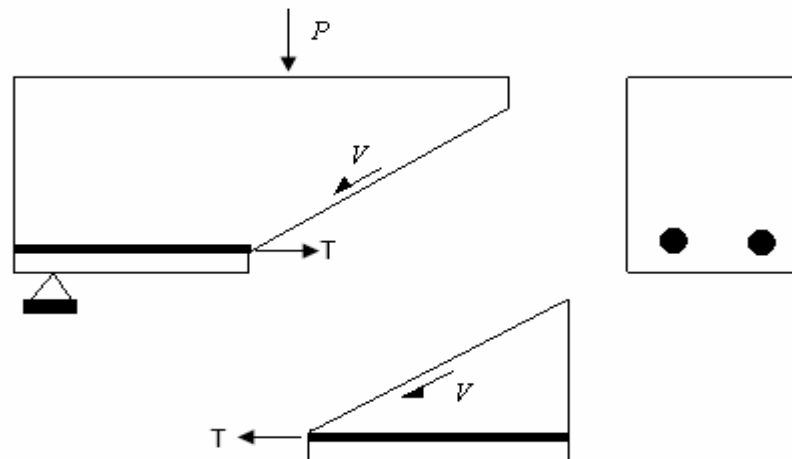


Fig 6.86 Shear Force in RC beam without web reinforcement

1. If a load path can be found where equilibrium is satisfied, the boundary conditions are fulfilled and the material does not exceed the yield condition anywhere, then the structure is safe. This is the lower bound theorem of the theory of plasticity.

2. On the other hand, the load that causes a failure mechanism compatible with the geometrical constraints of the structure is an upper bound of the strength of the structure (Duthinh and Carino, 1996).

For many years the application of plastic theory in practical design was restricted to Denmark and Switzerland. Now the interest in other countries is growing and plastic methods have been adopted in the Eurocode 2, the future common concrete code in Europe. The problem to be overcome is not to find the plastic solutions, although this is not always easy. The difficult problem is the pronounced softening of unconfined concrete which renders the perfectly plastic material model a rather crude one. What has been shown in the past decades is that by introducing empirically determined reduction factors, the so-called effectiveness factors, on the concrete strengths the theoretical solutions may be brought into close agreement with experiments (Hoang and Nielsen, 1998).

Empirical equations are of special concern in the design of shear strength of RC beams without web reinforcement. Current design codes in this field are summarized in Table 6.31.

Table 6.31 Current Design Codes

2002 Final Draft Of EC2 (2002)	$V_{Rd,c} = 0.18 k (100 \rho_l f_c)^{1/3} b_w d \geq 0.035 k^{3/2} f_c^{1/2} b_w d$ (6.44)	$f_c \leq 100(\text{MPa})$, $k = 1 + \sqrt{200/d} \rho_l \leq 2.0$, $\rho_l = \frac{A_l}{b_w d} \leq 0.02$
AASHTO LRFD 2000 [10]	$V_c = \beta \sqrt{f_c} b_w d$ (6.45)	β is given in tabular form as a function of the equivalent crack spacing and the longitudinal strain in the web.
ACI318-02 Eq. 11-3 [11]	$V_c = \frac{\sqrt{f_c}}{6} b_w d$ (6.46)	$f_c < 70 \text{ MPa}$
ACI318-02 (2002) Eq. 11-5	$V_c = (0.16 \sqrt{f_c} + 17 \rho_l \frac{Vd}{M}) b_w$ (6.47)	$f_c < 70 \text{ MPa}$, $Vd/M \leq 1$

The shear strength of RC beams without web reinforcement has been studied by numerous researchers (Cladera,2003, Morrow and Viest,1957, Kani et al.,1979, Mphonde and Frantz,1984, Elzanaty et al,1986, Ahmad et al,1986, Salandra and Ahmad,1989, Thorenfeldt and Drangsholt,1990, Kim and Park,1994, Yoon et al,1996, Adebar and Collins,1996, Islam et al,1998, Collins and Kuchma,1999, González-Fonteboa and Hormigones,2002). In this study an extensive literature review on experimental studies related to shear strength of RC beams without web reinforcement has been carried out and an experimental database has been constructed. A total of 161 specimens from 14 separate studies were included in the database shown in Table 6.32. Further details of the experimental database are given in Table A.4.

Table 6.32 Experimental database and range of variables

Reference	Number of Specimen	d (mm)	f_c (MPa)	ρ_l (%)	a/d
Morrow et al. (1957)	11	356 to 375	15 to 46	1.83 to 3.83	2.8 to 7.9
Kani et al. (1979)	31	137 to 1090	17 to 30	0.50 to 2.84	2.5 to 6.8
Mphonde et al.(1984)	11	298	22 to 102	2.32 and 3.36	2.5 and 3.6
Elzanaty et al. (1986)	11	273	21 to 79	1.00 to 3.30	4.0 and 6.0
Ahmad et al. (1986)	14	184 to 208	61 to 67	1.77 to 6.64	2.7 to 4.0
Salandra et al. (1989)	4	171	52 to 69	1.45	2.6 and 3.6
Thorenfeldt et al (1990)	16	150 and 300	54 to 98	1.82 and 3.23	3.0 and 4.0
Kim et al. (1994)	15	142 to 915	54	1.01 to 4.68	3.0 and 4.5
Yoon et al. (1996)	3	655	36 to 87	2.8	3.23
Adebar et al. (1996)	6	178 and 278	46 to 59	1.0 to 3.04	2.9 and 4.5
Islam et al.(1998)	10	203 to 207	27 to 83	2.02 to 3.22	2.9 to 3.9
Collins et al (1999)	21	110 to 925	36 to 99	0.50 to 1.03	2.5 to 3.1
González (2002)	4	305 and 306	40 to 47	2.9	2.3
Cladera (2003)	4	359	50 to 87	2.24	3.0

NNs have been widely applied to the prediction of shear strength of RC beams (Seleemah,2005, Adhikary and Mutsuyoshi,2004, Cladera and Mari,2004a, Cladera and Mari,2004b, Mansour etal,2004, Oreta and Winston,2004, Sanad and Saka,2001).

6.2.8.3 NN Results

The experimental database is randomly divided as training and test set given in Table A.1. Among 161 datasets 14 datasets were used as test and the rest as training set. The optimal NN architecture in this part was found to be 5-3-1 NN architecture with hyperbolic tangent sigmoid transfer function (tansig). The training algorithm was quasi-Newton back propagation (BFGS). The optimum NN model is given in Fig 6.87. Statistical parameters of learning and training sets of NN model are presented in Table 6.33. The % errors and Prediction of NN and actual values of learning and testing sets and their corresponding correlation are given in Figs. 6.88-6.91. Results of NN model is presented in Table A4.

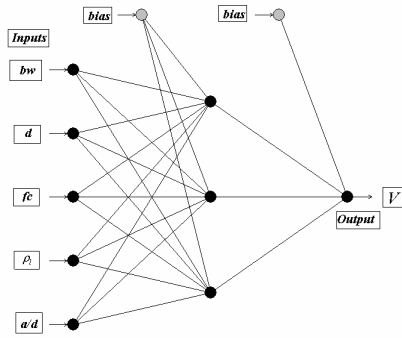


Fig 6.87 Optimum NN model

Table 6.33 Statistical parameters of the proposed NN Model

	MSE	RMSE	SSE	MAPE (%)
NN Test Set	346.2	18.61	5193	14.78
NN Training Set	80.9	9.0	11812	7.94

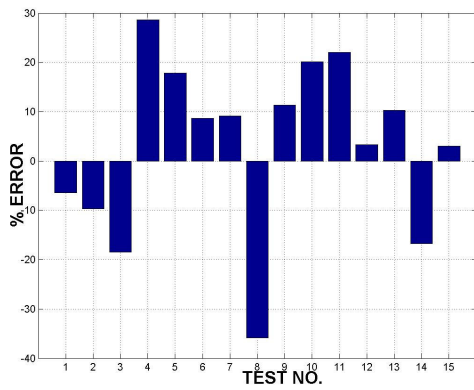


Fig 6.88 % Error of test set for NN model

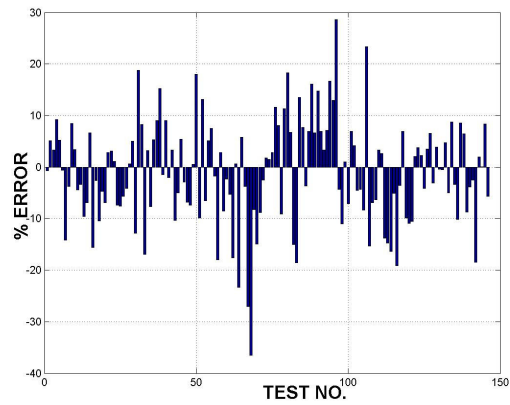


Fig 6.89 % Error of train set

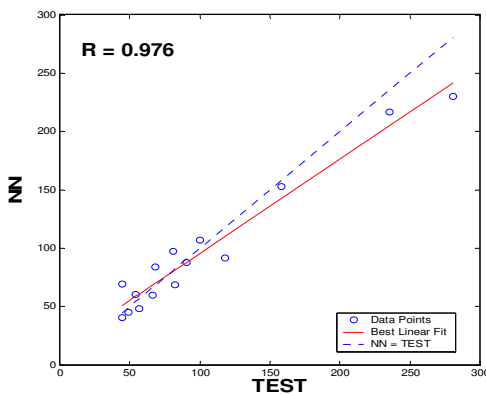


Fig 6.90 Performance of test set for NN model

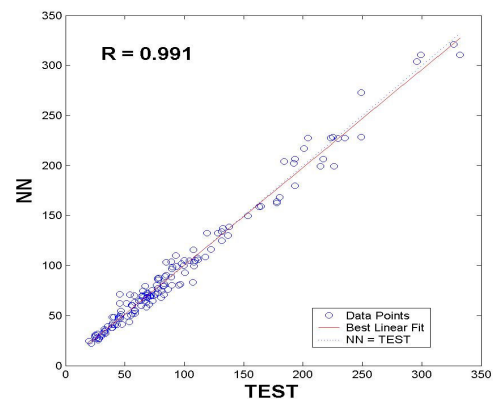


Fig 6.91 Performance of train set for NN model

The overall performance and accuracy of the proposed SC models and current design codes with respect to experimental results are shown in Figures 6.92-6.101 which is also summarized in Table A.4

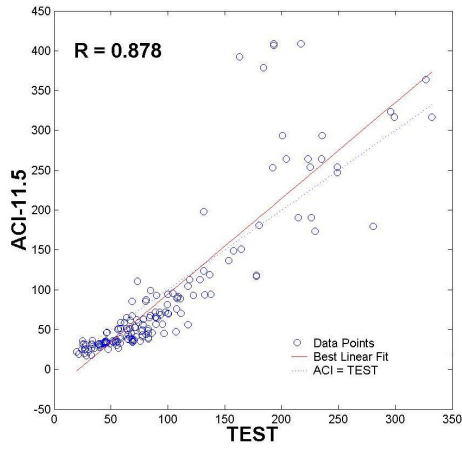


Fig 6.92 Overall performance ACI (11.5) code

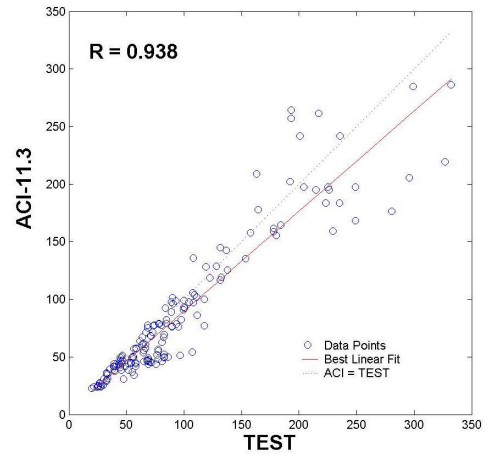


Fig 6.93 Overall performance ACI (11.3) code

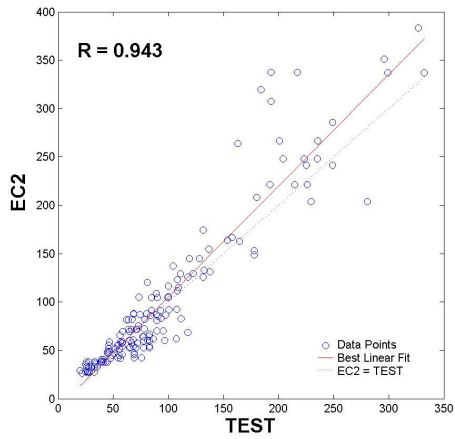


Fig 6.94 Overall performance EC2 code

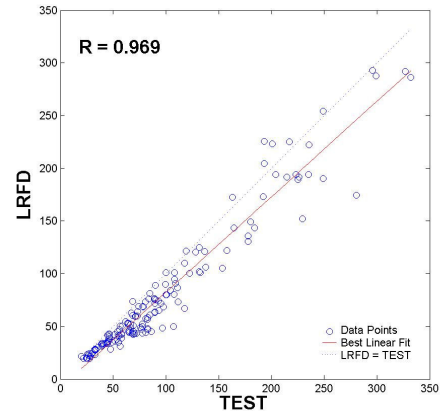


Fig 6.95 Overall performance LRFD code

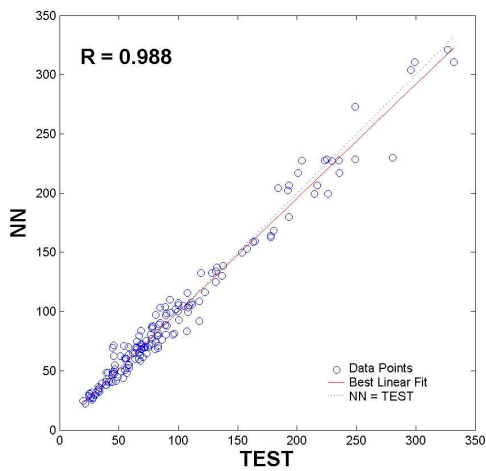


Fig 6.96 Overall Performance of NN model

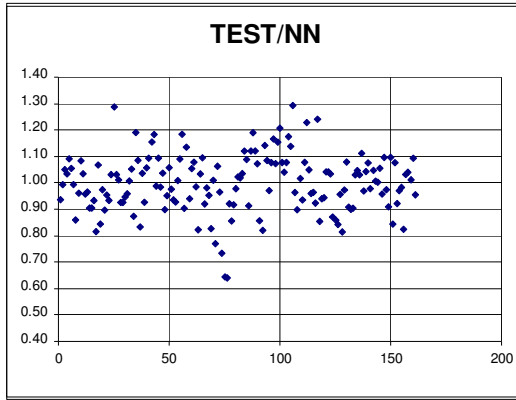


Fig 6.97 Distribution of mean of test/predicted for NN model

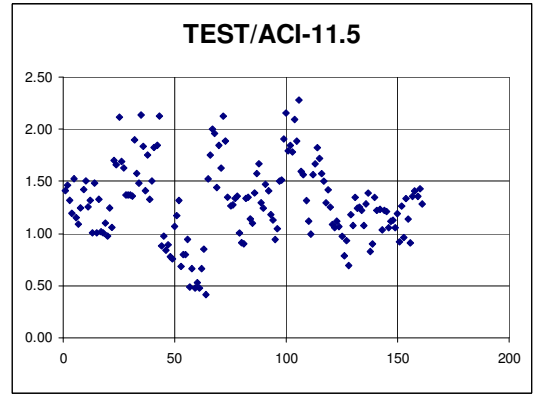


Fig 6.98 Distribution of mean of test/predicted for ACI 11.5

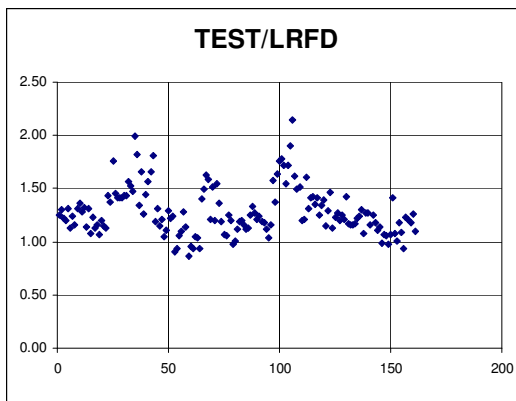


Fig 6.99 Distribution of mean of test/predicted for LRFD

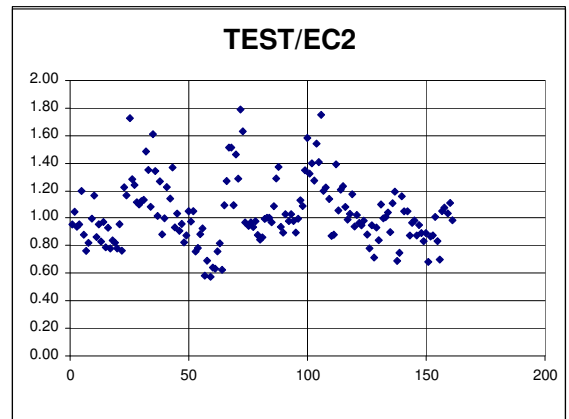


Fig 6.100 Distribution of mean of test/predicted for EC2 model

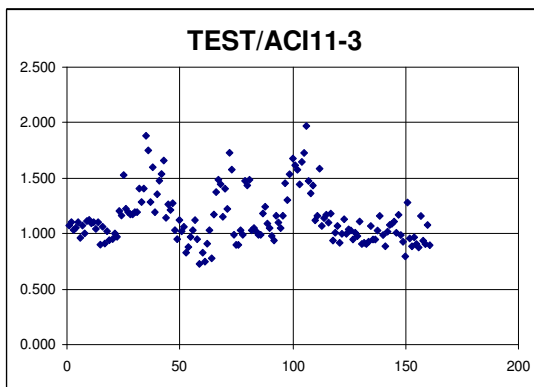


Fig 6.101 Distribution of mean of test/predicted for ACI 11.3 model

6.2.8.4 Explicit Formulation of the NN Model

The main focus is to obtain the explicit formulation of the shear capacity as a function of variables given as follows:

$$V = f(b_w, d, f_c, \rho_l, a/d)$$

The explicit formulation for the proposed NN model is obtained by using the well trained NN parameters which are biases, and weights for the input and hidden layer and the normalization factors both for inputs and output proposed NN model. The derivation of the explicit formulation is too complex particularly for those who do not have a neural network background. Detailed information about the derivation can be found in references [44, 45]. The same steps can be given in a simpler form as follows:

$$V = 400 * \left(\frac{2}{1 + e^{-2W}} - 1 \right)$$

$$\text{Where } W = (0.17) * \left(\frac{2}{1 + e^{-2U_1}} - 1 \right) + (0.615) * \left(\frac{2}{1 + e^{-2U_2}} - 1 \right) + (0.847) * \left(\frac{2}{1 + e^{-2U_3}} - 1 \right) - 0.0976$$

$$U_1 = (0.02 * b_w) + (0.0029 * d) + (-0.0015 * f_c) + (0.96 * \rho_l) + (0.07 * a/d) - 10.19$$

$$U_2 = (0.0045 * b_w) + (-0.0003 * d) + (-0.0025 * f_c) + (3.86 * \rho_l) + (-0.021 * a/d) - 1.145$$

$$U_3 = (-0.0036 * b_w) + (0.0012 * d) + (0.004 * f_c) + (-4.5 * \rho_l) + (-0.0086 * a/d) + 1.298$$

It should be noted that the proposed explicit formulation of the NN models presented above are valid only for the ranges of experimental database given in Table 6.32.

6.2.8.5 Conclusion

This case study that addresses the feasibility of NNs for the prediction of shear capacity of RC beams without web reinforcement. The proposed NN model is given in explicit form for practical use. The overall performances of the proposed NN

model in this case study is quite satisfactory as compared to current design codes (ACI, EC2 and LRD). The correlation coefficients of current design codes are lower than the proposed SC codes except the LRFD code which has a higher correlation coefficient than the proposed NR model. However if the standard deviation is also taken into account the proposed NR model (Std. Dev.=0.188) performs better than LRFD code (Std. Dev.=0.222). The results of the proposed NN model is seen to be more accurate than current design codes. The outcomes of this study prove the feasibility of the application of NNs for the prediction of shear capacity of RC beams without web reinforcement.

6.2.9 Strength Enhancement for CFRP Confined Concrete Cylinders

6.2.9.1 Introduction

This study presents the application of Neural Networks (NN) for the modeling of strength and ductility enhancement of CFRP (Carbon Fiber-Reinforced Plastic) confined concrete cylinders. The proposed NN model is based on experimental results collected from literature. It represents the ultimate strength of concrete cylinders after CFRP confinement which is also given in explicit form in terms of diameter, unconfined concrete strength, tensile strength CFRP laminate and total thickness of CFRP layer used. The accuracy of the proposed NN models are quite satisfactory as compared to experimental results. Moreover the result of proposed NN model is compared with 10 different theoretical models proposed by researchers so far and is found to be by far more accurate.

With over fifty years of excellent performance records in the aerospace industry, fiber-reinforced-polymer (FRP) composites have been introduced with confidence to the construction industry. These high-performance materials have been accepted by civil engineers and have been utilized in different construction applications such as repair and rehabilitation of existing structures as well as in new construction applications. One of the successful and most popular structural applications of FRP composites is the external strengthening, repair and ductility enhancement of reinforced

concrete (RC) columns in both seismic and corrosive environments (Hollaway,2004). Main types of FRP composites used in external strengthening and repair of RC columns are: Glass-fiber-reinforced polymers (GFRP), carbon-fiber-reinforced polymers (CFRP), and aramid-fiber-reinforced polymers (AFRP). Types of FRP confinement can be spiral, wrapped and tube. FRP composites offer several advantages due to extremely high strength-to-weight ratio, good corrosion behavior and electromagnetic neutrality. Thus the effect of FRP confinement on the strength and deformation capacity of concrete columns has been extensively studied and several empirical and theoretical models have been proposed (Lorenzis, 2001). This study proposes a new approach for the modeling of strength enhancement of CFRP wrapped concrete cylinders using NNs. The proposed NN model for the compressive strength of the confined concrete cylinder is presented in explicit form.

6.2.9.2 Behavior of FRP Confined Concrete

Being a frictional material, concrete is sensitive to hydrostatic pressure. The beneficial effect of lateral stresses on the concrete strength and deformation has been recognized nearly for a century. In other words when uniaxially loaded, concrete is restrained from dilating laterally, it exhibits increased strength and axial deformation capacity indicated as confinement which has been generally applied to compression members through steel transverse reinforcement in the form of spirals, circular hoops or rectangular ties, or by encasing the concrete columns into steel tubes that act as permanent formwork (Lorenzis, 2001). Besides steel reinforcement FRPs are also for confinement of concrete columns and offers several advantages as compared to steel (Fardis and Khalili,1982) such as continuous confining action to the entire cross-section, easiness and speed of application, no change in the shape and size of the strengthened elements, corrosive resistance (Lorenzis,2001).

Typical response of FRP-confined concrete is shown in Fig 6.102, where normalized axial stress is plotted against axial, lateral, and volumetric strains. The stress is normalized with respect to the unconfined strength of concrete core. The figure shows that both axial and lateral responses are bi-linear with a transition zone at or near the peak strength of unconfined concrete core. The volumetric response shows a

similar transition toward volume expansion. However, as soon as the jacket takes over, volumetric response undergoes another transition which reverses the dilation trend and results in volume compaction. This behavior is shown to be markedly different from plain concrete and steel-confined concrete (Mirmiran et al,2000).

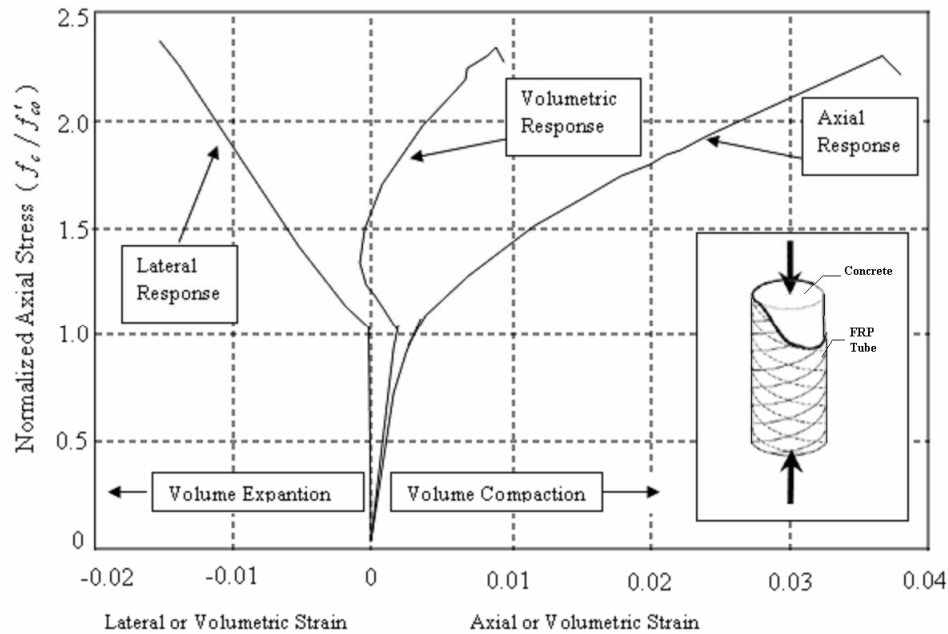


Fig 6.102 Typical response of FRP-confined concrete (Mirmiran et al,2000).

The characteristic response of confined concrete includes three distinct regions of uncracked elastic deformations, crack formation and propagation, and plastic deformations. It is generally assumed that concrete behaves like an elastic-perfectly plastic material after reaching its maximum capacity, and that the failure surface is fixed in the stress space. Constitutive models for concrete should be concerned with pressure sensitivity, path dependence, stiffness degradation and cyclic response. The existing plasticity models range from nonlinear elasticity, endo-chronic plasticity, classical plasticity, and multi-laminate or micro-plane plasticity to bounding surface plasticity. Many of these models, however, are only suitable in a specific application and loading system for which they are devised and may give unrealistic results in other cases. Also, some of these models require several parameters to be calibrated based on experimental results (Mirmiran et al,2000). Considerable experimental research has been performed on the behaviour of CFRP confined concrete columns (Miyachi et al,1997, Kono et al,1998, Matthys et al, 1999, Shahawy,2000, Rochette and Labossière,2000, Micelli et al,2001, Rousakis,2001). Several models are

proposed in literature for the strength enhancement of FRP confinement effect of concrete columns given in table 6.34.

Table 6.34. Models for strength enhancement of FRP confined concrete cylinders

Model	Expression (f'_{cc} / f'_{co})
Fardis & Khalili (1981)	$\frac{f'_{cc}}{f'_{co}} = 1 + 4.1 \frac{P_u}{f'_{co}}$ (6.48)
	$\frac{f'_{cc}}{f'_{co}} = 1 + 3.7 \left(\frac{P_u}{f'_{co}} \right)^{0.86}$ (6.49)
Saadatmanesh . et. al. (1994)	$\frac{f'_{cc}}{f'_{co}} = 2.254 \sqrt{1 + 7.94 \frac{P_u}{f'_{co}} - 2 \frac{P_u}{f'_{co}} - 1.254}$ (6.50)
Miyauchi et. al. (1997)	$\frac{f'_{cc}}{f'_{co}} = 1 + 3.485 \frac{P_u}{f'_{co}}$ (6.51)
Kono et. al. (1998)	$\frac{f'_{cc}}{f'_{co}} = 1 + 0.0572 p_u$ (6.52)
Saaman et. al. (1998)	$\frac{f'_{cc}}{f'_{co}} = 1 + 6.0 \frac{P_u^{0.7}}{f'_{co}}$ (6.53)
Tountanji (1999)	$\frac{f'_{cc}}{f'_{co}} = 1 + 3.5 \left(\frac{P_u}{f'_{co}} \right)^{0.85}$ (6.54)
Saafi et. al. 1999	$\frac{f'_{cc}}{f'_{co}} = 1 + 2.2 \left(\frac{P_u}{f'_{co}} \right)^{0.84}$ (6.55)
Spoelstra & Monti (2000)	$\frac{f'_{cc}}{f'_{co}} = 0.2 + 3 \left(\frac{P_u}{f'_{co}} \right)^{0.5}$ (6.56)
Xiao & Wu (2000)	$\frac{f'_{cc}}{f'_{co}} = 1.1 + \left(4.1 - 0.75 \frac{f'_{co}{}^2}{E_1} \right) \frac{P_u}{f'_{co}}$ (6.57)

This case study aims to propose an alternative approach and a new formulation by means of NNs for the prediction of strength enhancement of CFRP confined concrete cylinders.

6.2.9.3 Experimental database

In this case study an extensive literature review on experimental studies related to strength enhancement of CFRP wrapped concrete cylinders has been carried out and an experimental database has been gathered. It should be noted that all specimen used in the database have a length to diameter ratio of 2 ($L/D = 2$). A total of 101 specimens from 7 separate studies with the ranges of variables were included in the database shown in Table 6.35.

Table 6.35 Experimental database and ranges of variables

Reference	Number of Specimen	D (mm)	nt (mm)	Ef (MPa)	f'_{co} (MPa)
Miyauchi et al. (1997)	10	100,150	0.11 to 0.33	3481	31.2 to 51,9
Kono et al. (1998)	17	100	0.167 to 0.501	3820	32.3 to 34,8
Matthys et al. (1999)	2	150	0.117,0.235	2600,1100	34.9
Shahawy et al. (2000)	9	153	0.36 to 1.25	2275	19.4 to 49
Rochette and Labossiere (2000)	7	100, 150	0.6 to 5.04	230, 1265	42 to 43
Micelli et al. (2001)	8	100	0.16, 0.35	1520, 3790	32 to 37
Rousakis (2001)	48	150	0.169 to 0.845	2024	25.15 to 82.13

6.2.9.4 Results of NN model

The experimental database is randomly divided as training and test set. Among 101 datasets 10 datasets were used as test and the rest as training set. The optimal NN architecture in this part was found to be 4-15-1 NN architecture with hyperbolic tangent sigmoid transfer function (tansig). The training algorithm was quasi-Newton back propagation (BFGS). The optimum NN model is given in Fig 6.103. Statistical parameters of learning and training sets of NN model are presented in Table 6.36. The % errors and Prediction of NN and actual values of learning and testing sets and their corresponding correlation are given in Figs 6.104-6.107. The results of the

proposed NN models are quite satisfactory ($R=0.98$, $\text{std dev.}=0.06$). Moreover the results of proposed NN model are compared with 10 different FRP confinement models and are found to be by far more accurate as given in Table 6.37.

Table 6.36 Statistical parameters of the proposed NN model

	MSE	RMSE	SSE	MAPE (%)
NN Training Set	18.76	4.33	1895.6	3.88
NN Test Set	77.06	8.77	770.6	8.41

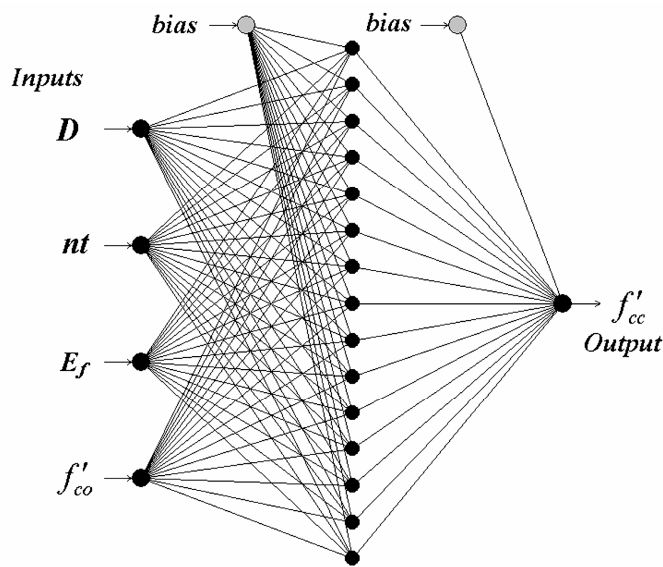


Fig 6.103 Proposed NN Model for the prediction of f'_{cc}

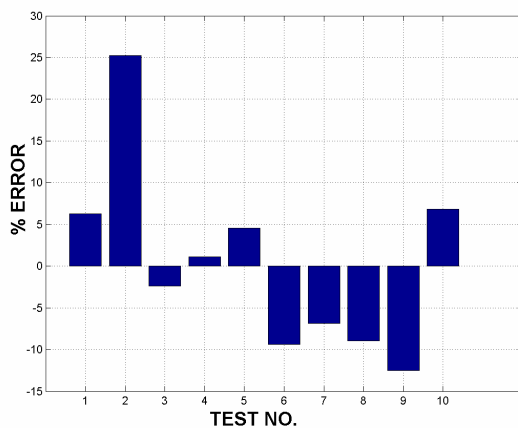


Fig 6.104 % Error of test set for NN model

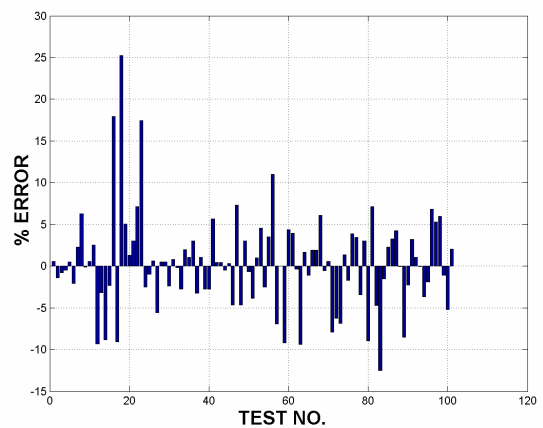


Fig 6.105 % Error of train set for NN model

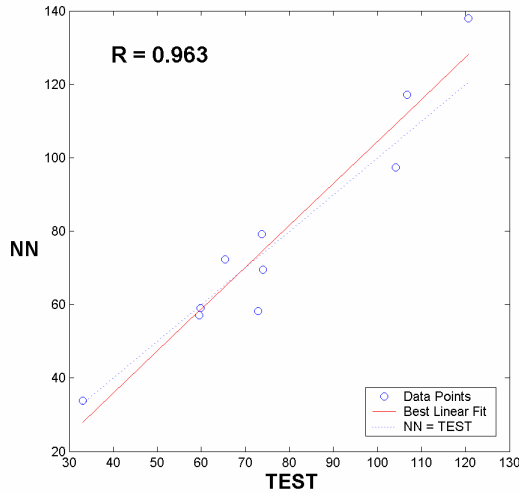


Fig 6.106 Performance of test set for NN model

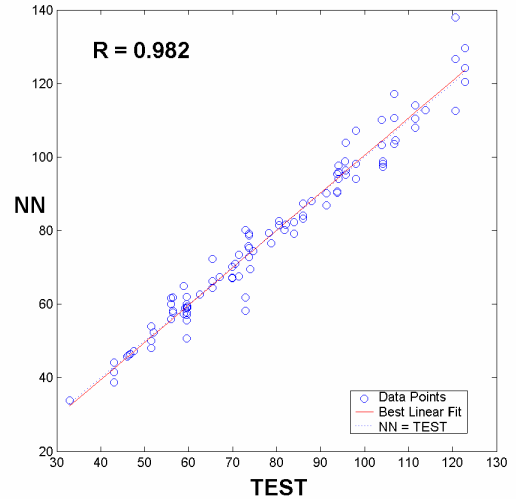


Fig 6.107 Performance of training set for NN model

Table 6.37. Statistics of performance and accuracy of (f'_{cc} / f'_{co}) of proposed NN model and various models compared to experimental results

Model	NN /Test	Eqn (6.48) /Test	Eqn (6.49) /test	Eqn (6.50) /Test	Eqn (6.51) /Test	Eqn (6.52) /Test	Eqn (6.53) /Test	Eqn (6.54) /Test	Eqn (6.55) /Test	Eqn (6.56) /Test	Eqn (6.57) /Test
Mean	1.00	1.31	1.33	1.25	1.20	0.98	1.06	1.29	1.03	1.01	1.00
Std. Dev.	0.06	0.34	0.28	0.19	0.28	0.18	0.17	0.26	0.16	0.19	0.46
R	0.98	0.87	0.87	0.85	0.86	0.77	0.87	0.87	0.87	0.87	0.87

6.2.9.5 Explicit Formulation of the NN Model

The main focus is to obtain the explicit formulation of the compressive strength of CFRP confined concrete cylinder as a function of variables given as follows:

$$f'_{cc} = f(D, nt, E_f, f_{co})$$

The explicit formulation for the proposed NN model is obtained by using the well trained NN parameters which are biases, and weights for the input and hidden layer and the normalization factors both for inputs and output proposed NN model. The derivation of the explicit formulation is too complex particularly for those who do

not have a neural network background. The same steps can be given in a simpler form as follows:

$$f'_{cc} = 150 * \left(\frac{2}{1 + e^{-2W}} - 1 \right)$$

$$\begin{aligned} \text{Where } W = & (0.63) * \left(\frac{2}{1 + e^{-2U1}} - 1 \right) + (0.74) * \left(\frac{2}{1 + e^{-2U2}} - 1 \right) + (-3.16) * \left(\frac{2}{1 + e^{-2U3}} - 1 \right) + \\ & (-2.62) * \left(\frac{2}{1 + e^{-2U4}} - 1 \right) + (-0.68) * \left(\frac{2}{1 + e^{-2U5}} - 1 \right) + (1.16) * \left(\frac{2}{1 + e^{-2U6}} - 1 \right) + \\ & (-1.36) * \left(\frac{2}{1 + e^{-2U7}} - 1 \right) + (0.61) * \left(\frac{2}{1 + e^{-2U8}} - 1 \right) + (0.83) * \left(\frac{2}{1 + e^{-2U9}} - 1 \right) + \\ & (-0.52) * \left(\frac{2}{1 + e^{-2U10}} - 1 \right) + (-0.61) * \left(\frac{2}{1 + e^{-2U11}} - 1 \right) + (-2.57) * \left(\frac{2}{1 + e^{-2U12}} - 1 \right) + \\ & (1.6) * \left(\frac{2}{1 + e^{-2U13}} - 1 \right) + (1.84) * \left(\frac{2}{1 + e^{-2U14}} - 1 \right) + (-3.77) * \left(\frac{2}{1 + e^{-2U15}} - 1 \right) + 0.25 \end{aligned}$$

$$\begin{aligned} U1 = & (0.024 * D) + (0.59 * nt) + (0.0004 * E_f) + (0.037 * f_{co}) + 14.02 \\ U2 = & (0.0217 * D) + (1.56 * nt) + (-0.0003 * E_f) + (0.0346 * f_{co}) - 4.42 \\ U3 = & (-0.07 * D) + (-0.1 * nt) + (-0.0013 * E_f) + (0.073 * f_{co}) + 16.12 \\ U4 = & (0.058 * D) + (-0.96 * nt) + (-0.0028 * E_f) + (-0.041 * f_{co}) + 1.42 \\ U5 = & (0.061 * D) + (-0.138 * nt) + (-0.0006 * E_f) + (-0.06 * f_{co}) - 4.02 \\ U6 = & (-0.0639 * D) + (-0.6017 * nt) + (-0.0014 * E_f) + (-0.0327 * f_{co}) + 15.32 \\ U7 = & (-0.0365 * D) + (-0.4598 * nt) + (-0.0004 * E_f) + (0.0691 * f_{co}) + 2.07 \\ U8 = & (-0.0684 * D) + (0.1734 * nt) + (0.0006 * E_f) + (-0.0381 * f_{co}) + 9.33 \\ U9 = & (0.0044 * D) + (0.2966 * nt) + (0.0008 * E_f) + (0.0736 * f_{co}) - 6.82 \\ U10 = & (0.0559 * D) + (1.3957 * nt) + (0.0004 * E_f) + (0.0160 * f_{co}) - 10.58 \\ U11 = & (0.0434 * D) + (-0.7968 * nt) + (0.0014 * E_f) + (-0.0164 * f_{co}) + 3.41 \\ U12 = & (-0.0309 * D) + (-1.0127 * nt) + (-0.0014 * E_f) + (-0.0326 * f_{co}) + 6.09 \\ U13 = & (-0.0638 * D) + (0.7750 * nt) + (0.0003 * E_f) + (0.0633 * f_{co}) + 1.34 \\ U14 = & (0.0920 * D) + (-0.6339 * nt) + (0.0007 * E_f) + (-0.0032 * f_{co}) - 2.86 \\ U15 = & (-0.0288 * D) + (-0.1202 * nt) + (0.0028 * E_f) + (0.0137 * f_{co}) - 5.91 \end{aligned}$$

It should be noted that the proposed explicit formulation of the NN models presented above are valid only for the ranges of experimental database given in Table 6.34 and for specimen that have a length to diameter ratio of 2 ($L/D = 2$).

6.2.9.6 Conclusion

This case study presents an alternative formulation for strength enhancement of CFRP wrapped concrete cylinders based on experimental results by means of NNs. The optimum NN architecture is obtained by a MATLAB program that automatically finds the best NN model. The results of the proposed NN model compared to experimental results are found to be quite satisfactory ($R=0.98$, std. dev. = 0.06). Moreover the accuracy of the proposed NN model is compared with several FRP confinement models proposed in literature and is found to be by far more accurate. The proposed NN model is also presented in explicit form which enables the NN model to be used for practical applications.

CHAPTER 7

CONCLUSIONS

This thesis presents an attempt to show the applicability of NNs for elastoplastic analysis of structures. It can be seen from previous chapters that all of the research objectives related to this study have been achieved. Thus the author has successfully presented the following original work:

1. Although NNs are widely used in the analysis of structural mechanics problems as well as for elastoplastic analysis of structures to an extent, no general study has been carried out covering a wide range of elastoplastic behavior of structures. Studies on this topic are specific studies in general. This thesis is the first study in literature investigating the feasibility of NNs for elastoplastic analysis of structures in a general aspect not only on theoretical basis of elastoplastic behavior but on realistic experimental results for various material types such as aluminum, steel, concrete and composite materials as well.
2. Case studies in this thesis also cover a wide range of material behaviour like flexural and buckling and complex behaviour as in the case of web crippling. It should be noted that the elastoplastic behavior in these case studies is quite complex and there exist almost no well established analytical solutions.
3. NNs are treated as black box in general. This thesis does not only verify NNs as alternative robust tools for elastoplastic analysis of structures but gives the solution in an explicit form of the proposed NN models as well. It aims to open the black box and to present the NN models in its implicit form. It should be noted that explicit formulation of NN models is of significant importance as it will serve for important advantages in the elastoplastic analysis and design of structures. This will also enable to open a new era in elastoplastic optimization analysis of structures.

4. The NN modeling in this thesis is based on FEM based data and experimental results collected from literature. Thus proposed NN models in this study are quite realistic as they are supported by experimental results.
5. One of the major tasks in NN studies which is quite difficult is the selection of Optimum NN architecture which is based on trial and error approaches. However, this thesis proposes an alternative algorithm for the selection of optimum NN architecture that automatically selects the best architecture.

The results of this thesis can be summarized as follows:

1. NNs can handle to model almost all complex plastic material behaviour being valid for almost all material types. In this thesis, NN models have shown satisfactory results for steel, aluminum, concrete and composite structures.
2. The optimum learning algorithm for modeling of elastoplastic behavior was found to be trainbfg. Another learning algorithm trainscg also gave satisfactory results where as trainlm algorithm should be used with a definite reserve. The optimum error learning algorithm was found to be SSE. It is impossible to define an optimum NN architecture but it can be concluded that single hidden layer architecture with less than 20 nodes is enough in general for the optimum NN architecture.
3. It should be stated that a proposed NN model should also show a good generalization capability i.e. it should give reasonable results for datasets different than test and training sets.
4. To attain flexibility, the NN toolbox offers significant advantages such as Hybrid NN models.
5. This study in fact proves the ultra high function approximation capability of NNs. It is almost impossible to reach this accuracy with other tools.

The author hopes that this study shall open a new era in NN studies of structural mechanics and analysis problems.

RECOMMENDATIONS FOR FUTURE WORK

It is obvious that artificial intelligence techniques or specifically soft computing approaches such as fuzzy logic, NNs, Genetic Algorithm and Genetic Programming will have much more profound application areas in the future for structural mechanics and structural analysis problems. For certain problems where no analytical solutions exist or the solution is extremely complex and difficult soft computing techniques will enable to obtain simple and explicit form solutions. Among these techniques, Genetic programming is worth to emphasize related to the subject of this thesis. Case studies performed in this thesis can also be modeled by Genetic programming. Furthermore, the proposed NN models in this thesis can also be used in inverse engineering analysis as well. These proposed NN models as they are all presented in explicit form, can be used in optimization applications of these problems. A new approach so called neuro-optimization can offer many advantages and open a new era in optimization studies.

REFERENCES

- AASHTO LRFD, (1998, 2000). Bridge design specifications and commentary. American Association of State Highway Transportation Official, Washington DC.
- Adebar, P. and Collins, M.P. (1996). Shear strength of members without transverse reinforcement, *Canadian Journal of Civil Engineering*, 23, 30–41
- Adeli, H. and Yeh. C.(1989). Peceptron learning in engineering design. *Microcomput Civil Engng*, 4:247-56.
- Adeli, H. and Hung, S.L. (1994). An Adaptive Conjugate Gradient Learning Algorithm for Efficient Training of Neural Networks. *Applied Mathematics and Computation*, Vol.62, pp.81-102.
- Adeli, H. Park,H.S. (1995). Counterpropagation Neural Networks in Structural Engineering, *Journal Of Structural Engineering*, 1205-1212
- Adhikary, B.B. and Mutsuyoshi, H. (2004). Artificial neural networks for the prediction of shear capacity of steel plate strengthened RC beams, *Construction & Building Materials*, 18:6 ,409-417
- Ahmad, S.H., Khaloo, A.R. and Poveda, A. (1986). Shear Capacity of Reinforced High-Strength Concrete Beams, *ACI Journal, Proceedings*,83:2, 297–305
- AISI (1996).*Specification for the Design of Cold-Formed Steel Structural Members*, American Iron and Steel Institute, Washington, D.C.
- AISC (1997). Specification for steel hollow structural sections. (AISC LRFD), American Institute of Steel Construction, Chicago, Il, USA
- Akhtar, S.and Sujiang, H. (1995). *Continuum Theory of Plasticity* , Wiley
- Chen,W.F. and Han, D.J.(1988). *Plasticity for Structural Engineers*, Springer

Allen, D. H. (1980). A note on the combined isotropic-kinematic work hardening rule. *IJNME*, 15, 1724-1728.

ACI (2002). ACI Building Code Requirements for Reinforced Concrete, ACI 318-02

Andersson, T. and Bergfors, A.(1973). Upplagstryckets inverkan på brottlasten hos trapetsprofilerad plåt, Examenarbeite i Stålbyggnad, Stockholm, K.T.H.

Arnault P.(1967). Recherche sur le flambement des profiles en alliages legers. Paris: Centre technique Industriel de la Construction Metallique (CTICM)

AS 4100 (1998). Standards Australia. *Australian standard AS 4100 steel structures*. Standards Australia, Sydney, Australia

ASCE (1971). *Plastic Design in Steel, A Guide and Commentary*, American Society of Civil Engineers, New York, New York,

ASCE (1991). Specification for the design of cold-formed stainless steel structural members. ANSI/ASCE-8-90. New York

Ashour, A.F.and Morley, C.T. (1994). The numerical determination of shear failure mechanisms in reinforced-concrete beams, *The Structural Engineer*, 72:23, 395–400.

Aust/NZS (2001). Cold-formed stainless steel structures. Australian/New Zealand Standard. Sydney, Australia: Standards Australia

Ayyub, B.M. (1997). *Uncertainty Modeling and Analysis in Civil Engineering*, CRC Press

Bakker, M.C.M. (1992). *Web Crippling of Cold-Formed Steel Members*, Dissertation Eindhoven University of Technology, The Netherlands

Banabic,D., Bunge,H.J., Pvhlandt,K. and Tekkaya, A.E.(2000). *Formability of Metallic Materials: Plastic Anisotropy, Formability Testing, Forming Limits*, Springer

Basheer, I. (1998).A. *Neuromechanistic-Based Modeling And Simulation Of Constitutive Behavior Of Fine-Grained Soils* , Ph.D. Thesis, Kansas State University

Bernard, A., Frey, F., Janss, J. and Massonnet, C. (1973). *Recherches sur le comportement au flambement de barres en aluminium*. IABSE Mem, 33(I):1–32.

Bezkorovainy, P., Burns, T. and Rasmussen, K.J.R. (2003). ,Strength Curves for Metal Plates in Compression, *Journal Of Structural Engineering*, ASCE , 1433-40

Bezkorovainy, P., Burns, T. and Rasmussen, K.J.R. (2002). Strength Curves for Metal Plates in Compression, Research Report No R821, Centre for Advanced Structural Engineering, University of Sydney

Boeraeve, P., Lognard, B., Janss, J., Gerardy, J.C. and Schleich, J. B.(1993). Elastoplastic behaviour of steel frameworks. *Journal of Constructional Steel Research*, 27, 3-21.

Faella,C., Mazzolani,F.M.,Piluso,V.,and Rizzano,G.(200). Local Buckling Of Aluminum Members: Testing And Classification, *Journal Of Structural Engineering*, 353-360

CSA (1995).Canadian Standards Association: S136-94 (with General Instruction No. 2), Cold Formed Steel Structural Members, Structures (Design), Rexdale (Toronto), Ontario, Canada

Chen, W.F. (1988). Evaluation of Plasticity Based Constitutive Models for Concrete Material. *Solid Mech. Arch.*, 13(1), 1-63.

Chou, S. M., Rhodes, J.(1997). Review And Compilation Of Experimental Results On Thin-Walled Structures, *Computers & Structures*, 65(1): 47-67

Chuang, P.H., Goh, T.C. and Wu.X. (1998). Modeling the Capacity of Pin-Ended Slender Reinforced Concrete Columns Using Neural Networks. *Journal of Structural Engineering*, 124(7), 830-838.

Cladera, A. and Mari, A.R.(2004). Shear design procedure for reinforced normal and high-strength concrete beams using artificial neural networks. Part I: beams without stirrups, *Engineering Structures*, 26:7, 917-926

Cladera, A. and Mari, A.R.(2004). Shear design procedure for reinforced normal and high-strength concrete beams using artificial neural networks. Part II: beams with stirrups, *Engineering Structures*, 26:7, 92-936

Cladera A. (2003). *Shear design of reinforced high-strength concrete beams*. PhD thesis published by ACHE (Spanish Concrete Association)

Coetzee, J.S., Van den Berg, G.J. and Van der Merwe, P.(1990). The effect of work hardening and residual stresses due to cold-work of forming on the strength of cold-formed stainless steel lipped channel section. In: *Proceedings of the tenth international specialty conference on cold-formed steel structures*, 143–62.

Collins, M.P.and Kuchma, D. (1999). How safe are our large, lightly reinforced concrete beams, slabs and footings? *ACI Structural Journal*, 96:4, 482-490

Drucker, D.C. and Prager,W. (1952). *Soil mechanics and plastic analysis or limit design*, *Quart. Appl. Math.*, 10: 157–165

David, R. O.(2002). *Plasticity and Geomechanics*. West Nyack, NY, USA: Cambridge University Press

Davies, J.M.and Jiang, C. (1997). Design Procedures for Profiled Metal Sheeting and Decking, *Thin-Walled Structures*, 27, 43-53

Davies, J.M.; Jiang, C. and Liu, Y.J. (1999). Web Crippling in Trapezoidally Profiled Sheeting and Decking, *Proceedings Eurosteel*, Praha, Czech Republic

Desai, C.S., and Siriwardane, H.J. (1984). *Constitutive Laws for Engineering Materials*. Prentice-Hall, Englewood Cliffs. N.J.

Djalaly, H., Sfintesco, D. (1972). Recherches sur flambement de barres en aluminium. Reports of the working commissions, IABSE, Vol. 23, *International Colloquium on Column Strength*

Duthinh, D. and Carino, N.J. (1996). *Shear Design of High-Strength Concrete Beams: A Review of the State-of-the-Art*, Building and Fire Research Laboratory, NIST, Gaithersburg

Dwight, J. (1999). *Aluminum design and construction*, E&FN Spon

ECCS (1978). *European recommendations for aluminium alloy structures*, 1st ed. European Convention for Constructional Steelwork, Brussels

Ellis, G. W., Yao, C., Zhao, R. and Penumadu, D. (1995). Stress-Strain Modeling of Sands Using Artificial Neural Networks." *Journal of Geotechnical Engineering Division*, ASCE. 121(5), 429-435.

Elzanaty, A.H., Nilson A.H. and Slate, F.O. (1986). Shear Capacity of Reinforced Concrete Beams Using High-Strength Concrete, *ACI Journal, Proceedings*, 83:2, 290-296

ENV (1993). European Prestandard Eurocode3, *Design of Steel Structures, Part 1-3: General rules-Supplementary rules for cold-formed thin gauge members and sheeting*, European Committee for Standardization CEN, Brussels

Erklig,A.,(2003), Finite Element Analysis of Finite strain Elastoplastic Impact Problems, PhD Thesis, University Of Gaziantep

Eurocode 3 (1996). *Design of steel structures, Part 1.4: supplementary rules for stainless steels*. Brussels: European Committee for Standardization

Eurocode 3 (2003). *Design of steel structures- Part 1-1: General rules and rules for buildings*, Brussels

Eurocode 9 (1998). *Design of aluminium alloy structures, part 1.1*. European Committee for Standardization, Brussels, Belgium.

Eurocode 2 (2002) *Design of Concrete Structures, Part 1: General rules and rules for buildings*. European Committee for Standardization

Fardis, M.N.and Khalili, H.(1982). FRP-encased concrete as a structural material. *Magazine of Concrete Research*, 34(121), 191-202.

Fardis, M.N.and Khalili, H. (1982).Concrete encased in fiberglass-reinforced-plastic. *Journal of the American Concrete Institute. Proceedings*, 78(6), 440-446.

Frey, F. and Rondal, J.(1978). *Aluminium alloy buckling curves a,b,c: table and equations*, ECCS Committee 16, Doc. 16-78-1

Galambos, T.V. (1998). *Guide to stability design criteria for metal structures*. New York: John Wiley & Sons

Gallagher, R. S. (1995). *Computer Visualization: Graphics Techniques for Scientific and Engineering Analysis*, CRC Press

Gao, X.W. and Davies, T.G.(2002).*Boundary Element Programming in Mechanics*, Cambridge University Press

Gardner, L. and Talja, A. (2003). *WP2: Structural hollow sections, ECSC project: structural design of cold-worked austenitic stainless steel*. Contract No. 7210 PR318; The Steel Construction Institute

Gardner, L. (2002). *A new approach to structural stainless steel design*. Ph.D. Thesis, Department of Civil and Environmental Engineering, Imperial College London, UK

Ghaboussi, J., Pecknold, D.A., Zhang, M. and Haj, R. (1998). Autoprogressive training of neural network constitutive models. *International Journal for Numerical Methods in Engineering*, 42(1), 105–126.

Ghaboussi, J., Garrett, J.H. and Wu, X. (1991). Knowledge-Based Modelling of Material Behaviour with Neural Networks. *Journal of Engineering Mechanics*, Vol.117, No.1, 132-153.

Ghaboussi, J., Garret, J. H., Jr., and Wu, X. (1990). Material Modeling with Neural Networks." *Proceedings of the International Conference on Numerical Methods in Engineering : Theory and Applications*, Swansea, U.K., 701-717.

Gioncu, V. and Petcu, D. (1997). Available Rotation Capacity of Wide-Flange Beams and Beam-Columns Part 1. Theoretical Approaches, *Journal of Constructional Steel Research*, 43(1-3), 161-217

Gioncu, V. and Petcu, D. (1997). Available Rotation Capacity of Wide-Flange Beams and Beam-Columns Part 2. Experimental and Numerical Tests, *Journal of Constructional Steel Research*, 43(1-3), 219-244

Goncalves, A. and Dinar, C. (2004). GBT local and global buckling analysis of aluminium and stainless steel columns Rodrigo, *Computers and Structures*, 82 (1): 1473–1484

González-Fonteboa, B.(2002).*Hormigones con áridos reciclados procedentes de demoliciones: dosificaciones, propiedades mecánicas y comportamiento estructural a cortante*, PhD Thesis, Universidad de la Coruña

Gozzi, J.(2004). *Plastic behaviour of steel: experimental investigation and modeling*, Licentiate Thesis , Civil and Environmental Engineering / Steel Structures, Lulea University of Technology,

Guzelbey, İ.H. (1992). *Finite and Boundary Analysis of Elasto-plastic Finite Strain Contact Problems*, PhD Thesis, Cranfield Institute of Technology

Hajela, P., and Berke, L. (1991). Neurobiological computational modes in structural analysis and design, *Computers and Struct.*, 41(4), 657-667.

Hancock, G. J.(2001). *Cold-Formed Steel Structures to the AISI Specification*, New York, Marcel Dekker Incorporated

Hashash, M. A., Jung, S. and Ghaboussi, J.(2004).Numerical implementation of a neural network based material model in finite element analysis, *Int. J. Numer. Meth. Engng*, 59,989–1005

Haykin, S. (1994). *Neural Networks: A Comprehensive Foundation*, NY:Macmillan.

Haykin, S. (1999). *Neural Networks: A Comprehensive Foundation*, 2nd ed. Englewood Cliffs, NJ: Prentice-Hall

Hebb, D.O.(1949). *The Organization of Behavior*. Wiley, New York

Hecht-Nielsen, R. (1990).*Neurocomputing*, Addison-Wesley, Reading, MA, 1990

Hetrakul, N. and Yu, W. W.(1978). *Structural Behaviour of Beam Webs Subjected to Web Crippling and a Combination of Web Crippling and Bending*, Final Report, Civil Engineering Study, 784, University of Missouri-Rolla, Rolla, MO

Hill,R.(1998). *The Mathematical Theory of Plasticity*, Oxford University Press

Hoang, L.C. and Nielsen, M.P.(1998). Plasticity Approach to Shear Design, *Cement and Concrete Composites*, 20:6, 437-453

Hofmeyer, H.(2000). *Combined Web Crippling and Bending Moment Failure of First-Generation Trapezoidal Steel Sheeting: Experiments, Finite Element Models, Mechanical Models*, PhD Thesis, Eindhoven University of Technology, The Netherlands

Hofmeyer, H., Kerstens, J. G. M., Snijder, H. H. and Bakker, M. C. M.(2001). New prediction model for failure of steel sheeting subject to concentrated load (web crippling) and bending *Thin-Walled Structures*,(39-9): 773-796

Hollaway, L.C. (2004). *Advanced Polymer Composites for Structural Applications in Construction*: ACIC 2004, Woodhead Publishing

Hu, H.-T. and Schnobrich, W.C. (1989). "Constitutive Modelling of Concrete by Using Non-Associated Plasticity." *Journal of Materials in Civil Engineering*. 1(4), 199-216.

Hung, S. L., and Adeli, H. (1991). A model of perceptron learning with a hidden layer for engineering design. *Neurocomputing*, 3(1), pp. 3-14

Ibell, M.M. (1998). An upper-bound plastic analysis for shear, *Magazine of Concrete Research*,50:1, 67-73.

Islam, M.S., Pam, H.J. and Kwan A.K.H.(1998). Shear capacity of high- strength concrete beams with their point of inflection within the shear span, *Proceedings of the Institution of Civil Engineers, Structures and buildings*, 128:1, 91-99

ISO (1992). Aluminium structures: material and design, part 1: ultimate limit state—static loading. Technical report, Doc. No. 188, International Standards Organization Committee TC 167/SC3

Iswandi, I. (1994). *Applications Of Non-Associated Plasticity In Modelling The Mechanical Response Of Concrete*, PhD Thesis, University Of Toronto

Jenkins, W.M. (1995). Neural Network-Based Approximations for Structural Analysis. *Developments in Neural Networks and Evolutionary Computing for Civil and Structural Engineering*, Edinburgh, UK, 25-35.

Jeroen Mennink (2002). *Cross-sectional stability of aluminium extrusions: Prediction of the actual local buckling behaviour*, PhD Thesis, Technical University of Eindhoven.

Kaczmarczyk L., and Waszczyszyn, Z. (2003). Neural procedures for the hybrid FEM/NN analysis of elastoplastic plates, *Numerical Methods in Continuum Mechanics*, Zilina, Slovak Slovak Republic

Kaliszuk J. and Waszczyszyn Z. (2003). Reliability analysis of structures by neural network supported Monte Carlo methods, *Neural Networks and Soft Computing*, 754-759, Springer, Physica-Verlag, Heildelberg

Kang, H.-T. and Yoon, C. J. (1994). Neural network approaches to aid simple truss design problems. *Microcomputers in Civ. Engrg.*, 9(3), pp. 211-218.

Kani, M.W., Huggins, M.W. and Wiltkopp, P.F. (1979). *On shear in reinforced concrete*, PhD Thesis, Department of Civil Engineering, University of Toronto, Canada

Karren, K.W.(1967). Corner properties of cold-formed steel shapes. *Journal of the Structural Division*, ASCE, 93(ST1):401–32.

Kasabov, K.N. (1996). *Foundations of Neural Networks, Fuzzy Systems, and Knowledge Engineering*, A Bradford Book The MIT Press Cambridge, Massachusetts, London, England

Kemp, A. R. and Dekker, N. W. (1991). Available rotation capacity in steel and composite beams. *The Structural Engineer*, 69(5), 88-97.

Kemp, A. R. (1985). Interaction of plastic local and lateral buckling. *Journal of Structural Engineering*, 111(10), 2181-2196.

Keulers, A.J.C.(1981). Buigproeven en Interactieproeven. Een vergelijking van proefresultaten met de ECCS-81 interactiecurve, waarbij deze curve gebaseerd is op testwaarden voor M_d en R_d , i.p.v. op volgens de ECCS-81 berekende waarden. Report THE171 BKO-S-81-01, Eindhoven University of Technology, Department of Structural Design, The Netherlands

Kim, J.K.and Park, Y.D.(1994). Shear Strength of Reinforced High Strength Concrete Beams without Web Reinforcement, *Magazine of Concrete Research*, 46,7-16

Kissell, J.R. and Ferry,R.L.(2002). *Aluminum Structures: A Guide to Their Specifications and Design*, Wiley

Kloppel, K.and Barsch, W. (1973). *Versuche zum Kapitel 'Stabilitatsfalle' der Neufassung von DIN 4113. Aluminium*, 10:690-9.

Konar , A. (1999). *Artificial Intelligence and Soft Computing* , CRC Press

Kono S., Inazumi M. and Kaku T. (1998). Evaluation of Confining Effects of CFRP Sheets on Reinforced Concrete Members. *Proceedings of the 2nd International Conference on Composites in Infrastructure ICCI'98*, 343-355.

Kortesis, S. and Panagiotopoulos, P.D. (1993). Neural networks for computing in structural analysis: Methods and prospects of applications, *Int. J. Numer. Meth. Engrg.* 36, 2305–2318.

Kuhlmann, U. (1989). Definition of flange slenderness limits on the basis of rotation capacity values. *Journal of Constructional Steel Research*, 14, 21-40.

Kuhlmann, U. (1986). *Rotations kapazität biegebeanspruchter IProfile unter Berücksichtigung des plastischen Beulens*. Technical Report, Mitteilung Nr. 86-5

Lade, P.V. (1988). Effects of Voids and Volume Changes on the Behaviour of Frictional Materials. *Int./ Num. Anal. Meth. Geomech.* 12, 351-370.

Landolfo, R. and Mazzolani, F.M. (1994). Ultimate Behaviour of Trapezoidal Steel Sheets in Bending, *Proceedings 12th International Specialty Conference on Recent Research and Developments in Cold-Formed Steel Design and Construction*, St. Louis, Missouri, U.S.A

Landolfo, R. and Mazzolani, F.M. (1995). *Comportamento flessionale di lamiera grecate in acciaio: analisi sperimentale*, *Costruzioni Metalliche*, 29

Langseth, M. and Hopperstad, O. S. (1995). Local buckling of square thin-walled aluminium extrusions. *Proc., 3rd Int. Conf. on Steel and Aluminium Struct.*, Istanbul, Turkey, 147–154.

Lay, M.G. and Galambos, T.V.(1965). Inelastic Steel Beams under Uniform Moment, *Journal of the Structural Division, ASCE*, Vol. 92, No. ST2, 207-228.

Lefik, M. and Schrefler, B.A. (2003). Artificial neural network as an incremental non-linear constitutive model for a finite element code. *Comput. Methods Appl. Mech. Engrg.* 192, 3265–3283

Lepi, S. M. (1998). *Practical Guide to Finite Elements*. CRC Press,

Li, S., and Reid, S. R. (1992). The plastic buckling of axially compressed square tubes. *J. Appl. Mech.*, 59, 201–210.

Lindner, J. and Shin, T. (1996). Interaction between Flexural Buckling and Plate Buckling on the Web Crippling Capacity of Trapezoidal Sheeting, *Conference Proceedings of the Second International Conference on Coupled Instabilities in Metal Structures CIMS*, Liege, Belgium

Lorenzis, L.A. (2001). *Comparative Study of Models on Confinement of Concrete Cylinders with FRP Composites*, PhD Thesis, Division for Building Technology, Chalmers University of Technology, Sweden

Lu JG, Zhou J and Wang H. (1994). Approach to structural approximation analysis by ANN, *Sci in China*, 37(8), 990-997

Lu, W. (2000). *Neural Network Model For Distortional Buckling Behaviour Of Cold-Formed Steel Compression Members*. MSc Thesis, Helsinki University of Technology, Finland

Lukaszyn, S. and Waszczyszyn, Z. (1999). Hybrid CPN / FDM analysis of an elastoplastic beam, *Proc. 4rd Conf. on Neural Networks and Their Applications*, Zakopane, 350-356.

Lukey, A. F. and Adams, P. F. (1969). Rotation capacity of beams under moment gradient. *Journal of the Structural Division, ASCE*, 95(ST6), 1173-1188.

M. Ashraf, L. and Gardner, D.A. (2005). Nethercot, Strength enhancement of the corner regions of stainless steel cross-sections, *Journal of Constructional Steel Research*, 61, 37–52

Mansour, M.Y., Dicleli, M., Lee, J.Y. and Zhang, J. (2004). Predicting the shear strength of reinforced concrete beams using artificial neural networks. *Engineering Structures*, 26:6, 781-799

- Masri, S. F., Chassiakos, A. G., and Caughey, T. K. (1993). Identification of nonlinear dynamics system using neural networks. *Appl.Mech.*, 60(1),123-133
- Matthys, S., Taerwe, L. and Audenaert, K. (1999). *Tests on Axially Loaded Concrete Columns Confined by Fiber Reinforced Polymer Sheet Wrapping*. 4th International Symposium on Fiber Reinforced Polymer Reinforcement for Reinforced Concrete Structures, 217-228.
- Mazzolani, F.M. (2001).EN1999 Eurocode 9: Design of aluminium structures, *Proceedings Of The Institution Of Civil Engineers-Civil Engineering* 144(2), 61-64
- Mazzolani, F. M. (1995). *Aluminium alloy structures*. E&FN Spon, London.
- Mazzolani, F. M., Faella, C., Piluso, V., and Rizzano, G. (1996a). *Experimental analysis of aluminium alloy SHS-members subjected to local buckling under uniform compression*. Proc., 5th Int. Colloquium on Struct. Stability, Structural Stability Research Council, Gainesville,Fla., 281–291.
- Mazzolani, F. M., Faella, C., Piluso, V., and Rizzano, G. (1996b). *Assessment of the stub column test for aluminium alloys*. Proc., 2nd Int. Conf. on Coupled Instabilities in Metal Struct., Imperial College Press, Liege, Belgium, 547–556.
- Messner, J.I., Sanvido, V.E. and Kumara, S.R.T. (1994). A Neural Network for Structural System Selection. *Microcomputers in Civil Engineering*, 9(2), 109-118.
- Micelli, F., Myers, J.J., and Murthy, S. (2001). *Effect of environmental cycles on concrete cylinders confined with FRP*, Proceedings of CCC 2001 International Conference on Composites in Construction, Porto, Portugal
- Miller, P. (1976). *Failure Mechanisms for reinforced concrete beams in torsion and bending*, International association for bridge and structural engineering (IABSE), 36:2, 147-163.

Minsky, M. and Pappert, S. (1969). *Perceptrons*. MIT Press, Cambridge, MA.

Mirmiran, A, Zagers, K. and Yuan, W. (2000). Nonlinear Finite element modeling of concrete confined by fiber composites, *Finite Elements in Analysis and Design* ,35, 79-96

Miyauchi, K, Nishibayashi, S. and Inoue, S. (1997). Estimation of strengthening effects with carbon fiber sheet for concrete column. Proceedings of the Third International Symposium (FRPRCS-3) on Non-Metallic (FRP) Reinforcement for Concrete Structures, Sapporo, Japan, 1, 217-224.

Moaveni, S. (2003). *Finite Element Analysis: Theory and Applications with ANSYS*, 2nd Ed. Prentice Hall

Morrow, J. and Viest, I.M. (1957). Shear strength of reinforced concrete frame members without web reinforcement, *ACI Journal*,28:9, 833-869

Mphonde, A.G. and Frantz, G.C. (1984). Shear Tests of High- and Low-Strength Concrete Beams Without Stirrups, *ACI Journal*, 81:4, 350-357

Mucha, G. and Waszczyszyn, Z. (1994). *Hybrid Neural Network computational program for bending analysis of elastoplastic beam*, 13. Polish Con. On Comp. Meth. In Mech. Ponzan, 949-954

Mucha, G and Waszczyszy, Z. (1997). *Hybrid neural-network / computational program for bending analysis of elastoplastic beams*”, in: Proc. 12th Polish Conf. Computer Meth. Mech., Poznań, Vol. 3, pp. 941-948.

Mukherjee, A. and Deshpande, J.M. (1995). Modeling Initial Design Process Using Artificial Neural Networks. *Journal of Computing in Civil Engineering*, 9(3),194-200.

Mukherjee, A. Deshpande, J.M. and Anmala, J. (1996), Prediction of Buckling Load of Columns Using Artificial Neural Networks. *Journal of Structural Engineering*, Vol. 122, No. 11, pp.1385-1387.

NAS (2001) *North American Specification for the Design of Cold-Formed Steel Structural Members*, Washington, D.C.

Nayak G.C. and Zienkiewicz O.C.(1972). Elasto-Plastic Stress Analysis:A generalisation for various Constitutive Relations Including Strain Softening. *Inter.J. Numer. Meth Engg.* 5, 113-135.

Nielsen, M.P. and Braestrup, M.W. (1975). Plastic Shear Strength of Reinforced Concrete Beams, *Bygningsstatistiske Meddelelser*, 46:3 , 61-99.

Nigrin, A. (1993). *Neural Networks for Pattern Recognition*, Cambridge, The MIT Press.

Oreta, A. and Winston, C.(2004). Simulating size effect on shear strength of RC beams without stirrups using neural networks, *Engineering Structures*, 26:5, 681-691

Pabisek, E. and Waszczysyn Z. (2001). *Neural analysis of elastoplastic plane stress problem with unilateral constraints*, Proc. European Conference on Computational Mechanics, EC-2001, CD-ROM, p.15, Cracow Univ. of Technology, Cracow, Poland,

Paik, J.K. and Anil, K.T. (2003). *Ultimate Limit State Design of Steel-Plated Structures*, Wiley

Papadrakakis, M., Papadopoulos, V. and Lagaros, N.D. (1996). Structural reliability analysis of elastic-plastic structures using neural network and Monte Carlo simulation, *Comp. Meth. Appl. Mech. Eng.*, 136,145-163

Park, M.S. and Lee, B.C. (1996). Prediction of Mode Parameters and Moment-Rotation Curves for Crushed Thin-Walled Trapezoidal Tubes in Bending, *Journal of Applied Mechanics*, 63: 453-459.

Peng, L. (1999). *Shear Strength of Beams by Shear-Friction*, PhD Thesis, The University Of Calgary

Penumadu, D., Jin-Nan, L., Chameau, J.-L., and Sandarajah. A. (1994). Anisotropic Rate Dependent Behavior of Clays Using Neural Networks. *Proc. XIIIICSMFE, ICSMFE*, New Delhi, India, 4, 1445-1448.

Petcu, D. and Gioncu V. (2003). Computer program for available ductility analysis of steel structures, *Computers&Structures*, 81(23), 2149-2164

Pham, D.T. and Pham, P.T.N. (1999). Artificial intelligence in engineering, *International Journal of Machine Tools & Manufacture*, 937-949

Prager, W. (1955). The Theory of Plasticity: A Survey of Recent Achievements. *Proc. Instn Mech. Engrs* , 169, 41-57.

Rasmussen, K.J.R. and Hancock, G.J. (1993). Design of cold-formed stainless steel tubular members. I Columns. *Journal of the Structural Engineering*, ASCE, 119(8):2349-67.

Rasmussen, K.J.R. and Rondal, J. (2000). Strength curves for aluminium alloy columns, *Engineering Structures*, 23 1505-1517

Rasmussen, K.J.R. and Rondal, J. (1996). J. Strength curves for metal columns. *J Struct Engng* ASCE ,123(6):721-8.

Rasmussen, K.J.R. and Rondal, J. (1997). Explicit approach to design of stainless steel columns. *J. Struct. Eng.*, 123;7;857-863.

Reddy, JN. (2004). *An Introduction to Nonlinear Finite Element Analysis*, Oxford University Press

Reinsch, W. (1983). *Das Kantenbeulen zur rechnerischen Ermittlung von Stahltrapezblechträger*, Dissertation, Technische Hochschule Darmstadt, Germany

Rhodes, J.; Nash, D. and Macdonald, M. (1999). An Examination of Web Crushing in Thin-Walled Beams, *Proceedings Light-Weight Steel and Aluminium Structures, Fourth International Conference on Steel and Aluminium Structures*, Espoo, Finland, 795-802

Rochette, P. and Labossière, P. (2000). Axial Testing of Rectangular Column Models Confined with Composites. *Journal of Composites for Construction*, ASCE, 4(3), 129-136.

Rogers, J. L. (1994). Simulating Structural Analysis with Neural Network. *Journal of Computing in Civil Engineering*, 8(2), 252-265.

Rondal, J. and Maquoi, R. (1979). Formulation d'Ayrton-Perry pour le flambement des barres métalliques. *Construct Metall*, 4:41-53.

Rondal, J. (1980). *Formulation simplifiée des courbes européennes de flambement des barres en alliage d'aluminium*. Report 95, MSM Institute of Civil Engineering, University of Liege

Rousakis, T. (2001). *Experimental investigation of concrete cylinders confined by carbon FRP sheets, under monotonic and cyclic axial compressive load*, Research Report, Chalmers University of Technology, Göteborg, Sweden

RSD (1974). *Richtlijnen voor de berekening van Stalen Dakplaten-RSD 1974*, Dumebo en Staalbouwkundig Genootschap, The Netherlands

Rumelhart, D.E., Hinton, G.E. and Williams, R.J. (1986). Learning internal representation by error propagation *Parallel Distributed Processing: Exploration in the Microstructure of Cognition*, Vol. 1. MIT Press, Cambridge, MA, Chapter 8

Saadatmanesh, H., Ehsani, M.R. and Li, M.W. (1994). Strength and Ductility of Concrete Columns Externally Reinforced with Fiber Composite Straps. *ACI Structural*, 91(4), 434-447.

Saafi, M., Toutanji, H.A. and Li, Z. (1999). Behavior of Concrete Columns Confined with Fiber Reinforced Polymer Tubes. *ACI Materials Journal*, 96(4), 500-509.

Salandra, M.A. and Ahmad, S.H. (1989). Shear capacity of reinforced lightweight high-strength concrete beams, *ACI Journal*, 86:6, 697-704

Salmon, C.G. and Johnson, J.E. (1996). *Steel Structures: Design and Behavior*, HarperCollins Publishers, Inc. New York, New York, USA

Samaan, M., Mirmiram, A. and Shahawy, M. (1998). Model of Concrete Confined by Fiber Composites. *Journal of Structural Engineering, ASCE*, 124(9,) 1025-1031.

Sanad, A. and Saka, M.P. (2001). Prediction Of Ultimate Shear Strength Of Reinforced-Concrete Deep Beams Using Neural Networks. *Journal of Structural Engineering*, 127:7, 818-828

Santaputra, C. (1986). *Eighth progress report, Design of Automotive Structural Components using High Strength Sheet Steels, Web Crippling of Cold Formed Steel Beams*, Civil Engineering Study 86-1, Structural Series, University of Missouri-Rolla, Department of Civil Engineering

Schafer, B.W. and Peköz, T. (1998). *Direct Strength Prediction of Cold-Formed Steel Members Using Numerical Elastic Buckling Solutions*, Proceedings 14th International Specialty Conference on Recent Research and Developments in Cold-Formed Steel Design and Construction, , St. Louis, Missouri, USA

Schafer, B.W. and Peköz, T. (1997). The Behaviour and Design of Longitudinally Stiffened Thin-Walled Compression Elements, *Thin-Walled Structures*, 27: 65-78.

Seleemah, A.A. (2005). A neural network model for predicting maximum shear capacity of concrete beams without transverse reinforcement, *Canadian Journal of Civil Engineering*, 32:4 , 644-657

Shahawy, M., Mirmiran, A. and Beitelmann, T. (2000). Tests and modeling of carbon-wrapped concrete columns, *Composites Part B: Engineering*, Elsevier Science Ltd., London, UK, 31, 471-480,

Sharp, M.L. (1990). Design parameters for web crippling of thin-walled members, report No. 57-90-21, Alcoa laboratories

Sidarta, D. E. (2000). *Neural Network-Based Constitutive Modeling Of Granular Material*, Ph.D. Thesis , University of Illinois at Urbana-Champaign,

Singer, J., Arbocz, J. and Weller, T. (2002). Buckling experiments: experimental methods in buckling of thin-walled structures, Wiley

Singer, J., Arbocz, J. and Weller, T. (2002). Buckling Experiments, Shells, Built-up Structures, Composites and Additional Topics (Buckling Experiments) , Wiley

Spangemacker, R. (1991). *Zum Rotationsnachweis von Stahlkonstruktion, die nach dem traglastverfahren berechnet werden*. Dissertation, Technischen Hochschule Aachen

Spoelstra, M.R. and Monti, G. (1999). FRP-Confined Concrete Model. *Journal of Composites for Construction*, 3(3),143-150.

Studnicka, J. (1990). *Web crippling of wide deck sections*, *Recent Research and Developments in Cold-Formed Steel Design and Construction*, Edited by W.W. Yu and R.A.Laboube, Rolla, University of Missouri-Rolla, Department of Civil Engineering,

Sun, D., Hu, Q. and Xu, H. (2000). A neurocomputing model for the elastoplasticity, *Comput. Methods Appl. Mech. Engrg.* 182, 177-186

Suong, V. H., Van, H. S., Van, H. and Feng W. F. (1998). *Hybrid Finite Element Method for Stress Analysis of Laminated Composites*. Kluwer Academic Publ.,

Suzuki, T., Ogawa, T. and Ikarashi, K. (1994). A study on local buckling behaviour of hybrid beams. *Thin-Walled Structures*, 19, 337-351.

Szewczyk, Z.P. and Noor, A.K. (1996). Hybrid neurocomputing/numerical strategy in nonlinear structural analysis, *Comp. & Struct.*, 58, 661-677

Szilard, R. (2004). *Theories and Applications of Plate Analysis: Classical Numerical and Engineering Methods*, Wiley

Talja, A. (1992). *Design of cold-formed HSS channels for bending and eccentric compression, Bending in the plane of symmetry*, VTT Research Notes 1403, Technical Research Centre of Finland, Espoo

Theocaris, P.S and Panagiotopoulos, P.D. (1993). Neural networks for computing in fracture mechanics, *Comp. Meth. Appl. Mech. Eng.*, 106, 231-228

Thomas J. S. (2000). *Cross Sectional Compactness And Bracing Requirements For Hps70w Girders*, MSc Thesis, The Pennsylvania State University,

Thorenfeldt, E. and Drangsholt, G. (1990). Shear capacity of reinforced high strength concrete beams, *ACI 2nd International Symposium on HSC*, 129-154

Tomà, A. and Stark, J.W.B. (1973). II. Vrij opgelegde platen op twee steunpunten zonder dimpels, Onderzoek geprofileerde stalen dakplaten, werkrapport van de werkgroep S.G.-T.C. 16 "Onderzoek van stalen dak- en gevelplaten", Instituut TNO voor bouwmaterialen en bouwconstructies

Tomà, A. and Stark, J.W.B. (1974). Twee veldsplaten zonder dimpel, Onderzoek geprofileerde stalen dakplaten, werkrapport van de werkgroep S.G.-T.C. 16

"Onderzoek van stalen dak- en gevelplaten", Instituut TNO voor bouwmaterialen en bouwconstructies

Topping, B.H.V. and Bahreininejad, A. (1997). *Neural Computing For Structural Mechanics*, Saxe-Coburg Publications,

Toutanji, H. (1963). Stress-Strain Characteristics of Concrete Columns Externally Confined with Advanced Fiber Composite Sheets. *ACI Materials Journal*, 96(3), 397-404.

Tsai, Y.M. and Crisinel, M. (1996). Moment redistribution in continuous profiled sheeting, Thin-walled metal structures in buildings, *IABSE proceedings*, 49,107-114, Zürich: IABSE-AIPC-IVBH

Vaessen, M.J. (1995). *On the elastic web crippling stiffness of thin-walled cold-formed steel members*, MSc. thesis, Eindhoven University of Technology, Department of Structural Design, The Netherlands

Van den Berg, G.J. and Van der Merwe, P. (1992). Prediction of corner mechanical properties for stainless steels due to cold forming. *Proceedings of the eleventh international specialty conference on cold-formed steel structures*. 571–86.

Vanluchene, D. and Sun, R. (1990). Neural networks in structural engineering." *Microcomputers in Civ. Engrg.*, 5(3), pp. 207-215.

Wang, C.M. and Reddy, J.N. (2004). *Exact Solutions for Buckling of Structural Members*, CRC Press

Wasserman, P.D. (1989). *Neural Computing Theory and Practice*. Van Nostrand Reinhold Co.New York

Waszczysz, Z. and Pabisek, E, Lukasz, S. (1999). Neural network supported computational analysis of elastoplastic structures, *Proc. 5th Intern. Conf. on Engineering Applications of Neural Networks*, Warsaw, pp. 273-279.

Waszczyszyn, Z. and Pabisek, E. (2000). *Neural networks in the analysis of elastoplastic plane stress problem with unilateral constraints.*, Computational Engineering Using Metaphors from Nature, pages 1-6, Civil-Comp Press, Edinburgh

Waszczyszyn, Z. and Pabisek, E.(1999a). Hybrid NN/FEM analysis of the elastoplastic plane stress problem. *Comp. Assis. Mech. Eng. Sci.*, 6, 177–188,

Waszczyszyn, Z. and Pabisek, E., (1999b). Hybrid BPNN / FEM analysis of the elastoplastic plate bending”, Proc. 4th Conf. on Neural Networks and Their Applications, Zakopane, Polit. Czestochowska, , pp. 369-374.

Waszczyszyn, Z. (1998). *Some new results in applications of backpropagation neural networks in structural and civil engineering.* Advances in engineering computational technology: Civil-Comp Press; Edinburgh,173–87.

Waszczyszyn, Z. (1996). *Some recent and current problems of neurocomputing in civil and structural engineering.* Advanced in computational structures technology. Edinburgh: Civil-Comp Pres,43–58.

Waszczyszyn, Z. (2003). Neurocomputing and finite element method *Computer Methods in Mechanics*, Gliwice, Poland

Waszczyszyn, Z. (1999). *Neural networks in the analysis and design of structures.* CISM Courses and Lectures no. 404. New York: Springer

Waszczyszyn, Z. (2000a). “Neural networks in plasticity: some new results and prospects of applications”, European Congress on Computational Methods in Applied Sciences and Engineering, ECCOMAS

Waszczyszyn, Z. (2000b). *Neural networks in structural engineering - some recent results and prospects for applications*, Ch.23 in: Computational Mechanics for the Twenty-First Century, Ed: B.H.V. Topping, Saxe Coburg Publications, Edinburgh, pp. 479-515,

Waszczyszyn, Z. and Ziemiański, L. (2001). Neural networks in mechanics of structures and materials—new results and prospects of applications, *Comput Struct* 79, 2261–2276.

Wilkinson, T. and Hancock, G. (2002). Predicting The Rotation Capacity Of Cold-Formed RHS Beams Using Finite Element Analysis, *Journal of Constructional Steel Research* 58, 1455–1471

Wing, B.A. (1981). *Web crippling and the interaction of bending and web crippling of unreinforced multi-web cold-formed steel sections*, Master's thesis, Waterloo, University of Waterloo

Winter, G. , Pian, R. H. J. Crushing Strength of Thin Steel Webs, *Cornell Bulletin* 35, pt. 1, April 1946

Wu X., (1991), Neural network-based material modeling. Ph.D. Thesis. Department of Civil Engineering, University of Illinois at Urbana-Champaign

Wu, Shaojie; Yu, Wei-Wen; LaBoube, Roger A. *Web Crippling Strength of Members using High-Strength Steels*, Proceedings 14th International Specialty Conference on Recent Research and Developments in Cold-Formed Steel Design and Construction, October, 15-16 1998

Wu. X. (1991). *Neural Network-Based Material Modeling*. Ph.D. thesis. University of Illinois at Urbana-Champaign, Urbana. Illinois.

www.comp.nus.edu.sg/~pris/ArtificialNeuralNetworks/BasicConcepts.html

www.igi.tugraz.at/lehre/EW/tutorials/nnt_intro/nnt_intro.pdf

Xiao Y., Wu H. (2000). Compressive Behaviour of Concrete Confined by Carbon Fiber Composite Jackets. *Journal of Materials in Civil Engineering*, ASCE, 12(2), 139-146.

- Yagawa C. and Okuda H. (1996), Neural networks in computational mechanics, *Arch.Comp. Meth. Eng.*, 4, 435-512
- Yeh, Y.C. (1999), Design of High-Performance Concrete Mixture using Neural Networks and Nonlinear Programming. *Journal of Computing in Civil Engineering*, Vol.13, No.1, pp. 36-57.
- Yoon, Y.S., Cook, W.D. Mitchell, D.(1996). Minimum shear reinforcement in normal, medium and high-strength concrete beams, *ACI Structural Journal*,93:5, 576-584
- Young, B; Hancock, Gregory J. (2001). Design Of Cold-Formed Channels Subjected To Web Crippling, *Journal of Structural Engineering*, 127 (10): 1137-45
- Yu, W. W. *Cold-formed steel design*, 3rd Ed., Wiley, New York, 2000
- Yu, W. W. 'Web crippling and combined web crippling and bending of steel decks. Civil Engineering Study 81-2, Structural Series, University of Missouri–Rolla, 1981
- Yura, J.A., Galambos, T.V., and Ravindra, M.K. (1978). The Bending Resistance of Steel Beams, *Journal of the Structural Division*, ASCE, 104:1355-69.
- Zeng, P.(1998). Neural Computing in mechanics, *Appl. Mech. Rev.*,51(2) ,173-197
- Zetlin, L. and Winter G.(1952) 65th and 66th. Progress reports on light gauge steel beams of cold-formed steel, Ithaca, Cornell University.
- Zhu. J-H.. Zaman, M.M.. and Anderson, S.A. (1998). "Modelling of Shearing Behaviour of a Residual Soil with Recurrent Neural Network." *International Journal for Numerical & Analytical Methods in Geomechanics*, 22(8), 671-687.
- Ziegler, H. (1959) A modification of Prager's Hardening Rule. *Quarterly Applied Mathematics*.17, 55-65.

Ziemiański, L.(1999). *Neural Networks in Structural Dynamics*, Ofic. Wyd. Polit. Rzesz., Rzeszów.

Zienkiewicz O.C., Taylor L.C.,(1991). *The Finite Element Method*. Mc Graw Hill.

Zupan, J., Gasteiger(1993), *J. Neural Networks for Chemists - An Introduction*; VCH: Weinheim,

Zurada, J.M. (1992), *Introduction to Artificial Neural Systems*, Boston:PWS Publishing Company.

APPENDIX

Table A.1 Results of NN models compared with Eqns. 6.8-6.11

*Bold cases are test sets

λ	e	n	FE $(\frac{\sigma_u}{\sigma_{0.2}})$	NN $(\frac{\sigma_u}{\sigma_{0.2}})$	FE/ NN	Eqn (8-11) (χ)	FE/ Eqn(8- 11)
0.500	0.001	3.0	0.970	0.991	0.979	1.000	0.970
0.750	0.001	3.0	1.267	1.304	0.972	1.293	0.980
1.000	0.001	3.0	1.516	1.603	0.946	1.613	0.940
1.250	0.001	3.0	1.863	1.914	0.973	1.941	0.960
1.500	0.001	3.0	2.227	2.252	0.989	2.273	0.980
2.000	0.001	3.0	3.029	3.016	1.005	2.941	1.030
2.500	0.001	3.0	3.866	3.874	0.998	3.613	1.070
3.000	0.001	3.0	4.629	4.685	0.988	4.286	1.080
0.500	0.001	5.0	1.118	1.027	1.089	1.107	1.010
0.750	0.001	5.0	1.237	1.208	1.024	1.275	0.970
1.000	0.001	5.0	1.417	1.411	1.004	1.523	0.930
1.250	0.001	5.0	1.629	1.645	0.991	1.793	0.909
1.500	0.001	5.0	1.890	1.912	0.988	2.070	0.913
2.000	0.001	5.0	2.478	2.535	0.978	2.636	0.940
2.500	0.001	5.0	3.112	3.222	0.966	3.208	0.970
3.000	0.001	5.0	3.821	3.812	1.002	3.783	1.010
0.500	0.001	10.0	1.083	1.101	0.983	1.105	0.980
0.750	0.001	10.0	1.214	1.253	0.969	1.238	0.980
1.000	0.001	10.0	1.451	1.440	1.008	1.466	0.990
1.250	0.001	10.0	1.683	1.665	1.011	1.717	0.980
1.500	0.001	10.0	1.918	1.928	0.995	1.977	0.970
2.000	0.001	10.0	2.510	2.543	0.987	2.510	1.000
2.500	0.001	10.0	3.111	3.119	0.997	3.050	1.020
3.000	0.001	10.0	3.808	3.809	1.000	3.592	1.060
0.500	0.001	100.0	0.976	1.031	0.946	0.996	0.980
0.750	0.001	100.0	1.174	1.207	0.973	1.174	1.000
1.000	0.001	100.0	1.471	1.418	1.037	1.415	1.040
1.250	0.001	100.0	1.672	1.663	1.005	1.672	1.000
1.500	0.001	100.0	1.916	1.934	0.991	1.935	0.990
2.000	0.001	100.0	2.496	2.518	0.991	2.471	1.010
2.500	0.001	100.0	3.073	3.117	0.986	3.013	1.020
3.000	0.001	100.0	3.771	3.747	1.006	3.557	1.060

Table A.1 cont'd

0.500	0.002	3.0	0.971	0.956	1.016	0.971	1.000
0.750	0.002	3.0	1.289	1.247	1.034	1.240	1.040
1.000	0.002	3.0	1.539	1.527	1.008	1.539	1.000
1.250	0.002	3.0	1.846	1.820	1.015	1.846	1.000
1.500	0.002	3.0	2.201	2.140	1.029	2.158	1.020
2.000	0.002	3.0	2.955	2.867	1.031	2.787	1.060
2.500	0.002	3.0	3.830	3.683	1.040	3.420	1.120
3.000	0.002	3.0	4.581	4.438	1.032	4.054	1.130
0.500	0.002	5.0	1.110	1.014	1.095	1.068	1.040
0.750	0.002	5.0	1.245	1.187	1.049	1.232	1.010
1.000	0.002	5.0	1.400	1.384	1.012	1.474	0.950
1.250	0.002	5.0	1.648	1.611	1.023	1.734	0.950
1.500	0.002	5.0	1.903	1.874	1.016	2.003	0.950
2.000	0.002	5.0	2.526	2.485	1.016	2.552	0.990
2.500	0.002	5.0	3.231	3.163	1.021	3.106	1.040
3.000	0.002	5.0	3.810	3.742	1.018	3.664	1.040
0.500	0.002	10.0	1.082	1.081	1.001	1.082	1.000
0.750	0.002	10.0	1.213	1.228	0.987	1.213	1.000
1.000	0.002	10.0	1.421	1.411	1.007	1.435	0.990
1.250	0.002	10.0	1.631	1.631	1.000	1.681	0.970
1.500	0.002	10.0	1.878	1.888	0.995	1.936	0.970
2.000	0.002	10.0	2.482	2.494	0.995	2.457	1.010
2.500	0.002	10.0	3.045	3.030	1.005	2.986	1.020
3.000	0.002	10.0	3.728	3.739	0.997	3.517	1.060
0.500	0.002	100.0	0.967	1.010	0.958	0.977	0.990
0.750	0.002	100.0	1.151	1.181	0.974	1.151	1.000
1.000	0.002	100.0	1.442	1.388	1.038	1.386	1.040
1.250	0.002	100.0	1.621	1.628	0.996	1.637	0.990
1.500	0.002	100.0	1.877	1.895	0.990	1.895	0.990
2.000	0.002	100.0	2.445	2.473	0.989	2.420	1.010
2.500	0.002	100.0	3.039	3.065	0.992	2.951	1.030
3.000	0.002	100.0	3.692	3.684	1.002	3.483	1.060
0.500	0.002	3.0	0.934	0.928	1.006	0.943	0.990
0.750	0.002	3.0	1.250	1.199	1.042	1.190	1.050
1.000	0.002	3.0	1.471	1.462	1.006	1.471	1.000
1.250	0.002	3.0	1.778	1.740	1.022	1.761	1.010
1.500	0.002	3.0	2.096	2.044	1.025	2.055	1.020
2.000	0.002	3.0	2.808	2.739	1.025	2.649	1.060
2.500	0.002	3.0	3.539	3.519	1.006	3.247	1.090
3.000	0.002	3.0	4.115	4.228	0.973	3.846	1.070
0.500	0.002	5.0	1.041	1.000	1.041	1.030	1.010
0.750	0.002	5.0	1.204	1.167	1.032	1.192	1.010
1.000	0.002	5.0	1.370	1.357	1.009	1.427	0.960
1.250	0.002	5.0	1.596	1.579	1.011	1.680	0.950
1.500	0.002	5.0	1.863	1.836	1.015	1.941	0.960
2.000	0.002	5.0	2.473	2.437	1.015	2.473	1.000
2.500	0.002	5.0	3.101	3.106	0.998	3.011	1.030

Table A.1 cont'd

3.000	0.002	5.0	3.658	3.674	0.996	3.552	1.030
0.500	0.002	10.0	1.081	1.061	1.019	1.060	1.020
0.750	0.002	10.0	1.188	1.205	0.986	1.188	1.000
1.000	0.002	10.0	1.392	1.382	1.007	1.406	0.990
1.250	0.002	10.0	1.581	1.597	0.990	1.647	0.960
1.500	0.002	10.0	1.839	1.850	0.994	1.896	0.970
2.000	0.002	10.0	2.431	2.446	0.994	2.407	1.010
2.500	0.002	10.0	3.012	2.972	1.014	2.924	1.030
3.000	0.002	10.0	3.617	3.671	0.985	3.445	1.050
0.500	0.002	100.0	0.950	0.989	0.960	0.959	0.990
0.750	0.002	100.0	1.140	1.156	0.986	1.129	1.010
1.000	0.002	100.0	1.400	1.359	1.030	1.359	1.030
1.250	0.002	100.0	1.605	1.594	1.007	1.605	1.000
1.500	0.002	100.0	1.839	1.857	0.990	1.857	0.990
2.000	0.002	100.0	2.372	2.429	0.977	2.372	1.000
2.500	0.002	100.0	3.064	3.014	1.017	2.891	1.060
3.000	0.002	100.0	3.413	3.622	0.942	3.413	1.000
0.500	0.003	3.0	0.899	0.906	0.993	0.917	0.980
0.750	0.003	3.0	1.191	1.159	1.028	1.145	1.040
1.000	0.003	3.0	1.409	1.407	1.001	1.409	1.000
1.250	0.003	3.0	1.649	1.670	0.987	1.682	0.980
1.500	0.003	3.0	1.980	1.961	1.010	1.961	1.010
2.000	0.003	3.0	2.650	2.629	1.008	2.524	1.050
2.500	0.003	3.0	3.492	3.378	1.034	3.090	1.130
3.000	0.003	3.0	3.988	4.048	0.985	3.659	1.090
0.500	0.003	5.0	0.986	0.987	0.999	0.996	0.990
0.750	0.003	5.0	1.155	1.147	1.007	1.155	1.000
1.000	0.003	5.0	1.328	1.332	0.997	1.383	0.960
1.250	0.003	5.0	1.548	1.548	1.000	1.629	0.950
1.500	0.003	5.0	1.826	1.799	1.015	1.882	0.970
2.000	0.003	5.0	2.375	2.390	0.994	2.399	0.990
2.500	0.003	5.0	3.097	3.049	1.015	2.921	1.060
3.000	0.003	5.0	3.584	3.607	0.994	3.446	1.040
0.500	0.003	10.0	1.060	1.043	1.016	1.039	1.020
0.750	0.003	10.0	1.164	1.182	0.985	1.164	1.000
1.000	0.003	10.0	1.364	1.355	1.007	1.378	0.990
1.250	0.003	10.0	1.549	1.565	0.990	1.614	0.960
1.500	0.003	10.0	1.802	1.812	0.995	1.858	0.970
2.000	0.003	10.0	2.358	2.399	0.983	2.358	1.000
2.500	0.003	10.0	2.980	2.916	1.022	2.865	1.040
3.000	0.003	10.0	3.477	3.605	0.964	3.375	1.030
0.500	0.003	100.0	0.942	0.969	0.972	0.942	1.000
0.750	0.003	100.0	1.118	1.132	0.988	1.107	1.010
1.000	0.003	100.0	1.386	1.330	1.042	1.332	1.040
1.250	0.003	100.0	1.589	1.561	1.018	1.573	1.010
1.500	0.003	100.0	1.803	1.820	0.990	1.821	0.990
2.000	0.003	100.0	2.394	2.385	1.004	2.324	1.030

Table A.1 cont'd

2.500	0.003	100.0	2.918	2.964	0.985	2.833	1.030
3.000	0.003	100.0	3.612	3.562	1.014	3.344	1.080
0.500	0.003	3.0	0.848	0.887	0.956	0.893	0.950
0.750	0.003	3.0	1.136	1.124	1.010	1.103	1.030
1.000	0.003	3.0	1.324	1.358	0.975	1.351	0.980
1.250	0.003	3.0	1.579	1.610	0.981	1.611	0.980
1.500	0.003	3.0	1.838	1.888	0.973	1.875	0.980
2.000	0.003	3.0	2.458	2.532	0.971	2.410	1.020
2.500	0.003	3.0	3.213	3.256	0.987	2.948	1.090
3.000	0.003	3.0	3.698	3.893	0.950	3.488	1.060
0.500	0.003	5.0	0.935	0.973	0.961	0.964	0.970
0.750	0.003	5.0	1.120	1.128	0.993	1.120	1.000
1.000	0.003	5.0	1.288	1.307	0.986	1.342	0.960
1.250	0.003	5.0	1.502	1.517	0.990	1.581	0.950
1.500	0.003	5.0	1.736	1.762	0.985	1.827	0.950
2.000	0.003	5.0	2.306	2.344	0.984	2.329	0.990
2.500	0.003	5.0	2.979	2.975	1.001	2.837	1.050
3.000	0.003	5.0	3.414	3.542	0.964	3.347	1.020
0.500	0.003	10.0	1.039	1.024	1.014	1.019	1.020
0.750	0.003	10.0	1.141	1.160	0.984	1.141	1.000
1.000	0.003	10.0	1.324	1.328	0.997	1.351	0.980
1.250	0.003	10.0	1.503	1.533	0.980	1.582	0.950
1.500	0.003	10.0	1.749	1.775	0.985	1.821	0.960
2.000	0.003	10.0	2.312	2.353	0.982	2.312	1.000
2.500	0.003	10.0	2.893	2.862	1.011	2.809	1.030
3.000	0.003	10.0	3.441	3.540	0.972	3.309	1.040
0.500	0.003	100.0	0.934	0.949	0.985	0.925	1.010
0.750	0.003	100.0	1.108	1.108	1.000	1.087	1.020
1.000	0.003	100.0	1.359	1.302	1.044	1.307	1.040
1.250	0.003	100.0	1.559	1.529	1.020	1.543	1.010
1.500	0.003	100.0	1.804	1.784	1.011	1.786	1.010
2.000	0.003	100.0	2.371	2.343	1.012	2.279	1.040
2.500	0.003	100.0	2.945	2.916	1.010	2.778	1.060
3.000	0.003	100.0	3.476	3.503	0.992	3.279	1.060
				Mean	1.000		1.008
				Std dev.	0.023		0.040

Table A.2 Results of NN models compared with Rasmussen’s Equations, EC9 and ISO

*Bold sets are used as test sets for NN training

RAS¹ : Proposed formulation by Rasmussen and Rondal (2000) for $\alpha = 0.4$

RAS² : Proposed formulation by Rasmussen and Rondal (2000) for $\alpha = 0.3$

Ref	E (MPa)	$\sigma_{0.2}$ (MPa)	n	L/r	λ	σ_u TEST (MPa)	TEST/RAS ¹	TEST/RAS ²	TEST/EC9	TEST/ISO	σ_u NN (MPa)	TEST/NN
Djalaly and Sfantesco (1972)	72600	310	7.15	10	0.211	312.9	1.008	1.008	1.011	1.008	297.5	1.05
	72600	310	7.15	50	1.055	225.4	1.143	1.085	1.147	1.121	235.3	0.958
	72600	310	7.15	70	1.477	143.8	1.165	1.129	1.203	1.189	147	0.978
	72600	310	7.15	85	1.793	97.6	1.108	1.085	1.15	1.141	102.2	0.955
	72600	310	7.15	100	2.109	74.4	1.139	1.122	1.183	1.177	72.7	1.023
	72600	310	7.15	120	2.531	51.4	1.112	1.1	1.153	1.149	49.73	1.034
	72600	310	7.15	150	3.164	33.8	1.12	1.117	1.163	1.16	34.24	0.987
	72600	310	7.15	10	0.214	321.5	1.004	1.004	1.007	1.004	347.1	0.925
	70630	320	18.12	50	1.072	237.4	1.186	1.127	1.193	1.166	231.4	1.026
	70630	320	18.12	70	1.5	137.8	1.111	1.077	1.148	1.135	143.7	0.959
	70630	320	18.12	85	1.822	97.2	1.1	1.077	1.141	1.134	100	0.972
	70630	320	18.12	100	2.143	71	1.084	1.068	1.125	1.12	71.38	0.995
	70630	320	18.12	120	2.572	47.7	1.029	1.018	1.067	1.064	49.05	0.973
	70630	320	18.12	150	3.215	30.7	1.022	1.014	1.056	1.054	34	0.903
	70630	320	18.12	10	0.203	288.2	1	1	1.001	1	286	1.008
	68670	288	16.16	50	1.016	213.6	1.124	1.066	1.123	1.095	213.8	0.999
	68670	288	16.16	70	1.423	144	1.182	1.143	1.219	1.204	132.7	1.086
	68670	288	16.16	85	1.728	93.7	1.071	1.047	1.111	1.102	92.44	1.014
	68670	288	16.16	100	2.033	65.6	1.009	0.992	1.048	1.042	66.41	0.988
	68670	288	16.16	120	2.44	46.7	1.013	1.001	1.05	1.047	46.32	1.008
68670	288	16.16	150	3.049	29.3	0.976	0.969	1.01	1.008	32.9	0.891	
Bernard et al. (1973)	68670	288	16.16	48.3	1.022	226	1.027	0.974	1.026	1.001	248.5	0.909
	75880	335	24.15	48.3	1.022	255.7	1.162	1.102	1.161	1.133	248.5	1.029
	75880	335	24.15	48.3	1.022	263.3	1.196	1.135	1.196	1.167	248.5	1.06
	75880	335	24.15	48.3	1.022	278.1	1.263	1.198	1.263	1.232	248.5	1.119
	75880	335	24.15	64.5	1.311	178.9	1.167	1.122	1.198	1.18	183.2	0.977
	78264	325	26.56	64.5	1.311	197.6	1.289	1.239	1.323	1.303	183.2	1.079
	78264	325	26.56	64.5	1.311	224.9	1.467	1.411	1.506	1.483	183.2	1.228
	78264	325	26.56	64.5	1.311	178.9	1.167	1.122	1.198	1.18	183.2	0.976
	78264	325	26.56	64.5	1.311	215	1.403	1.348	1.44	1.418	183.2	1.174
	78264	325	26.56	64.5	1.311	161.6	1.054	1.013	1.082	1.065	183.2	0.882
	78264	325	26.56	64.5	1.311	159.6	1.041	1.001	1.068	1.052	183.2	0.871
	78264	325	26.56	64.5	1.311	166.5	1.086	1.044	1.114	1.098	183.2	0.909
	78264	325	26.56	48.3	0.982	251.4	1.156	1.097	1.15	1.121	258.6	0.972

Table A.2 cont'd

	78264	325	26.56	48.3	0.982	286.9	1.32	1.251	1.313	1.279	258.6	1.11
	78264	325	26.56	48.3	0.982	263.2	1.211	1.148	1.204	0.173	258.6	1.018
	78264	325	26.56	48.3	0.982	242	1.113	1.055	1.107	0.179	258.6	0.936
	78264	325	26.56	48.3	0.982	262	1.205	1.143	1.199	1.168	258.6	1.013
	78264	325	26.56	48.3	0.982	263.2	1.211	1.148	1.204	1.173	258.6	1.018
	78264	325	26.56	48.3	0.982	257	1.182	1.121	1.176	1.146	258.6	0.994
	78264	325	26.56	48.3	0.982	281.9	1.297	1.23	1.29	1.257	258.6	1.09
	78264	325	26.56	32.4	0.659	290	1.083	1.042	1.042	1.015	295.1	0.983
	78264	325	26.56	32.4	0.659	288.7	1.078	1.038	1.038	1.01	295.1	0.978
	78264	325	26.56	32.4	0.659	298.7	1.116	1.074	1.074	1.046	295.1	1.012
	78264	325	26.56	32.4	0.659	310.1	1.158	1.115	1.115	1.085	295.1	1.051
	78264	325	26.56	32.4	0.659	282.9	1.057	1.017	1.017	0.99	295.1	0.959
	78264	325	26.56	32.4	0.659	283.7	1.06	1.02	1.02	0.993	295.1	0.962
	78264	325	26.56	32.4	0.659	301.6	1.126	1.084	1.084	1.055	295.1	1.022
	78264	325	26.56	32.4	0.659	295	1.102	1.06	1.06	1.032	295.1	1
	78264	325	26.56	41.2	0.9	271.4	1.094	1.076	1.076	1.047	275.5	0.985
	72170	340	35.78	41.2	0.9	265.6	1.07	1.053	1.053	1.024	275.5	0.964
	72170	340	35.78	41.2	0.9	274.9	1.108	1.09	1.09	1.06	275.5	0.998
	72170	340	35.78	41.2	0.9	264	1.064	1.047	1.047	1.018	275.5	0.958
	72170	340	35.78	41.2	0.9	275.7	1.111	1.093	1.093	1.063	275.5	1.001
	72170	340	35.78	51.2	1.086	201.7	1.095	1.041	1.103	1.079	203.6	0.991
	67300	299	29.45	51.2	1.086	197.6	1.073	1.02	1.081	1.057	203.6	0.971
	67300	299	29.45	51.2	1.086	206.5	1.121	1.066	1.13	1.105	203.6	1.014
	67300	299	29.45	51.2	1.086	219.9	1.194	1.135	1.203	1.176	203.6	1.08
	67300	299	29.45	51.2	1.086	203.9	1.107	1.052	1.115	1.09	203.6	1.002
	67300	299	29.45	51.2	1.086	194.2	1.055	1.002	1.063	1.039	203.6	0.954
	67300	299	29.45	51.2	1.086	202.8	1.101	1.046	1.109	1.085	203.6	0.996
	67300	299	29.45	51.2	1.086	203.2	1.103	1.048	1.111	1.087	203.6	0.998
	67300	299	29.45	28.9	0.527	208.6	0.963	0.936	0.926	0.903	202	1.033
	74650	245	19.94	28.9	0.527	200.3	0.925	0.899	0.889	0.867	202	0.992
	74650	245	19.94	28.9	0.527	197.9	0.914	0.888	0.878	0.857	202	0.98
	74650	245	19.94	28.9	0.527	192.7	0.89	0.865	0.855	0.834	202	0.954
	74650	245	19.94	51.9	0.947	163.6	0.951	0.902	0.941	0.916	164.3	0.996
	74650	245	19.94	51.9	0.947	155.1	0.901	0.854	0.892	0.868	164.3	0.944
	74650	245	19.94	51.9	0.947	191.4	1.112	1.054	1.101	1.072	164.3	1.165
	74650	245	19.94	51.9	0.947	158.8	0.923	0.875	0.913	0.889	164.3	0.966
	74650	245	19.94	51.9	0.947	153.3	0.891	0.845	0.882	0.859	164.3	0.933
	74650	245	19.94	51.9	0.947	163.6	0.951	0.902	0.941	0.916	164.3	0.996
	74650	245	19.94	51.9	0.947	153.2	0.89	0.844	0.881	0.858	164.3	0.932
	74650	245	19.94	51.9	0.947	157.1	0.912	0.865	0.903	0.879	164.3	0.956
Kloppel and Barsch (1973)	74650	245	19.94	90	1.937	82.2	1.011	0.992	1.049	1.043	85.81	0.958
	72100	330	33.6	90	1.827	81.5	1.013	0.992	1.051	1.044	82.83	0.984
	72100	293	29.9	90	1.827	79	0.981	0.961	1.018	1.011	82.83	0.954
	72100	293	29.9	60	1.291	180.5	1.115	1.07	1.143	1.125	176.6	1.022
	72100	330	33.6	60	1.291	169.7	1.048	1.006	1.074	1.057	176.6	0.961
	72100	330	33.6	82	1.765	98.1	1.018	0.996	1.057	1.049	103.3	0.95

Table A.2 cont'd

	72100	330	33.6	82	1.765	98.1	1.018	0.996	1.057	1.049	103.3	0.95
	72100	330	33.6	60	1.218	162.8	1.04	0.995	1.061	1.042	170.4	0.956
	72100	293	29.9	82	1.665	101	1.063	1.037	1.102	1.092	99.71	1.013
Arnault (1967)	72100	293	29.9	50	1.036	225.6	1.117	1.06	1.119	1.092	230.2	0.98
	73575	312	11.9	70	1.451	144.2	1.125	1.089	1.161	1.147	143.7	1.004
	73575	312	11.9	85	1.762	97.6	1.067	1.044	1.107	1.099	99.74	0.979
	73575	312	11.9	100	2.073	74.5	1.097	1.079	1.138	1.133	71.13	1.047
	73575	312	11.9	120	2.487	51.4	1.068	1.056	1.108	1.104	48.91	1.051
	73575	312	11.9	150	3.109	33.8	1.082	1.074	1.119	1.116	34.24	0.987
	73575	312	11.9	50	0.996	213.6	1.102	1.045	1.098	1.071	217.9	0.98
	68670	288	66.3	70	1.394	143.9	1.144	1.104	1.178	1.163	133.3	1.079
	68670	288	66.3	85	1.693	93.7	1.033	1.009	1.072	1.063	92.38	1.014
	68670	288	66.3	100	1.992	65.6	0.972	0.955	1.009	1.003	66.51	0.986
	68670	288	66.3	120	2.39	46.7	0.974	0.962	1.011	1.007	46.71	1
	68670	288	66.3	150	2.988	29.2	0.937	0.929	0.969	0.967	33.38	0.875
	68670	288	66.3	50	1.078	241.1	1.233	1.171	1.241	1.213	225.6	1.069
	68670	315	22.5	70	1.509	149	1.233	1.196	1.274	1.261	140	1.064
	68670	315	22.5	85	1.832	98.5	1.145	1.122	1.189	1.18	97.53	1.01
	68670	315	22.5	50	1.071	237.4	1.179	1.12	1.186	1.159	218	1.089
	71120	322	37.3	70	1.499	137.8	1.103	1.07	1.14	1.128	134.1	1.028
	71120	322	37.3	85	1.82	97.2	1.093	1.07	1.134	1.126	93.53	1.039
	71120	322	37.3	100	2.141	70.9	1.076	1.06	1.117	1.112	67.46	1.051
	71120	322	37.3	120	2.569	47.7	1.022	1.011	1.106	1.056	47.26	1.009
	71120	322	37.3	150	3.212	30.8	1.017	1.009	1.051	1.049	33.47	0.92
						Mean:	1.089	1.052	1.1	1.064		0.998
						Stan Dev.	0.103	0.095	0.109	0.165		0.06

Table A.3 Results Of NN Models

*Bold values are Test set

Specimen	L	λ	E	ft	n	TEST	NN	Test/N	Form.	Test /Form.	TESTS	NN	Test/NN
RHS1	46.8	19.86	62.8	250.9	24	19.39	19.39	1.00	20.3	0.96	77.5	82.65	0.94
RHS1	46.8	19.86	62.8	250.9	24	19.41	19.39	1.00	20.3	0.96	78.7	82.65	0.95
RHS2	120.4	34.52	69.8	214.3	31	24.54	24.54	1.00	29.8	0.82	122.4	68.14	1.80
RHS2	73.6	21.1	69.8	214.3	31	24.93	24.93	1.00	29.8	0.84	124.3	152.46	0.82
RHS3	52.3	22.62	68.4	233.3	27	15.1	15.11	1.00	16.34	0.92	134.8	159.97	0.84
RHS3	52.3	22.62	68.4	233.3	27	15.12	15.11	1.00	16.34	0.93	136.8	159.97	0.86
RHS4	149	39.81	70.9	242.5	20	6.45	6.45	1.00	7.69	0.84	109.2	111.3	0.98
RHS4	80.7	21.56	70.9	242.5	20	6.7	6.70	1.00	7.69	0.87	109.8	121.67	0.90
RHS5	211	42.23	69.7	244.5	48	3.28	3.28	1.00	4.31	0.76	109.1	123.56	0.88
RHS5	104.5	20.92	69.7	244.5	48	3.75	7.35	0.51	4.31	0.87	108.5	80.21	1.35
RHS6	88.8	20.62	77.8	235	19	3.83	3.83	1.00	5.59	0.69	122.4	124.65	0.98
RHS6	179	41.56	77.8	235	19	4.15	4.15	1.00	5.59	0.74	122.9	127.05	0.97
RHS7	176	34.52	62.8	258.9	31	1.63	1.69	0.96	2.29	0.71	118.7	117.3	1.01
RHS7	179.5	35.21	62.8	258.9	31	1.94	1.88	1.03	2.29	0.85	120.6	112.66	1.07
RHS8	233.5	45.95	63.5	258.6	27	2.88	2.92	0.99	4.36	0.66	212	206.86	1.02
RHS8	234.5	46.14	63.5	258.6	27	2.9	2.86	1.01	4.36	0.67	212	208.29	1.02
RHS9	236	45.6	70.2	242.2	45	1.88	1.88	1.00	3.13	0.60	224.9	192.34	1.17
RHS9	236	46.09	68.5	236.6	33	1.95	1.85	1.05	3.13	0.62	248.1	243.71	1.02
RHS10	361	54.7	68.9	227.3	25	1.35	1.35	1.00	2	0.68	255.6	255.37	1.00
RHS10	361	54.7	68.9	227.3	25	1.6	1.60	1.00	2	0.80	271.2	281.8	0.96
RHS11	225	41.54	68.8	255.5	14	1.09	1.05	1.04	1.171	0.93	290.8	270.97	1.07
RHS11	224.5	41.45	68.8	255.5	14	1.09	1.13	0.97	1.171	0.93	261.2	267.74	0.98
RHS12	237	43.37	74.5	246.8	19	0.99	0.97	1.02	0.934	1.06	315.6	311.82	1.01
RHS12	242	44.29	74.5	246.8	19	1.04	1.06	0.98	0.934	1.11	313.2	326.02	0.96
RHS13	298	45.94	68.5	236.6	33	1.88	1.98	0.95	2.53	0.74	248.2	239.83	1.03
RHS13	299	45.6	70.2	242.2	45	1.95	1.88	1.04	2.53	0.77	222.6	192.34	1.16
RHS14	176	34.02	62.4	242.8	35	1.15	1.15	1.00	1.213	0.95	79.7	86.98	0.92
RHS14	191	34.98	69.3	253.3	38	1.24	1.24	1.00	1.213	1.02	89.4	80.15	1.12
RHS14	178	34.4	62.4	242.8	35	1.26	1.26	1.00	1.213	1.04	79.1	83.06	0.95
RHS15	235.5	46.5	69.3	212.4	27	4.16	4.16	1.00	5.833	0.71	190.7	191.72	0.99
RHS15	234.5	46.3	69.3	212.4	27	4.64	4.74	0.98	5.833	0.80	185.7	186.64	0.99
RHS15	233.9	46.18	69.3	212.4	27	5.21	5.11	1.02	5.833	0.89	185.2	183.55	1.01
RHS16	238	44.75	60	260.5	53	1.08	1.15	0.94	0.437	2.47	92.8	94.43	0.98
RHS16	239	44.94	60	260.5	53	1.12	1.05	1.06	0.437	2.56	92.5	93.97	0.98
RHS17	180	34.99	62.4	242.8	35	1.24	1.30	0.95	1.245	1.00	85.1	78.93	1.08
RHS17	178	34.59	69.3	253.3	38	1.28	1.53	0.84	1.245	1.03	88.6	79.71	1.11
RHS18	125	36.13	68	285	28	0.98	1.03	0.95	0.546	1.79	92.7	93.17	0.99
RHS18	127	36.71	68	285	28	1.02	0.98	1.05	0.546	1.87	89.4	91.29	0.98
RHS19	359	43.97	69.3	229.4	34	0.83	0.79	1.05	0.518	1.60	137.7	168.94	0.82
RHS19	355	43.48	69.3	229.4	34	0.83	0.87	0.95	0.518	1.60	139.6	156.71	0.89
RHS20	601	45.27	65.2	282.8	15	0.89	0.91	0.98	0.477	1.87	513.5	512.37	1.00
RHS20	601	45.27	65.2	282.8	15	0.93	0.91	1.02	0.477	1.95	506.5	512.37	0.99
RHS21	140	28.57	67.5	276.9	33	2.77	2.80	0.99	5.08	0.55	115.3	128.14	0.90
RHS21	141	28.78	67.5	276.9	33	3.26	3.22	1.01	5.08	0.64	116.5	125.26	0.93
RHS22	540	57.73	72	353.4	84	0.92	0.92	1.00	0.487	1.89	497	498.48	1.00
RHS22	540	57.73	72	353.4	84	0.97	0.92	1.05	0.487	1.99	493	498.48	0.99

Table A.3 Cont'd

RHS23	411.5	45.45	71.9	329.9	91	0.99	1.02	0.97	0.916	1.08	612	614.02	1.00
RHS23	411	45.4	71.9	329.9	91	1	0.97	1.03	0.916	1.09	621.5	620.89	1.00
RHS24	531.2	23.46	71.4	362.1	77	2.83	2.82	1.00	5.06	0.56	2939.4	2945	1.00
RHS24	535	23.63	71.4	362.1	77	2.85	2.86	1.00	5.06	0.56	2934	2925	1.00
RHS25	361	29.93	68.8	342.8	30	1.37	1.38	0.99	1.415	0.97	669	679.13	0.99
RHS25	361	29.93	68.8	342.8	30	1.39	1.38	1.01	1.415	0.98	670.5	679.13	0.99
RHS26	601	26.2	71.6	184.8	84	1.92	1.95	0.98	1.733	1.11	852	867.13	0.98
RHS26	601	26.2	71.6	184.8	84	1.95	1.95	1.00	1.733	1.13	865	867.13	1.00
RHS27	508	56.18	69	325	53	1.17	1.22	0.96	0.317	3.69	808.5	818.85	0.99
RHS27	508	56.17	69	325	53	1.28	1.23	1.04	0.317	4.04	831	818.32	1.02
SHS1	44.5	26.13	67.5	241.3	22	30.04	30.03	1.00	47.34	0.63	30.6	27.58	1.11
SHS1	46	27.01	67.5	241.3	22	32.51	32.52	1.00	47.34	0.69	29.7	18.87	1.57
SHS2	120	24.86	72.3	244.3	19	18.36	18.36	1.00	25.28	0.73	158.4	150.55	1.05
SHS2	115.7	25.78	72.3	244.3	19	21.07	21.07	1.00	25.28	0.83	160.8	156.15	1.03
SHS3	149.4	24.59	64.9	244.8	29	4.94	4.94	1.00	5.38	0.92	132.4	185.88	0.71
SHS3	149.4	24.59	64.9	244.8	29	5.07	4.94	1.03	5.38	0.94	131.3	185.88	0.71
SHS4	149.4	25.07	64.1	225.2	31	11.65	12.48	0.93	13.59	0.86	186.6	171.06	1.09
SHS4	149.3	25.05	64.1	225.2	31	13.26	12.43	1.07	13.59	0.98	180.9	171.64	1.05
SHS5	209.5	24.6	70.2	202.9	21	6.88	7.38	0.93	7	0.98	213.8	215.73	0.99
SHS5	209.5	24.6	70.2	202.9	21	7.89	7.38	1.07	7	1.13	208.7	215.73	0.97
SHS6	239	24.49	71.7	220.3	27	3.52	3.83	0.92	4.85	0.73	264.4	261.99	1.01
SHS6	239	24.49	71.7	220.3	27	4.13	3.83	1.08	4.85	0.85	263.8	261.99	1.01
SHS7	296	23.9	70.8	228.3	28	1.43	1.43	1.00	1.93	0.74	300.2	245.02	1.23
SHS7	299	24.14	70.8	228.3	28	1.47	1.61	0.91	1.93	0.76	304.8	241.36	1.26
SHS8	179	23.88	72	186.6	12	1.71	1.81	0.95	2.49	0.69	83.3	83.73	0.99
SHS8	179	23.88	72	186.6	12	1.9	1.81	1.05	2.49	0.76	82.7	83.73	0.99
SHS9	239	23.71	65.1	203.9	28	0.76	0.79	0.96	0.63	1.21	84.6	72.02	1.17
SHS9	239.5	23.75	65.1	203.9	28	0.81	0.78	1.04	0.63	1.29	84.7	71.46	1.19
SHS10	303	25	65.3	323.7	27	2.91	2.91	1.00	3.75	0.78	728.5	709.19	1.03
SHS10	303	25	65.3	323.7	27	3.26	2.91	1.12	3.75	0.87	731.5	709.19	1.03
SHS11	451	24.12	75.3	252.1	11	1.29	1.29	1.00	1.18	1.09	592.5	615.86	0.96
SHS11	437	23.37	75.3	252.1	11	1.56	1.56	1.00	1.18	1.32	605.5	582.41	1.04
SHS12	452	24.2	68.4	300.1	13	1.06	1.07	0.99	0.902	1.18	643.5	636.77	1.01
SHS12	451.5	24.17	68.4	300.1	13	1.13	1.12	1.01	0.902	1.25	626.5	634.05	0.99
							Mean:	0.99		1.09			1.02
							St.	0.07		0.61			0.15

TABLE A.4 Experimental database vs. NN and design code results

*Bold sets are test sets

Ref.	B(mm)	D(mm)	fc(MPa)	%Reinf	a/d	Vtest (kN)	NN (kN)	EC2 (kN)	LRFD (kN)	ACI11-5 (kN)	ACI 11-3 (kN)	TEST/ NN	TEST/ EC2	TEST/ LRFD	TEST/ ACI11-5	TEST/ ACI11-3
	305	368	14.7	1.85	3.9	100.1	107	105.5	80.1	70.70	93.5	0.936	0.949	1.250	1.416	1.071
	305	375	25	2.41	3.8	137.9	138.9	131.2	106.1	94.13	125.4	0.993	1.051	1.300	1.465	1.100
	305	368	27.2	1.85	3.9	122.3	116.3	129.6	100.3	92.85	118.8	1.051	0.944	1.219	1.317	1.029
	305	368	28.4	1.24	3.9	109	105.5	115	90.8	91.63	103.8	1.033	0.948	1.200	1.190	1.050
	308	356	39.9	3.79	4	177.9	162.8	148.7	135.8	116.75	161.8	1.093	1.196	1.310	1.524	1.100
	305	372	45.7	1.83	3.8	136.8	130	154.8	121	118.87	142.5	1.053	0.884	1.131	1.151	0.960
	305	365	32.6	1.87	7.9	104.3	105	137.2	84.1	95.34	97.5	0.994	0.760	1.240	1.094	1.070
	305	365	16.3	1.87	4.9	88.96	103.6	108.9	76.7	71.54	89	0.858	0.817	1.160	1.244	1.000
	305	368	27.2	2.46	4.8	132.3	137.5	133	101	93.42	119.2	0.962	0.995	1.310	1.416	1.110
	305	356	45	3.83	5	177.9	164	153.2	130.8	118.31	158.9	1.085	1.161	1.360	1.504	1.120
Morrow and Viest (1957)	305	363	27.2	1.88	5.9	111.2	107.6	128.9	86.9	88.57	102	1.034	0.863	1.280	1.256	1.090
	177.8	273	20.6	1.2	4	44.81	46.89	47.2	33.9	33.97	40.7	0.956	0.949	1.322	1.319	1.101
	177.8	273	39.9	1	4	45.97	47.56	55.4	40.3	45.88	44.2	0.967	0.830	1.141	1.002	1.040
	177.8	273	20.6	2.5	4	54.48	60.32	56	41.6	36.67	49.5	0.903	0.973	1.310	1.486	1.101
	177.8	273	39.9	1.2	4	46.35	51.25	58.9	42.9	46.30	51.5	0.904	0.787	1.080	1.001	0.900
	177.8	273	39.9	2.5	4	64.93	69.76	69.8	52.8	49.00	61.3	0.931	0.930	1.230	1.325	1.059
	177.8	273	79.2	2.5	4	68.29	83.77	87.7	60.4	66.91	75	0.815	0.779	1.131	1.021	0.911
	177.8	273	65.5	1.2	4	58.69	55.05	69.5	50.6	58.62	57.5	1.066	0.844	1.160	1.001	1.021
	177.8	273	65.5	2.5	4	67.21	79.68	82.4	62.8	61.32	71.5	0.844	0.816	1.070	1.096	0.940
	177.8	273	79.2	1.6	4	63.67	65.36	81.4	53.1	65.04	67	0.974	0.782	1.199	0.979	0.950
	177.8	273	65.5	3.3	4	78.53	87.67	82.4	68.3	62.98	78.5	0.896	0.953	1.150	1.247	1.000
Elzanaty et al (1986)	177.8	273	63.4	2.5	6	61.9	64.94	81.5	54.8	58.68	63.8	0.953	0.760	1.130	1.055	0.970
	152	298	22.6	3.36	3.6	64.6	69.42	52.8	45.2	38.01	53.8	0.931	1.223	1.429	1.700	1.201
	152	298	29.5	2.32	3.6	66.8	64.93	57.7	48.8	40.15	57.6	1.029	1.158	1.369	1.664	1.160
	152	298	49.1	3.36	2.5	117.9	91.69	68.4	67	55.78	77.1	1.286	1.724	1.760	2.114	1.529

Table A.4 cont'd

Mphonde and Frantz (1984)	152	298	40.9	3.36	3.6	82.16	79.71	64.4	56.7	48.63	67.3	1.031	1.276	1.449	1.689	1.221
	152	298	45.2	3.36	3.6	82.79	81.9	66.6	58.7	50.75	69.6	1.011	1.243	1.410	1.631	1.190
	152	298	81.4	3.36	3.6	89.69	96.86	81	63.6	65.63	76.7	0.926	1.107	1.410	1.367	1.169
	152	298	81.1	3.36	3.6	89.38	96.76	80.9	63.4	65.52	76.4	0.924	1.105	1.410	1.364	1.170
	152	298	88.4	3.36	3.6	93.45	99.04	83.2	65.3	68.09	78.5	0.944	1.123	1.431	1.373	1.190
	152	298	99.8	3.36	3.6	97.84	102.1	86.7	68.4	71.89	82.2	0.958	1.128	1.430	1.361	1.190
	152	298	22.4	3.36	2.5	77.77	77.31	52.7	49.9	41.06	55.2	1.006	1.476	1.559	1.894	1.409
	152	298	86.2	3.36	2.5	111.3	106	82.6	73.2	70.51	86.3	1.050	1.347	1.520	1.578	1.290
Islam et al (1998)	150	203	83.3	3.22	3.9	65	74.56	60.1	44.2	43.97	46.1	0.872	1.082	1.471	1.478	1.410
	150	203	83.3	3.22	3	96.9	81.57	60.1	48.7	45.38	51.5	1.188	1.612	1.990	2.135	1.882
	150	203	83.3	3.22	3.9	80.7	74.56	60.1	44.3	43.97	46.1	1.082	1.343	1.822	1.835	1.751
	150	203	72.2	3.22	3.9	58	69.84	57.3	43.3	41.23	45	0.831	1.012	1.339	1.407	1.289
	150	203	72.2	3.22	3.9	72.1	69.84	57.3	43.4	41.23	45.1	1.032	1.258	1.661	1.749	1.599
	150	207	50.8	2.02	3.9	45.5	49.27	51.7	36.1	34.40	38.2	0.924	0.880	1.260	1.323	1.191
	150	207	50.8	2.02	3.9	51.9	49.27	51.7	36	34.40	38.2	1.053	1.004	1.442	1.509	1.359
	150	205	34.4	3.19	3.9	55	50.42	45.1	35	30.08	37.2	1.091	1.220	1.571	1.829	1.478
	150	207	26.6	2.02	3.9	47.5	41.23	41.7	28.6	25.66	30.8	1.152	1.139	1.661	1.851	1.542
Islam et al (1998)	150	207	26.6	2.02	2.9	56.5	47.94	41.7	31.2	26.58	34	1.179	1.355	1.811	2.125	1.662
	300	925	36	1	2.9	225	228.4	241.6	189.1	254.15	197.5	0.985	0.931	1.190	0.885	1.139
	300	925	36	1	2.9	249	228.4	241.6	190.1	254.15	197.5	1.090	1.031	1.310	0.980	1.261
	300	925	39	1	2.9	223	227.6	248.2	193.9	263.86	183.5	0.980	0.898	1.150	0.845	1.215
	300	925	39	1	2.9	235	227.6	248.2	194.2	263.86	183.6	1.033	0.947	1.210	0.891	1.280
	300	925	39	1	2.9	204	227.6	248.2	194.3	263.86	197.3	0.896	0.822	1.050	0.773	1.034
	300	925	37	0.75	2.9	192	202	221.5	173	253.36	202.1	0.950	0.867	1.110	0.758	0.950
	300	450	37	0.81	3	131.7	124.9	125.8	102.1	123.56	116.8	1.054	1.047	1.290	1.066	1.128
	300	225	37	0.88	3	72.9	75.06	75.4	59.8	62.05	71.2	0.971	0.967	1.219	1.175	1.024
	300	110	37	0.9	3.1	40	42.91	38.2	32.3	30.33	37.6	0.932	1.047	1.238	1.319	1.064
	295	920	50	1.03	2.5	200.8	216.9	266.5	223.1	293.32	242	0.926	0.753	0.900	0.685	0.830
	169	459	53	1.03	2.7	68.6	68.21	87.9	73.8	85.71	77.7	1.006	0.780	0.930	0.800	0.883

Table A.4 cont'd

	295	920	50	1.03	2.5	235.7	216.9	266.5	222.4	293.32	242	1.087	0.884	1.060	0.804	0.974
Collins and Kuchma (1999)	169	459	53	1.03	2.7	80.5	68.21	87.9	73.2	85.71	77.7	1.180	0.916	1.100	0.939	1.036
	295	920	86	1.03	2.5	184	204.1	319.3	143.3	378.72	164.3	0.902	0.576	1.284	0.486	1.120
	169	459	91	1.03	2.7	73.1	64.63	105.3	64.3	110.75	76.9	1.131	0.694	1.137	0.660	0.951
	300	925	98	1	2.9	193	206.5	337.4	225.5	408.74	264.4	0.935	0.572	0.856	0.472	0.730
	300	925	98	1	2.9	217	206.5	337.4	225.3	408.74	261.4	1.051	0.643	0.963	0.531	0.830
	300	925	99	0.75	2.9	193	179.6	307.6	204.7	406.66	257.3	1.075	0.627	0.943	0.475	0.750
	300	450	99	0.81	3	131.7	134.1	174.6	125.1	198.14	144.7	0.982	0.754	1.053	0.665	0.910
	300	225	99	0.88	3	84.8	103.4	104.6	81.3	99.34	82.3	0.820	0.811	1.043	0.854	1.030
	300	925	94	0.5	2.9	163	158.5	264.1	172.7	392.50	209	1.028	0.617	0.944	0.415	0.780
		127	208	60.8	1.77	3	48.92	44.82	44.8	34.9	32.10	41.8	1.092	1.092	1.402	1.524
Ahmad et al (1986)	127	203	60.8	3.93	4	57.83	63.21	45.8	38.8	33.06	41.9	0.915	1.263	1.490	1.749	1.380
	127	203	60.8	3.93	3	68.95	70.57	45.8	42.3	34.51	46.3	0.977	1.505	1.630	1.998	1.489
	127	203	60.8	3.93	2.7	68.95	72.78	45.8	43.4	35.15	47.6	0.947	1.505	1.589	1.962	1.449
	127	202	67	5.04	4	51.21	62.12	47.1	42.3	35.54	44.5	0.824	1.087	1.211	1.441	1.151
	127	202	67	5.04	3	68.94	68.5	47.1	45.7	37.39	48.9	1.006	1.464	1.509	1.844	1.410
	127	184	64.3	6.64	4	54.28	70.81	42.5	45.2	33.42	44.5	0.767	1.277	1.201	1.624	1.220
	127	184	64.3	6.64	3	75.63	71.47	42.5	49.1	35.64	43.7	1.058	1.780	1.540	2.122	1.731
	127	184	64.3	6.64	2.7	68.95	71.66	42.5	50.7	36.62	43.6	0.962	1.622	1.360	1.883	1.581
	127	207	64.3	3.26	4	45.39	62.21	47.4	38.1	33.79	45.8	0.730	0.958	1.191	1.343	0.991
		127	207	64.3	3.26	3	44.48	69.38	47.4	41.6	35.01	49.4	0.641	0.938	1.069	1.270
Yoon and Cook ()	127	207	64.3	3.26	2.7	45.39	71.53	47.4	42.8	35.56	50.4	0.635	0.958	1.061	1.277	0.901
	127	208	66.9	2.25	4	44.62	48.64	48.2	35.7	33.41	43.3	0.917	0.926	1.250	1.335	1.030
	127	208	66.9	2.25	3	46.7	54.87	48.2	38.9	34.26	47.2	0.851	0.969	1.201	1.363	0.989
Yoon and Cook ()	375	655	36	2.8	3.2	249	273.1	285.6	254.1	247.04	168.2	0.912	0.872	0.980	1.008	1.480
	375	655	67	2.8	3.2	296	303.8	351.3	293.1	323.72	205.6	0.974	0.843	1.010	0.914	1.440
	375	655	87	2.8	3.2	327	321.3	383.2	292	363.79	219.5	1.018	0.853	1.120	0.899	1.490
Yoon and Cook ()	170	270	53.7	1.87	3	70.68	69.63	71.5	59.4	52.96	68.6	1.015	0.989	1.190	1.335	1.030
	170	270	53.7	1.87	3	71.6	69.63	71.5	59.7	52.96	68.2	1.028	1.001	1.199	1.352	1.050

Table A.4 cont'd

	170	272	53.7	1.01	3	58.26	52.19	58.5	50.2	51.08	57.1	1.116	0.996	1.161	1.141	1.020
	170	272	53.7	1.01	3	56.41	52.19	58.5	50.4	51.08	57	1.081	0.964	1.119	1.104	0.990
	170	267	53.7	3.35	3	78.07	85.85	72.4	69.1	56.21	78.9	0.909	1.078	1.130	1.389	0.989
	170	255	53.7	4.68	3	89.73	80.59	69.9	71.8	56.97	76	1.113	1.284	1.250	1.575	1.181
	170	255	53.7	4.68	3	95.37	80.59	69.9	71.7	56.97	76.3	1.183	1.364	1.330	1.674	1.250
	170	270	53.7	1.87	4.5	66.55	59.76	71.5	52.4	51.32	61.1	1.114	0.931	1.270	1.297	1.089
	170	270	53.7	1.87	4.5	63.8	59.76	71.5	52.7	51.32	60.8	1.068	0.892	1.211	1.243	1.049
	170	142	53.7	1.87	3	41.03	48.31	40.4	33	27.85	41.9	0.849	1.016	1.243	1.473	0.979
	170	142	53.7	1.87	3	39.34	48.31	40.4	33	27.85	41.9	0.814	0.974	1.192	1.413	0.939
	300	550	53.7	1.87	3	226.1	199.2	221.3	191.6	190.36	194.9	1.135	1.022	1.180	1.188	1.160
	300	550	53.7	1.87	3	214.5	199.2	221.3	191.5	190.36	195	1.077	0.969	1.120	1.127	1.100
	300	915	53.7	1.87	3	299.2	310.7	337	287.7	316.70	285	0.963	0.888	1.040	0.945	1.050
Kim and Park (1994)	300	915	53.7	1.87	3	332.1	310.7	337	286.3	316.70	286.3	1.069	0.985	1.160	1.049	1.160
	150	221	77.8	1.82	3	67.93	58.52	60.7	43	45.22	46.5	1.161	1.119	1.580	1.502	1.461
	150	221	54	1.82	3	58.12	54.51	53.7	42.4	38.25	44.4	1.066	1.082	1.371	1.520	1.309
	150	207	54	3.23	4	70.46	61.41	52.8	43	36.89	45.8	1.147	1.334	1.639	1.910	1.538
	150	207	54	3.23	3	82.63	68.78	52.8	46.9	38.33	49.2	1.201	1.565	1.762	2.156	1.679
	150	207	77.8	3.23	4	77.82	72.78	59.6	43.7	43.42	48	1.069	1.306	1.781	1.792	1.621
	150	207	77.8	3.23	3	82.63	79.97	59.6	48	44.86	52.3	1.033	1.386	1.721	1.842	1.580
	150	207	58	3.23	4	68.01	63.5	54.1	44.2	38.08	46.9	1.071	1.257	1.539	1.786	1.450
	150	207	58	3.23	3	82.63	70.84	54.1	48	39.51	50.1	1.166	1.527	1.721	2.091	1.649
	150	207	86.4	3.23	4	86.16	76.26	61.7	45.3	45.53	49.8	1.130	1.396	1.902	1.892	1.730
	150	207	86.4	3.23	3	107.2	83.37	61.7	50.1	46.96	54.4	1.286	1.737	2.140	2.283	1.971
	150	207	97.7	3.23	4	76.84	80.31	64.3	47.4	48.14	51.9	0.957	1.195	1.621	1.596	1.481
	150	207	97.7	3.23	3	77.72	87.31	64.3	52.2	49.58	56.7	0.890	1.209	1.489	1.568	1.371
	300	414	77.8	3.23	4	229.4	227.1	203.8	151.9	173.69	159.3	1.010	1.126	1.510	1.321	1.440
	150	221	97.7	1.82	3	56.16	60.46	65.5	46.8	50.26	50.1	0.929	0.857	1.200	1.117	1.121
	300	442	77.8	1.82	3	180.3	168.5	208.1	149	180.87	155.4	1.070	0.866	1.210	0.997	1.160
Thorenfeldt and Drangsholt (1990)	300	414	77.8	3.23	3	280.7	230	203.8	174.3	179.42	176.5	1.220	1.377	1.610	1.564	1.590

Table A.4 cont'd

	150	137	25	2.73	3.9	28.6	27.45	27.3	21.9	17.13	26.6	1.042	1.048	1.306	1.670	1.075
	150	137	25	2.8	3	32.7	34.26	27.3	23.2	17.94	28.7	0.955	1.198	1.409	1.822	1.139
	156	270	27	2.74	3	65.1	68.03	53.3	45.9	37.86	55.6	0.957	1.221	1.418	1.719	1.171
	151	270	27	2.84	4	55.4	60.46	51.6	41.1	35.23	50.4	0.916	1.074	1.348	1.573	1.099
	155	270	30	2.66	6.5	53.6	43.46	54.9	37.9	35.70	45.3	1.233	0.976	1.414	1.501	1.183
	156	543	26	2.77	4	93.1	109.9	91.5	74.3	71.76	98.5	0.847	1.017	1.253	1.297	0.945
	156	543	27	2.77	3.1	107.8	115.8	92.6	80.5	75.77	106	0.931	1.164	1.339	1.423	1.017
	156	543	26	2.72	6.8	84.6	90.32	91.5	60.8	67.48	79.1	0.937	0.925	1.391	1.254	1.070
	154	1090	27	2.71	3	164.4	159.1	163.1	143.5	150.60	177.7	1.033	1.008	1.146	1.092	0.925
	152	1090	30	2.72	4	158	152.9	166.8	122.1	149.05	157.7	1.033	0.947	1.294	1.060	1.002
	155	1090	27	2.7	7	153.6	149.7	164.2	105.5	136.58	135.2	1.026	0.935	1.456	1.125	1.136
	152	270	17	0.5	3	27.2	31.54	28.1	24	25.35	27.2	0.862	0.968	1.133	1.073	1.000
	152	270	17	0.5	3.5	24.5	28.72	28.1	20	25.17	23.4	0.853	0.872	1.225	0.973	1.047
	152	270	28	0.5	3.5	25.4	30.36	33.1	20	32.04	24.6	0.837	0.767	1.270	0.793	1.033
	152	270	35	0.5	2.6	33.6	35.39	35.7	28	36.05	35.2	0.949	0.941	1.200	0.932	0.955
	152	270	35	0.5	3.5	24.9	30.81	35.7	20	35.68	24.7	0.808	0.697	1.245	0.698	1.008
	152	270	17	0.8	4	30.2	31.31	32.8	24.9	25.59	30.7	0.965	0.921	1.213	1.180	0.984
	152	270	17	0.8	5	27.3	25.52	32.8	19.3	25.29	24.6	1.070	0.832	1.415	1.079	1.110
	152	270	17	0.8	2.5	35.6	39.51	32.8	30.4	26.44	39.2	0.901	1.085	1.171	1.346	0.908
	152	270	17	0.8	3	32.5	36.5	32.8	27.9	26.04	35.4	0.890	0.991	1.165	1.248	0.918
	152	270	17	0.8	3	32.8	36.67	32.8	28.4	26.06	36	0.895	1.000	1.155	1.259	0.911
	152	270	26	0.8	3	38.8	38	37.8	33.3	31.78	41.8	1.021	1.026	1.165	1.221	0.928
	152	270	26	0.8	4	33.6	32.36	37.8	27.7	31.29	31.3	1.038	0.889	1.213	1.074	1.073
	152	270	26	0.8	2.5	41.5	40.59	37.8	33.6	32.15	43.6	1.022	1.098	1.235	1.291	0.952
	152	270	26	0.8	2.5	44.6	40.43	37.8	34.4	32.12	47	1.103	1.180	1.297	1.389	0.949
	152	270	26	0.8	5.1	25.7	26.8	37.8	23.8	31.00	24.9	0.959	0.680	1.080	0.829	1.032
	152	270	26	0.8	5.1	27.9	26.96	37.8	22	31.01	23.9	1.035	0.738	1.268	0.900	1.167
	152	270	26	0.8	2.5	43.3	40.65	37.8	34.2	32.16	43.8	1.065	1.146	1.266	1.347	0.989
	152	270	26	0.8	2.5	39.4	40.65	37.8	34.1	32.16	44.1	0.969	1.042	1.155	1.225	0.893
	152	270	26	0.8	3	39.3	37.84	37.8	31.5	31.76	38.5	1.039	1.040	1.248	1.237	1.021

Table A.4 cont'd

Kani et al (1979)	152	270	26	0.8	4	32.6	32.74	37.8	27.6	31.32	30	0.996	0.862	1.181	1.041	1.087
Cladera (2003)	200	359	49.9	2.24	3	99.69	100.2	104.7	90	81.62	91	0.995	0.952	1.108	1.221	1.095
	200	359	60.8	2.24	3	108.1	103.2	111.8	95	89.14	97	1.047	0.967	1.138	1.213	1.114
	200	359	68.9	2.24	3	99.93	105.2	116.6	101	94.30	99	0.950	0.857	0.989	1.060	1.009
	200	359	87	2.24	3	117.9	108.4	126	110	104.83	100	1.088	0.936	1.072	1.125	1.179
	360	278	52.5	1.57	2.9	128	132.4	144.9	120.8	112.95	128.6	0.967	0.883	1.060	1.133	0.995
Adebar and Collins (1996)	360	278	52.5	1.57	2.9	119	132.4	144.9	121.4	112.95	128.2	0.899	0.821	0.980	1.054	0.928
	290	278	49.3	1.95	2.9	108	99.48	122.9	100.9	90.22	135.7	1.086	0.879	1.070	1.197	0.796
	290	278	46.2	1.95	2.9	81	97.24	120.2	57.4	87.64	62.8	0.833	0.674	1.411	0.924	1.290
	290	178	51.5	3.04	4.5	74.3	69.78	87.1	68.8	58.91	77.4	1.065	0.853	1.080	1.261	0.960
	290	278	58.9	1	2.9	90	98.6	104.4	89.1	93.19	101.5	0.913	0.862	1.010	0.966	0.887
Salandra and Ahmad (1989)	101.6	171.4	53.7	1.45	2.6	26.68	27.75	26.8	22.6	19.90	27.5	0.962	0.996	1.181	1.341	0.970
	101.6	171.4	52.1	1.45	3.6	21.79	22.35	26.5	20	19.15	23.9	0.975	0.822	1.090	1.138	0.912
	101.6	171.4	69.1	1.45	3.6	20.02	24.55	29.1	21.5	21.87	22.8	0.816	0.688	0.931	0.915	0.878
	101.6	171.4	66.8	1.45	2.6	29.8	29.22	28.8	24.2	22.00	25.7	1.020	1.035	1.231	1.354	1.160
	200	305	39.65	2.93	3.3	90.64	87.97	85.4	75	64.21	96.4	1.030	1.061	1.209	1.412	0.940
Gonzalez (2002)	202	306	40.2	2.88	3.3	88.86	88.77	86.8	75.6	65.32	97.7	1.001	1.024	1.175	1.360	0.910
	203	306	46.77	2.87	3.3	100.5	92.72	91.8	79.8	70.03	92.5	1.084	1.095	1.259	1.435	1.086
	199	305	41.45	2.93	3.3	83.88	88.93	86.2	76.2	65.12	92.6	0.943	0.973	1.101	1.288	0.906
	Mean											0.993	1.026	1.282	1.301	1.144
	Std Dev.											0.109	0.232	0.222	0.375	0.238
R											0.988	0.943	0.969	0.878	0.938	

CURRICULUM VITAE

PERSONAL INFORMATION

Surname, Name: ÇEVİK, Abdulkadir
Nationality: Turkish (TC)
Date and Place of Birth: 10 September 1971 , Gaziantep
Marital Status: Married
Phone: 90 342 3601200 2409
Fax: 90 342 3601107
email: akcevik@gantep.edu.tr

EDUCATION

Degree	Institution	Year of Graduation
MS	METU-Civil Engineering (Construction Management)	1998
BS	METU-Civil Engineering	1994
High School	Gaziantep Anatolian High School	1990

WORK EXPERIENCE

Year	Place	Enrollment
1999- Present	GAZÜ- Civil Engineering Department	Instructor
1997-1999	GAZÜ-Vocational High School	Instructor

FOREIGN LANGUAGES

German and English

PUBLICATIONS

- 1.Guzelbey IH, Cevik A, Gogus MT, Prediction of rotation capacity of wide flange beams using neural Networks, Journal of Constructional Steel Research (Under Publication), 2006
2. Guzelbey IH, Cevik A, Erklig A, Prediction of web crippling strength of cold-formed steel sheetings using neural Networks , Journal of Constructional Steel Research (Under Publication), 2006